Implementing advanced neo-associationist analyses of the brain

Chris Foulon

THÈSE DE DOCTORAT
DE L'UNIVERSITÉ PIERRE ET MARIE CURIE

Spécialité : Neurosciences

École doctorale : "Cerveau Cognition Comportement"

réalisée

à l'Institut du Cerveau et de la Moelle épinière

présentée par

Chris FOULON

pour obtenir le grade de :

DOCTEUR DE L'UNIVERSITÉ PIERRE ET MARIE CURIE

Sujet de la thèse :

Implementing Advanced Neo-Associationist Analyses of the Brain.

Dirigée par Pr. Michel THIEBAUT DE SCHOTTEN et Pr. Emmanuelle VOLLE

soutenue le 27/08/2018

devant le jury composé de :

Pr.	Laure ZAGO	Rapporteur
Pr.	Parashkev NACHEV	Rapporteur
Pr.	Pascale PRADAT-DIEHL	Examinateur
Pr	Cameron CRADDOCK	Examinateur
Pr	Roberto TORO	Examinateur

Acknowledgement

Une thèse, en tant que formation mais également en tant que travail de recherche ne peut s'effectuer seul, et celle-ci ne fait pas exception, bien au contraire. J'ai eu le plaisir et l'honneur d'interagir avec de très nombreuses personnes, qui ont toutes, à leur manière, participé à l'élaboration de ce travail. Ne voulant pas assommer les lecteurs avant même le début de cette thèse, je me contenterais de remerciements non-exhaustif.

Je pourrais certainement écrire une seconde thèse uniquement sur ce que je dois à mon directeur Michel Thiebaut de Schotten. Merci de m'avoir donné cette opportunité d'entrer dans le monde de la recherche et qui plus est, dans un cadre aussi stimulant et passionnant. Merci de m'avoir appris tant de choses, d'avoir été si patient et généreux. J'espère seulement que je serais capable de faire honneur à tout le temps et cette énergie consacrés à ma formation et à tout le reste.

Je voudrais également remercier Emmanuelle Volle qui m'a prodigué de nombreux conseils et m'a également supervisé tout au long de cette thèse. Merci pour sa patience pour répondre à mes nombreuses questions d'une clarté bien souvent douteuse.

Merci à Leonardo Cerliani pour son aide et ses conseils. Merci de m'avoir accompagné en Allemagne pendant deux mois. Et surtout merci pour ses talents culinaires qui m'ont donné goût à la bonne cuisine. J'ai bien peur, en revanche, qu'en ce domaine, l'élève que je suis ne surpassera jamais le maître.

Un chaleureux merci à Daniel Margulies, qui m'a accueilli dans son laboratoire à Leipzig pendant deux mois puis nous a rejoints à Paris au début de cette année. Merci d'être si généreux, et d'apporter toute cette énergie et cette originalité.

Un grand merci à Justine Mertz pour sa gentillesse et son soutien. Merci pour avoir enduré mon flot constant de réflexions et de complaintes aléatoires ! Ce fut un grand plaisir de suivre ses aventures, merci de me les avoir partagées.

Merci à Lydia Bessaï pour sa joie, sa bonne humeur et l'énergie qu'elle a apporté, pendant son passage au laboratoire comme après.

Merci à Chloé Stengel qui a commencé son doctorat en même temps que moi et qui a donc dû me supporter pendant ces presque trois années. Merci pour toutes les discussions passionnantes que l'on a partagé.

Merci à Clara Sanches qui a également dû supporter mes sujets de discussion aléatoires. Merci pour sa gentillesse, sa bonne humeur et son addiction au soleil.

Merci à Marcela Ovando Téllez qui fut d'un grand soutien, toujours joviale et souriante. Merci d'avoir partagé toutes ces discussions pendant nos pauses café !

Merci à Valentina Pacella pour avoir amené le soleil italien durant le dernier automne. Merci pour sa gaieté, son humour et son soutien.

.

Merci à Richard Levy, notre chef d'équipe au Frontlab, pour ses innombrables conseils et ses questions avisées lors des réunions, motivant tous les membres du laboratoire à donner le meilleur d'eux-mêmes.

Je remercie également tous les autres membres du BCBlab et du Frontlab pour votre aide et pour ces magnifiques années que j'ai passé à vos côtés. Ces trois années furent les plus heureuses et enrichissantes (et éprouvantes) de ma vie.

Un énorme et chaleureux merci à Michel Foulon, mon père, pour sa foi en moi indéfectible pour mes débuts dans le monde de la recherche. J'ai ouï dire qu'une bonne partie de Beaumont-le-Roger subit des rapports réguliers et passionnés de mes activités, relatant parfois des avancements de carrière avant même que j'en fusse moi-même au courant. Et merci de m'avoir transmis la curiosité et la soif d'apprendre qui m'ont mené jusqu'ici.

Merci à ma mère, Sylvie Bannier, pour m'avoir mis au monde, me transmettant ainsi un cerveau capable de s'étudier lui-même.

Merci à Igor de Schotten, pour m'avoir partagé son amour des légumes, du fromage vegan et des smoothies. Et merci pour m'avoir laissé une petite place dans sa voiture pour sortir en douce de la capitale, malgré le fait de devoir supporter mes discussions.

Je me dois également de remercier tous les amis de notre serveur Discord pour leur patience et leur endurance à supporter mes interminables complaintes, réflexions en tout genre et mes débats stériles. Avec des remerciements particuliers à Maxime Michotte, Guillaume Corré et Thomas Grenier pour m'avoir maintes fois aidé sur toutes sortes de questions techniques et théoriques dans les domaines informatiques.

Merci beaucoup à mes rapporteurs d'avoir accepté d'évaluer mon travail. J'espère que la lecture de cette thèse n'aura pas été trop ennuyeuse.

Et finalement, merci à l'Agence Nationale de la Recherche (ANR-13-JSV4-0001-01) et la Fondation pour la Recherche Médicale (FRM-RAD15008DDA) qui ont permis de financer cette thèse.

Contents

Introduction

Advanced brain imaging techniques have brought revolutionary tools to study the living human brain. Over the last few decades, our understanding of how our brain works grew faster than ever before. Neuroimaging devices brought new methods of analyses that refined models of brain functioning.

In this context, the comparison of dysfunction with normal functioning, as we know it, brought about fundamental breakthroughs. The investigation of abnormalities is a well-known method to attempt to understand complex systems. Indeed, brain function cannot be summarised with a mathematical equation, which prevents us from predicting its state from initial conditions. Therefore, we need to improve our knowledge of brain disorders if we wish to understand the functioning of the brain, prevent, cure, and rehabilitate patients with brain pathologies.

The study of brain damage dates far back in history. The focal brain lesions, i.e. damage restricted to an area, constitutes, since the 19th century, the most common way to study brain dysfunctions—pathologies such as strokes and tumours. These observations go hand in hand with hypotheses that lead to theoretical models used to interpret results. The theoretical models that have emerged in the last two centuries still significantly influence modern research. Even though the technical advances opened numerous perspectives to learn more about our minds, this knowledge is far from being served on a silver platter. The design and the choice of the strategy to account for the potential physical biases and match with the current knowledge about brain's functioning require the creation of new methods. Indeed, the biological changes following a lesion generate nearly unpredictable artefacts. It requires additional or alternative computations. We will see that this task is anything but trivial as the inherent complexity of this problem sometimes led to an oversimplification of what we know about the brain's mechanisms.

Theories of the functioning of the human brain, methods and tools to investigate the relationship between anatomy and behaviour as well as observations that corroborate or rebut these theories are intricated since the dawn of the study

of the human mind. What we understand about our brain is the result of their conjoint evolution all along history.

1 Historical context

Understanding the human mind obsessed philosophers, physicians, and later neuroscientists over millennia (Crivellato and Ribatti, 2007). How can a human think, store memories, have emotions, produce language as well as all the amazingly diverse and complex behaviours? One prior question to investigate these mechanisms is "Where?". Where are the colossal amounts of information we receive every second processed into our wide range of behaviours and thoughts? Nowadays, the first answer a person will give is: "In the brain!", but this has not been the case for most of human history. Ancient Egyptians did not believe the brain was the source of our thoughts; for them, the heart was the seat of intellect (Catani and Thiebaut de Schotten, 2012). Despite a surgical treatise written about 5,000 years ago (Breasted, 1930) describing cases of brain injuries, including one where a penetrating wound in the temple prevented the patient from speaking, Egyptians did not associate the mind with the brain. This example illustrates a misinterpretation occurring because of an incorrect theory. The ancient Greeks began to consider the brain as a central organ for behaviour and cognition. Indeed, during the 6th and 5th century BC, mentions of this organ shift can be found in the texts of pre-Socratic philosophers. However, for several centuries, strong partisans of the heart-centred theory, notably Aristotle, Empedocles, and Democritus, held considerable sway over the scientific community. The prohibition of human dissection for millennia hampered our progress in understanding of the brain. Nevertheless, during the 3rd century BC, thanks to the thirst of Greek rulers of Alexandria for scientific knowledge, human dissection became a useful means of studying human anatomy (Breasted, 1930) and hence brain anatomy. During this period, by comparing animals with humans, Erasistratus described the cerebral convolutions and was the first to attempt to correlate morphometric features of the brain with intelligence (Clarke and O'Malley, 1996). Unfortunately, Galen (129-200 AD) rejected this hypothesis and advocated for the ventricles as the centre of the body control system (Catani and Thiebaut de Schotten, 2012). With the burning down of the Alexandria library, scientific learning ambition was demoted, and the ancient ventricles

dogma remained set in stone for the next fourteen centuries—particularly since human dissection became yet again prohibited, considered as blasphemous.

It is only during the late eleventh century that human dissection slowly came back, for scientific purposes only (Ghosh, 2015). Nevertheless, it was not until the sixteenth century that people like Andreas Vesalius finally began to question Galen's teaching of the human brain's functioning. Even if human dissection was not always practised legally and conscientiously, the next two centuries of research on brain anatomy and functioning were incredibly prolific. It progressively led to the elaboration of the first comprehensive models of the brain as the organ of thoughts. The 19th century witnessed the birth of the three seminal theories that would shape the landscape of the study of the brain's global functioning. Vesalius described the convolutions as "storerooms" and "warehouses" of memories—an idea that can be considered as the forerunner of the localisationism introduced by Franz Joseph Gall (1758-1828). Gall expanded these ideas to the whole brain and tried to explain and localise every human function in the brain. His theory described the brain as the organ of the mind; as a mosaic of multiple independent organs. Each organ identified with the convolutions, performing its own distinct function (Gall and Spurzheim, 1810). This theory of the organisation of brain functions is the foundation of the localisationist school of thought. He also hypothesised that the bigger the brain region, the better the person should be at a given task. Most importantly, he argued that the size of a brain region should impact the shape of the skull. Clearly, the external skull shape is not an indirect measure of the fine brain morphology (Jones et al., 2018), and his ideas fell into disrepute. It should be noted that the size of a cortical region is still used nowadays by thousands of neuroscientists as a tool to study the brain and its disorders (Ashburner and Friston, 2000). Even though Gall's idea of the morphometric change of the brain was correct, he just had the wrong hypothesis about how it can be measured. Segregating brain functions was not a satisfying model for everyone. Another theory emerged, championed by Marie-Jean-Pierre Flourens (1794-1867), claiming the "equipotentiality" of brain areas. In this holistic model, every cortical area can be recruited to perform any function—the overall brain size becoming a pivotal measure to explain intellectual capabilities. Fortunately for geniuses with small brains (i.e. see the brain dissection of Anatole France, Keith 1927), the overall brain volume is too simple a criterion to explain intellectual capabilities. Lastly, the associationism came to

life with the work of Theodor Hermann Meynert (1833-1892) who aimed to map the morphology and distribution of both cortical cells and myelinated fibres. He was able to classify the white matter connections and developed a model suggesting that interactions between different brain areas subserve higher cognitive functions (Meynert, 1885). Considering these three theories yet constitute the limits of the possible models of the brain functioning, it is all the more impressive they were formalised at a time before the neuron was precisely described (Deiters, 1865) Indeed, the localizationism could be entirely correct if neurons were devoid of axons. Neurons would only be locally connected with their neighbours, and that would explain the segregation of functions. Alternatively, the initial holistic idea of equipotentiality of cortical regions would only be possible if every neuron of the brain was connected to every other neuron. The associationist theory lay somewhere in between localisationism and holism and agreed with their understanding of brain anatomy, integrating the knowledge of connections conveyed by the fibre bundles of the white matter with the involvement of cortical and subcortical region networks in the elaboration of functions. The study of brain damage solidified this position as Carl Wernicke (1848-1904), who studied six months with Meynert, collected cases of brain disconnections associated with specific disorders. He interpreted these disorders as the consequence of severed white matter fibres disrupting the connections among the network of regions that performed a function. That was the beginning of the disconnection syndrome era. Carl Wernicke subsequently applied the disconnection paradigm to other neurological pathologies (Wernicke, 1906) and psychiatric disorders (Lissauer, 1890; Liepmann, 1900). Seemingly strongly lateralised function, however, drove Wernicke and other associationists to include a form of cortical specialisation in their model, bringing back some localisationist concepts. Hugo Liepmann, one of Wernicke's students, came up with an alternative explanation—the anatomical lateralisation of connections (Liepmann, 1900). This model, however, needed extensive anatomy methods not available at the time. The associationist concept was perfected by Constantin Von Monakow (1853-1930), who discovered and described diaschisis—a degeneration in a cortical or subcortical region following the loss of its connections (von Monakow, 1914; Finger et al., 2004). Associationist models defined at that time are the origin of current networks approaches. Nevertheless, the associationism was not the only model to produce persuasive arguments and evidence. For instance, Karl Lashley brought back the

equipotentiality of cortical regions—the original holistic idea—and stated the irrelevance of damage localisation (Lashley, 1950). He rejected the idea of memory storehouses in localised regions and, instead, promoted the equivalence of all cortical areas for the retention of memories. During the last 50 years of research, however, no anatomical or functional evidence, either on animal or humans, supported this principle. On the contrary, many regions are unable to compensate for the loss of a function. On the other hand, the famous case series reported by Paul Broca (Broca, 1861) of patients showing a language production impairment after a brain lesion in the posterior third of the ventral left frontal lobe, propelled the localisationism as a prominent theory to investigate and explain human behaviour. This particular language deficit now bears his name "Broca's aphasia". Contrary to the holistic school of thoughts, the movement initiated by Broca gathered many partisans and these ideas never really left Neuroscience. Hence, Paul Broca brought the localisationism at the forefront of the scene. His systematic description of patients' cases and his methodology made him the father of modern cognitive neuroscience and neuropsychology and inspired modern neuroimaging analyses.

For instance, the magnetic resonance imaging (MRI) techniques rapidly became the source of numerous discoveries. In a nutshell, the MRI machine generates a strong homogeneous magnetic field—centred on the body part of interest—to align all the hydrogen atoms' spin magnetic moment. A radio frequency pulse is then applied to excite these atoms—and the time the atoms will take to align back with the magnetic field is used to constitute the MRI image (Friedman et al., 1989). Depending on the tissue's atomic composition, this time will differ—it will be the contrast used in the images to distinguish the different tissues. This principle allows scientists to have an anatomical image of a living brain—enabling the study of brain pathologies before the death of the patients. MRI sequences can be adapted to the observation of different aspects of brain functioning. For instance, functional magnetic resonance imaging (fMRI) can estimate a brain region's activity. Given that deoxygenated and oxygenated haemoglobin have different magnetic properties, the consumption of oxygen by the neurons creates a contrast called Blood Oxygen Level Dependent (BOLD) signal. Hence, recording the subject's BOLD for several minutes allows for the estimation of brain region activity—regions that are more active will need more oxygen and thus require more blood carrying it. Even if this method suffers from

a low temporal resolution, it enabled many discoveries and is still the most used MRI modality today. One way to use this modality is to record the subject's brain activity while performing a well-controlled task and perform analyses of the evolution of the blood flow with time. However, when our brain is not focusing its attention on a particular task, it does not stop its activity and can also be recorded with resting-state functional magnetic resonance imaging (rs-fMRI). This recording condition is used differently than task-related fMRI and allows exploration of the synchronisation of brain regions (i.e. functional connectivity) (Biswal et al., 1995; Smith et al., 2009). Another modality, diffusion magnetic resonance imaging (dMRI) focuses on the microscopic movement (i.e. diffusion) of the water molecules. If nothing constrains the water molecules, water diffuses homogeneously in every direction; however, in the white matter, molecules diffuse preferentially in the direction of the fibres. Therefore, recording the direction of water diffusion can inform us about the organisation of the white matter. A noteworthy usage of the dMRI data is tractography—the estimation of the trajectory of fibres by following the preferential direction of water diffusion. It is the first and so far the only way to reconstruct an estimation of the white matter connections in the living human brain. Together, we will see that these measures derived from the four MRI methods now feed at least 2 of the 3 theories of the functioning of the brain with compelling results.

Thus far, we saw that the pure holism did not resist the careful investigation of the last half-century. The localisationism, however, kept the support of the neuroscientists, though not in its original form. We will see in the following that the new imaging techniques and the advances of these past decades have brought a new light to the associationist theories of the brain functioning.

2 Problem

The theoretical model we choose drives hypotheses and interpretations. The work of Paul Broca has substantially influenced the attempts to explain how the human brain functions, preaching the localisation of functions. Probably defending—as every good scientist—reproducible science, Broca preserved the brains of several of his patients. It gave the opportunity, almost two centuries later, to re-analyse his cases, taking into account the advances of neuroscience methods. MRI studies showed that Broca solely observed brain surface in his patients,

underestimated the extent of the damages, leading to question his interpretation of the localisation of language in the human brain (Dronkers et al., 2007). The fresh MRI view of these historic brain injuries indicated that a much more complicated model was needed to explain language production. Hence, re-examining the seminal cases which enforced the localisationism using modern technologies might debunk old beliefs. By doing so, Thiebaut de Schotten et al. (2015) showed that the associationism framework could also explain patients' symptoms as a disruption of structural networks. Associationism also has the advantage to explain the symptoms implied by pure white matter lesions (Ciaraffa et al., 2013). Indeed, if the brain regions were performing distinct functions, solely damaging the white matter fibres should not affect the functions and, thus, not produce any deficit. Even though local connections and long-range white matter connections are inter-connecting the brain, the last century of research failed to show the equipotentiality of the cortical areas—as well as discarding the pure holistic interpretations. Therefore, it is crucial to carefully choose a model integrating the last discoveries of the field. We cannot discard the prominent role of the white matter connections. A more comprehensive theory, however, often requires the investigation of new features. In our case, exploring the white matter connections and their damages requires new techniques and methods, which are the focus of the present Ph.D. thesis. Dozens of billions of neurons (Bartheld et al., 2016) have at least an axon; these axons go through the white matter, which constitutes about half of the brain volume. The white matter seems to be a common denominator of many brain disorders (Fields, 2008). It is nonetheless particularly tricky to study the white matter in patients with a focal brain lesion. After a focal brain lesion, mapping white matter pathways disconnection is a thorny question. If we try to map disconnection using dMRI soon after a stroke or surgical resection, artefactual information in the regions surrounding the damages will perturb fibre tracking, thus leading to over- or underestimation of brain disconnections. A cascade of reactions occurs after a stroke, including oedema, diaschisis (i.e. a mechanism causing the partial degeneration of the brain areas that suffered from severed connections), inflammation, and cell death (Lo et al., 2003; Bartolomeo and Thiebaut de Schotten, 2016). This battlefield-like environment makes the work arduous for those who plan to map the vestiges of the severed connections. At the chronic stage, after three months or more following the injury, it is just impossible to track the remaining

disconnected fibres because of the Wallerian degeneration (Waller, 1850). Deafferentation—the loss of fibres in interconnecting regions—can either increase or decrease the excitability of disconnected regions (Bartolomeo and Thiebaut de Schotten, 2016), lessening the possibilities to detect them indirectly by observing activity changes. Additionally, even if the lesion occurs in only one hemisphere, diaschisis and deafferentation can also affect the other hemisphere. Hence, to map disconnections and their effects accurately, one might think that we should improve methods to disentangle severed fibres from the biological noise created by the damage. Albeit logical, improving such methods would not reveal fibres lost at the chronic stage. An alternative to analyse brain disconnections must be developed.

Medical scientists must develop accurate predictive methods for them to be adopted by the healthcare community. The translational part of lesion study requires additional and meticulous research, and these approaches have to prove their robustness before being widely adopted. Unfortunately, lesion studies demand substantial statistical power and large groups of patients and are unfit for clinical practice. On the other hand, the use of lesion studies with the purpose of deciphering brain functions also suffers from various flaws. The blossoming of MRI and other technologies—allowing the observation of brain damages in vivo—opened new methodological perspectives. It is now possible to compare many people's brains. Damasio and Damasio (1989) well understood this advance and developed a new way to study brain lesions by using their overlap coupled with behavioural measurement. By doing so, they performed, as well as thousands of neuroscientists after them, many group analyses to understand the underlying mechanisms of the human brain's functioning. Fifteen years later, voxel-based lesion-symptom mapping (VLSM; Bates et al. 2003), a more powerful and larger-scale method, emerged. This approach was more precise as it overlapped lesions digitally and performed a statistical test at the voxel level. The significant advance made with that method was enabling the use of unselected lesions and continuous behavioural scores. Indeed, a common bias was to group the patients according to their lesion location, influencing the hypotheses and interpretations. When patients are selected for their lesion location, one cannot circularly conclude that the region studied is performing the function alone. Further, the use of continuous behavioural measures in VLSM was more accurate than previous binary approaches. The method nonetheless inherits sub-

stantial flaws from the classic lesion overlapping methods. In the case of ischemic damage, from example as a result of strokes, the overlapping methods may bring more information on the vascular organisation than on the functional arrangement (Bartolomeo, 2011). Mah et al. (2014) explored this question and indeed discovered that the locations of the critical regions found by that method are mislocated—this mislocation following the vascular tree. Ultimately, the overlapping methods may mislocate a critical spot when the symptoms are resulting from damage along a particular white matter pathway (see Figure 1; Catani and Mesulam, 2008). This error can occur in the study of every kind of tissue—grey or white matter—if the studied lesions are hitting a critical area on different locations while the most robust overlap is in a non-critical spot (Nachev, 2015).

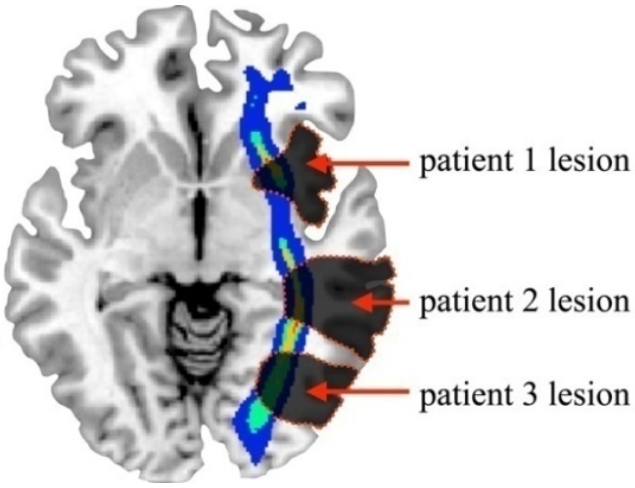

Figure 1: Brain damages can occur in different locations but disconnect the same white matter tract; they can have the same behavioural consequences without any overlap. By Thiebaut de Schotten.

Hence, the future methods used to study focal brain lesions must be coherent with the models of the functioning of the human brain, but also solve or circumvent the numerous biological flaws and technical limitations, as well as the methodological shortfalls of current methods.

According to associationist principles, a lesion is not merely damage to an independent functional node but rather the disruption of a complex system of brain structures that are anatomically and functionally interconnected. This thesis aims to provide tools to map this disruption and, using these tools, demonstrate that the effects of brain lesions extend way beyond the damaged area alone.

We will see that accurate mapping of lesions' impact and their link with patients' symptoms reveal many details about the underlying mechanisms of cognitive functions. It allowed us to show that high-level cognitive functions require interaction between various brain structures. By using different MRI modalities, enabling us to record a broader set of complementary measures, we will see how we can overcome some of the flaws of classical lesion-symptom mapping methods. As these methods are often performed using only structural images, they do not integrate information about the connexions between brain regions and how they are affected by injuries. To better consider the connexions, we used the diffusion MRI and the tractography computed from it. As we mentioned, these measures suffer from different flaws when applied to patient data; this thesis will discuss how we managed to circumvent these flaws using healthy subject tractographies to estimate the white matter disconnections. We also used a third MRI modality, the resting-state functional MRI (rs-fMRI). It gives us additional information about connections between brain areas. Besides, while tractography only maps direct connections, rs-fMRI provides data about the indirect connections. The fMRI calculates blood oxygenation level variations and areas can be activated together but be separated by more than one structural connection. We will see the value of combining these complementary modalities and their different measures, extending the range of information to which we have, and we will look at how we can use the advantages of the different approaches to making up for the flaws of the others.

In the following part of this thesis, we present the methods and results obtained with this work through three studies and a scientific commentary. We first propose a set of multimodal methods to map the indirect effects of lesions that we implemented in a freely available open-source software, the BCBtoolkit. Following the associationist principles, we applied these methods to explore the effects of focal frontal brain lesions on the category fluency performance through their impact on both structural and functional networks. The second article focuses on the study of analogical reasoning, a cornerstone of creative cognitive processes. Using a dataset of focal frontal lesions, we identified the regions and connections that critically impair patients' performance in analogy tasks. In the third article, we investigated the impact of focal brain lesions on other aspects of creativity, the generation and combination of distant associations. Once again, we identified regions and structural connections involved in these cognitive pro-

cesses, but we also explored the impact of the damage to functional networks and how it is linked to behavioural impairment. Finally, the commentary about the article 'High-dimensional therapeutic inference in the focally damaged human brain' by Xu et al. (2018) gave us the opportunity to discuss the potential advances that may overtake the flaws of classical methods used to assess how brain lesions cause symptoms.

Methods and results

3 Advanced lesion symptom mapping analyses and implementation as BCBtoolkit

Résumé :

Introduction : Les nouvelles techniques de neuroimagerie telles que la tractographie à partir de l'imagerie de diffusion par résonance magnétique et l'imagerie par résonance magnétique fonctionnelle (IRMf) permettent respectivement de cartographier les connexions structurelles entre les régions cérébrales et de mesurer l'activité et les interactions entre ces différentes régions. Bien qu'elles aient permis de nombreuses découvertes en les appliquant à des sujets sains, ces techniques restent peu utilisées chez les patients atteints de lésions cérébrales. L'étude des lésions cérébrales constitue pourtant une opportunité unique pour comprendre le fonctionnement de l'esprit humain. Cependant, les méthodes classiquement utilisées dans ce contexte considèrent généralement la zone endommagés comme directement responsable des symptômes comportementaux. Pourtant, plusieurs études ont montré qu'il est important de prendre en compte les connexions anatomiques affectées par les lésions pour explorer les déficits cognitifs (Geschwind, 1965a,b). Il a également été démontré que les lésions peuvent également affecter des régions, distantes des dommages cérébraux, faisant partie de réseaux fonctionnels plus larges (Carrera and Tononi, 2014; Finger et al., 2004; Corbetta et al., 2005). Les déconnexions peuvent avoir un impact, sur des régions distantes des zones endommagées, à cause de réactions biologiques inadaptées ou d'une propagation pathologique (Fornito et al., 2015). Une région privée de ses connexions entrantes et sortantes ne peut plus contribuer aux fonctions qu'elle supportait. Ce phénomène, nommé diaschisis (Carrera and Tononi, 2014; Finger et al., 2004; Feeney and Baron, 1986), va provoquer, dans les régions déconnectées, la diminution du nombre de synapses et de dendrites, l'altération de la myéline ainsi que le rétrécissement de neurones ou bien leur mort programmée via le mécanisme de l'apoptose (Cowan, 1970; Bredesen, 1995; Capurso et al., 1997). Bien que des méthodes existent pour estimer les effets indirects des lésions

grâce aux différentes modalités de l'imagerie par résonance magnétique (IRM), la façon de combiner ces méthodes et les informations provenant des différentes techniques reste incertaine. Une incertitude qui est amplifiée par le manque d'outils open-source et facilement accessibles, ce qui menace la reproductibilité des études dans ce domaine. En réponse à ces besoins, nous avons développé et implémenté plusieurs méthodes multimodales pour étudier les effets indirects des lésions cérébrales que nous avons réuni dans un logiciel gratuit et open-source : le BCBtoolkit. Nous avons appliqué ces méthodes pour étudier l'impact de lésions focales sur la performance en fluence catégorielle (c'est à dire, énumérer le plus de noms d'animaux possible en deux minutes), chez 37 patients ayant subi un accident vasculaire cérébral ou une résection chirurgicale.

Résultats : Nous nous sommes tout d'abord intéressés aux déconnexions structurelles diminuant la performance des patients à l'aide du Tractotron. La comparaison des lésions cérébrales avec un atlas des principaux faisceaux de fibres de la matière blanche nous a permis d'identifier cinq faisceaux critiques, tous dans l'hémisphère gauche, pour ce test neuropsychologique. Les déconnexions du long segment ou du segment antérieur du faisceau arqué, du faisceau aslant frontal ou bien des parties inférieures ou supérieures du faisceau longitudinal frontal sont liées à une baisse de performance comparée aux patients n'ayant pas de déconnexion de ces faisceaux. Il existe cependant différents atlas des connexions de la matière blanche et ceux-ci permettent de cartographier uniquement les plus connu et les plus important des faisceaux de fibres. Pour obtenir des informations plus complètes sur les déconnexions engendrées par les lésions cérébrales, nous avons utilisé une méthode plus dirigée par les données nommée *disconnectome maps*. Cette approche permet de cartographier les faisceaux de fibres touchés par la lésion en calculant quelles connexions passent par celle-ci dans la tractographie de 10 sujets contrôles sains. Une fois les cartes d'estimation des déconnexions, les disconnectomes, obtenues pour chaque patient, nous les avons combinées à une méthode statistique, AnaCOM2, pour identifier les régions qui, lorsqu'elles sont déconnectées, sont liées à un score en fluence catégorielle inférieur à celui des 54 sujets contrôles sains de notre jeu de données. Cette approche a révélé l'implication d'au moins douze régions (clusters) corticales et sous-corticales, dans les deux hémisphères, dans l'exécution de la tâche. Les régions corticales critiques trouvées dans l'hémisphère gauche sont l'aire motrice pré-supplémentaire,

la partie inférieure du sillon intrapariétal, les gyri cingulaires moyen et antérieur et le gyrus frontal moyen. Dans l'hémisphère droit ressortent également l'aire motrice pré-supplémentaire, les gyri cingulaires antérieur et moyen ainsi que le gyrus frontal moyen. Nous avons également trouvé plusieurs structures sous-corticales importantes pour la fluence catégorielle. Dans l'hémisphère gauche, le noyau caudé, le putamen et plusieurs noyaux thalamiques dont le ventral antérieur, ventro-latéral antérieur et le ventro-latéral postérieur ainsi que la pars opercularis font partie du même cluster critique pour l'exécution de la tâche. Et enfin, nous avons identifié deux clusters sous-corticaux dans l'hémisphère droit : le striatum et le noyau thalamique ventral. Nous avons ensuite comparé ces clusters aux cartes des activations fonctionnelles lors des tâches de fluence ou de catégorisation effectuées par des sujets contrôles sains, en utilisant la méthode de méta-analyse Neurosynth (Yarkoni et al., 2011; Yarkoni, 2011). Ainsi, nous avons pu montrer que les zones déconnectées que nous avons identifiées comme liées à une faible performance en fluence catégorielle correspondent avec les zones classiquement activées en imagerie par résonance magnétique fonctionnelle (IRMf) lors de tâches de catégorisation et de fluence. Jusqu'ici, les méthodes que nous avons implémentées ne nous permettent d'étudier que les déconnexions structurelles et donc les connexions directes impactées par les dommages cérébraux. Pour nous permettre d'étudier des dégradations sur des régions qui ne sont pas directement connectées aux zones lésées, nous nous sommes intéressés à la connectivité fonctionnelle calculée à partir de l'IRMf au repos. Nous avons ainsi calculé quelles régions, chez les sujets contrôles, ont une activité corrélée avec celle des différents clusters de déconnexions critiques obtenues par la méthode précédente. Cette méthode permet d'identifier les réseaux fonctionnels associés aux clusters et donc les zones qui y sont fonctionnellement connectées que ce soit par des connexions structurelles directes ou indirectes. Nous avons donc obtenu 12 réseaux fonctionnels, un pour chacun des clusters. Certains réseaux ayant des motifs d'activations similaires, nous avons utilisé une analyse en composantes principales pour déterminer si un moins grand nombre de réseaux pourrait les résumer. Nous avons ainsi identifié 3 méta-réseaux expliquant plus de 80% de la variance de la connectivité fonctionnelle : un réseau ventral fronto-pariétal (VFP) majoritairement dans l'hémisphère gauche, un réseau cingulo-operculaire (CO) et un réseau cortico-striatal (CS). Nous avons ensuite exploré si ces réseaux, bien qu'ils impliquent des zones très distantes des dommages, sont bel et bien

endommagés et si l'on pouvait relier ces dommages avec les différences de performance. Pour cela, nous avons tout d'abord comparé la mesure de connectivité fonctionnelle, et nous avons observé une diminution significative entre celle des sujets sains et celle des patients ayant une déconnexion dans le VFP et le CS. Nous avions également comme hypothèse que les réseaux fonctionnels affectés devraient présenter des changements micro-structurels et qu'ils devraient être relié à une baisse de score en fluence catégorielle. Pour mesurer des changements structurels, nous avons utilisé deux mesures : l'épaisseur corticale et l'entropie du signal IRMf au repos. Nous avons comparé l'épaisseur corticale dans les réseaux fonctionnels et nous avons pu relier une diminution de l'épaisseur corticale dans le réseau ventral fronto-pariétal avec une baisse de performance en fluence catégorielle. Pour ce qui est de l'entropie du signal IRMf, qui peut être interprétée comme une mesure indirecte de la complexité des réseaux neuronaux (Tononi et al., 1998), nous avons constaté une différence significative d'entropie dans les deux hémisphères entre les patients et les contrôles. Les différences d'entropie dans les réseaux ou les régions déconnectées n'ont en revanche pas passé les seuils statistiques après la correction pour comparaisons multiples.

Conclusion : Cette étude nous a permis de démontrer, à l'aide de méthodes multimodales d'analyses de l'imagerie par résonnance magnétique implémentées dans notre logiciel le BCBtoolkit, que les lésions cérébrales focales affectent de façon indirecte de nombreuses régions et réseaux fonctionnels dans l'ensemble du cerveau. En appliquant ces méthodes à l'étude de l'influence des lésions sur les performances en fluence catégorielle, nous avons pu étudier avec précisions les réseaux nécessaires à la réalisation de cette tâche. Le Tractotron nous a permis d'identifier les faisceaux de matière blanche affectant la performance lorsqu'ils sont déconnectés, en particulier le long segment ainsi que le segment antérieur du faisceau arqué, connus pour leur implication dans les réseaux du langage (Catani and Ffytche, 2005; Dronkers et al., 2007; Forkel et al., 2014). Les cartes de disconnectomes nous ont permis de pallier à certaines limitations des atlas des connexions cérébrales pour prendre en compte les sous-portions de faisceaux déconnectés et les faisceaux cortico-sous-corticaux affectés par les lésions. La combinaison de ces cartes avec l'analyse statistique AnaCOM2 nous a permis d'identifier des clusters de déconnexions corticales et sous-corticales critiques pour la performance en fluence catégorielle. Ces clusters sont cohérents

avec des études antérieures sur les tâches de fluence (MacPherson et al., 2015) et correspondent quasi systématiquement avec les activations trouvées chez les sujets sains lors de tâches de fluence et/ou de catégorisation en IRMf. Ces résultats étant focalisés sur les connexions structurelles affectées par les lésions, nous nous sommes demandé si une cascade de connexions polysynaptiques peut influencer le comportement et si les déconnexions et dysfonctions de régions pourraient affecter des zones connectées de manière indirecte. Pour explorer cette dimension supplémentaire des connexions indirectes, nous avons calculé la connectivité fonctionnelle des régions déconnectées précédemment identifiées (clusters). Nous avons pu montrer que, dans le contexte de la fluence catégorielle, les zones déconnectées font partie des 3 grands réseaux fonctionnels. Un réseau ventral fronto-pariétal majoritairement à gauche, miroir du réseau attentionnel ventral latéralisé à droite (Fox et al., 2006), qui lie les territoires clés du langage (Smith et al., 2009) et qui est associé aux fonctions exécutives (Parlatini et al., 2017; Power and Petersen, 2013). Nous avons également montré l'implication d'un réseau cingulo-operculaire, interagissant avec le réseau de contrôle fronto-pariétal pour le contrôle des comportements dirigés vers un but (Gratton et al., 2017) qui, avec le troisième, le réseau cortico-striatal, peut être relié à une réduction de performance dans les tâches de fluence (Chouiter et al., 2016). Les réseaux cingulo-operculaire et cortico-striatal peuvent aussi contribuer à la performance de par leur rôle dans l'initiation du comportement ou la capacité des sujets à allouer et coordonner les ressources durant la tâche (Bonnelle et al., 2012). Finalement, nous avons montré un lien entre une baisse de connectivité fonctionnelle et une déconnexion du réseau ventral fronto-pariétal ou du réseau cortico-striatal. Ces deux réseaux étant fortement latéralisés, ce résultat suggère que la partie des réseaux dans l'hémisphère intact contribue à maintenir la connectivité fonctionnelle. Des changements de connectivité devraient induire des changements de la microstructure des zones de projection et provoquer des conséquences cognitives ou comportementales. Nous avons mesuré les différences d'épaisseur corticale pour évaluer les changements structurels liés à des déconnexions directes ou indirectes des structures cérébrales. Nous avons pu montrer un lien entre un amincissement du cortex au sein du réseau ventral fronto-pariétal et une diminution de performance dans le test de fluence catégorielle. Ce résultat indique un lien fort entre l'intégrité des réseaux fonctionnels dérivée des mesures d'épaisseur cortical et les performances cognitives, et pourrait être exploité dans

de futures recherches pour stratifier des populations de patients ou prédire une récupération potentielle. Enfin, nos résultats concernant une diminution globale de l'entropie du signal IRMf au repos répliquent les résultats publiés récemment qui montrent une importante diminution de l'entropie dans les deux hémisphères de patients en comparaison de celle de sujets contrôles (Saenger et al., 2017). Ceci démontre un effet global des lésions sur la dynamique du signal IRMf. L'absence de résultats significatifs entre les patients ayant, ou non, des déconnexions dans des régions plus localisées suggèrent en revanche que l'entropie, bien que prometteuse, pourrait être trop bruitée pour détecter des changement micro-structurels fins. Ces résultats montrent que les différentes mesures de neuro-imagerie implémentées dans le BCBtoolkit nous aident à comprendre et à prendre en compte les différents retentissements anatomiques et fonctionnels d'une lésion en lien avec ses conséquences cognitives, nous renseignant ainsi sur les mécanismes sous-jacents des fonctions cognitives. Cette étude suggère qu'en utilisant les méthodes du BCBtoolkit, les chercheurs et cliniciens peuvent mesurer les effets indirects des lésions cérébrales et les associer aux conséquences neuropsychologiques. Cependant ces méthodes requièrent, en aval, la délimitation manuelle des lésions, dont l'automatisation reste un défi complexe, particulièrement pour les IRM structurels (Liew et al., 2018).

GigaScience, 7, 2018, 1–17

doi: 10.1093/gigascience/giy004
Advance Access Publication Date: 8 February 2018
Technical Note

TECHNICAL NOTE

Advanced lesion symptom mapping analyses and implementation as *BCBtoolkit*

Chris Foulon[1,2,3,*], Leonardo Cerliani[1,2,3], Serge Kinkingnéhun[1], Richard Levy[2], Charlotte Rosso[3,4,5], Marika Urbanski[1,2,6], Emmanuelle Volle[1,2,3] and Michel Thiebaut de Schotten[1,2,3,*]

[1]Brain Connectivity and Behaviour Group, Sorbonne Universities, Paris France, [2]Frontlab, Institut du Cerveau et de la Moelle épinière (ICM), UPMC UMRS 1127, Inserm U 1127, CNRS UMR 7225, Paris, France, [3]Centre de Neuroimagerie de Recherche CENIR, Groupe Hospitalier Pitié-Salpêtrière, Paris, France, [4]Abnormal Movements and Basal Ganglia team, Inserm U 1127, CNRS UMR 7225, Sorbonne Universities, UPMC Univ Paris 06, Institut du Cerveau et de la Moelle épinière, ICM, Paris, France, [5]APHP, Urgences Cérébro-Vasculaires, Groupe Hospitalier Pitié-Salpêtrière, Paris, France and [6]Medicine and Rehabilitation Department, Hôpitaux de Saint-Maurice, Saint-Maurice, France

[*]**Correspondence address.** Chris Foulon, E-mail: hd.chrisfoulon@gmail.com and Michel Thiebaut de Schotten, michel.thiebaut@gmail.com

Abstract

Background: Patients with brain lesions provide a unique opportunity to understand the functioning of the human mind. However, even when focal, brain lesions have local and remote effects that impact functionally and structurally connected circuits. Similarly, function emerges from the interaction between brain areas rather than their sole activity. For instance, category fluency requires the associations between executive, semantic, and language production functions. **Findings:** Here, we provide, for the first time, a set of complementary solutions for measuring the impact of a given lesion on the neuronal circuits. Our methods, which were applied to 37 patients with a focal frontal brain lesions, revealed a large set of directly and indirectly disconnected brain regions that had significantly impacted category fluency performance. The directly disconnected regions corresponded to areas that are classically considered as functionally engaged in verbal fluency and categorization tasks. These regions were also organized into larger directly and indirectly disconnected functional networks, including the left ventral fronto-parietal network, whose cortical thickness correlated with performance on category fluency. **Conclusions:** The combination of structural and functional connectivity together with cortical thickness estimates reveal the remote effects of brain lesions, provide for the identification of the affected networks, and strengthen our understanding of their relationship with cognitive and behavioral measures. The methods presented are available and freely accessible in the *BCBtoolkit* as supplementary software [1].

Keywords: Brain; MRI; Lesion; Statistics; Software; Open source; Connectivity; Disconnection; Behaviour

Received: 6 July 2017; **Revised:** 15 November 2017; **Accepted:** 23 January 2018

Recent advances in neuroimaging techniques have allowed for further examination of the structural and functional organization of the human brain. While diffusion weighted imaging (DWI) tractography [2] depicts how brain areas are connected together, functional magnetic resonance imaging (*f*MRI) measures the activity within and interaction between brain areas [3]. These methods have been successfully applied to the healthy human brain; however, they remain underused in patients with brain lesions.

Patients with brain lesions provide a unique opportunity to understand the functioning of the human mind. Lesion symptom mapping analyses traditionally assume that visible and directly damaged areas are responsible for a patient's symptoms [4–7]. Following this logic, the areas that are the most frequently damaged by the lesion are considered as the neuronal substrate for the function. Previous studies that used this method have identified critical areas dedicated to, for example, language production [8], comprehension [9], spatial awareness [10–13], and other high-level cognitive functions [14–17]. However, anatomical disconnections between regions are also important considerations for the exploration of cognitive deficits [18, 19]. The dysfunction of distant areas that are connected to the lesioned tissue has also been reported in *f*MRI studies. These studies have shown that the networks are disrupted even by distant lesions through disconnection and diaschisis mechanisms [20–22].

Nonlocal effects of lesions have previously been explored using various forms of atlas-based analyses of tract damage [23–32], lesion-driven tractography [32–34], disconnectome mapping [35–39], and lesion-driven resting-state *f*MRI (rs-*f*MRI) connectivity [34, 40]. However, determining what these methods actually measure and identifying how to properly combine them are not always clear to the scientific community. Furthermore, there is an extremely limited availability of free, open-source software that applies methods to measure the nonlocal effects of lesions. These resources and scientific tools remain very much inaccessible and present a potential threat to reproducible science [41].

Disconnections and diaschisis can have an impact on distant regions in several respects through maladaptive responses and pathological spread [42]. When disconnected from its inputs and outputs, a region can no longer contribute to the elaboration of the supported function. This phenomenon is called diaschisis [20, 21, 43]. Once deprived from its inputs and/or outputs, transneuronal degeneration in the region will occur [42], dendrite and synapse density will decrease in number, myelin content will be altered, and neurons will reduce in size or die through a mechanism called apoptosis, a programmed cell death [44–46]. Hence, a white matter disconnection leads to both functional and anatomical changes that extend well beyond the visible damage. New approaches are therefore required to capture the long-range effects that follow brain disconnections. For instance, cortical thickness [see, 47] and other volumetric [eg, voxel-based morphometry 48] analyses have been used to study the structural changes associated with brain lesions but have not been applied in the context of brain disconnection.

In response to this need, here, we provide a set of complementary solutions to measure both the circuit and the subsequent changes within the circuit that are caused by a lesion. We applied these methods to 37 patients with focal brain lesions following a stroke or surgical resection. We first assessed the risk of disconnection in well-known white matter tracts and tested their relationship with category fluency performance. Category fluency is an appropriate test to explore disconnection since it requires the associations between executive, semantic, and language production functions [49, 50]. We then developed a tractography-based approach in order to produce maps of the areas that are directly disconnected by the lesion and tested their relationship with category fluency performance. We additionally calculated the rs-*f*MRI connectivity of these areas to reveal the whole network of directly and indirectly disconnected regions that participate in category fluency. Finally, we explored potential microstructural changes in the latter disconnected regions by estimating neuronal loss or local connectivity degeneration derived from magnetic resonance-based measures of cortical thickness and resting-state *f*MRI entropy.

Methods

Participants and category fluency task

Thirty-seven right-handed patients (French native speakers; 19 females; mean age 48 ±14.2 years, age ranging from 23 to 75 years) who presented with a frontal lobe lesion at the chronic stage (>3 months) were included in this study (see Table 1 for demographics). These patients were recruited from the stroke unit and the neuroradiology department at Salpêtrière Hospital, the neurological unit at Saint-Antoine Hospital, and the neuroradiology department at Lariboisière Hospital in Paris. Patients with a history of psychiatric or neurological disease, drug abuse, or MRI contraindications were not included. Additionally, we gathered behavioral data from 54 healthy participants (French native speakers; 27 females; mean age 45.8 ±14.4 years, age ranging from 22 to 71 years) in order to constitute a normative group.

All participants performed a category fluency task [51] in French. They were instructed to enumerate as many animals as possible during a timed period of 120 seconds. A clinical neuropsychologist (M. U.) recorded the results. Repetition and declination of the same animal were not taken into account in the final category fluency score.

The local ethics committee (Comités de protection des personnes, CPP Ile de France VI, Groupe hospitalier Pitie Salpetriere, reference project number 16-10) approved the experiment. All participants provided written, informed consent in accordance with the Declaration of Helsinki. Participants also received a small indemnity for their participation.

Magnetic resonance imaging

An axial 3-dimensional magnetization prepared rapid gradient echo dataset covering the entire head was acquired for each participant (176 slices, voxel resolution = 1 × 1 × 1 mm, echo time = 3 msec, repetition time = 2300 msec, flip angle = 9°).

Additionally, the same participants underwent an *f*MRI session of resting state. During the resting-state session, participants were instructed to relax, keep their eyes closed, and avoid falling asleep. Functional images were obtained using T2-weighted echo-planar imaging with blood oxygenation level–dependent contrast using SENSitivity Encoding (SENSE) imaging, an echo time of 26 msec, and a repetition time of 3000 msec. Each dataset comprised 32 axial slices acquired continuously in ascending order covering the entire cerebrum with a voxel resolution of 2 × 2 × 3 mm; 200 volumes were acquired using these parameters for a total acquisition time of 10 minutes.

Finally, DWI was also acquired for 54 participants of the normative group (French native speakers; 27 females; mean age 45.8 ±14.4 years, age ranging from 22 to 71 years) and consisted of 70 near-axial slices acquired using a fully optimized acquisition sequence for the tractography of DWI, which provided isotropic

Table 1: Demographical and clinical data

ID	Age (years)	Education (years)	Gender	Lesion side	Lesion volume (mm^3)	Lesion delay (months)	Etiology
P01	56	17	F	Right	255	7	Stroke
P02	55	19	M	Left	34374	76	Hematoma
P03	46	17	F	Left	14847	126	Stroke
P04	50	11	F	Left	110145	137	Surgery
P05	64	14	M	Right	59048	119	Stroke
P06	32	16	F	Right	15946	129	epilepsy
P07	51	11	M	Bilateral	113170	54	Stroke
P08	70	5	F	Left	51530	85	Surgery
P09	47	11	M	Right	7809	115	Hematoma
P10	62	13	F	Bilateral	21295	14	Hematoma
P11	41	16	M	Right	55848	29	Surgery
P12	46	12	M	Bilateral	2542	51	Hematoma
P13	67	15	M	Left	4102	133	Stroke
P14	49	9	M	Bilateral	14929	19	Hematoma
P15	36	14	F	Right	40854	82	Surgery
P16	40	22	F	Left	24829	56	Hematoma
P17	40	14	M	Bilateral	14364	7	Hematoma
P18	23	16	F	Right	21681	47	Surgery
P19	54	22	M	Right	51897	48	Stroke
P20	71	17	M	Left	25779	91	Hematoma
P21	23	15	F	Right	29513	36	Surgery
P22	27	9	F	Left	12986	30	Surgery
P23	26	13	F	Left	2640	19	Surgery
P24	32	14	F	Left	12653	4	Surgery
P25	59	16	F	Left	97	9	Hematoma
P26	26	13	F	Left	26928	32	Stroke
P27	58	12	M	Left	1026	3	Stroke
P29	75	12	F	Left	14938	16	Hematoma
P30	52	13	F	Right	11978	20	Surgery
P31	58	12	M	Right	13263	21	Surgery
P32	62	5	M	Right	20281	9	Surgery
P33	41	17	M	Left	7463	29	Surgery
P34	42	17	M	Left	24319	6	Infection
P35	60	12	M	Right	41897	24	Surgery
P36	51	14	F	Right	39213	17	Surgery
P37	51	12	F	Right	8133	48	Surgery
P38	33	17	M	Right	140947	48	Surgery

($2 \times 2 \times 2$ mm) resolution and coverage of the entire head with a posterior–anterior phase of acquisition. The acquisition was peripherally gated to the cardiac cycle [52], with an echo time = 85 msec. We used a repetition time equivalent to 24 RR (ie, interval of time between 2 heart beat waves). At each slice location, 6 images were acquired with no diffusion gradient applied. Additionally, 60 diffusion-weighted images were acquired in which gradient directions were uniformly distributed on the hemisphere with electrostatic repulsion. The diffusion weighting was equal to a *b*-value of 1500 s/mm^2.

Stereotaxic space registration

As spatial normalization can be affected by the presence of a brain lesion, additional processing was required before the normalization could be calculated. For instance, in the case of bilateral lesions, the registration was weighted as previously reported [53]. For unilateral lesions, the first step was to produce an enantiomorphic filling of the damaged area [54]. Each patient's lesion (or signal abnormalities due to the lesion) was manually segmented (using FSLview; [55]). Unilateral lesions were replaced symmetrically by the healthy tissue of the contralateral hemisphere. Enantiomorphic T1 images were fed into FMRIB's Automated Segmentation Tool (FAST) [56] for estimation of the bias field and subsequent correction of radiofrequency field inhomogeneity. This improved the quality of the automated skull stripping performed using a brain extraction tool (BET) [57] and the registration to the MNI152 using affine and diffeomorphic deformations [58]. The original T1 images (non enantiomorphic) were registered to the MNI152 space using the same affine and diffeomorphic deformations as calculated above. Subsequently, lesions were segmented again in the MNI152 space under the supervision of an expert neurologist (E. V.). This method has been made freely available as the tool *normalisation* as part of *BCBtoolkit* [1].

The following sections are hypotheses driven and outlined in Supplementary Fig. 1.

White matter tracts disconnection

Each patient's lesion was compared with an atlas of white matter tracts [59], indicating for each voxel, the probability of finding a white matter tract such as the arcuate fasciculus, the frontal aslant tract, or the uncinate fasciculus in the MNI152 coordinate system. We considered a tract to be involved when the likelihood of a tract being present in a given voxel was estimated

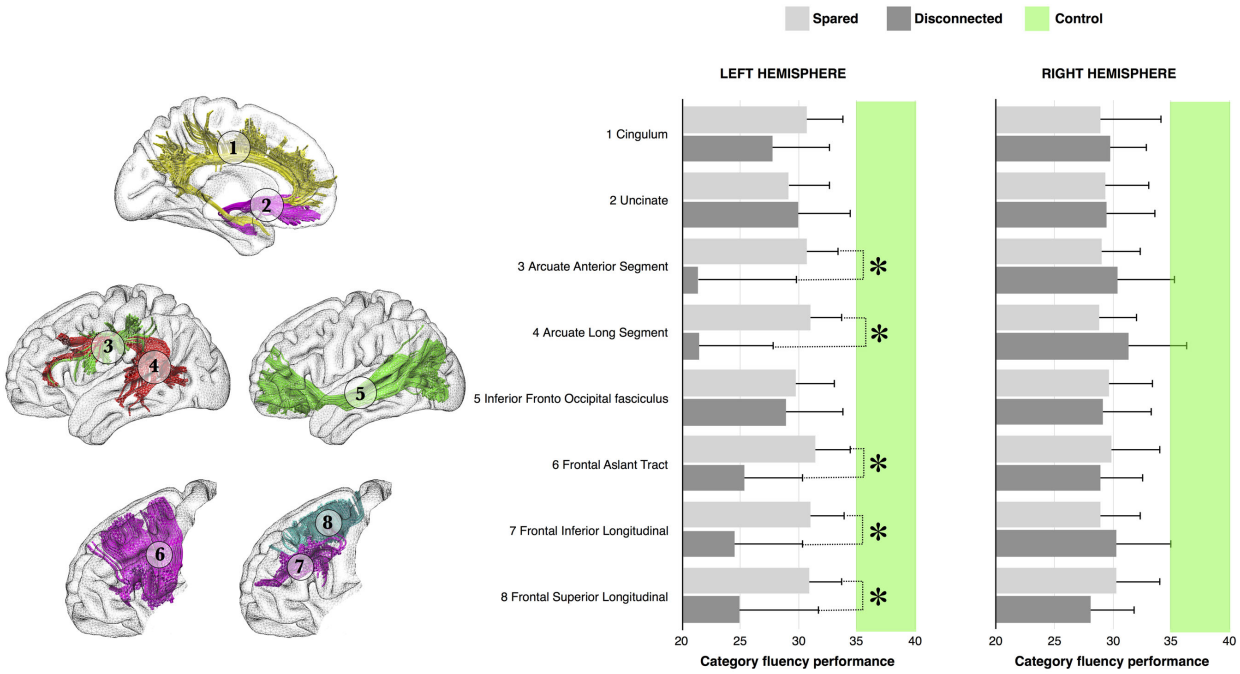

Figure 1: Category fluency performance (mean performance with 95% confidence intervals [CIs]) for patients with (dark gray) or without (light gray) disconnection of each tract of interest. The green intervals indicate the range of controls' performance corresponding to 95% CIs. $* P < 0.05$.

above 50% [23]. This method is freely available as *tractotron* in *BCBtoolkit* [1]. We focused on frontal lobe tracts with a potential effect on executive, semantic, and language functions since all of the patients had a frontal lesion. These tracts included the cingulum, the frontal aslant, and the frontal superior and inferior longitudinal tracts for the executive functions [60]; the uncinate and the inferior fronto-occipital fasciculi for the semantic access [61, 62]; and the anterior and long segment of the arcuate fasciculi for the phonemic system [63, 64]. A Kruskal-Wallis test was used to compare performance on the category fluency test for each tract between both preserved and disconnected patients and control participants. Subsequently, for each significant tract between patients, Mann-Whitney post hoc comparisons were performed (Fig. 1).

Direct disconnection of brain areas: structural connectivity network

This approach used the DWI datasets of 10 participants in the normative group to track fibers that passed through each lesion.

For each participant, tractography was estimated as indicated in [65].

Patients' lesions in the MNI152 space were registered to each control native space using affine and diffeomorphic deformations [58] and, subsequently, used as seed for the tractography in Trackvis [66]. Tractography from the lesions were transformed in visitation maps [67, 68], binarized, and brought to the MNI152 using the inverse of precedent deformations. Finally, we produced a percentage overlap map by summing at each point in the MNI space the normalized visitation map of each healthy patient. Hence, in the resulting *disconnectome map*, the value in each voxel took into account the interindividual variability of tract reconstructions in controls and indicated a probability of disconnection from 50% to 100% for a given lesion (ie, thus explaining more than 50% of the variance in disconnection and corresponding to a large effect size). This procedure was repeated for all lesions, allowing the construction of a *disconnectome map* for each patient/lesion. These steps were automatized in the tool *disconnectome map* as part of the *BCBtoolkit*. Note that sample size and age effects are carefully explored and reported in the Supplementary Material. Overall, 10 patients are sufficient to produce a good enough *disconnectome map* that matches the overall population (more than 70% of shared variance). We also demonstrate in the Supplementary Material that *disconnectome maps* show a very high anatomical similarity between decades and no decrease of this similarity with age.

Thereafter, we used *AnaCOM2*, which is available within the *BCBtoolkit*, in order to identify the disconnections that are associated with a given deficit, that is, connections that are critical for a given function (Fig. 2). *AnaCOM2* is comparable to *AnaCOM* [69] but has been reprogrammed and optimized to work on any Linux or Macintosh operating systems.

Initially, *AnaCOM* is a cluster-based lesion symptom mapping approach that identifies clusters of brain lesions that are associated with a given deficit, that is, the regions that are critical for a given function. In the context of this article, *AnaCOM2* used *disconnectome maps* instead of lesion masks to identify clusters of disconnection that are associated with category fluency deficits, that is, the connections that are critical for a given function. Compared to standard voxel-based lesion-symptom mapping (VLSM) [8], *AnaCOM2* regroups voxels with the same distribution of neuropsychological scores into clusters of voxels. Then, for each cluster larger than 8 mm^3, *AnaCOM2* will perform a Kruskal-Wallis test between patients with a disconnection, patients spared of disconnection, and controls. Resulting *P* values are Bonferroni-Holm corrected for multiple comparisons. Subsequently, significant clusters (*P* value < 0.05) are used to perform a post hoc Mann-Whitney comparison between 2 subgroups of interest (ie, disconnected patients and healthy participants). Post hoc results are Bonferroni-Holm corrected for multiple comparisons

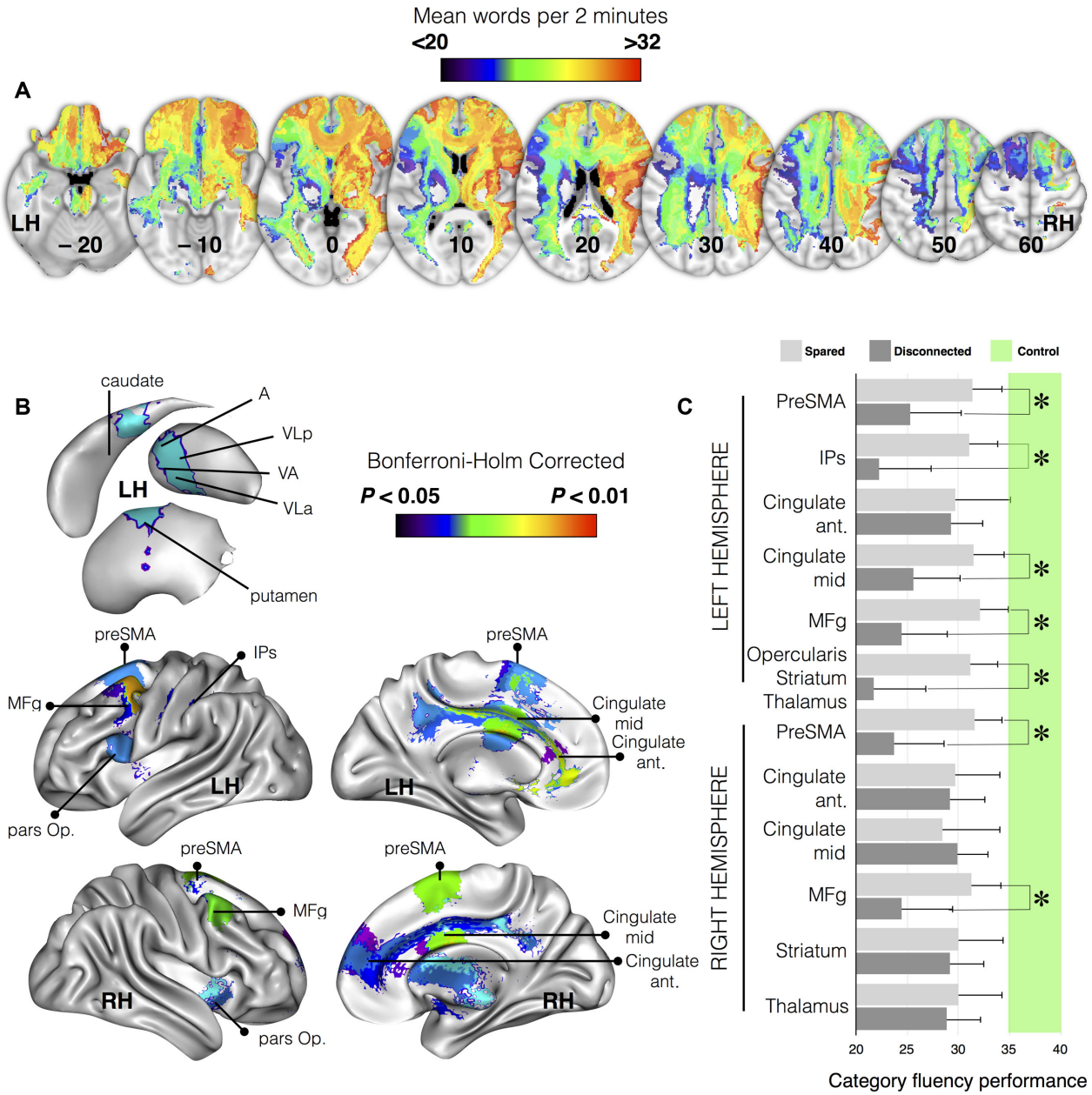

Figure 2: Areas directly disconnected by the lesion that significantly contributed to a decreased score on category fluency task (referred to as "disconnected areas" in the manuscript). A) Representative slices from *disconnectome maps* computed for category fluency performance; blue clusters indicate group average low performance and red clusters indicate high performance. B) Brain areas contributing significantly after correction for multiple comparisons. C) Category fluency performance (mean performance with 95% confidence intervals [CIs]) for patients with (dark gray) or without (light gray) disconnection of each of the examined cortical regions. The green interval indicates performance in matched controls with 95% CIs. Abbreviations: A, anterior group of thalamic nuclei; LH, left hemisphere; IPs, intraparietal sulcus; MFg, middle frontal gyrus; pars Op., frontal pars opercularis; PreSMA, presupplementary motor area; RH, right hemisphere; VA, ventral anterior; VLa, ventrolateral anterior; VLp, ventrolateral posterior. $*$ $P < 0.05$ Bonferroni-Holm corrected for multiple comparisons.

(statistical tests and corrections are computed using R language [70]).

Patient–control comparisons have been chosen as a first step in order to avoid drastic reduction of statistical power when 2 or more nonoverlapping areas are responsible for patients' reduced performance [69]. Nonparametric statistics have been chosen, as it is fair to consider that some clusters will not show a Gaussian distribution. *AnaCOM2* resulted in a statistical map that reveals, for each cluster, the significance of a deficit in patients who undertake a given task as compared to controls.

In the following sections, the term "clusters" systematically refers to the result of the post hoc Mann-Whitney comparison between disconnected patients and healthy participants who survived Bonferroni-Holm correction for multiple comparisons.

fMRI meta-analyses

A method described by Yarkoni et al. [71, 72] was used to identify the functional networks involved in category fluency. We searched for brain regions that are consistently activated in

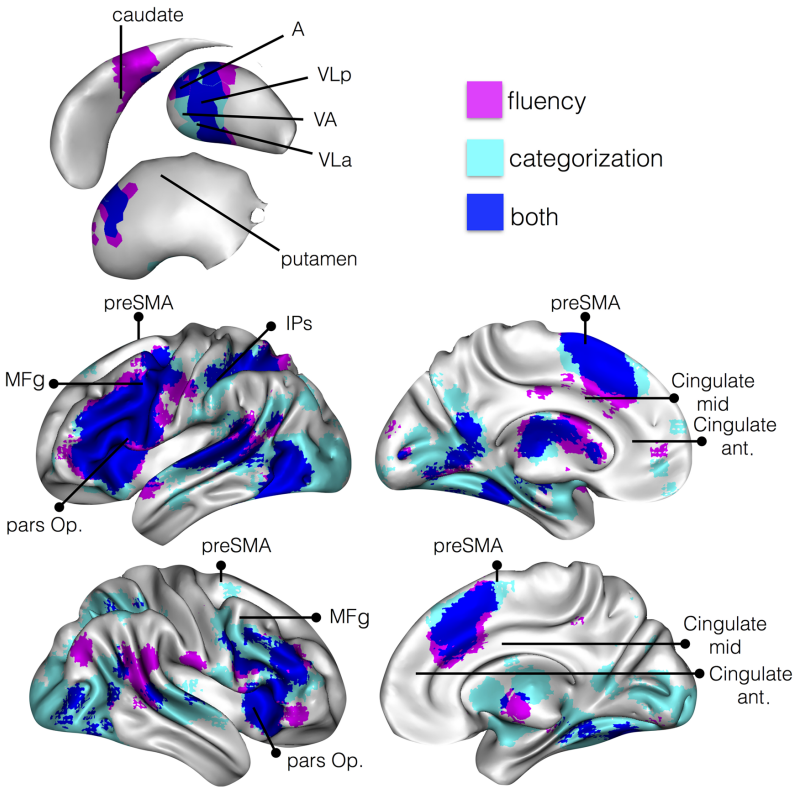

Figure 3: Areas classically activated with functional magnetic resonance imaging ($P < 0.01$ corrected for False Discovery Rate) during fluency (pink) and categorization (cyan) tasks. Areas involved in both fluency and categorization are highlighted in dark blue. Abbreviations: A, anterior group of thalamic nuclei; IPs, intraparietal sulcus; MFg, middle frontal gyrus; PreSMA, presupplementary motor area; VA, ventral anterior; VLa, ventrolateral anterior; VLp, ventrolateral posterior.

studies that load highly on the following 2 features: "fluency" (120 studies, 4214 activations) and "category" (287 studies, 10179 activations). The results were superimposed on the 3D reconstruction of the MNI152 images (Fig. 3).

Indirect disconnection of brain areas: functional connectivity network

Rs-*f*MRI images were first motion corrected using MCFLIRT [73], then corrected for slice timing, smoothed with a full half width maximum equal to 1.5 times the largest voxel dimension, and finally filtered for low temporal frequencies using a Gaussian-weighted local fit to a straight line. These steps are available in Feat as part of the FSL package [74].

Rs-*f*MRI images were linearly registered to the enantiomorphic T1 images and, subsequently, to the MNI152 template (2 mm) using affine transformations. Confounding signals were discarded from rs-*f*MRI by regressing out a confound matrix from the functional data. The confound matrix included the estimated motion parameters obtained from the previously performed motion correction, the first eigenvariate of the white matter and cerebrospinal fluid (CSF) as well as their first derivative. Eigenvariates can easily be extracted using fslmeants combined with the –eig option. White matter and CSF eigenvariates were extracted using masks based on the T1-derived 3-classes segmentation thresholded to a probability value of 0.9, registered to the rs-*f*MRI images, and binarized. Finally, the first derivative of the motion parameters, white matter, and CSF signal was calculated by linear convolution between their time course and a [–1 0 1] vector.

For each control participant, we extracted the time course that corresponded to each significant cluster, which was identified by the statistical analyses of the *disconnectome maps*. These time courses were subsequently correlated to the rest of the brain so as to extract seed-based resting-state networks. In order to obtain the most representative networks at the group level, for each seed-based resting-state network, we calculated the median network across the group. The median network resulting from a seed contains, in each voxel, the median of functional connectivity across all the controls. Medians were chosen instead of average as they are less sensitive to outliers and are more representative of the group-level data [75]. The calculation of the functional connectivity was automatized and made available inside the *funcon* tool as part of *BCBtoolkit*. Medians were calculated using the function fslmaths.

Visual inspection revealed that several of these resting-state networks shared a very similar distribution of activations. Therefore, an "activation" matrix was derived from the seed-based resting-state networks. This matrix consisted of columns that indicated each seed-based resting-state network and rows that represented the level of activation for each voxel in the cortex. This activation matrix was entered into a principal component analysis in SPSS (Chicago, Illinois) using a covariance matrix and varimax rotation (with a maximum of 50 iterations for convergence) in order to estimate the number of principal components to extract for each function. Components were plotted according to their eigenvalue (*y*; lower left panel in Fig. 4); we applied a scree test to separate the principal from residual components. This analysis revealed that 3 factors were enough to explain 82% of the variance of the calculated seed-based resting-state networks. This means that 3 factors are good enough to

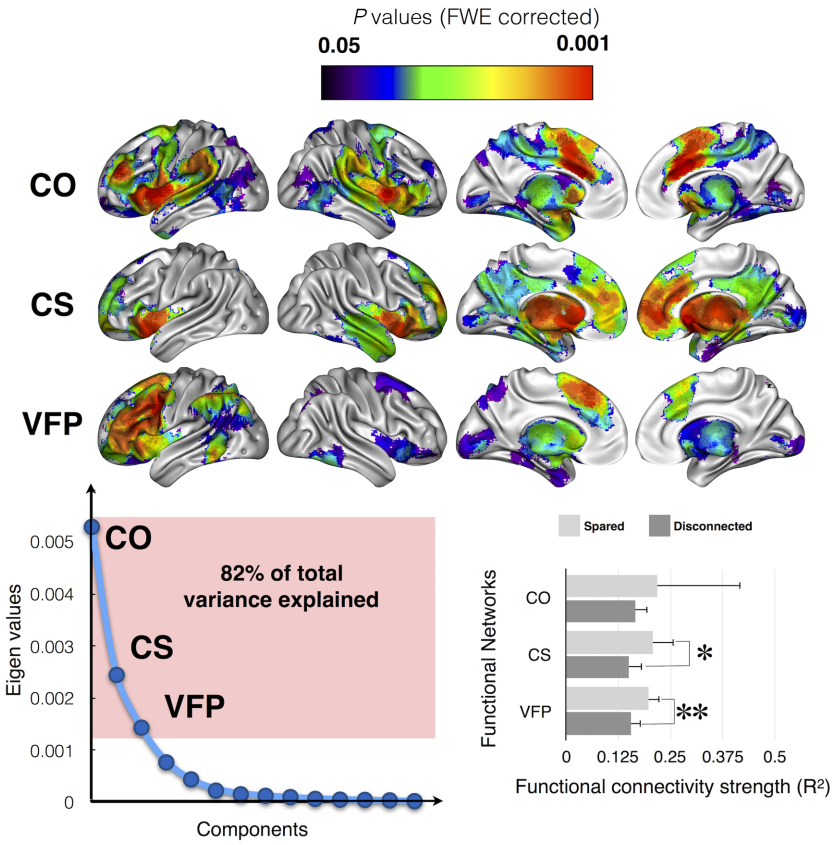

Figure 4: Functional networks involving the identified disconnected areas, as defined by resting state functional connectivity. Top panel, Main cortical networks involving the disconnected areas revealed by a principal component analysis. Bottom left panel, Principal component analysis of the raw functional connectivity result. Bottom right panel, Strength of the functional connectivity for patients with (dark gray) or without (light gray) involvement of the functional network. Abbreviations: CO, cingulo-opercular network; CS, cortico-striatal network; VFP, ventral fronto-parietal network. * $P < 0.05$; **, $P < 0.01$.

summarize most of the seed-based resting-state network results. Finally, brain regions that had a statistically significant relationship with the 3 components (ie, factor-networks) were detected using a linear regression with 5.000 permutations, in which the eigenvalues of the 3 components represented the independent variable and the seed-based resting-state networks represented the dependent variable. Results were Family Wise Error–corrected for multiple comparisons and projected onto the average 3D rendering of the MNI152 template in the top panel of Fig. 4. In the following sections, the term "factor-networks" systematically refers to brain regions that have a statistically significant relationship with the 3 components.

Additionally, for each patient, we extracted the time course that corresponded to each factor-network. These time courses were subsequently correlated to the rest of the brain so as to extract seed-based factor-networks in each patient. FSLstats was used to extract the strength of factor-networks functional connectivity and, subsequently, to compare patients according to their disconnection status. Note that a patient disconnected in a factor-network is a patient who has a disconnection in at least 1 of the clusters that contributed significantly to the factor-network.

Structural changes in disconnected regions

A distant lesion can affect cortical macro- and microstructures remotely. Conscious of this, we attempted to estimate these structural changes and their relationship with category fluency within each functional factor-network. To this aim, we explored the properties of each functional network using the following 2 complementary measures: T1w-based cortical thickness to identify fine local volumetric changes and the Shannon entropy of rs-*f*MRI as a surrogate for the local complexity of the neural networks [76]. Each original functional network seeded from each cluster was thresholded and binarized at $r > 0.3$ and used as a mask to extract cortical thickness and entropy. Patients' lesions were masked out for these analyses.

For the cortical thickness, a registration-based method (Diffeomorphic Registration based Cortical Thickness, DiReCT) was used [77] from the T1-weighted imaging dataset. The first step, as for the *normalization*, was to produce an enantiomorphic filling of the damaged area in order to prevent the analysis from being contaminated by the lesioned tissue. The second step of this method consisted of creating two 2-voxel thick sheets, 1 laying just between the gray matter and the white matter and the second laying between the gray matter and the CSF. The gray–white interface was then expanded to the gray–CSF interface using diffeomorphic deformation estimated with Advanced Normalization Tools (ANTs). The registration produced a correspondence field that allowed an estimate of the distance between the gray–white and the gray–CSF interfaces and thus corresponded to an estimation of cortical thickness. Voxels that belonged to the lesion were subsequently removed from the cortical thickness maps (see Supplementary Fig. S2). This approach has good

scan–rescan repeatability and good neurobiological validity as it can predict with a high statistical power the age and gender of the participants [78] as well as atrophy following brain lesions [79]. Note that the striatum and thalamus were excluded from the cortical thickness analysis since they do not have a cortical ribbon.

Shannon entropy is an information theory–derived measure that estimates signal complexity [80, 81]. In the context of rs-*f*MRI, the entropy measures the local complexity of the blood oxygen level–dependent (BOLD) signal as a surrogate of the complexity of the spontaneous neuronal activity [82, 83]. Since "cells that fire together wire together" [84], for each gray matter voxel, Shannon entropy of rs-fMRI can be considered as a surrogate for the complexity of the connections within this voxel and between this voxel and the rest of the brain. Shannon entropy was extracted from the previously preprocessed rs-*f*MRI using the following formula: − sum (p∗log(p)), where p indicates the probability of the intensity in the voxel [76].

FSLstats was used to extract the average cortical thickness and resting state *f*MRI entropy for each cluster and factor-network. Statistical analysis was performed using SPSS software. In our analysis, Gaussian distribution of the data was not confirmed for the cortical thickness and the entropy measures using the Shapiro–Wilk test. Therefore, nonparametric statistics were chosen to compare cortical thickness and entropy levels between patients disconnected, patients spared, and controls in each cluster and factor-network. Additionally, bivariate Spearman rank correlation coefficient analyses were performed between the cortical thickness or entropy measurement of each functional network and each patient's category fluency performance. Correlation significant at $P < 0.0041$ survives Bonferroni correction for multiple comparisons (12 networks).

Results

White matter tracts disconnection

Patients' lesions were compared to an atlas of white matter connections in order to identify the probability of tract disconnections [59]. A Kruskal-Wallis test indicated that for each tract, patients (ie, connected and disconnected) and control participants showed a significantly different performance on the category fluency test (all $P < 0.001$; full statistics reported in Table 2). Between patients, post hoc comparisons revealed that disconnections of the left frontal aslant ($U = 90.0$; $P = 0.0389$), frontal inferior longitudinal ($U = 69.0$; $P = 0.0216$) and frontal superior longitudinal ($U = 75.0$; $P = 0.0352$) tracts, and the anterior ($U = 28.5$; $P = 0.0116$) and long segment ($U = 31.5$; $P = 0.0059$) of the arcuate fasciculus were associated with a poorer performance in category fluency (Fig. 1). However, these post hoc comparisons did not survive Bonferroni-Holm correction for multiple comparisons.

These results indicate that poor performance measured in patients with brain damage can be associated to some extent with white matter tract disconnections.

Direct disconnection of brain areas: structural connectivity network

As different white matter atlases exist for the interpretation of the white matter tract disconnection [85] and atlas-based approaches cannot assess the disconnection of the subportion of tracts nor the involvement of multiple tracts by a lesion, data-driven maps of disconnection or "disconnectomes" were produced. Using tractography in a group of 10 healthy controls, the registered lesions were used as a seed to reveal white matter tracts that passed through the injured area so as to produce maps of disconnections, later referred to as *disconnectome maps*. Category fluency scores were attributed to each patient's *disconnectome map* (see Fig. 2A). A Kruskal-Wallis test indicated that for several clusters, patients (ie., connected and disconnected) and control participants showed a significantly different performance on the category fluency test (all $P < 0.001$; full statistics reported in Table 3).

Results were further statistically assessed using Mann-Whitney post hoc comparisons in order to identify areas that, when deafferented due to a disconnection mechanism, lead to a significant decrease in performance in category fluency when compared to controls.

The following results are Bonferroni-Holm corrected for multiple comparisons. Main cortical areas in the left hemisphere included the pre supplementary motor area (preSMA; cluster size = 1449; Mann Whitney $U = 88.5$; $P = 0.025$), the anterior portion of the intraparietal sulcus (IPs; cluster size = 1143; $U = 18$; $P = 0.030$), anterior cingulate gyrus (cluster size = 837; $U = 304$; $P = 0.025$) and middle cingulate gyrus (cluster size = 898; $U = 95.5$; $P = 0.014$), the middle frontal gyrus (MFg; cluster size = 829; $U = 81.5$; $P = 0.005$), and the pars opercularis of the inferior frontal gyrus (cluster size = 5314; $U = 16$; $P = 0.025$).

In the right hemisphere, the preSMA (cluster size = 1050; $U = 50.5$; $P = 0.014$), the MFg (cluster size = 552; $U = 54$; $P = 0.018$), the anterior cingulate gyrus (cluster size = 572; $U = 44.5$; $P = 0.009$), and the middle cingulate gyrus (cluster size = 817; $U = 317$; $P = 0.041$) were also involved (Fig. 2B).

Subcortical areas in the left hemisphere involved the caudate, the putamen, and several ventral thalamic nuclei including the ventral anterior, the ventrolateral anterior, and the ventrolateral posterior as a part of the same cluster (cluster size = 5314; $U = 16$; $P = 0.025$).

In the right hemisphere, the striatum (cluster size = 527; $U = 310$; $P = 0.031$) and the ventral thalamic nuclei (cluster size = 935; $U = 202.0$; $P = 0.025$) were also involved (Fig. 2B).

Additionally, between-patient (ie, connected and disconnected, uncorrected for multiple comparisons) comparisons confirmed the critical involvement of the preSMA ($U = 212$; $P = 0.0456$), the MFg ($U = 237$; $P = 0.01$), the pars opercularis ($U = 179$; $P = 0.004$), and the IPs ($U = 172$; $P = 0.01$) in the left hemisphere. The preSMA ($U = 208$; $P = 0.01$) and the MFg ($U = 196$; $P = 0.038$) were also involved in the right hemisphere (Fig. 2C). Full statistics are reported in Table 3.

fMRI Meta-analyses

We further examined whether the disconnected areas in patients with poor performance are functionally engaged in tasks related to fluency and categorization using a meta-analysis approach [71, 72].

The result indicates that disconnected areas reported as significantly contributing to category fluency performance in patients are classically activated by functional MRI tasks that require either fluency or categorization in healthy controls (Fig. 3).

Indirect disconnection of brain areas: functional connectivity network

As the *disconnectome mapping* method cannot measure the indirect disconnection produced by a lesion (ie, it fails to measure

Table 2: White matter tracts disconnection relationship with category fluency statistical report

	3 groups comparison		Patients disconnected and connected		Patients disconnected and controls		Patients connected and controls		n1[a]	n2[b]
Tract	K	*P* value	U	*P* value	U	*P* value	U	*P* value		
Cingulum left	19	0.0001	141	0.2035	189	0.0003	277	0.0003	16	21
Cingulum right	19	0.0001	161	0.5	280	0.0001	187	0.0019	23	14
Uncinate left	19	0.0001	148	0.3994	176	0.0027	291	0.0001	13	24
Uncinate right	19	0.0001	167	0.4635	209	0.0004	258	0.0003	17	20
Arcuate anterior segment left	22	0.0000	29	0.0116	12	0.0004	454	0.0001	5	32
Arcuate anterior segment right	19	0.0001	126	0.3855	118	0.0025	348	0.0001	16	21
Arcuate long segment left	23	0.0000	32	0.0059	13	0.0001	453	0.0002	6	31
Arcuate Long segment right	19	0.0001	107	0.2559	117	0.0068	349	0.0001	9	28
Inferior fronto-occipital fasciculus left	19	0.0001	165	0.5	196	0.0011	271	0.0001	15	22
Inferior fronto-occipital fasciculus right	19	0.0001	157	0.3457	199	0.0002	268	0.0004	17	20
Frontal aslant tract left	21	0.0000	90	0.0389	90	0.0001	377	0.0004	11	26
Frontal aslant tract right	19	0.0001	155	0.3131	194	0.0001	272	0.0012	18	19
Frontal inferior longitudinal left	21	0.0000	69	0.0216	54	0.0001	413	0.0004	9	28
Frontal inferior longitudinal right	19	0.0001	140	0.3051	171	0.0022	295	0.0001	13	34
Frontal superior longitudinal left	20	0.0000	75	0.0352	73	0.0004	393	0.0002	9	28
Frontal superior longitudinal right	19	0.0001	129	0.1992	120	0.0001	346	0.0005	13	34

Results are not corrected for multiple comparisons.
[a]Number of disconnected patients.
[b]Number of spared patients.

the disconnection in a region that is not directly anatomically connected to a damaged area but that nonetheless remains a part of the same large network of functionally connected areas), we used functional connectivity in healthy controls. This allowed us to reveal the entire network of regions that are functionally connected to the areas that were reported as contributing significantly to the category fluency performance when directly disconnected. When compared to tractography, functional connectivity has the added advantage of revealing the areas that contribute to the network through both direct and indirect structural connections.

Principal component analysis indicated that the significant areas that contributed to category fluency performance belonged to 3 main functional networks (ie, factor-networks) (Fig. 4), which accounted for more than 80% of the total variance of the functional connectivity results.

The left cingulate clusters (anterior and middle), the right anterior cingulate, the middle frontal gyrus, the thalamus, and the operculum all belonged to the cingulo-opercular network (CO) [86], including the right preSMA, posterior cingulate, and rostral portion of the middle frontal gyrus.

The middle of the cingulate gyrus and the striatum in the right hemisphere both belonged to a cortico-striatal network (CS) [87] that involves the right thalamus and striatum.

Finally, the left MFg, preSMA, IPs, pars opercularis, thalamus, and striatum were all involved in a larger, left ventral fronto-parietal network (VFP), which also included other areas such as the right preSMA, the frontal eye field, and the temporo-parietal junction [88].

Additional analyses revealed the differences in the functional connectivity of these factor-networks relative to the disconnected status of areas involved in category fluency. Between-patient (ie, connected and disconnected) comparisons revealed significantly lower functional connectivity in the left VFP network ($U = 54.0$; $P = 0.006$) and in the CS network ($U = 63.0$; $P = 0.027$) when anatomically disconnected. The CO network, however, did not show any significant difference ($U = 40.0$; $P = 0.213$). Overall, the strength of the functional connectivity for each patient did not correlate significantly with the fluency performance.

Structural changes in disconnected regions

Additional exploratory analyses revealed structural changes related to the disconnections. We estimated these changes using the following 2 complementary measures: T1w-based cortical thickness to identify fine local volumetric changes and the Shannon entropy of rs-*f*MRI as a surrogate for the local complexity of the neural networks [76].

Table 3: Direct disconnection of brain areas relationship with category fluency statistical report

Fluency score		3 groups comparison		Patients disconnected and connected (uncorrected)		Patients disconnected and controls		Patients connected and controls		n1[a]	n2[b]
	Disconnected areas	Kruskal-Wallis	*P* value	U	*P* value	U	*P* value	U	*P* value		
Left hemisphere	PreSMA	21.34128456	0.0059	212	0.0456	88.5	0.0248	377.5	0.0329	12	25
	IPs	23.35102548	0.0023	172	0.0098	18	0.0295	448	0.0324	7	30
	Cingulate ant	18.6697471	0.0125	160.5	0.7452	304	0.0248	162	0.0329	25	12
	Cingulate mid	21.52289636	0.0054	219	0.0464	95.5	0.0141	370.5	0.0329	13	24
	MFg	23.12826675	0.0026	237	0.0103	81.5	0.0054	384.5	0.0329	13	24
	Opercularis, striatum, thalamus	23.99647373	0.0017	179	0.0043	16	0.0249	450	0.0324	7	30
Right hemisphere	PreSMA	22.92724537	0.0028	208	0.0130	50.5	0.0138	415.5	0.0329	10	27
	Cingulate ant	18.8698263	0.0125	185.5	0.6470	225	0.0330	241	0.0329	20	17
	Cingulate mid	18.62681983	0.0125	137.5	0.6966	317	0.0415	149	0.0329	25	12
	MFg	22.06856039	0.0042	196	0.0382	54	0.0180	412	0.0329	10	27
	Striatum	18.604408	0.0125	154.5	0.8966	310	0.0313	156	0.0329	14	23
	Thalamus	19.117101	0.0125	192	0.5326	202	0.0248	264	0.0329	14	23

Unless specified, *P* values are Bonferroni-Holms corrected for multiple comparisons.
Abbreviation: MFg, middle frontal gyrus; SMA, supplementary motor area.
[a]Number of disconnected patients.
[b]Number of connected patients.

When compared to controls, patients showed a reduced cortical thickness in the left pars opercularis (H = 13; $P = 0.0012$), MFg (H = 8; $P = 0.0143$), preSMA (H = 8; $P = 0.0224$), IPs (H = 9; $P = 0.0131$), and right anterior (H = 7; $P = 0.0296$) and middle cingulate gyrus (H = 23; $P = 0.000$). When compared to patients with no disconnection, only the right middle cingulate gyrus survived the Bonferroni-Holm correction for multiple comparisons (U = 67; $P = 0.004$). When compared to controls, disconnected patients showed reduced entropy for all regions (all $P < 0.05$, except for the right middle frontal gyrus). However, when compared to patients with no disconnection, none of the comparisons survived the Bonferroni-Holm correction for multiple comparisons. Uncorrected *P* values are reported as an indication in Table 4 and the bar chart in Supplementary Fig. S3.

None of these measures correlated significantly with the fluency performance.

In order to further assess the integrity of the whole network of regions that were functionally connected to the areas reported as having significantly contributed to category fluency performance, we also extracted the cortical thickness and entropy from the regions that were functionally connected to the disconnected areas. Correlation analyses indicated that a thinner cortex in the ventral fronto-parietal network seeded from the left MFg (Spearman Rho = .464 ± 0.341; $P = .004$), IPs (Rho = .475 ± 0.341; $P = .003$), and left pars opercularis/striatum/thalamus (Rho = .512 ± 0.341; $P = .001$) corresponded to a reduced performance in category fluency (Fig. 5). Additionally, a thinner cortical thickness in the left preSMA functional network (Rho = .376 ± 0.341; $P = .024$) and a higher rs-*f*MRI entropy (Rho = −.420 ± 0.370; $P = .019$) in the mid cingulate gyrus functional network were associated with poorer performance in category fluency. These last 2 results, however, did not survive Bonferroni-Holm correction for multiple comparisons.

The same analyses were repeated controlling for age and lesion size and confirmed the results for the ventral fronto-parietal network seeded from the left MFg (Spearman Rho = .423; $P = .01$), IPs (Rho = .538; $P = .001$), and left opercularis (Rho = .590 ± 0.341; $P < .001$) and corresponded to a reduced performance in category fluency (Fig. 5). Additionally, a thinner cortical thickness in the left preSMA functional network (Rho = .439; $P = .007$) and a higher rs-*f*MRI entropy (Rho = −.420 ± 0.370; $P = .019$) in the mid cingulate gyrus functional network were associated with poorer performance in category fluency.

Discussion

A large set of complementary methods can capture the impact of lesions on distant regions and expose the subsequent consequences on patients' neuropsychological performance. Several of these methods are built directly into our freely available software package *BCBtoolkit*. This package can be used to measure the pathophysiological mechanisms that cause cognitive deficits and to assess the relationship between these mechanisms and their consequential effects. Here, we evaluated the risk of disconnection of classically defined white matter tracts and tested their relationship with category fluency performance. We then used a tractography-based approach to reveal regions that were structurally disconnected by the lesion and to assess their relationship with category fluency performance as compared to controls and other patients. Functional connectivity from the disconnected regions revealed large networks of interconnected areas. Within these regions/networks, measures of cortical thickness and entropy of the rs-*f*MRI images were correlated to fluency performance, suggesting that some structural changes that occurred within these networks were due to the remote effect of a lesion that led to cognitive impairments. Consequently, the *BCBtoolkit* provided investigators with an ability to quantify the effect of brain damage on the whole brain and to explore its relationship to behavioral and cognitive abilities.

The investigation into the contribution of white matter tract disconnection is an approach that is more than a century old and postulates an interruption in the course of white matter tracts in single case patients [89, 90]. Our method provides an anatomical rationale and puts forth a statistical methodology that enables it to be extended to group-level studies. In the case of category fluency performance, this analysis particularly revealed a significant involvement of the anterior and long segments of the arcuate fasciculus, which are implicated in the language network [90–92]. However, these tracts have been defined, for convenience, by their shape (eg, uncinate for hook-shaped connections and arcuate for arched-shaped connections) and should not be considered as a single unit, as, ultimately, subportions could contribute differently to the elaboration of the cognition and behavior.

Data-driven maps of disconnection, or *disconnectomes*, were consequently produced in order to identify the subportion of disconnected tracts and reveal the pattern of cortico-subcortical areas that were disconnected by the lesion. For the first time, we exemplify that this method goes beyond assessing only lesions and can be used to assess the relationship between disconnected areas and the patient's neuropsychological performance. Here, this approach revealed that category fluency performance significantly decreased when several cortical and subcortical clusters were directly disconnected. The observed areas are consistent with previous lesion studies on fluency tasks [93]. Furthermore, each area identified as significantly involved in this analysis corresponded, almost systematically, to activation loci derived from *f*MRI studies in healthy controls who performed fluency and/or categorization tasks. This result suggests that the method appropriately identified altered functional networks that contribute to the category fluency test. Nonetheless, one might argue that a cascade of polysynaptic events can influence behavior and that dysfunctional, disconnected areas will also impact other indirectly connected areas.

In order to explore this additional dimension, we calculated the functional connectivity of the previously identified disconnected regions (ie, clusters). In the case of the present analysis on category fluency performance, we revealed that the disconnected areas belonged to the following 3 large functional networks (ie, factor-networks): a left-dominant ventral fronto-parietal network; a mirror of the right-lateralized ventral attention network [94], which links key language territories [88] and is associated with executive functions [95, 96]. In addition, we showed the involvement of the cingulo-opercular network, a network that interacts with the fronto-parietal control network for the control of goal-directed behaviors [97], which together with the cortico-striatal network may also be linked to a reduced performance in fluency tasks [98]. The cingulo-opercular and cortico-striatal networks may also have contributed to performance through the global inertia or the ability of participants to allocate and coordinate resources during the task [99]. Finally, disconnection was associated with a significant reduction of functional connectivity in 2 of the 3 factor-networks investigated. This is an important result, as functional connectivity appeared to be less significantly impaired in bilateral networks, suggesting that the proportion of the preserved functional net-

Table 4: Cortical thickness and functional magnetic resonance imaging entropy measures in disconnected areas

Cortical thickness		3 groups comparison		Patients disconnected and connected		Patients disconnected and controls		Patients connected and controls		n1[a]	n2[b]
	Disconnected areas	Kruskal-Wallis	*P* value	U	*P* value	U	*P* value	U	*P* value		
Left hemisphere	PreSMA	8	0.0224	109	0.0944	168	0.0057	514	0.0565	12	25
	IPs	9	0.0131	54	0.0251	59	0.0019	667	0.1134	7	30
	Cingulate ant	5	0.0822	110	0.1000	465	0.0175	269	0.2061	25	12
	Cingulate mid	5	0.0759	139	0.2998	278	0.1436	435	0.0137	13	24
	MFg	8	0.0143	109	0.0695	172	0.0028	502	0.0710	13	24
	Opercularis	13	0.0012	40	0.0061	44	0.0006	583	0.0225	7	30
Right hemisphere	PreSMA	4	0.1328	134	0.4931	214	0.1711	523	0.0254	10	27
	Cingulate ant	7	0.0296	167	0.4696	362	0.0191	295	0.0169	20	17
	Cingulate mid	23	0.0000	61	0.0020	223	0.1414	254	0.1415	25	12
	MFg	6	0.0587	116	0.2634	163	0.0359	538	0.0359	10	27
Shannon entropy											
Left hemisphere	PreSMA	24	0.0000	86	0.2171	85	0.0004	210	0.0000	12	25
	IPs	27	0.0000	40	0.0422	18	0.0002	260	0.0000	7	30
	Cingulate ant	44	0.0000	84	0.1158	109	0.0000	3	0.0000	25	12
	Cingulate mid	36	0.0000	97	0.3029	45	0.0000	127	0.0000	13	24
	MFg	16	0.0004	100	0.4246	125	0.0043	272	0.0003	13	24
	Opercularis, striatum, thalamus	17	0.0002	65	0.3680	75	0.0181	287	0.0001	7	30
Right hemisphere	PreSMA	8	0.0177	82	0.2364	117	0.0078	413	0.0243	10	27
	Cingulate ant	55	0.0000	81	0.0640	16	0.0000	4	0.0000	20	17
	Cingulate mid	22	0.0000	111	0.4596	203	0.0001	114	0.0003	25	12
	MFg	22	0.0000	55	0.0497	136	0.0533	209	0.0000	10	27
	Striatum	23	0.0000	110	0.4436	202	0.0001	100	0.0001	14	23
	Thalamus	58	0.0000	67	0.0204	0	0.0000	6	0.0000	14	23

Results are not corrected for multiple comparisons.

Abbreviation: IPs, intraparietal sulcus; MFg, middle frontal gyrus; SMA, supplementary motor area.

[a]Number of disconnected patients.

[b]Number of spared patients.

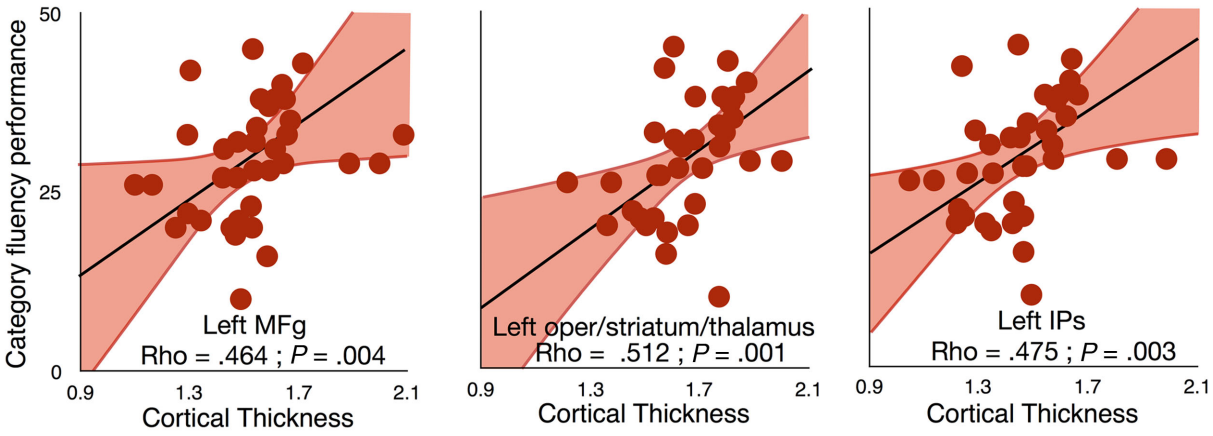

Figure 5: Dimensional relationship between cortical thickness measured in rs-fMRI disconnected networks and category fluency. Note that regression lines (in black) and intervals (mean confidence intervals in red) are for illustrative purposes since we performed a rank-order correlation. Abbreviations: IPs, intraparietal sulcus; MFg, middle frontal gyrus.

work in both of the intact hemispheres may contribute to the strength of functional connectivity.

Changes in connectivity should induce changes in the microstructure of the areas of projection and provoke cognitive or behavioural consequences. Measures of the cortical thickness revealed a significant thinning for some, but not all, directly disconnected areas. This result may reflect a potential transneuronal degeneration mechanism [42]. However, current limitations in spatial resolution and MRI signal might have biased this measure in some regions due to changes in myelination in the lower layers of the cortex [100]. Cortical thickness analyses revealed that the left dominant ventral fronto-parietal network, whether it is seeded from MFg, IPs, or subcortical structures in the left hemisphere, had a reduced cortical thickness associated with the category fluency performance. This result indicates a strong and encouraging relationship between the integrity of a network derived from measures of cortical thickness and behavioral performances. Future research can benefit from this approach to stratify patient populations and predict potential recovery.

Additionally, we explored whether structural changes such as other neural (eg, synaptic plasticity) or nonneural factors (eg, altered properties of the vasculature) could also be captured by measures of rs-*f*MRI entropy. Our results replicated recently published results that showed a strong decrease of entropy in both hemispheres when patients were compared to controls [101]. This indicates a large-scale effect of brain lesion on the overall BOLD dynamic of the brain. Finally, the result between patients (connected and disconnected) did not survive the correction for multiple comparisons, suggesting that, although promising, Shannon entropy measures of BOLD may be too noisy of a measure to capture very fine microstructural events with high enough statistical power.

Previous reports indicated that *AnaCOM* suffers from lower specificity than VLSM (Rorden et al. [102]. *AnaCOM* compares performance of patients with that of controls, an approach that has previously been criticized [102]. In the context of our study, classic VLSM did not reveal any significant area involved with category fluency. In classic VLSM approaches, nonoverlapping lesions are competing for statistical significance, fundamentally assuming that a single region is responsible for the symptoms. In the present study, we followed Associationist principles [19, 18], assuming that several interconnected regions will contribute to the elaboration of the behavior. By comparing the performance between patients and a control population using *AnaCOM2*, several nonoverlapping regions can reach significance without competing for it. Hence, our results differ theoretically and methodologically from previous approaches. Perhaps more importantly, the network of disconnected areas revealed by *AnaCOM2* is typically considered as functionally engaged during fluency and categorization tasks in healthy controls.

Newer multivariate methods have also been shown to provide superior performance compared to traditional VLSM (ie, support vector regression lesion-symptom mapping) [7, 103]. For instance, such approaches have been used to model the statistical relationship between damaged voxels in order to reduce false positives. In the *disconnectome maps*, this relationship has been preestablished using an anatomical prior derived from tractography in healthy controls. Therefore, it is not recommended to use multivariate approaches with the *disconnectome maps*, as they might come into conflict with the prebuilt anatomical association between the voxels. Additionally, these approaches require a much larger database of patients than the current study. Future research that uses large lesion databases will be required to explore the effect of multivariate statistical analysis on *disconnectome maps*.

Multivariate approaches also elegantly demonstrated that false positives can be driven by the vascular architecture [7]. This is an important limitation concerning any voxel and vascular lesion symptom mapping. Here, the group of patients explored had stroke and surgical lesions. Although we cannot exclude the participation of the vascular architecture in the present findings, the heterogeneity of the lesions included in our analyses may have limited this factor. Additionally, the statistical interaction between vascular architecture and the *disconnectome map* results remain to be explored in large databases of lesions.

Methods used to estimate cortical thickness have previously been reported to perform poorly in peri-infarct regions, and the quality of the tissue segmentation may be particularly poor for stroke patients [79]. Here, we followed previously published recommendations for applying DiReCT [77] to the data from stroke patients; the lesion was masked out, the tissue segmentations

were visually inspected, and manual boundary correction was performed when necessary (see Supplementary Fig. S2 for an example).

Finally, we applied our methods to the neural basis of category fluency as a proof of concept. The anatomy of category fluency should be, ideally, replicated in a larger sample of patients that includes adequate lesion coverage of the entire brain to provide a more comprehensive understanding of category fluency deficit after a brain lesion. While gathering such a large dataset of patients with brain lesions would have been impossible to achieve before, it might soon become possible thanks to collaborative initiatives such as the Enigma Consortium stroke recovery initiative [104, 105].

Conclusion

Overall, using *BCBtoolkit*, researchers and clinicians can measure distant effects of brain lesions and associate these effects with neuropsychological outcomes. However, our methods require the manual delineation of lesion masks, automatization remaining a big challenge, especially on T1 images [105]. Taken together, these neuroimaging measures help discern the natural history of events that occur in the brain after a lesion, as well as assist in the localization of functions. These methods, gathered in the *BCBtoolkit*, are freely available as supplementary software [1, 107].

Availability of supporting data

Patients' lesions registered to the reference map MNI152 are available as supplementary material via the BCBlab website [106] and via the GigaScience database GigaDB [107]. However, we are not able to fully share the actual clinical sample data because sharing of the clinical raw data is not covered by the participants' consent. A copy of the consent form as signed by the participants is available via GigaDB.

Availability of supporting source code and requirements

- Project name: BCBtoolkit
- Project home page: http://toolkit.bcblab.com
- Operating system(s): Linux, MacOS
- Programming language: Java, Bash, R
- Other requirements: FSL, R, Python 2.7, Numpy
- License: BSD 3-Clause

An archival copy of the supporting source code is also available via GigaDB [107].

Additional material

Figure S1: Step by step, hypotheses-driven analyses with BCBtoolkit.

Figure S2: Native T1, enantiomorphic deformation and derived cortical thickness of 3 representative patients.

Figure S3: Cortical thickness and Shannon entropy measures (mean with 95% confidence intervals) in patients with (dark gray) or without (light gray) disconnection for each of the disconnected areas. The green interval indicates performance in matched controls with 95% confidence intervals.

Competing interests

The authors declare that they have no competing interests.

Author contributions

C.F. implemented the methods inside the *BCBtoolkit*, performed the analyses, and wrote the manuscript. L.C. created the pipeline for the preprocessing of the resting state and for the functional correlation and revised the manuscript. S.K. conceived and helped to upgrade the statistical analyses. C.R. collected the neuroimaging data. M.U. and E.V recruited the participants; collected and built the database of patients; matched healthy controls, including the neuropsychological and neuroimaging data; and revised the manuscript. E.V. also participated in the conception of the lesion study and provided funding for the database acquisition. R.L. provided funding for the study and revised the manuscript. M.T.d.S. wrote the manuscript, provided funding, conceived and coordinated the study, and reviewed and collected neuroimaging data.

Acknowledgments

We thank Lauren Sakuma, Roberto Toro, Jean Daunizeau, Emmanuel Mandonnet, Beatrice Garcin, Stephanie J. Forkel, and the BCBlab and Brainhack for useful discussions. We also thank Mozilla spaces for their support, the participants of this study as well as Prof. Claude Adam, Dr. Carole Azuar, Dr. Marie-Laure Bréchemier, Dr. Dorian Chauvet, Dr. Frédéric Clarençon, Dr. Vincent Degos, Prof. Sophie Dupont, Prof. Damien Galanaud, Dr. Béatrice Garcin, Dr. Florence Laigle, Dr. Marc-Antoine Labeyrie, Dr. Anne Leger, Prof. Vincent Navarro, Prof. Pascale Pradat-Diehl, and Prof. Michel Wager for their help in recruiting the patients. The research leading to these results was funded by the Agence Nationale de la Recherche (grants ANR-09-RPDOC-004-01 and ANR-13- JSV4-0001-01) and from the Fondation pour la Recherche Médicale. Additional financial support was provided by the program Investissements d'avenir (ANR-10-IAIHU-06).

References

1. Brain Connectivity Behaviour Toolkit (BCBtoolkit), http://toolkit.bcblab.com/.
2. Jones DK, Simmons A, Williams SC et al. Non-invasive assessment of axonal fiber connectivity in the human brain via diffusion tensor MRI. Magn Reson Med 1999;**42**(1):37–41.
3. Logothetis N. What we can do and what we cannot do with fMRI. Nature 2008;**453**(7197):869–78.
4. Broca P. Perte de la parole, ramollissement chronique et destruction partielle du lobe antérieur gauche du cerveau. Bull Soc Anthropol 1861;**2**:235–8, 301–321.
5. Damasio H, Damasio A. Lesion analysis in Neuropsychology, ed. O.U. Press, New York, 1989.
6. Rorden C, Karnath HO, Bonilha L. Improving lesion-symptom mapping. J Cogn Neurosci 2007;**19**(7): 1081–8.
7. Mah YH, Husain M, Rees G et al. Human brain lesion-deficit inference remapped. Brain 2014;**137**(9):2522–31.
8. Bates E, Wilson SM, Saygin AP et al. Voxel-based lesion-symptom mapping. Nat Neurosci 2003;**6**(5):448–50.
9. Dronkers NF, Wilkins DP, Van Valin RD, Jr et al. Lesion analysis of the brain areas involved in language comprehension. Cognition 2004;**92**(1-2):145–77.

10. Karnath HO, Ferber S, Himmelbach M. Spatial awareness is a function of the temporal not the posterior parietal lobe. Nature 2001;**411**(6840):950–3.
11. Bird CM, Malhotra P, Parton A et al. Visual neglect after right posterior cerebral artery infarction. Journal of Neurology, Neurosurgery & Psychiatry 2006;**77**(9):1008–12.
12. Husain M, Kennard C. Visual neglect associated with frontal lobe infarction. J Neurol 1996;**243**(9):652–7.
13. Mort DJ, Malhotra P, Mannan SK et al. The anatomy of visual neglect. Brain 2003;**126**(9):1986–97.
14. Coulthard EJ, Nachev P, Husain M. Control over conflict during movement preparation: role of posterior parietal cortex. Neuron 2008;**58**(1):144–57.
15. Volle E, Kinkingnéhun S, Pochon JB et al. The functional architecture of the left posterior and lateral prefrontal cortex in humans. Cereb Cortex 2008;**18**(10):2460–9.
16. Volle E, Levy R, Burgess PW. A new era for lesion-behavior mapping of prefrontal functions, in Principles of Frontal Lobe Function, Stuss DT, Knight RT, Eds. 2013, p. 500–23.
17. Badre D, Hoffman J, Cooney JW et al. Hierarchical cognitive control deficits following damage to the human frontal lobe. Nat Neurosci 2009;**12**(4):515–22.
18. Geschwind N. Disconnexion syndromes in animals and man - Part I. Brain 1965;**88**(2):237–94.
19. Geschwind N. Disconnexion syndromes in animals and man - Part II. Brain 1965;**88**(3):585–644.
20. Carrera E, Tononi G. Diaschisis: past, present, future. Brain 2014;**137**(9):2408–22.
21. Finger S, Koehler PJ, Jagella C. The Monakow concept of diaschisis. Arch Neurol 2004;**61**(2):283–8.
22. Corbetta M, Kincade MJ, Lewis C et al. Neural basis and recovery of spatial attention deficits in spatial neglect. Nat Neurosci 2005;**8**(11):1603–10.
23. Thiebaut de Schotten M, Tomaiuolo F, Aiello M et al. Damage to white matter pathways in subacute and chronic spatial neglect: a group study and 2 single-case studies with complete virtual "in vivo" tractography dissection. Cereb Cortex 2014;**24**(3):691–706.
24. Thiebaut de Schotten M, Kinkingnéhun S, Delmaire C et al. Visualization of disconnection syndromes in humans. Cortex 2008;**44**(8):1097–103.
25. Urbanski M, Bréchemier ML, Garcin B et al. Reasoning by analogy requires the left frontal pole: lesion-deficit mapping and clinical implications. Brain 2016;**139**(6):1783–99.
26. Cazzoli D, Hopfner S, Preisig B et al. The influence of naturalistic, directionally non-specific motion on the spatial deployment of visual attention in right-hemispheric stroke. Neuropsychologia 2016;**92**:181–9.
27. Piai V, Meyer L, Dronkers NF et al. Neuroplasticity of language in left-hemisphere stroke: evidence linking subsecond electrophysiology and structural connections. Hum Brain Mapp 2017;**38**(6):3151–3162.
28. Rudrauf D, Mehta S, Grabowski TJ. Disconnection's renaissance takes shape: formal incorporation in group-level lesion studies. Cortex 2008;**44**(8):1084–96.
29. Fridriksson J, Dazhou G, Paul F et al. Damage to the anterior arcuate fasciculus predicts non-fluent speech production in aphasia. Brain 2013;**136**(11):3451–60.
30. Hope TM, Seghier ML, Prejawa S et al. Distinguishing the effect of lesion load from tract disconnection in the arcuate and uncinate fasciculi. Neuroimage 2016;**125**:1169–73.
31. Corbetta M, Ramsey L, Callejas A et al. Common behavioral clusters and subcortical anatomy in stroke. Neuron 2015;**85**(5):927–41.
32. Griffis JC, Nenert R, Allendorfer JB et al. Damage to white matter bottlenecks contributes to language impairments after left hemispheric stroke. NeuroImage: Clinical 2017;**14**:552–65.
33. He BJ, Snyder AZ, Vincent JL et al. Breakdown of functional connectivity in frontoparietal networks underlies behavioral deficits in spatial neglect. Neuron 2007;**53**(6):905–18.
34. Turken AU, Dronkers NF. The neural architecture of the language comprehension network: converging evidence from lesion and connectivity analyses. Front Syst Neurosci 2011;**5**:1.
35. Bonilha L, Jensen JH, Baker N et al. The brain connectome as a personalized biomarker of seizure outcomes after temporal lobectomy. Neurology 2015;**84**(18):1846–53.
36. Thiebaut de Schotten M, Dell'Acqua F, Ratiu P et al. From Phineas Gage and Monsieur Leborgne to H.M.: revisiting disconnection syndromes. Cereb Cortex 2015;**25**(12):4812–27.
37. Kuceyeski A, Navi BB, Kamel H et al. Structural connectome disruption at baseline predicts 6-months post-stroke outcome. Hum Brain Mapp 2016;**37**(7):2587–601.
38. Yourganov G, Fridriksson J, Rorden C et al. Multivariate connectome-based symptom mapping in post-stroke patients: networks supporting language and speech. J Neurosci 2016;**36**(25):6668–79.
39. Kuceyeski A, Maruta J, Relkin N et al. The Network Modification (NeMo) Tool: elucidating the effect of white matter integrity changes on cortical and subcortical structural connectivity. Brain Connectivity 2013;**3**(5):451–63.
40. Boes AD, Prasad S, Liu H et al. Network localization of neurological symptoms from focal brain lesions. Brain 2015;**138**(10):3061–75.
41. Munafo M. Metascience: reproducibility blues. Nature 2017;**543**(7647):619–20.
42. Fornito A, Zalesky A, Breakspear M. The connectomics of brain disorders. Nat Rev Neurosci 2015;**16**(3):159–72.
43. Feeney DM, Baron JC. Diaschisis. Stroke 1986;**17**(5):817–30.
44. Cowan W. *Contemporary Research Methods in Neuroanatomy*. Springer, 1970.
45. Bredesen DE. Neural apoptosis. Ann Neurol 1995;**38**(6):839–51.
46. Capurso SA, Calhoun ME, Sukhov RR et al. Deafferentation causes apoptosis in cortical sensory neurons in the adult rat. J Neurosci 1997;**17**(19):7372–84.
47. Schaechter JD, Moore CI, Connell BD et al. Structural and functional plasticity in the somatosensory cortex of chronic stroke patients. Brain 2006;**129**(10):2722–33.
48. Xing S, Lacey EH, Skipper-Kallal LM et al. Right hemisphere grey matter structure and language outcomes in chronic left hemisphere stroke. Brain 2016;**139**(1):227–41.
49. Gladsjo JA, Schuman CC, Evans JD et al. Norms for letter and category fluency: demographic corrections for age, education, and ethnicity. Assessment 1999;**6**(2):147–78.
50. MacPherson SE, Della Sala S. Handbook of Frontal Lobe Assessment. Oxford: Oxford University Press, 2015.
51. Lezak M. Neuropsychological Assessment. Oxford: Oxford University Press, 1995.
52. Jones DK, Griffin LD, Alexander DC et al. Spatial normalization and averaging of diffusion tensor MRI data sets. Neuroimage 2002;**17**(2):592–617.
53. Brett M, Leff AP, Rorden C et al. Spatial normalization of brain images with focal lesions using cost function masking. Neuroimage 2001;**14**(2):486–500.

54. Nachev P, Coulthard E, Jäger HR et al. Enantiomorphic normalization of focally lesioned brains. Neuroimage 2008;**39**(3):1215–26.
55. http://fsl.fmrib.ox.ac.uk.
56. Zhang Y, Brady M, Smith SM. segmentation of brain MR images through a hidden Markov random field model and the expectation-maximization algorithm. IEEE Trans Med Imaging 2001;**20** 1:45–57.
57. Smith SM. Fast robust automated brain extraction. Hum Brain Mapp 2002;**17**(3):143–55.
58. Avants BB, Tustison NJ, Song G et al. A reproducible evaluation of ANTs similarity metric performance in brain image registration. Neuroimage 2011;**54**(3):2033–44.
59. Rojkova K, Volle E, Urbanski M et al. Atlasing the frontal lobe connections and their variability due to age and education: a spherical deconvolution tractography study. Brain Struct Funct 2016;**221**(3):1751–66.
60. Catani M, Dell'acqua F, Vergani F et al. Short frontal lobe connections of the human brain. Cortex 2012;**48**(2): 273–91.
61. Von Der Heide RJ, Skipper LM, Klobusicky E et al. Dissecting the uncinate fasciculus: disorders, controversies and a hypothesis. Brain 2013;**136**(6):1692–707.
62. Duffau H, Gatignol P, Mandonnet E et al. New insights into the anatomo-functional connectivity of the semantic system: a study using cortico-subcortical electrostimulations. Brain 2005;**128**(4):797–810.
63. Catani M, Jones DK, Ffytche DH. Perisylvian language networks of the human brain. Ann Neurol 2005;**57**(1):8–16.
64. Catani M, Bambini V. A model for social communication and language evolution and development (SCALED). Curr Opin Neurobiol 2014;**28**:165–71.
65. Thiebaut de Schotten M, Dell'Acqua F, Forkel SJ et al. A lateralized brain network for visuospatial attention. Nat Neurosci 2011;**14**(10):1245–6.
66. *Trackvis*, http://trackvis.org/.
67. Ciccarelli O, Toosy AT, Parker GJ et al. Diffusion tractography based group mapping of major white-matter pathways in the human brain. Neuroimage 2003;**19**(4):1545–55.
68. Thiebaut de Schotten M, Ffytche DH, Bizzi A et al. Atlasing location, asymmetry and inter-subject variability of white matter tracts in the human brain with MR diffusion tractography. Neuroimage 2011;**54**(1):49–59.
69. Kinkingnehun S, Volle E, Pélégrini-Issac M et al. A novel approach to clinical-radiological correlations: Anatomo-Clinical Overlapping Maps (AnaCOM): Method and validation. Neuroimage 2007;**37**(4):1237–49.
70. *R Core Team 2016*, https://www.r-project.org/.
71. Yarkoni T, Poldrack RA, Nichols TE et al. Large-scale automated synthesis of human functional neuroimaging data. Nat Methods 2011;**8**(8):665–70.
72. *Neurosynth*, http://neurosynth.org/.
73. Jenkinson M, Bannister P, Brady M et al. Improved optimization for the robust and accurate linear registration and motion correction of brain images. Neuroimage 2002;**17**(2): 825–41.
74. Woolrich MW, Jbabdi S, Patenaude B et al. Bayesian analysis of neuroimaging data in FSL. Neuroimage 2009;**45**(1): S173–86.
75. Kenney J. Mathematics of Statistics. London: Chapman & Hall, 1939.
76. Tononi G, Edelman GM, Sporns O. Complexity and coherency: integrating information in the brain. Trends Cogn Sci 1998;**2**(12):474–84.
77. Das SR, Avants BB, Grossman M et al. Registration based cortical thickness measurement. Neuroimage 2009;**45**(3):867–79.
78. Tustison NJ, Cook PA, Klein A et al. Large-scale evaluation of ANTs and FreeSurfer cortical thickness measurements. Neuroimage 2014;**99**:166–79.
79. Li Q, Pardoe H, Lichter R et al. Cortical thickness estimation in longitudinal stroke studies: a comparison of 3 measurement methods. NeuroImage: Clinical 2015;**8**:526–35.
80. Shannon CE. The mathematical theory of communication. 1963; MD Comput, 1997;**14**(4):306–17.
81. Gray R. Entropy and Information Theory. Springer US, 2011.
82. Ogawa S, Lee TM, Kay AR et al. Brain magnetic resonance imaging with contrast dependent on blood oxygenation.. Proc Natl Acad Sci 1990;**87**(24):9868–72.
83. Biswal B, Yetkin FZ, Haughton VM et al. Functional connectivity in the motor cortex of resting human brain using echo-planar MRI. Magn Reson Med 1995;**34**(4):537–41.
84. Hebb DO. The Organization of Behavior: A Neuropsychological Theory. New York: Wiley and Sons, 1949.
85. de Haan B, Karnath HO. 'Whose atlas I use, his song I sing?' - The impact of anatomical atlases on fiber tract contributions to cognitive deficits after stroke. Neuroimage 2017;**163**:301–9.
86. Sadaghiani S, D'Esposito M. Functional characterization of the cingulo-opercular network in the maintenance of tonic alertness. Cereb Cortex 2015;**25**(9):2763–73.
87. Voorn P, Vanderschuren LJ, Groenewegen HJ et al. Putting a spin on the dorsal-ventral divide of the striatum. Trends Neurosci 2004;**27**(8):468–74.
88. Smith SM, Fox PT, Miller KL et al. Correspondence of the brain's functional architecture during activation and rest. Proc Natl Acad Sci 2009;**106**(31):13040–5.
89. Lichtheim L. On aphasia. Brain 1885;**7** 4:433–84.
90. Catani M, Ffytche DH. The rises and falls of disconnection syndromes. Brain 2005;**128**(10):2224–39.
91. Dronkers NF, Plaisant O, Iba-Zizen MT et al. Paul Broca's historic cases: high resolution MR imaging of the brains of Leborgne and Lelong. Brain 2007;**130**(5):1432–41.
92. Forkel SJ, Thiebaut de Schotten M, Dell'Acqua F et al. Anatomical predictors of aphasia recovery: a tractography study of bilateral perisylvian language networks. Brain 2014;**137**(7):2027–39.
93. MacPherson SE, Sala SD. Handbook of Frontal Lobe Assessment. Oxford: Oxford University Press, 2015.
94. Fox MD, Corbetta M, Snyder AZ et al. Spontaneous neuronal activity distinguishes human dorsal and ventral attention systems. Proc Natl Acad Sci 2006;**103**(26):10046–51.
95. Parlatini V, Radua J, Dell'Acqua F et al. Functional segregation and integration within fronto-parietal networks. Neuroimage 2017;**146**:367–75.
96. Power JD, Petersen SE. Control-related systems in the human brain. Curr Opin Neurobiol 2013;**23**(2):223–8.
97. Gratton C, Neta M, Sun H et al. Distinct stages of moment-to-moment processing in the cinguloopercular and frontoparietal networks. Cereb Cortex 2016.
98. Chouiter L, Holmberg J, Manuel AL et al. Partly segregated cortico-subcortical pathways support phonologic and semantic verbal fluency: A lesion study. Neuroscience 2016;**329**:275–83.

99. Bonnelle V, Ham TE, Leech R et al. Salience network integrity predicts default mode network function after traumatic brain injury. Proc Natl Acad Sci 2012;**109**(12): 4690–5.
100. Wagstyl K, Ronana L, Goodyer IM et al. Cortical thickness gradients in structural hierarchies. Neuroimage 2015;**111**:241–50.
101. Saenger VM, Ponce-Alvarez A, Adhikari M et al. Linking entropy at rest with the underlying structural connectivity in the healthy and lesioned brain. Cereb Cortex 2017;(in press)(2017).
102. Rorden C, Fridriksson J, Karnath HO. An evaluation of traditional and novel tools for lesion behavior mapping. Neuroimage 2009;**44**(4):1355–62.
103. Zhang Y, Kimberg DY, Coslett HB et al. Multivariate lesion-symptom mapping using support vector regression. Hum Brain Mapp 2014;**35**(12):5861–76.
104. http://enigma.ini.usc.edu/ongoing/enigma-stroke-recovery/.
105. Liew S-L et al. A large, open source dataset of stroke anatomical brain images and manual lesion segmentations. bioRxiv 179614; doi: https://doi.org/10.1101/179614 2017.
106. *Open Database Brain Connectivity Behaviour Laboratory (BCBlab)*, http://opendata.bcblab.com/.
107. Foulon C, Cerliani L, Kinkingnéhun S et al. Supporting data for "advanced lesion symptom mapping analyses and implementation as BCBtoolkit". GigaScience Database 2018; http://dx.doi.org/10.5524/100399.

Advanced lesion symptom mapping analyses and implementation as BCBtoolkit

Supplementary material

Foulon C[a,b,c*], Cerliani L[a,b,c], Kinkingnéhun S[a], Levy R[b], Rosso C[c,d], Urbanski M[a,b,e], Volle E[a,b,c], Thiebaut de Schotten M[a,b,c*]

[a] Brain Connectivity and Behaviour Group, Brain and Spine Institute, Paris France.

[b] Frontlab, Institut du Cerveau et de la Moelle épinière (ICM), UPMC UMRS 1127, Inserm U 1127, CNRS UMR 7225, Paris, France.

[c] Centre de Neuroimagerie de Recherche CENIR, Groupe Hospitalier Pitié-Salpêtrière, Paris, France.

[d] APHP, Urgences Cérébro-Vasculaires, Groupe Hospitalier Pitié-Salpêtrière, Paris, France.

[e] Medicine and Rehabilitation Department, Hôpitaux de Saint-Maurice, Saint-Maurice, France.

* Corresponding authors hd.chrisfoulon@gmail.com and michel.thiebaut@gmail.com

Competing interests:

The authors declare that they have no competing interests

The optimal number of participants was calculated for *disconnectome maps* from separate paired populations of equal gender distribution. This approach was repeated for groups consisting of 4, 6, 8, 10, 12, 14, 16, 18 and 20 subjects. Squared spatial Pearson's correlations between each pair (i.e. square of fslcc from FSL) were employed to calculate the percentage of shared variance (i.e. the similarity). This analysis indicates a steep increase of shared variance between disconnectome maps produced from 4 to 10 participants followed by a slower increase from 10 to 20 participants. This result indicates that, using the disconnectome, 10 subjects are sufficient to produce a good enough disconnectome map that matches the overall population (above 70% of shared variance). A larger dataset (n = 36) can be downloaded on our website (http://www.bcblab.com/opendata). Additionally, HCP 7T data (n = 166) have been prepared for the disconnectome and are available on demand to the authors (hd.chrisfoulon@gmail.com or michel.thiebaut@gmail.com).

We also measured whether the shape of the disconnectome changes over age. We assessed this question by producing disconnectome maps for each decade. We quantified similarities using squared spatial Pearson's for the 21-30-year-old maps and the maps for the other decades. The result indicates that disconnectome maps show a very high anatomical similarity between decades. Hence disconnectome maps in our sample did not show any age-related changes.

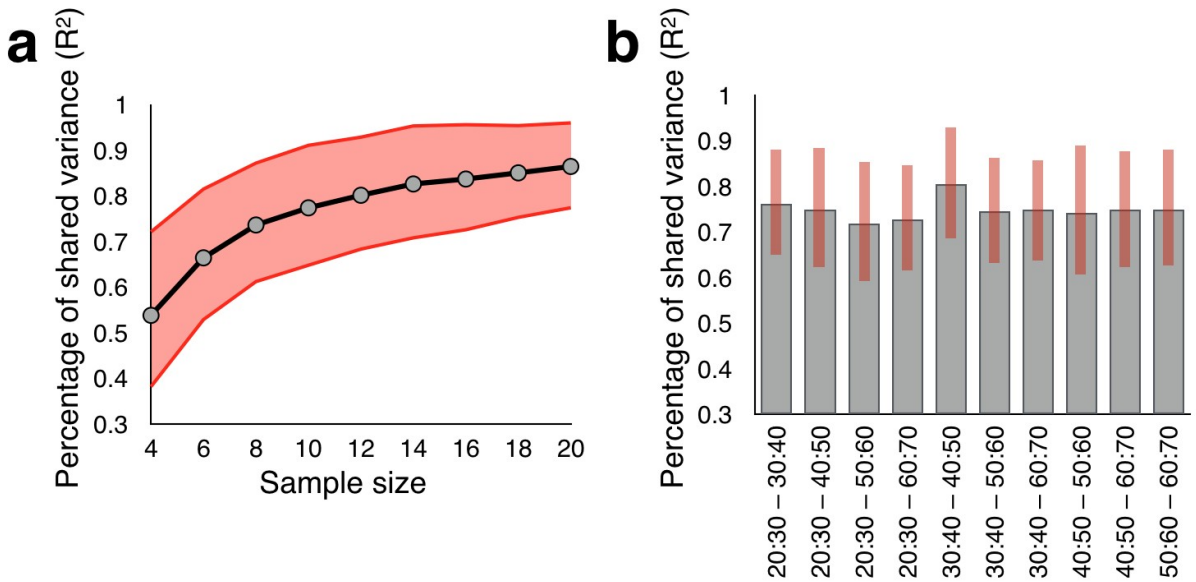

Disconnectome maps optimisation. a) Percentage of shared variance according to sample size. Red areas indicate standard deviations b) Cross-correlation between decades. Red bars indicate standard deviations.

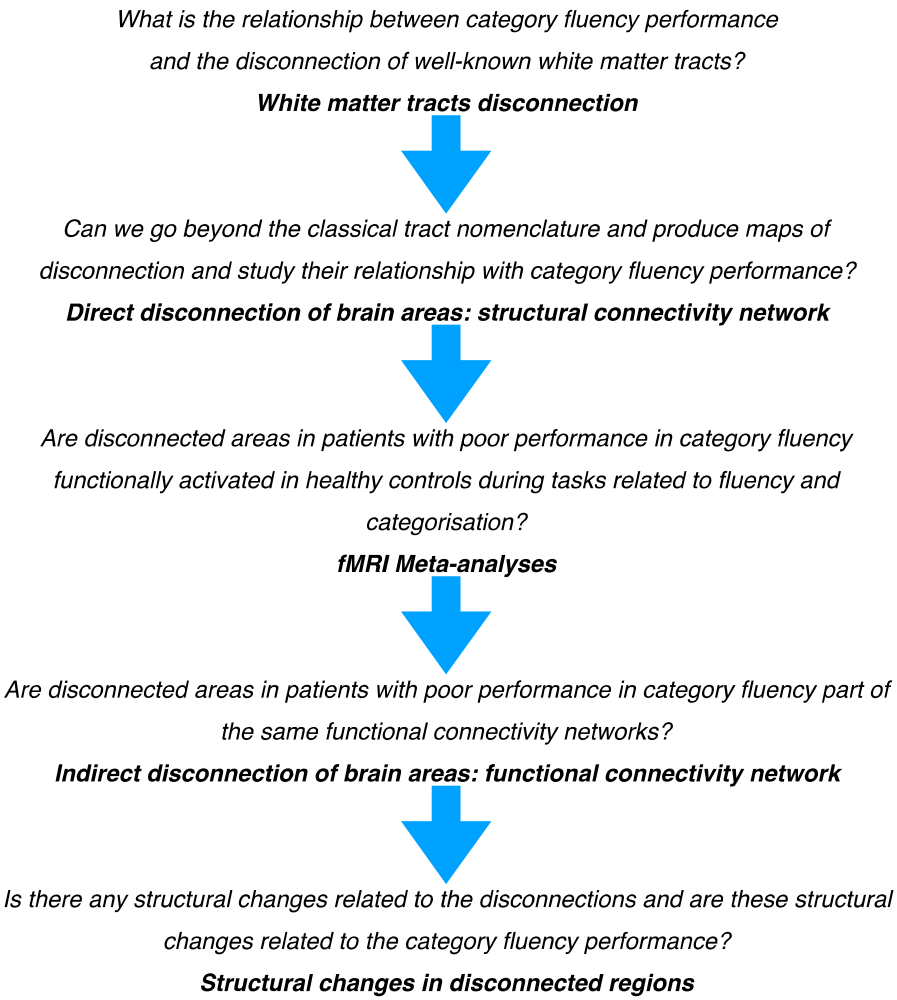

Sup Fig. 1: Step by step, hypotheses-driven analyses with BCBtoolkit.

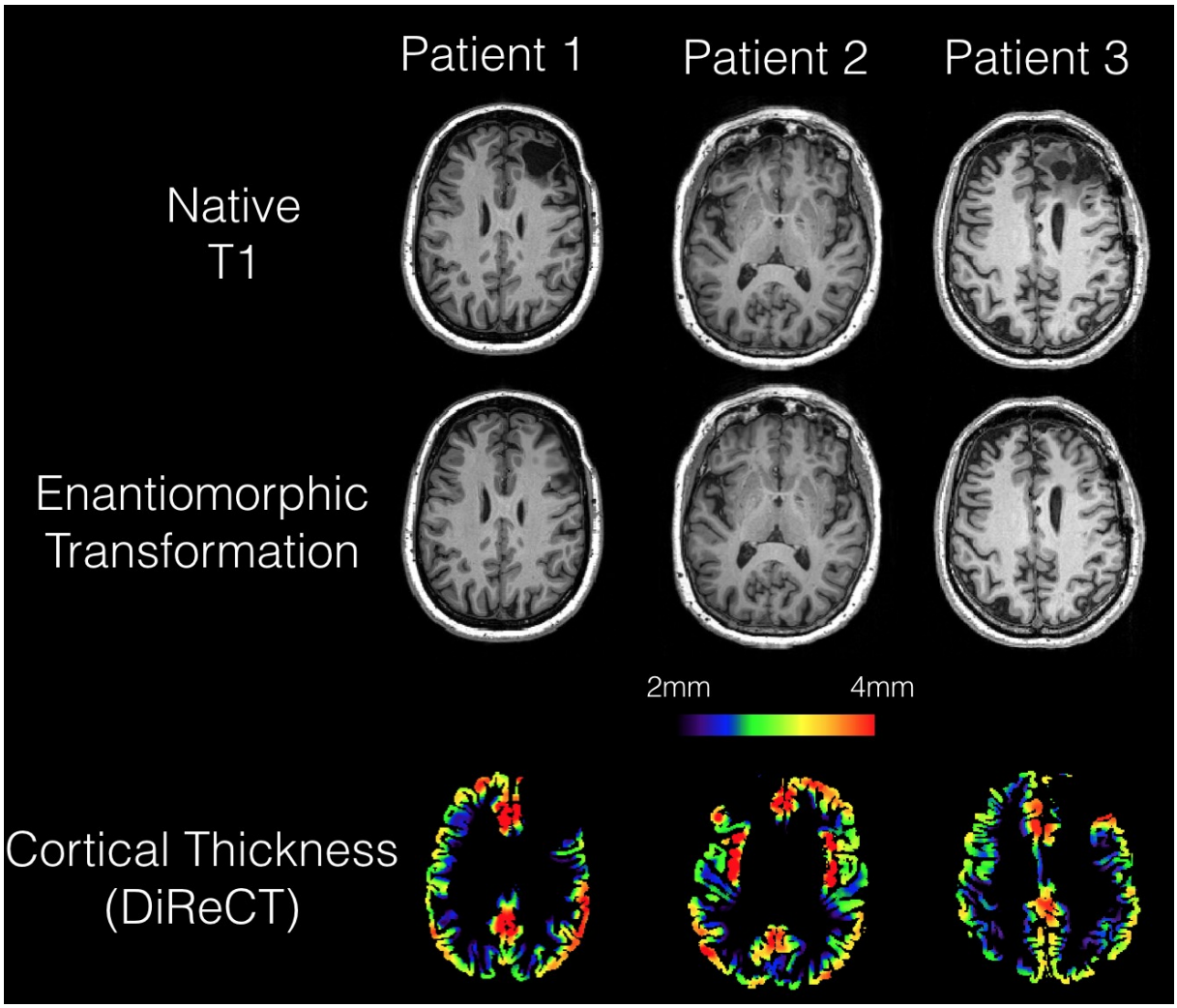

Sup Fig. 2: Native T1, enantiomorphic deformation and derived Cortical Thickness of three representative subjects

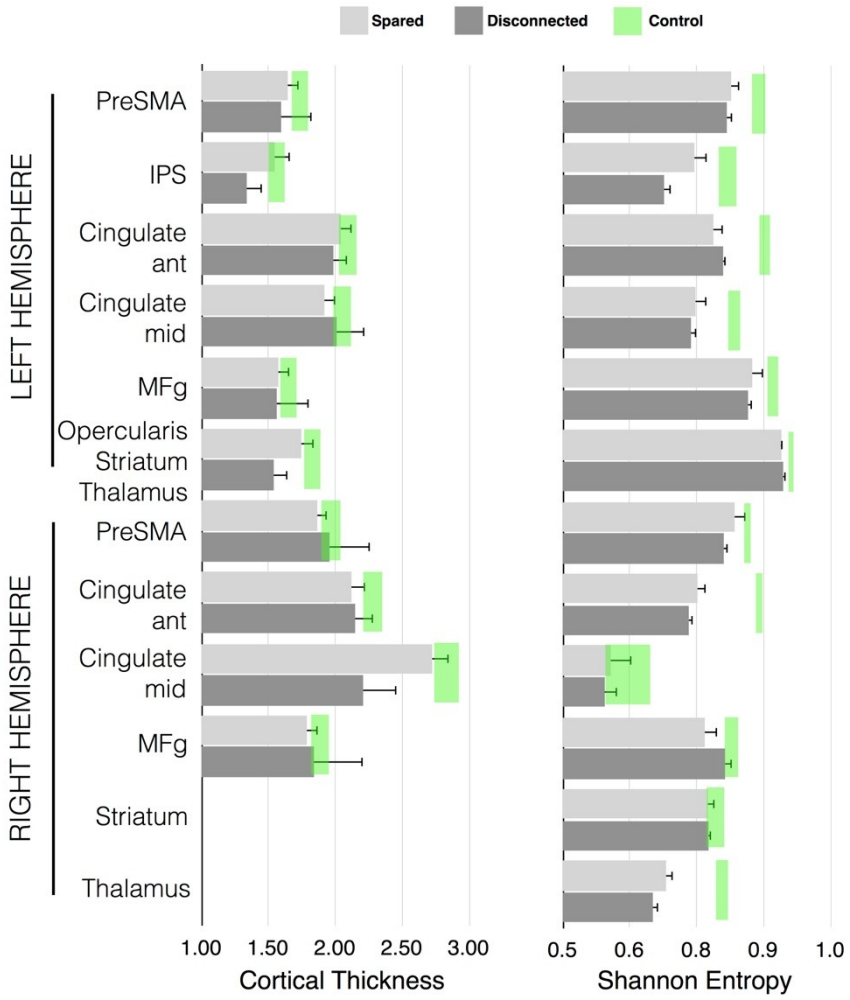

Sup Fig. 2: Cortical thickness and Shannon entropy measures (mean with 95% confidence intervals) in patients with (dark grey) or without (light grey) disconnection for each of the disconnected areas. The green interval indicates performance in matched controls with 95% confidence intervals.

4 High-level cognitive functions arise from the interaction between various brain structures

This first article had two fundamental purposes. The first one was methodological, with the disconnectome maps method as its pivotal advance. We wanted to provide a set of complementary tools to explore the variety of indirect effects due to focal brain lesions. The disconnectome maps enable an estimate of the disconnections, which is information that is mostly lost in patient data. We demonstrated that its combination with various methods allows the investigation of different aspects of the lesions' consequences, showing the importance of considering brain damage as the disruption of complex structural and functional networks interacting together rather than discrete functional units. Our second goal was the implementation of these methods gathered in the BCBtoolkit. It was essential for us to provide an open-source package to diffuse it freely as it should be for the sake of reproducible science but also to give the possibility to modify and improve it for future users. Besides, we also endeavoured to make it as user-friendly as possible to facilitate its use for clinicians and in general researchers who are not experts in neuroimaging methodologies. Although the open-source allows the modification of every parameter of the software, we provide with this package the default parameters that we optimised all along the development of these tools—profiting, for instance, from studies using some of these methods, like the next two, to make it more efficient and easier to use.

The two following studies were the opportunity to develop and test different methods to investigate how lesions impact brain dynamics. They aim to investigate the brain mechanisms supporting other high-level cognitive functions and, in particular, different processes known to be involved in creative thinking. That was the perfect opportunity to work with different teams of neuroscientists, who had different skills and usages of neuroimaging analyses, to develop and refine our tools. It allowed us to study the impact of brain lesions on different cognitive mechanisms from different angles.

The first of these articles, (Urbanski et al., 2016), aimed at identifying the critical brain regions for analogical reasoning, using a lesion approach. Analogical reasoning was mainly explored using fMRI images showing a set of interconnected brain areas, including several frontal regions. However, this method does not

inform us of the critical areas or networks. For this purpose, we performed a voxel-based lesion study, combined with the use of new methods, to explore the impact of disconnections that cannot be analysed with the VLSM approach. This study thus triggered the development of the early version of some modules of the BCBtoolkit, including Tractotron and disconnectome maps.

Contribution: As a co-author of this study, I mainly participated in the methodologies, especially how to further the voxel-based lesion symptom analysis to explore the impact of damage through the prism of the associationist paradigm. To this end, we developed and improved Tractotron and the disconnectome method, the first modules implemented in the BCBtoolkit. I developed and programmed these methods. I also participated in the writing and editing of the article.

Résumé :

Introduction : Le raisonnement par analogie est au coeur des processus de généralisation et d'abstraction qui permettent l'élaboration de concepts et la créativité. Les analogies permettent d'inférer une représentation générale à partir de similarités entre des objets ou situations et de transférer ce schéma général à de nouveaux cas. Elles sont par conséquent primordiales pour différents processus cognitifs de haut niveau comme l'apprentissage. Malgré l'importance du raisonnement par analogie pour la vie de tous les jours et dans la société, il reste assez peu étudié (Ahmed and Miller, 2015). De plus, les effets des pathologies cérébrales sur cette capacité sont rarement mesurés en pratique clinique, rendant difficile l'évaluation de leur impact sur la vie des patients et limitant notre compréhension des bases anatomiques des fonctions impliquées dans le raisonnement par analogie. Le peu d'études ayant exploré cette fonction chez des sujets sains ont montré l'importance du cortex préfrontal dans sa réalisation (Morrison et al., 2004; Krawczyk, 2012). Plusieurs études montrent des activations fonctionnelles dans le cortex rostro-latéral préfrontal gauche lors de tâches d'analogie (Vartanian, 2012). Cependant, elles ne permettent pas de déterminer si cette région est critique pour le raisonnement par analogie.

Résultats : Dans cette étude, nous explorons la capacité de raisonnement par analogie de 27 patients atteints de dommages focaux dans les lobes frontaux. Nous avons utilisé une approche (voxel-based lesion symptom mapping; VLSM) comparant les voxels des données IRM pour identifier les régions lésées diminuant significativement la performance dans le raisonnement analogique. Cette méthode nous a permis de montrer qu'une lésion dans le cortex rostro-latéral préfrontal gauche diminue significativement les performances dans le raisonnement par analogie. Pour comprendre plus précisément quel rôle joue cette région dans la fonction étudiée, nous nous sommes intéressés aux connexions de la matière blanche impactées par les lésions. Pour cela, nous avons utilisé la méthode du Tractotron, qui nous permet de comparer les lésions avec un atlas des connexions pour ensuite associer les déconnexions qu'elles provoquent avec un changement comportemental. Nous avons ainsi identifié 4 faisceaux de fibres de l'hémisphère gauche : le faisceau fronto-occipital inférieur, unciné et fronto-marginal ainsi que les radiations thalamiques antérieures, qui, lorsqu'ils sont déconnectés, sont associés à une baisse de performance lors de la tâche d'analogie. Nous avons également cartographié les connexions potentiellement interrompues par la région identifiée par l'analyse VLSM à l'aide des disconnectome maps. Nous avons ainsi identifié l'ensemble des faisceaux connectés au cortex rostro-latéral préfrontal gauche. De plus, nous avons montré que l'atteinte du raisonnement par analogie était corrélée au nombre de déconnexions parmis ces faisceaux. Enfin, nous sommes également parvenu à démontrer la validité d'une version raccourcie de la tâche utilisée pour retrouver le lien entre le cortex rostro-latéral préfrontal gauche et une baisse de performance.

Conclusion : Grâce à cette étude, nous avons tout d'abord confirmé la nécessité de l'intégrité du cortex rostro-latéral préfrontal gauche, et de ses connexions, dans les processus liés au raisonnement par analogie. La comparaison des lésions avec l'atlas des faisceaux majeurs montrent, au delà de la zone lésée, un lien entre déconnexions et baisse de performance, des résultats cohérents avec d'autres études utilisant la tractographie. Les faisceaux critiques pour l'analogie connectent notamment le lobe frontal aux cortex temporaux (via le faisceau unciné), au cortex occipital (via le faisceau fronto-occipital inférieur) et aux structures sous-corticales par la radiation thalamique antérieure. L'étude des connexions passant par la région identifiée à l'aide de VLSM montrent que cette

dernière a une forte connectivité anatomique et est à l'intersection de nombreux faisceaux. La corrélation entre le nombre de ces connexions interrompues et la baisse de performance suggèrent que le cortex rostro-latéral préfrontal gauche est un point de convergence entre les différents systèmes impliqués dans le raisonnement par analogie. Ces résultats confirment l'importance d'explorer la connectivité anatomique pour expliquer les effets des lésions sur les fonctions cognitives de haut niveau. Nos résultats démontrent également que l'utilisation des tâches expérimentales d'analogie permettrait d'affiner l'évaluation neuropsychologique des patients souffrant de lésions du lobe frontal.

Brain Advance Access published April 13, 2016

doi:10.1093/brain/aww072 BRAIN 2016: Page 1 of 17 | 1

BRAIN
A JOURNAL OF NEUROLOGY

Reasoning by analogy requires the left frontal pole: lesion-deficit mapping and clinical implications

Marika Urbanski,[1,2,3,4,5] Marie-Laure Bréchemier,[1,2,3,4] Béatrice Garcin,[1,2,3,4] David Bendetowicz,[1,2,3,4] Michel Thiebaut de Schotten,[1,2,3,4,6] Chris Foulon,[1,2,3,4,6] Charlotte Rosso,[1,2,3,7] Frédéric Clarençon,[8] Sophie Dupont,[9] Pascale Pradat-Diehl,[10] Marc-Antoine Labeyrie,[11] Richard Levy,[1,2,3,12] and Emmanuelle Volle,[1,2,3,4,6,13]

Analogical reasoning is at the core of the generalization and abstraction processes that enable concept formation and creativity. The impact of neurological diseases on analogical reasoning is poorly known, despite its importance in everyday life and in society. Neuroimaging studies of healthy subjects and the few studies that have been performed on patients have highlighted the importance of the prefrontal cortex in analogical reasoning. However, the critical cerebral bases for analogical reasoning deficits remain elusive. In the current study, we examined analogical reasoning abilities in 27 patients with focal damage in the frontal lobes and performed voxel-based lesion-behaviour mapping and tractography analyses to investigate the structures critical for analogical reasoning. The findings revealed that damage to the left rostrolateral prefrontal region (or some of its long-range connections) specifically impaired the ability to reason by analogies. A short version of the analogy task predicted the existence of a left rostrolateral prefrontal lesion with good accuracy. Experimental manipulations of the analogy tasks suggested that this region plays a role in relational matching or integration. The current lesion approach demonstrated that the left rostrolateral prefrontal region is a critical node in the analogy network. Our results also suggested that analogy tasks should be translated to clinical practice to refine the neuropsychological assessment of patients with frontal lobe lesions.

1 Inserm, U 1127, 75013 Paris, France
2 CNRS, UMR 7225, 75013 Paris, France
3 Sorbonne Universités, UPMC Univ Paris 06, UMR S 1127, 75013 Paris, France
4 ICM, FrontLab, 75013 Paris, France
5 Hôpitaux de Saint-Maurice, Medicine and Rehabilitation Department, 94410 Saint-Maurice, France
6 ICM, Brain Connectivity and Behaviour, 75013 Paris, France
7 AP-HP, Hôpital de la Salpêtrière, Stroke Centre, 75013 Paris, France
8 AP-HP, Hôpital de la Salpêtrière, Neuroradiology Department, 75013 Paris, France
9 AP-HP, Hôpital de la Salpêtrière, Epileptology Department, 75013 Paris, France
10 AP-HP, Hôpital de la Salpêtrière, Physical Medicine and Rehabilitation Department, 75013 Paris, France
11 AP-HP, Hôpital Lariboisière, Neuroradiology Department, 75010 Paris, France
12 AP-HP, Hôpital de la Salpêtrière, Behavioural Neuropsychiatry Unit, 75013 Paris, France
13 CENIR, ICM, 75013 Paris, France

Correspondence to: Emmanuelle Volle,
FrontLab – ICM, Hôpital Pitié Salpêtrière, 47,
bd de l'hôpital, 75013 Paris
E-mail: emmavolle@gmail.com

Received September 17, 2015. Revised February 18, 2016. Accepted February 19, 2016.

Keywords: analogy; reasoning; rostral prefrontal; abstraction; relational integration

Abbreviations: AUC = area under the curve; IFOF = inferior fronto-occipital fasciculus; PFC = prefrontal cortex; ROC = receiver operating characteristic; VLSM = voxel-based lesion–symptom mapping

Introduction

Using analogies, we can learn abstract concepts and create new associations between distant ideas. Analogies are a powerful tool that allows us to infer general representations from similarities between objects/situations and to transfer this general schema to new cases (Gentner, 1983; Gick and Holyoak, 1983; Gentner *et al.*, 1993; Holyoak and Thagard, 1995, 1997; Gentner and Holyoak, 1997). Hence, analogical reasoning is at the core of generalization and abstraction processes (Holyoak and Thagard, 1995; Thibaut *et al.*, 2010*a*; Hofstadter and Sander, 2013).

Analogical reasoning combines three key mechanisms: relational processing, similarity processing, and schema inference. Reasoning by analogy depends on the ability to consider, integrate, and compare multiple relationships between components of mental representations (Gentner *et al.*, 1993; Robin and Holyoak, 1995; Gentner and Markman, 1997; Holyoak and Thagard, 1997; Halford *et al.*, 2010). The consideration and integration of multiple relationships (relational reasoning) is also thought to be a key factor for fluid intelligence and to rely on prefrontal functions (Duncan *et al.*, 1995; Robin and Holyoak, 1995; Waltz *et al.*, 1999; Geake and Hansen, 2005; Jung and Haier, 2007). In addition, analogical reasoning depends on the ability to detect similarities between these relational representations (Gentner *et al.*, 1993; Gentner and Medina, 1998; Blanchette and Dunbar, 2000). The comparison and mapping of relational representations composing analogous situations result in the inference of an analogy schema, i.e. a general representation of a pattern of relational similarities (Gick and Holyoak, 1983; Bethell-Fox *et al.*, 1984; Gentner *et al.*, 1993; Gentner and Markman, 1997). When a new analogy schema is inferred, new concepts are formed in a flexible manner. Therefore, analogical reasoning allows the study of the relational integration, similarity matching and schema inference processes that are required for abstract thinking and reasoning.

Despite the importance of these high-level functions in human cognition, deficits in analogical reasoning are rarely assessed in clinical practice, leading to poor understanding of their impacts on patients' daily lives and of their neuroanatomical bases (Ahmed and Miller, 2015). However sparse, previous patient studies have revealed deficits on pictorial and verbal analogy tasks in patient with frontotemporal dementia, suggesting that the prefrontal cortex (PFC) is critical for analogical reasoning (Morrison *et al.*, 2004; Krawczyk *et al.*, 2008). As patients with frontotemporal dementia have diffuse prefrontal damage and no voxel-based morphometry analyses have been performed, these studies have not provided evidence of a precise anatomical correlate. In a voxel-based morphometry study of adolescents, traumatic brain injury has been shown to impair performance on a scene analogy task and to alter its correlation with cortical thickness in prefrontal regions (Krawczyk *et al.*, 2010*a*). The one study that examined focal lesions in adults used a voxel-based lesion–symptom mapping (VLSM) approach on (mainly) stroke patients (Schmidt *et al.*, 2012). The results revealed several posterior prefrontal and temporal areas critical for semantic verbal analogies. However, the poor representation of prefrontal damage ($n = 17$) and of anterior prefrontal lesions in particular in this stroke population limited the conclusions that could be drawn regarding the role of anterior cerebral regions. Among studies that used relational reasoning tasks that are similar to analogy tasks, such as matrix problem tasks (Raven, 1938; Wechsler, 1997), voxel-based lesion studies have also lacked coverage of the rostral PFC region despite larger sample sizes (Gläscher *et al.*, 2009; Baldo *et al.*, 2010), and the conclusions drawn regarding the critical brain regions for these tasks have not always been consistent among studies (Waltz *et al.*, 1999; Tranel *et al.*, 2008; Gläscher *et al.*, 2009; Baldo *et al.*, 2010; Woolgar *et al.*, 2010; Waechter *et al.*, 2013). In related fields that explored abstraction or reasoning, studies in brain-damaged patients have highlighted the critical importance of the left PFC for proverb interpretation (McDonald *et al.*, 2008; Kaiser *et al.*, 2013; Murphy *et al.*, 2013), conceptualization (Dubois *et al.*, 2000; Delis *et al.*, 2001; Hoffman *et al.*, 2010; Lagarde *et al.*, 2015), and inductive reasoning (Reverberi *et al.*, 2005).

In healthy volunteers, functional imaging studies on analogy have shown the involvement of various prefrontal regions, including the rostrolateral PFC, in addition to parietal and temporal regions (for a review, see Krawczyk, 2012). A variety of analogy tasks have used verbal, figurative or abstract material that involved semantic (Bunge *et al.*, 2005; Wendelken *et al.*, 2008; Green *et al.*, 2010), role-based (Krawczyk *et al.*, 2010*a*), visuospatial, mathematical, or logical relationships (Christoff *et al.*, 2003; Geake and Hansen 2005; Smith *et al.*, 2007; Wartenburger *et al.*, 2009; Cho *et al.*, 2010; Volle *et al.*, 2010; Preusse *et al.*, 2011; Watson and Chatterjee, 2012). Although domain-oriented or relation-oriented brain regions have been observed (Krawczyk *et al.*, 2011), the rostrolateral PFC has been demonstrated to be a domain-general region involved in both semantic and visuospatial analogies (Wendelken *et al.*, 2012) and in both classical analogy and matrix problem-solving tasks (Krawczyk *et*

al., 2011). A recent meta-analysis of functional imaging results has shown that the left rostrolateral PFC and dorsolateral PFC are the most consistently activated regions across different analogy studies and tasks (Vartanian, 2012). Other approaches such as voxel-based morphometry on healthy volunteers (Aichelburg *et al.*, 2016) and developmental studies of children (Wright *et al.*, 2007; Crone *et al.*, 2009; Thibaut *et al.*, 2010*b*; Dumontheil, 2014), have also indicated that the left rostrolateral PFC is important for various relational reasoning tasks.

In other words, the literature on healthy subjects indicates that the rostrolateral PFC, among other regions, plays an important and domain-general role in analogy but the available evidence cannot demonstrate whether it is critical for this process. Patient studies have provided limited conclusions regarding the roles of rostral frontal areas. To the best of our knowledge, no study has examined whether analogical or relational reasoning depends on the integrity of frontal lobe connections. Hence, the precise cerebral bases for analogical reasoning deficits and the effect of rostral PFC damage on analogical reasoning abilities remain to be clarified.

In this study, we used a lesion-behaviour mapping approach in 27 patients with a focal brain lesion in the PFC, to explore the crucial prefrontal regions for analogy and to test whether the left rostrolateral PFC is critical. The patients were administered a visuospatial analogy task that has been previously associated with the left rostrolateral PFC in healthy subjects (Volle *et al.*, 2010; Aichelburg *et al.*, 2016). The analogy schemas of this task are comparable to those used in previous studies (Gentner and Medina, 1998; Krawczyk *et al.*, 2008; Wartenburger *et al.*, 2009; Watson and Chatterjee, 2012) or in matrix problems. The two analogy conditions used each required relational reasoning and differed only in whether the analogy schema must be inferred. These conditions were compared to a control task that did not require relational processing. Lesion-deficit relationships were explored using a VLSM technique (Bates *et al.*, 2003). In addition, we used a track-wise lesion-deficit analysis (Thiebaut de Schotten *et al.*, 2014, 2015) to explore the impact of tract disconnection on analogical reasoning. Finally, we examined the sensitivity and specificity of this analogy task in patients with damaged frontal lobes and estimated the potential value of the task in clinical practice.

Materials and methods

Participants

Twenty-seven right-handed patients (16 females, mean age of 47.2 years, ranging from 23 to 75 years) who each presented with a single, focal frontal lesion and were seen at the chronic stage (>2 months) participated in this study. The patients were recruited from the departments of nervous system diseases and neuroradiology at Salpêtrière Hospital, the neurological unit at Saint-Antoine Hospital and the neuroradiology department at Lariboisière Hospital in Paris. Patients with a history of psychiatric or neurological disease, drug or psychotropic abuse, MRI contraindication or who were not able to understand the task instructions were excluded. All patients were native French speakers. Descriptive and clinical data are reported in Table 1.

The patient performances were compared to those of a normative group of 54 healthy right-handed, French native speaker control subjects (Supplementary Table 1), who were matched for age and years of formal education and who had no history of psychiatric or neurological disease, drug or psychotropic abuse, or MRI contraindication and no cognitive impairment [Mini-Mental State Examination (MMSE) $\geqslant$ 27/30; Folstein *et al.*, 1975].

The experiment was approved by the local ethics committee; all participants provided written informed consent according to the Declaration of Helsinki and were paid for their participation.

Neuropsychological testing

A battery of neuropsychological tests was administered to all participants (Supplementary material). Cognitive status was measured with the MMSE (Folstein *et al.*, 1975). A short assessment of cognitive and behavioural executive functions was performed using the Frontal Assessment Battery (FAB, Dubois *et al.*, 2000), a semantic and lexical fluency task (Cardebat *et al.*, 1990) and the Stroop test (Stroop, 1935). Semantic knowledge was assessed using short French versions of a naming test and a semantic matching test (as described in Merck *et al.*, 2011).

Experimental design

The Analogy and Match (control) tasks of the current study have been used in previous studies in healthy volunteers (Volle *et al.*, 2010; Aichelburg *et al.*, 2016). All of the experimental conditions followed the same design and used the same types of stimuli (Fig. 1 and Supplementary material). After the instructions were displayed, a first set of stimuli appeared on the left part of the screen (the source set), and two other sets appeared on the right part of the screen (the target sets). The participants were asked to select the target set that matched the source set based on the relationships between the stimuli that composed the sets (Analogy tasks) or based on the similarity of their visual features (Match tasks). The subjects had 11.5 s to respond by a button press. The stimuli were letters, numbers or abstract figures, presented in different colours, numbers, sizes or patterns.

Analogy tasks were divided into two conditions: an AnalogyFind and an AnalogyApply condition. In the AnalogyFind condition, the participants had to find the analogy schema by considering the similarities between the structures of each set. The instruction 'find analogy' was displayed, and the task required comparing the sets, finding an analogy schema and choosing the target set accordingly (e.g. symmetry of the size of the stimuli). In the AnalogyApply condition, the analogy schema was indicated to the participants by providing them with a verbal term that described it (e.g. 'Proportion'). The instruction that contained the verbal description of the schema

Table 1 Clinical, descriptive information, and performance for the 27 patients included in the study

Patient	Age (years)	Gender	Education (years)	Aetiology	Lesion side and location	Interval (months)	Lesion volume (cm^3)	VLSM	Deficit-short task
P01	56	F	17	Ischaemic stroke	R - Semi-oval centre	7	0.27		
P02	55	M	19	Haemorrhage S	L - rostral PFC/VMPFC[a]	76	38.87	+	+
P03	46	F	17	Ischaemic stroke	L - posterior MFG	126	21.22		
P04	50	F	11	Low-grade glioma (excision)	L - rostral PFC + /VMPFC[a]	137	150.85	+	+
P05	64	M	14	Ischaemic stroke	R - IFG and MFG	121	76.63		+
P06	32	F	16	Epilepsy surgery	R - posterior SFG	133	22.43		
P08	70	F	5	Meningioma (excision)	L - rostral PFC + [a]	85	55.60	+	+
P09	47	M	11	Haemorrhage RA	R - Cingulate/VMPFC	115	13.79		
P10	62	F	13	Haemorrhage RA	B - Cingulate/VMPFC	14	44.12		
P11	41	M	16	Epilepsy surgery	R - IFG/MFG/posterior SFG	29	67.13		
P12	46	M	12	Haemorrhage RA	B - Cingulate/VMPFC	51	9.29		
P13	67	M	15	Ischaemic stroke	L - anterior IFG	133	4.71		
P14	49	M	9	Haemorrhage RA	B - Cingulate/VMPFC	19	23.17		
P15	36	F	14	Epilepsy surgery	R - rostral PFC/VMPFC	82	49.67		
P16	40	F	22	Haemorrhage S	L - rostral PFC[a]	56	27.59		+
P17	40	M	14	Haemorrhage RA	B - rostral PFC/VMPFC	7	26.71		
P18	23	F	16	Epilepsy surgery	R - rostral PFC	47	32.13		
P19	54	M	22	Ischaemic stroke	R - IFG/MFG white matter	48	60.11		
P20	71	M	17	Haemorrhage RA	L - rostral PFC/VMPFC[a]	91	37.06		
P21	23	F	15	Epilepsy surgery D	R - rostral PFC	36	37.79		
P22	27	F	9	Epilepsy surgery	L - lateral rostral PFC[a]	30	16.45	+	+
P23	26	F	13	Epilepsy surgery D	L - precentral gyrus	19	2.95		
P24	32	F	14	Epilepsy surgery	L - posterior medial PFC	4	14.81		
P25	59	F	16	Haemorrhage RA	L - VMPFC	9	0.87		
P26	26	F	13	Haemorrhage	L - posterior IFG	32	29.19		
P27	58	M	12	Ischaemic stroke	L - precentral sulcus	3	1.22		
P29	75	F	12	Haemorrhage S	L - rostral PFC[a]	16	14.1	+	+

[a]Patients belonging to the 'damaged left rostrolateral PFC' group as defined anatomically. Patients who participated in the VLSM Analogy region are indicated in the 'VLSM' column. Patients impaired in the short version of the task (Analogy index) are indicated in the 'Deficit-short task' column. Ischaemic strokes affected the middle cerebral artery territory. Haemorrhages were caused by a ruptured aneurism (RA), or due to a spontaneous haematoma (S), or to a vascular malformation for one patient (Patient P26). Epileptic patients underwent a surgical resection of their epileptic focus, whose origin was cryptogenic, except for two patients who had a dysplasia removed (D). Education level corresponds to the number of years since beginning of school (usually at age 6; 12 years correspond to a high school degree). Interval is the delay between lesion and testing in months. B = bilateral; F = female; L = left; IFG = inferior frontal gyrus; M = male; MFG = middle frontal gyrus; R = right; Rostral PFC + = damage to rostral PFC extending to anterior part of MFG, SFG, IFG; SFG = superior frontal gyrus; VMPFC = ventromedial PFC.

was displayed on the screen together with the sets; thus, participants still had to consider and compare the multiple relationships between the stimuli, but there was no need to infer or retrieve the schema. Six geometrical or mathematical schemas (proportion, subtraction, addition, mirroring, symmetry and progression) were used and applied to the identity of the stimuli (letters or figures) or to their size, number, brightness, or texture. The features of the stimuli that were not relevant for the analogy schema varied between the source and target, to avoid perceptual matching. For AnalogyApply and AnalogyFind, two types of analogy trials were proposed in the same proportion: intra- and cross-dimensional analogies (Fig. 1).

In the Match tasks, the source and target sets had to be matched on the basis of six perceptual attributes: colour, quantity, size, texture, figures and letters. As with the Analogy tasks, the Match tasks included two separate conditions, a MatchFind and a MatchApply condition. In the MatchFind condition, the instruction 'find match' was displayed, and the participants had to find the perceptual relationship between the source and the correct target set. In the MatchApply condition, the participants were instructed to apply a given matching rule. The instruction that contained a verbal description of the matching rule was displayed on the screen (e.g. 'same colours') together with the sets.

All participants understood the instructions and were able to perform the tasks correctly after training. They performed one session of each of the four experimental conditions in the following order: 28 MatchApply trials, 28 MatchFind trials, 48 AnalogyApply trials and 48 AnalogyFind trials. The trials were randomized within each session.

Behavioural analysis

The accuracy (percentage of correct responses) was measured for each condition. Analogy and Match mean accuracies were calculated by averaging performance on the AnalogyFind and AnalogyApply conditions and on the MatchApply and MatchFind conditions, respectively. Similarly, the Find and Apply performances were calculated by averaging the Find (AnalogyFind and MatchFind) and Apply (AnalogyApply and MatchApply) conditions. We also examined the performance at cross- and intra-dimensional trials for the AnalogyApply and AnalogyFind tasks separately. To assess the possible specificity of the deficits in the Analogy tasks

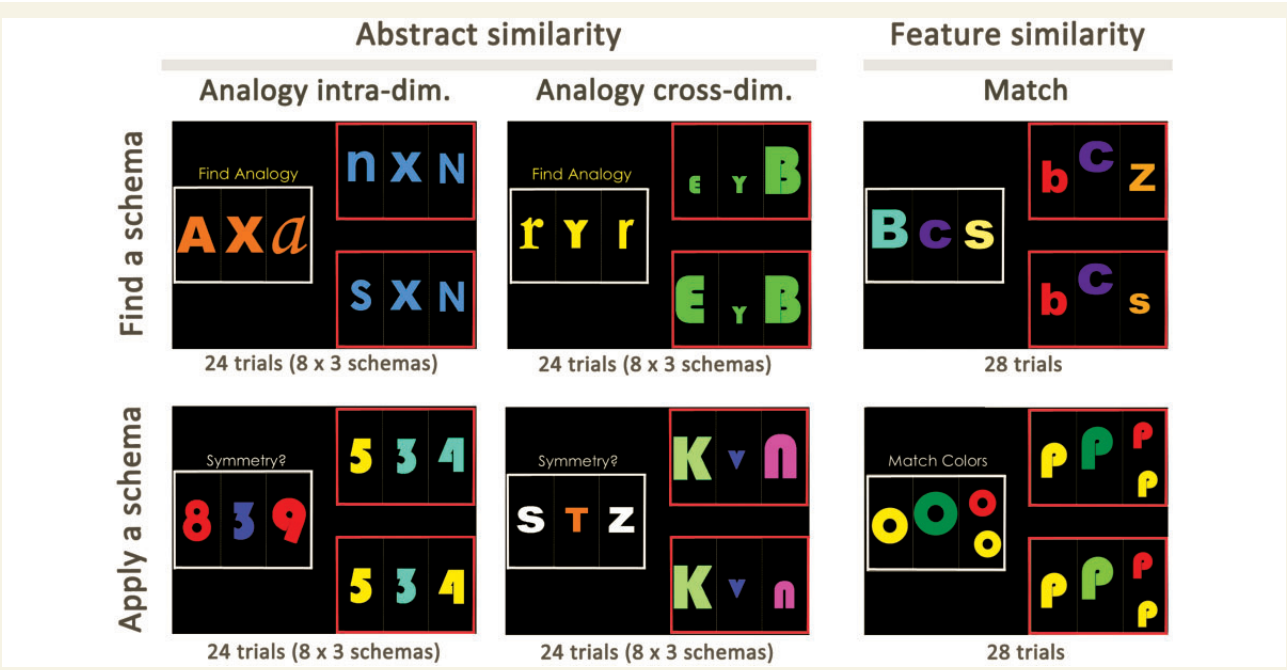

Figure 1 Examples of intra- and cross-dimensional Analogy and Match trials. In each example, for clarity, source sets are framed in white, and target sets are framed in red, although in the real tasks, the sets were all framed in light grey when they were displayed to the participants. The *left column* displays an intra-dimensional analogy, and the *middle column* displays a cross-dimensional analogy, using the same analogy schema 'symmetry'. In the intra-dimensional analogy, the symmetry is on the same dimension in the source and target sets. The correct answer in the top left example (AnalogyFind) is the top target, in which there is symmetry of the letter identity in both the target and source sets. The correct answer in the bottom left example (AnalogyApply) is the bottom target, in which there is symmetry of the colour in both the target and source sets. In cross-dimensional analogy, the symmetry concerns different dimensions in the source and target sets. The correct answer in the top middle example (AnalogyFind) is the bottom target, in which there is symmetry of size, whereas the source set has symmetry of letter identity. In the bottom middle example (AnalogyApply), the correct answer is the top target. The *right column* displays a Match trial. Correct answers are the bottom target for the top trial and the top target for the bottom trial. For each of these tasks, the participants performed Find and Apply conditions. The *upper row* presents Find trials, in which the abstract similarity (in the Analogy task) or the feature similarity (in the Match task) was not given to the participant. The *bottom row* presents Apply trials, in which the abstract similarity or feature similarity was given in the instruction. Three distinct analogy schemas were used in the AnalogyFind condition, and three other schemas were used in the AnalogyApply condition, although in the figure the same schema 'symmetry' is used for an easier understanding of the distinct conditions. The three matching rules used in the MatchFind condition were distinct from the three rules used in the MatchApply condition.

relative to the control task, we also calculated an index [Analogy index = (Analogy mean accuracy – Match mean accuracy) × 100/mean accuracy in all Analogy and Match tasks averaged]. Similarly, we calculated indices to test for possible specificity of deficits in the Find condition relative to the Apply condition [Find index = (mean accuracy in Find conditions – mean accuracy in Apply conditions) × 100/mean accuracy in the average of all conditions], and in the cross relative to the intra-dimensional analogies [Cross index = (mean accuracy in cross-dimension Analogy trials – mean accuracy in intra-dimension Analogy trials) × 100/mean accuracy in the average of all analogy conditions].

Statistical analyses were performed using SPSS software (v22.0; LEAD Technologies, Inc.). Between-group differences were analysed using parametric *t*-tests (when the assumption of normality was met) or non-parametric tests otherwise (Mann-Whitney test), using exact *P*-values for comparison within our patient group. Correlations between the performances of the patients and age, education, delay or volume of the lesion were analysed using the non-parametric Spearman test (r_s).

Image acquisition and preprocessing

Magnetic resonance acquisition

Patients and controls underwent the same high-resolution T_1-weighted structural MRI acquisition on a Siemens 3 T VERIO TIM system that was equipped with a 32-channel head coil. A 3D MPRAGE (magnetization-prepared rapid-acquisition gradient echo) dataset that covered the whole brain was acquired for each participant across 176 axial slices with a voxel isometric resolution of 1 mm^3 (echo time = 2.98 ms, repetition time = 2300 ms, and flip angle = 9°). MRI and behavioural testing took place on the same day for most of the participants or a few days apart at most.

MRI spatial normalization

T_1-weighted 3D sequences were preprocessed with SPM8 software (Wellcome Department of Imaging Neuroscience, London, UK), which ran on Matlab (Mathworks Inc., Natick, USA; www.mathworks.com/matlabcentral). The MRIs were spatially normalized to the Montreal Neurological Institute (MNI)

template. The 'unified segmentation' approach was combined with lesion masking to limit the impact of a brain lesion on the spatial normalization (Crinion *et al.*, 2007; Andersen *et al.*, 2010). This approach has been identified as the best compromise between the normalization accuracy and lesion shrinkage in a recent study (Ripollés *et al.*, 2012). The segmentation parameters were set to the defaults, except for regularization, which was set to medium (Andersen *et al.*, 2010; Ripollés *et al.*, 2012). Spatially normalized images were resliced with a final voxel size of $1.5 \times 1.5 \times 1.5\,mm^3$. Each normalized MRI was visually checked and compared with the MNI template to evaluate the normalization accuracy (B.G., M.L.B., D.B. and E.V.). No patient had to be excluded due to difficulties with normalization.

Lesion-behaviour mapping approach

To investigate lesion-deficit relationships, we ran a VLSM analysis (Bates *et al.*, 2003) using NPM software (http://www.mccauslandcenter.sc.edu/mricro/npm/). The preprocessed and normalized MRIs were used for lesion segmentation. Signal abnormalities due to the lesion were manually segmented using MRIcron (http://www.mccauslandcenter.sc.edu/mricro/mricron/) by trained neurologists (B.G., M.L.B., and D.B.) supervised by an experienced neurologist (E.V.), who were blind to the performances of the patients at the time of the lesion segmentation. The resulting segmented lesion volumes in the MNI space were then introduced in the statistical procedure.

Given the non-normal distribution of the performance and the small sample of the patients, we used the non-parametric Brunner-Munzel test and corrected for multiple comparisons for family-wise errors using permutations, with a significance threshold of $P < 0.05$. Only the voxels that concerned at least three lesions were considered (all of the lesions together covered 74% of the frontal lobes; overlaps of at least three lesions represented 30% of the frontal lobes). These analyses provided statistical maps for Analogy and Match mean accuracy scores as well as for the Analogy index.

Track-wise lesion-deficit analysis

To explore the impact of tract disconnection on analogical reasoning, we used two track-wise lesion-deficit approaches.

A priori approach

First, independent of the VLSM results, we used a diffusion-based atlas of frontal lobe connections (Rojkova *et al.*, 2015) combined with Tractotron software as part of the BCB toolkit (http://www.brainconnectivitybehaviour.eu/), to identify the tracts that could be affected by the lesion of each patient. Tractotron automatically computes the overlap of each segmented lesion with the map of the tracts. We mapped the lesion from each patient onto tractography reconstructions of white matter pathways obtained from a group of healthy controls (Rojkova *et al.*, 2015). We quantified the severity of the disconnection by measuring the probability of the tract to be disconnected (Thiebaut de Schotten *et al.*, 2014). A tract was considered disconnected when a lesion overlapped with a voxel that belonged to this tract with a probability that was above the chance level (probability > 0.5). We *a priori* selected several projection tracts that have been associated with Analogy performance according to Aichelburg *et al.* (2016): the long segment of the arcuate fasciculus, the fronto-marginal tract, the inferior fronto-occipital fasciculus (IFOF), the uncinate fasciculus and the anterior thalamic radiations. Then, we examined the impact of the disconnection of each tract in the left and right hemispheres on analogical reasoning. For each tract of interest, we compared the performance of the patients with and without its disconnection using non-parametric Mann-Whitney tests (with exact *P*-values significant at $P < 0.05$).

VLSM-based approach

Second, based on the VLSM results, we created a map of the tracts connecting the VLSM Analogy region ('VLSM connectome map') and calculated the probability that each lesion intersects this map. We built the VLSM connectome map using Disconnectome map software (Aichelburg *et al.*, 2016; Thiebaut de Schotten *et al.*, 2015) as part of the BCB toolkit (http://www.brainconnectivitybehaviour.eu). The VLSM region was registered to the tractography of a group of healthy controls (Rojkova *et al.*, 2015) using affine and diffeomorphic deformations. The registered VLSM region was used as a seed point to track streamlines passing through the region in a normative dataset. The software creates a probability map of the streamlines intersecting the seed such that the value in each voxel of the map varies based on inter-subject variability. Then, we used Tractotron (Thiebaut de Schotten *et al.*, 2014) (http://www.brainconnectivitybehaviour.eu/), to compute the probability that each lesion intersects the VLSM connectome map. Tractotron also identified the tracts connected to the VLSM region (Rojkova *et al.*, 2015). Among these VLSM connected tracts, we calculated the number of tracts that were disconnected by the lesion of each patient (with probability > 0.5) and examined its correlation with analogy performance.

Sensitivity and specificity of analogy tasks and conditions for clinical use

Finally, we aimed to evaluate the clinical value of the analogy tasks for patients with frontal lobe damage. First, our original tasks in their current form might not be suitable for clinical practice because they take time to perform (between 45 and 50 min). Therefore, we ran a new analysis on a subsample of the trials, which was composed of the 28 first AnalogyFind trials (intra- and cross-dimensional) and the 28 MatchFind trials that had been administered to each participant. As the order was randomized for each participant, the 28 first Analogy trials were not the same among individuals and were randomly selected. We also checked the reliability of all trials statistically and observed good item reliability (Spearman-Brown coefficient = 0.761). The Apply conditions were discarded because the Find conditions may correspond better to real-life analogies, and they were more strongly impacted by brain lesions. The estimated duration of this subsample of trials did not exceed 15 min.

Second, to examine the ability of this shorter version to discriminate among patients, we grouped the patients according to their lesion location, independent of the VLSM results. For analysis of accuracy of the short version, the patients were divided into two *a priori*-defined groups based on integrity of the left rostrolateral PFC. The definition of the group was based on previous literature indicating the importance of the left rostrolateral PFC in analogy. Because the rostral PFC is

difficult to delineate anatomically, a pragmatic definition was used, as described in Tisserand *et al.* (2002): the rostral prefrontal region corresponds to the most anterior 25 coronal slices (2.5 cm), $y > 44$ in the MNI coordinates. Within this rostral prefrontal region, we selected its left lateral part (defining the 'left rostrolateral PFC region') by selecting MNI x coordinates that were lower than −25. Seven patients had a lesion that affected this anatomically defined rostrolateral PFC region and were pooled in the 'damaged left rostrolateral PFC' group (indicated in Table 1). Their performances were compared to patients who had an intact left rostrolateral PFC ('intact left rostrolateral PFC' group).

We then examined the sensitivity and specificity of this shorter subtask to discriminate brain lesions, by building receiver operating characteristic (ROC) curves for each score. These ROC curves show the trade-off between the sensitivity and specificity, and the area under the curve (AUC) estimates the accuracy of the task for predicting the left rostrolateral damage in patients who had frontal lesions. Based on the obtained predictive value of the analogy and index scores and on the normative scores of controls, we grouped the patients according to the presence or absence of a deficit in analogical reasoning (Table 1) and compared their cognitive profiles and lesion locations.

Results

Behavioural results

The patients exhibited significantly poorer performances compared with the controls on the FAB, fluency tasks, and MMSE, and they showed a greater interference effect on the Stroop test, but their semantic knowledge was preserved (Supplementary Table 1 and Supplementary Fig. 1).

The patients performed significantly more poorly than the healthy participants in terms of both the Analogy conditions separately and the Analogy mean accuracy score. They had lower Match mean accuracy scores, whereas their accuracy in each Match condition separately did not differ from that of the controls. The Analogy index was significantly higher in the patient group, which suggests that their deficit was larger in the Analogy than the Match tasks. The patients scored lower than the healthy subjects in the Find and Apply conditions, but not in the Find index, which suggests that they were equally impaired in the Apply and Find conditions.

Although age, lesion volume and lesion delay, and in some cases education, can be confounding factors in VLSM analysis, there was no significant correlation between Analogy mean accuracy score and age ($r_s = -0.276$, ns), education ($r_s = 0.336$, ns), lesion volume ($r_s = -0.314$, ns), or lesion delay ($r_s = -0.201$, ns), which have not been covaried out.

VLSM results

The statistical map of the Analogy mean accuracy score (Fig. 2) showed that a deficit in the Analogy tasks was associated with a left rostral prefrontal area (MNI coordinates centred on −31, 51, −3; $z = 3.48$; volume = 0.33 cm^3) that encompassed Brodmann area (BA) 47/10 and was located at the rostral junction between the superior and middle frontal gyrus, extending into pars triangularis. A smaller cluster was located posteriorly, centred on coordinates −34, 41, 3, and another in the orbitofrontal cortex, BA 47 and 11, centred on coordinates −30, 41, −10. These clusters are gathered under the term 'the VLSM Analogy region' in the further analyses below.

Table 2 shows that the patients who contributed to the 'VLSM Analogy region' ($n = 5$) did not differ from the other patients in terms of their age, education, lesion volume, delay between lesion and inclusion, and general neuropsychological testing, except for the Stroop test, in which they had a stronger interference effect. The patients contributing to the 'VLSM Analogy region' had lesions caused by various mechanisms, including haemorrhage (Patients P02 and P29), tumour excision (Patients P04 and P08) or epilepsy surgery (Patient P22), as indicated in Table 1.

Patients with a lesion in the 'VLSM Analogy region' showed significantly greater impairment than the other patients on the Analogy tasks but not on the Match tasks, as shown by a significant between-group difference in the Analogy index (Fig. 3 and Table 2). There was no between-group difference in the Find index or the Cross index. In other words, the 'VLSM Analogy' patients were not differentially affected compared with the other patients by the need to infer the analogy schema (no significant difference in the Find index) or to transfer the schema to different dimensions in the source and target (no significant difference in the Cross index). For subsequent analyses, intra- and cross-dimensional trials, as well as Apply and Find analogy trials, were pooled.

We also ran VLSM maps for the mean Match score and found no significant results.

The statistical map for the Analogy Index (Fig. 2) revealed a region that was very close to the 'VLSM Analogy region' in the middle frontal gyrus and pars triangularis, which encompassed BA 10, 47, 45 and 46 and was centred on the MNI coordinates −35, 48, and 9 (volume of 1.57 cm^3). Although the VLSM Analogy and VLSM Index regions did not fully overlap, they both included BA10 and 47 in the left rostrolateral PFC, indicating that the left rostrolateral PFC was specifically critical to Analogy relative to Match.

Track-wise lesion-deficit approach

A priori approach

Several tract disconnections had impacts on analogical reasoning abilities. Table 3 shows that disconnections of the left IFOF, uncinate fasciculus and fronto-marginal tract were associated with a greater deficit in Analogy tasks (Analogy mean accuracy score and Analogy index). Disconnection of the left anterior thalamic radiation was associated with a deficit in the Analogy tasks, but no

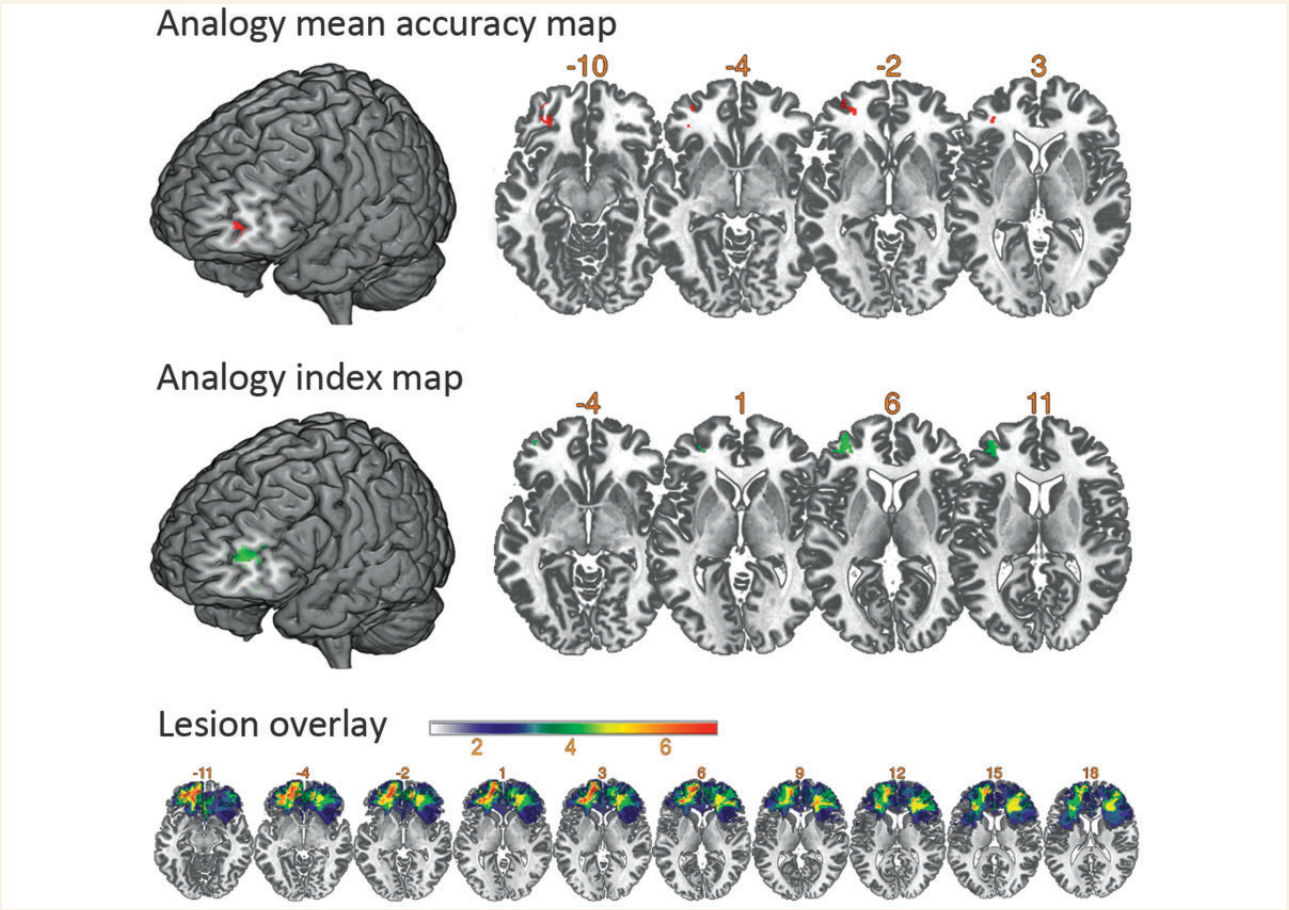

Figure 2 Overlap of patient lesions and statistical VLSM maps obtained for the Analogy mean accuracy and Analogy Index scores. The VLSM maps are superimposed on a normalized T_1 MRI from a single subject in MNI space. Statistical maps were generated using the Brunner-Munzel test. Maps were thresholded at a $P < 0.05$ and corrected for multiple comparisons (family-wise error correction by permutations).

significant association was observed with the Analogy index. Age, education, lesion delay and lesion volume did not significantly differ between the 'Disconnected' and 'Intact' groups for these four analogy-related tracts, except that the patients with a uncinate fasciculus disconnection had an increased age. Disconnection of the left arcuate fasciculus was not associated with a significant deficit, perhaps because it was disconnected in only five patients. None of the selected tracts in the right hemisphere was associated with a deficit in an Analogy or Match tasks when disrupted.

Both the VLSM and disconnection approaches show that left-brain lesions were associated with analogical difficulties. Note that none of the descriptive, clinical or neuropsychological data significantly differed between the right brain-damaged ($n = 9$) and left brain-damaged patients ($n = 14$) (Supplementary Table 2).

VLSM-based approach

In a second approach, we built the VLSM connectome map composed of the tracts connected to the VLSM Analogy region. This map is shown in Supplementary Fig. 2. For each patient, the probability of disconnection of the VLSM connectome map and the number of disconnected tracts among the VLSM connected tracts are provided in Supplementary Table 3. The probability of disconnection of the VLSM connectome map was significantly correlated with the Analogy mean accuracy score ($r_s = -0.511$; $P = 0.006$) and with the Analogy Index ($r_s = -0.471$; $P = 0.013$). This result indicates that a lesion that disconnected the 'VLSM Analogy region' affected analogical reasoning. The correlations of the probability of disconnection of the VLSM connectome map with age ($r_s = 0.262$), education ($r_s = -0.201$) and lesion volume ($r_s = 0.366$) were not significant.

Tracts connected to the VLSM Analogy region included the left anterior thalamic radiation, fronto-marginal tract, IFOF, uncinate fasciculus, orbitopolar tract, superior longitudinal fasciculus (branch 3), fronto-pontine projections, and frontostriatal fasciculus. Among these tracts, we observed significant correlations between the number of disconnected tracts per patient and the Analogy mean

Table 2 Descriptive data, neuropsychological scores, analogy performance, and statistical group comparisons between the VLSM Analogy group and other patient group

	VLSM Analogy group (n = 5)	Other patient group (n = 22)	Statistical comparisons
Descriptive data: mean (SD)			
Age (years)	55.40 (18.93)	45.36 (14.75)	U = 34.0, ns
Education (years)	11.20 (5.12)	14.91 (3.08)	U = 25.0, ns
Lesion volume (cm^3)	55.20 (56.12)	27.40 (21.89)	U = 37.0, ns
Lesion-testing delay (months)	68.8 (38.11)	53.45 (45.91)	U = 42.0, ns
Neuropsychological data: mean (SD)			
FAB (/18)	15.20 (0.84)	15.82 (1.79)	U = 36.5, ns
Semantic fluency	30.00 (7.84)	27.91 (7.83)	U = 49.5, ns
Lexical fluency	19.60 (5.13)	19.86 (7.46)	U = 47.5, ns
Stroop interference	−3.81 (1.56)	1.56 (5.22)	**U = 9.0, P = 0.002**
Experimental conditions: mean % (SD)			
MatchApply	87.14 (6.49)	92.69 (8.85)	U = 25.0, ns
MatchFind	86.43 (7.74)	89.29 (12.42)	U = 36.0, ns
AnalogyApply	61.72 (14.31)	79.78 (11.90)	**U = 10.5, P = 0 .003**
Cross trials	61.67 (14.78)	77.18 (13.27)	**U = 21.5, P = 0.035**
Intra trials	61.67 (15.13)	82.20 (13.37)	**U = 10.5, P = 0.003**
AnalogyFind	53.75 (9.81)	76.20 (10.24)	**U = 7.0, P = 0.001**
Cross trials	44.52 (18.74)	70.30 (14.51)	**U = 16.5, P = 0.014**
Intra trials	61.67 (9.03)	81.63 (9.24)	**U = 7.0, P = 0.001**
Indices			
Analogy index	−41.30 (20.04)	−15.79 (8.56)	**U = 9.0, P = 0.002**
Find index	−7.75 (8.94)	−4.41 (6.97)	U = 39.0, ns
Cross index	−17.53 (25.14)	−11.21 (11.46)	U = 50.5, ns

Values are means (SD) or mean percentage of correct responses (SD) for experimental tasks. Exact P-values significant at $P < 0.05$ are provided. ns = non-significant.

accuracy score ($r_s = -0.553$; $P = 0.003$) as well as the Analogy Index ($r_s = -0.416$; $P = 0.031$). Correlations with age ($r_s = 0.334$), education ($r_s = -0.131$) and lesion volume ($r_s = 0.024$) were not significant. Among all other tracts (tracts not connected to the VLSM analogy region), the Analogy mean accuracy score and Analogy index were not correlated with the number of disconnected tracts per patient [$r_s = 0.126$ and 0.122, respectively; not significant (ns)], but lesion volume was correlated ($r_s = 0.693$; $P < 0.001$). These findings indicate that analogical reasoning depends on connectivity of the VLSM region independent of lesion size.

Value of Analogy tasks in clinical practice

To further explore the value of our Analogy task in clinical practice, we analysed a subsample of the original trials. Patients in the 'damaged left rostrolateral PFC' group (with left rostrolateral PFC anatomically defined, $n = 7$) had poorer performances than those in the 'intact left rostrolateral PFC' group ($n = 20$) in the AnalogyFind-short version condition but not in the MatchFind-short version condition, and their Analogy index-short version was significantly greater (Supplementary Table 4).

We explored the discriminative value of the short version of the analogy tasks with regard to brain damage location (damaged versus intact left rostrolateral PFC) using ROC curves (Supplementary Fig. 3). The AUCs showed that the accuracies of the AnalogyFind-short version performance (AUC = 0.925; $P = 0.001$) and of the Analogy index-short version (AUC = 0.954; $P < 0.001$) were very good, but that the MatchFind-short version poorly discriminated among the patients (AUC = 0.707; $P = 0.109$).

Examination of the coordinate points of the ROC curves showed that an AnalogyFind-short version score of below 65.3% [which corresponds to the mean performance of the controls minus 1.5 standard deviation (SD)] had a sensitivity of 85.7% and a specificity of between 85 and 90%. An Analogy index-short version that was lower than –33% (absolute value > 33) had a sensitivity of 85.7% and a specificity of between 90 and 95%. The Analogy index-short version was as sensitive as the AnalogyFind-short version when discriminating the patients, and it had a slightly better specificity. Thus, an Analogy index-short version score that exceeded 1.5 SD from the mean score of the healthy controls (< –33%) was used as a cut-off to define an analogical reasoning impairment.

To further characterize the value of such a cut-off in brain-damaged patients, we analysed the cognitive profile and visualized the lesion location of the patients as a function of their deficit in analogical reasoning.

Table 4 shows that the two groups did not differ significantly in age, education, lesion volume, mean lesion-testing

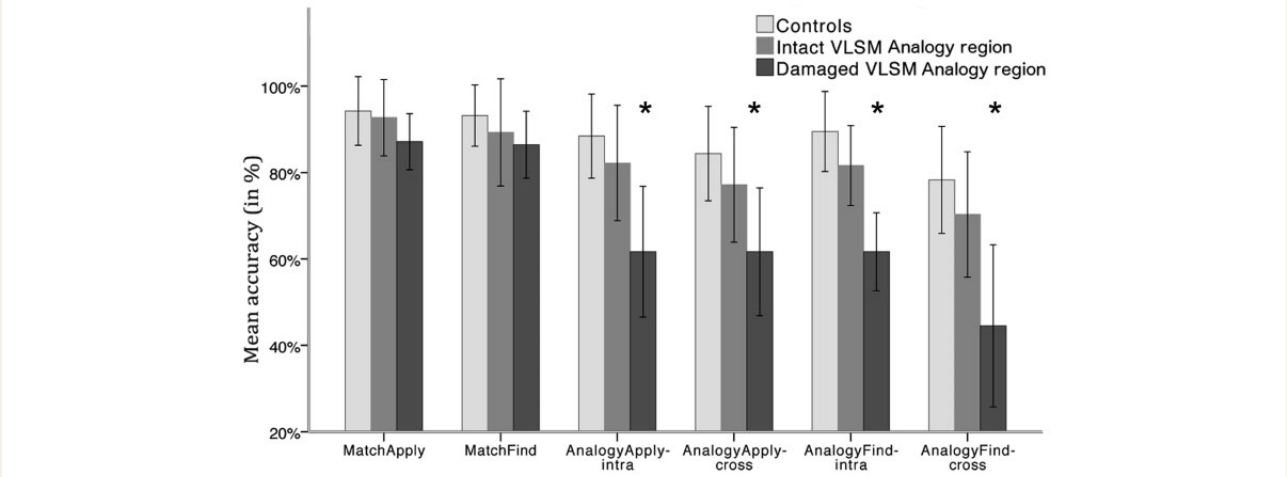

Figure 3 Analogy performance of patients with a lesion involving the 'VLSM Analogy region' compared to those with a lesion that spares this region and to healthy subjects. The mean accuracy (in %) and SD (error bars) under each experimental condition are displayed for patients with a lesion involving the VLSM Analogy region associated with a deficit in Analogy mean accuracy scores (dark grey), for patients with a lesion that spares this region (light grey) and for healthy subjects (very light grey). The performance on the Analogy tasks (but not on the Match tasks) differed significantly between the two patient groups. *Significant difference at a $P < 0.05$ between patients with a lesion involving the 'VLSM Analogy region' compared to those with a lesion that spares this region.

delay or neuropsychological scores, especially for those tasks that tap into executive functions (Table 1). This finding suggests that other cognitive deficits cannot explain the analogy difficulties. Figure 4 shows that the lesions of the patients with impaired analogical reasoning overlapped mainly in the left rostrolateral PFC region, whereas the lesions of the patients with preserved analogical reasoning overlapped in the right PFC.

In summary, the short version of the tasks was sufficiently sensitive to confirm the critical role of the left rostrolateral PFC in analogical reasoning, with a high accuracy of the Analogy index in distinguishing the patients with a left rostrolateral PFC lesion.

Discussion

The current study focused on the impacts of prefrontal lesions on analogical reasoning. The results obtained using three distinct approaches (VLSM, disconnection, and ROC analyses) converge to show the critical role of the left rostral prefrontal region in analogical reasoning. Two new findings emerge from this work. First, analogical reasoning specifically depends on the integrity of the left rostrolateral PFC and/or on the integrity of some of its long-range connections. Second, our analogy task very accurately predicts a left rostrolateral PFC lesion and could be used as a new tool to assess brain-damaged patients. These findings have important clinical implications because analogical reasoning and the more general functions of the rostral part of the PFC are poorly assessed in clinical practice.

Analogy and the integrity of the prefrontal cortex and/or its connections

Few data are available regarding analogical reasoning abilities in patients with brain damage. Following the two studies that explored neurological patients with diffuse frontal damage (Morrison *et al.*, 2004; Krawczyk *et al.*, 2008), the current VLSM analysis specifies which area in the PFC is critical for analogical reasoning. This critical area is located in the rostrolateral PFC, encompasses BA 10 and 47 and is left lateralized (Fig. 2). A lesion of this region is not associated with a deficit in the perceptual matching condition, which suggests that analogical reasoning is relatively specifically impaired when this region is damaged (Table 2 and Fig. 3). As illustrated in Supplementary Fig. 4, this result converges with the conclusions drawn from other approaches, such as functional imaging (Volle, *et al.*, 2010; and for reviews see Krawczyk, 2012; Vartanian, 2012) and morphometry (Aichelburg *et al.*, 2016). The left rostrolateral PFC has been observed in functional imaging studies using different analogy tasks that involved distinct types of relationships in the semantic or visuospatial domains, which suggests a domain-general role of the left rostrolateral PFC in analogies. However, the precise role of this rostrolateral PFC region in analogy, and in cognition in general, is not clearly understood. Previous studies have suggested that this rostrolateral PFC region is involved in relational integration (Christoff *et al.*, 2001; Kroger *et al.*, 2002; Ruff *et al.*, 2003; Ramnani and Owen, 2004; Krawczyk *et al.*, 2011), abstraction (Christoff *et al.*, 2009), and the mapping of similarities (Bunge *et al.*, 2005; Garcin *et al.*, 2012). Our task manipulation did

Table 3 Impact of tract disconnection on age, education, lesion volume, delay between lesion and testing, and analogy performance

	Age (years)	Education (years)	Lesion volume (cc)	Lesion-testing delay (months)	Match mean (%)	Analogy mean (%)	Analogy-index	Find-index	Cross-index
Left									
IFOF-L	U = 51.5, ns	U = 81.0, ns	U = 79.0, ns	U = 84.5, ns	U = 60.0, ns	**U = 36.6, *P* = 0.008**	**U = 39.0, *P* = 0.012**	U = 84.0, ns	**U = 47.5, *P* = 0.038**
Disconnected (*n* = 12)	53.50 (16.96)	13.83 (4.51)	37.19 (39.20)	57.17 (46.87)	90.08 (4.40)	68.92 (12.30)	−27.86 (17.43)	−5.64 (8.78)	−18.50 (15.57)
Intact	42.20 (13.09)	14.53 (3.09)	28.84 (24.55)	55.60 (46.52)	90.40 (11.31)	78.33 (12.49)	−14.63 (9.58)	−4.54 (6.14)	−7.49 (11.87)
UF-L	**U = 39.0, *P* = 0.014**	U = 83.0, ns	U = 79.0, ns	U = 80.5, ns	U = 57.0, ns	**U = 35.0, *P* = 0.007**	**U = 35.0, *P* = 0.008**	U = 78.0, ns	U = 55.5, ns
Disconnected (*n* = 11)	56.00 (15.29)	13.91 (4.72)	37.91 (41.03)	59.45 (48.45)	89.82 (4.51)	68.09 (12.55)	−28.83 (17.94)	−6.00 (9.11)	−18.00 (16.22)
Intact	41.19 (13.28)	14.44 (3.01)	28.86 (23.72)	54.13 (45.33)	90.56 (10.95)	78.31 (12.06)	−14.79 (9.28)	−4.35 (5.98)	−8.52 (12.19)
FMT-L	U = 49.0, ns	U = 68.0, ns	U = 51.0, ns	U = 76.5, ns	**U = 39.0, *P* = 0.029**	**U = 30.5, *P* = 0.008**	**U = 34.0, *P* = 0.015**	U = 59.0, ns	U = 54.5, ns
Disconnected (*n* = 9)	54.44 (16.53)	13.56 (5.20)	45.72 (41.55)	56.89 (43.96)	88.67 (4.15)	66.00 (13.03)	−30.78 (19.46)	−7.37 (9.05)	−18.49 (18.04)
Intact	43.61 (14.40)	14.56 (2.85)	25.97 (23.83)	56.00 (47.91)	91.06 (10.38)	78.22 (11.34)	−15.38 (8.88)	−3.85 (6.20)	−9.33 (11.73)
ATR-L	U = 79.0, ns	U = 81.0, ns	U = 86.0, ns	U = 84.0, ns	U = 54.5, ns	**U = 38.0, *P* = 0.009**	U = 57.0, ns	U = 85.0, ns	**U = 46.5, *P* = 0.03**
Disconnected (*n* = 14)	49.07 (17.83)	13.86 (4.20)	34.60 (36.61)	59.00 (48.69)	88.71 (7.80)	69.29 (11.94)	−25.40 (17.30)	−5.49 (8.57)	−18.19 (14.53)
Intact	45.23 (13.49)	14.62 (3.25)	30.35 (26.25)	53.38 (44.21)	91.92 (9.77)	79.38 (12.58)	−15.25 (10.05)	−4.53 (5.94)	−6.13 (11.98)
AF-L	U = 53.0, ns	**U = 17.5, *P* = 0.016**	U = 52.0, ns	U = 53.5, ns	U = 54.5, ns	U = 44.0, ns	U = 42.0, ns	U = 44.0, ns	U = 30.0, ns
Disconnected (*n* = 5)	46.00 (19.60)	10.80 (3.35)	47.96 (61.66)	55.20 (55.12)	92.00 (3.46)	68.20 (17.88)	−31.93 (25.20)	−2.83 (6.23)	−21.96 (15.54)
Intact	47.50 (15.23)	15.00 (3.41)	29.05 (20.87)	56.55 (44.89)	89.86 (9.61)	75 50 (11.84)	−17.92 (10.81)	−5.52 (7.56)	−10.21 (13.66)
Right									
IFOF-R	U = 69.0, ns	U = 80.5, ns	**U = 48.0, *P* = 0.05**	U = 84.0, ns	U = 78.5, ns	U = 62.0, ns	U = 73.0, ns	U = 75.0, ns	U = 50.0, ns
Disconnected (*n* = 11)	44.09 (13.54)	14.18 (3.34)	40.05 (21.79)	51.55 (38.39)	90.64 (10.32)	77.36 (13.43)	−16.53 (11.23)	−3.94 (6.69)	−5.79 (12.81)
Intact	49.38 (17.13)	14.25 (4.07)	27.39 (36.53)	59.56 (51.20)	90.00 (7.91)	71.94 (12.77)	−23.25 (16.81)	−5.77 (7.81)	−16.91 (14.14)
UF-R	U = 88.0, ns	U = 76.5, ns	**U = 44.0, *P* = 0.025**	U = 70.0, ns	U = 75.5, ns	U = 74.0, ns	U = 89.0, ns	U = 84.0, ns	U = 65.5, ns
Disconnected (*n* = 11)	45.55 (14.71)	14.00 (3.55)	44.06 (38.45)	58.82 (42.38)	91.36 (10.19)	76.09 (14.50)	−19.36 (13.86)	−5.24 (6.92)	−7.33 (13.00)
Intact	48.38 (16.73)	14.38 (3.95)	24.63 (23.89)	54.56 (49.27)	89.5 (7.93)	72.81 (12.29)	−21.31 (16.02)	−4.87 (7.77)	−15.86 (14.80)
FMT-R	U = 57.5, ns	U = 55.5, ns	**U = 20.0, *P* = 0.002**	U = 67.5, ns	U = 61.0, ns	U = 57.5, ns	U = 63.0, ns	U = 63.0, ns	U = 53.0, ns
Disconnected (*n* = 8)	42.88 (15.97)	15.50 (2.83)	49.29 (17.51)	47.75 (36.92)	93.13 (4.79)	79.25 (7.32)	−16.18 (8.66)	−3.49 (6.93)	−5.58 (15.01)
Intact	49.05 (15.66)	13.68 (3.99)	25.50 (33.73)	59.89 (49.51)	89.05 (9.86)	72.00 (14.47)	−22.33 (16.76)	−5.67 (7.53)	−15.25 (13.63)
ATR-R	U = 82.5, ns	U = 83.5, ns	**U = 48.0, *P* = 0.041**	U = 73.5, ns	U = 65.5, ns	U = 52.0, ns	U = 67.0, ns	U = 88, ns	**U = 46.5, *P* = 0.033**
Disconnected (*n* = 15)	46.27 (14.16)	14.47 (3.16)	43.41 (36.60)	62.07 (46.23)	91.53 (9.04)	77.47 (12.88)	−17.47 (12.35)	−4.98 (6.70)	−7.14 (11.88)
Intact	48.42 (18.03)	13.92 (4.46)	18.97 (16.71)	49.08 (46.16)	88.67 (8.56)	70.00 (12.60)	−24.31 (17.44)	−5.08 (8.29)	−18.94 (15.20)
AF-R	U = 58.5, ns	U = 34.5, ns	U = 30.0, ns	U = 62.5, ns	U = 37.0, ns	U = 45.5, ns	U = 54.0, ns	U = 42.0, ns	U = 39.0, ns
Disconnected (*n* = 6)	45.67 (15.11)	16.33 (3.01)	48.60 (27.26)	53.50 (40.50)	94.33 (5.85)	79.83 (7.41)	−16.60 (7.98)	−1.89 (4.66)	−4.32 (14.74)
Intact	47.67 (16.21)	13.62 (3.75)	27.96 (31.71)	57.10 (48.07)	89.10 (9.24)	72.52 (13.99)	−21.63 (16.37)	−5.92 (7.75)	−14.69 (13.89)

Tracts were defined *a priori* based on Aichelburg *et al.* (2016).

Table 4 Descriptive data, neuropsychological scores, analogy scores for the short version of the task, and statistical comparisons between patients with an impaired versus preserved analogy performance

	Patients with impaired analogy scores (n = 7)	Patients with preserved analogy scores (n = 20)	Group comparisons
Descriptive data: mean (SD)			
Age (years)	54.43 (17.02)	44.70 (14.84)	U = 44.5, ns
Education (years)	13.14 (5.81)	14.60 (2.78)	U = 52.0, ns
Lesion volume (cc)	48.66 (47.24)	48.18 (21.84)	U = 39.0, ns
Lesion-testing delay (months)	70.14 (0.63)	68.00 (37.40)	U = 45.0, ns
Neuropsychological scores: mean (SD)			
FAB (/18)	15.57 (1.27)	15.75 (1.80)	U = 57.5, ns
Semantic fluency	30.86 (7.17)	27.40 (7.88)	U = 55.5, ns
Lexical fluency	21.00 (7.30)	19.40 (7.04)	U = 66.5, ns
Stroop interference	−1.66 (4.27)	1.34 (5.35)	U = 36.0, ns
Experimental conditions short version: mean % (SD)			
MatchFind-short version	87.77 (7.39)	89.11(12.93)	U = 51.5, ns
AnalogyFind-short version	51.33 (9.64)	77.68 (11.67)	**U = 7.0, P < 0.001**
Analogy index-short version	−53.43 (11.71)	−13.67 (11.65)	**U < 1.0, P < 0.001**

Values are mean scores (SD) or mean percentage of correct responses (SD) for the short experimental task. Exact P-values significant at a $P < 0.05$ are provided. FAB = frontal assessment battery; ns = non-significant

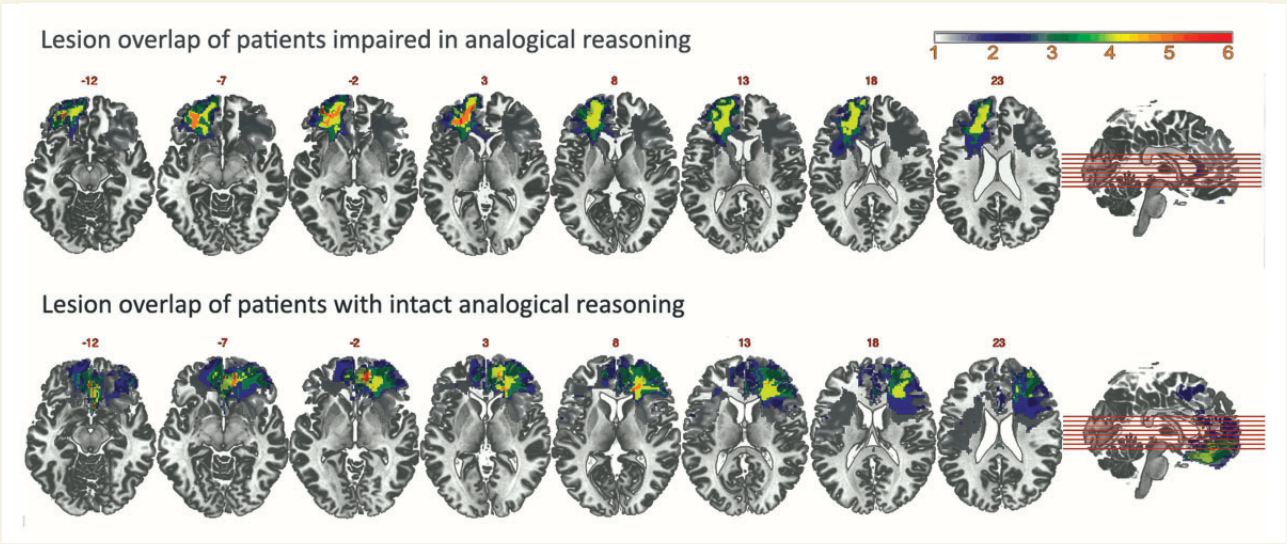

Figure 4 Overlaps of lesions from patients with specific impairment in analogical reasoning and from patients with normal performance. Patients with impaired analogical reasoning were defined by an Analogy index < −1.5 SD of the mean score of the healthy subjects (n = 7 patients) in the short version of the tasks. Analogical reasoning was considered 'intact' when the Analogy index was within 1.5 SD of the mean score of the healthy subjects (n = 20 patients). The colour code is represented on the upper right-hand side, and it ranges from white (n = 1) to red (n = 6), indicating maximum overlap. The axial slices range from z = −12 to z = 23 in the MNI.

not provide evidence of a significant difference that would have suggested a role in inference processes (Find versus Apply) or in remote mapping that allows for abstract generalization (Cross- versus Intra-dimensional analogy), although there is evidence from other studies that the left PFC is important for rule induction (Reverberi *et al.*, 2005) and for distant analogies (Green *et al.*, 2010). However, in patients with left rostrolateral PFC damage, the deficit was deeper for inferences based on cross-dimensional mapping (Table 2 and Fig. 3). Thus, it remains possible that these differences exist but were missed because of a lack of sufficient statistical power or due to insufficient lesion overlap.

A left dominance of PFC for analogical reasoning was previously highlighted in functional imaging studies (Bunge *et al.*, 2009; Vartanian, 2012) and in one repetitive transcranial magnetic stimulation study (Boroojerdi *et al.*, 2001). However, the lateralization of rostrolateral PFC functions is not understood. The role of language in analogies could be at play, but it cannot entirely explain a left lateralization because tasks that used non-verbal analogies also recruited the left rostrolateral PFC (Wharton *et al.*,

2000; Christoff *et al.*, 2003; Bunge *et al.*, 2009; Hampshire *et al.*, 2011; Watson and Chatterjee, 2012; Wendelken *et al.*, 2012), and analogical reasoning difficulties are not associated with reduced fluencies in our patients.

VLSM analysis did not identify other critical prefrontal areas for analogies, although previous functional imaging studies have shown that several prefrontal regions are involved in analogical reasoning (Christoff *et al.*, 2001; Bunge *et al.*, 2005; Geake and Hansen, 2005, 2010; Green *et al.*, 2006, 2012; Cho *et al.*, 2007; Wendelken *et al.*, 2008, 2012; Krawczyk, *et al.*, 2010*b*, 2011; Volle, *et al.*, 2010; Hampshire *et al.*, 2011; Preusse *et al.*, 2011; Krawczyk, 2012), as well as temporal and parietal regions. Within the PFC, it is possible that the other prefrontal regions that support analogical reasoning are less lateralized, which allows for the contralateral cortex to compensate for this function. However, we cannot exclude the possibility that the analyses missed some other critical prefrontal region because of the lack of statistical power achieved for some of the regions and because only partial coverage of the frontal lobes was obtained. It is likely that the left rostrolateral PFC operates via interaction with more posterior regions in the prefrontal, parietal and temporal lobes (Aichelburg *et al.*, 2016; Cocchi *et al.*, 2014; Rojkova *et al.*, 2015). Because we examined only patients with prefrontal brain lesions, no conclusion could be made on the critical roles of the parietal and temporal lobes. Nevertheless, our track-wise lesion-deficit approach provided some clues about the roles of the interactions of the left rostrolateral PFC with other brain regions for analogy performance.

We found that disconnection of the left IFOF, uncinate fasciculus, fronto-marginal tract, or anterior thalamic radiation was associated with a deficit in Analogy tasks (Table 3). These results are consistent with a previous tractography study in healthy subjects (Aichelburg *et al.*, 2016) and confirm the importance of the left hemisphere for analogical reasoning. Here, anatomical connections between the temporal cortices (via the uncinate fasciculus), the occipital cortex (via the IFOF), and subcortical structures via the anterior thalamic radiations appear to play a role in analogical reasoning. The VLSM-based approach further showed that an analogical reasoning impairment was associated with a disconnection of the VLSM Analogy region. Owing to these connections, information can converge within the left rostrolateral PFC, coming from distinct domains or networks (Sakai and Passingham, 2003; Parkin *et al.*, 2015).

Recent resting-state studies have emphasized the importance of functional networks for high-level cognitive functions and that the disruption of these networks could better explain a deficit in high-level cognition than lesion location *per se* (Woolgar *et al.*, 2010; Gratton *et al.*, 2012; Warren *et al.*, 2014; Corbetta *et al.*, 2015). In this context, the result that a very circumscribed lesion site is critical for analogical reasoning is puzzling. This lesion site may be critical because damage to this area cannot be compensated for and/or because several tracts that converge at this site must be conjointly damaged to provoke a deficit, as suggested by the correlation between analogy performance and the number of tracts connected to this region that were affected by the lesions. This latter interpretation would match the cortical disconnection mechanism that was previously hypothesized by Norman Geschwind (1965). Overall, these results suggest that the left rostrolateral PFC region is a functional 'hub' or an essential relay station in the analogy network. This interpretation argues for the role of this region in integrating information of different natures or domains.

Clinical application of the study: a new assessment tool

Although recent cognitive theories based on functional imaging place the rostral PFC at the top of a frontal hierarchical functioning model that subserves reasoning, problem solving, behavioural adaptation and abstraction (Badre and D'Esposito, 2007; Koechlin and Summerfield, 2007; Badre, 2008; Christoff *et al.*, 2009; Krawczyk *et al.*, 2011), functions of the rostral PFC are poorly assessed in clinical practice. Only recently has Burgess and Shallice's work on multitasking (Shallice and Burgess, 1991) generated specific tasks for physicians (Burgess *et al.*, 2006, 2009). Existing neuropsychological tools offer very few tests of abstract thinking or reasoning, and the critical brain networks for these tests are not well understood, as mentioned in the 'Introduction' section. The conceptual framework of analogical reasoning provides cognitive tasks that tap into abstract thinking and relational reasoning abilities, and the cerebral networks associated with these tasks have begun to be clarified. Hence, patients could benefit from the transfer of analogical reasoning tasks to clinical practice. In this study, we simulated a short version of our analogy task that could be transferred to clinical practice and showed that it had very good sensitivity and specificity for predicting left rostrolateral PFC injury, which demonstrates that even a small set of analogy trials is valuable for discriminating among different types of patient damage (Supplementary Fig. 3). The Analogy index appeared to be the most specific measure for analogical reasoning deficits.

Impairment in our Analogy tasks was not associated with global executive dysfunction, which suggests that analogical reasoning is a cognitive ability that is not entirely captured by classical executive neuropsychological tests (Table 4). Our results rather support a functional specialization within the PFC, with a distinct role of the rostral PFC compared with the more posterior areas. Previous studies have highlighted the role of inhibition abilities and interference control for analogical reasoning (Morrison *et al.*, 2004; Krawczyk *et al.*, 2008; Bugaiska and Thibaut, 2015). These studies suggest the possibility that analogy deficit in patients with left rostrolateral PFC lesion may

be due to poor inhibition abilities. Although our VLSM analysis cannot rule out this explanation, other parts of our findings do not favour this hypothesis because patients with impaired analogy scores did not have more interference sensitivity than patients with preserved analogy scores (Table 4). In addition, response inhibition is usually associated with right or medial frontal regions (Stuss *et al.*, 2001; van Veen and Carter, 2005; Volle *et al.*, 2012; Tsuchida and Fellows, 2013; Aron *et al.*, 2014; Hornberger and Bertoux, 2015; Robinson *et al.*, 2015).

Finally, patients with frontal lesions of different aetiologies have been included in this study, which is a limitation because different pathologies affect the brain differently with distinct time courses and mechanisms of plasticity. However, a recent study has demonstrated that frontal lesions of different vascular and tumour aetiologies have similar effects on executive testing and fluid reasoning (Cipolotti *et al.*, 2015). This finding supports the idea that the pooling of lesions with various physiopathological mechanisms in the same analysis is a valid methodological approach to exploring the organization of frontal functions. This approach has been used previously (Volle *et al.*, 2008, 2012; Tsuchida and Fellows, 2013; Azuar *et al.*, 2014), including lesions caused by epilepsy surgery (Tranel *et al.*, 2008; Gläscher *et al.*, 2009; Chapados and Petrides, 2013). The pooling of lesions with different physiopathological mechanisms allowed us to more completely cover the possible lesion locations in the PFC, including the rostral part, which is rarely affected by ischaemic strokes. Furthermore, this approach could mitigate statistical and spatial biases due to stroke locations (Nachev *et al.*, 2008; Volle *et al.*, 2013; Mah *et al.*, 2014). In this context, our findings suggest that assessing analogical reasoning in brain-damaged patients has a clinical value that is independent of the lesion aetiology.

Overall, the short version of our analogy task could enrich the classical neuropsychological toolbox for the assessment of high-level cognitive functions that depend on the rostral PFC. The ecological validity of this test in real-world problem-solving remains to be demonstrated. Hence, the short version of the Analogy test will be validated in an independent and larger sample of patients with more homogeneous lesions and in a group of controls matched for age and education. We will examine correlations to other relational reasoning or problem-solving tasks to further improve the value of the test as a tool for the evaluation of analogical reasoning abilities in clinical practice.

Conclusions

Analogical reasoning plays a significant role in inferring general representations from similarities, which in turn can be applicable to solving new problems. The current lesion study has demonstrated for the first time, using three distinct approaches, that the left rostrolateral PFC (along with its long-range anatomical connections) is specifically critical for analogical reasoning and that a left rostrolateral PFC lesion could impair the relational integration and matching processes that are involved in abstract thinking. Despite a relatively small sample size examined in this study, these results converge clearly with existing neuroimaging findings on analogy. Furthermore, our study provides a sensitive and specific new neuropsychological test that can be transferred to everyday clinical practice, for the assessment of analogical reasoning in patients. These findings could be useful to clinicians by informing them of the expected consequences of rostral prefrontal damage on high-level cognitive functions and proposing a tool for their assessment.

Acknowledgements

The authors thank Prof. Claude Adam, Dr Carole Azuar, Dr Dorian Chauvet, Dr Vincent Degos, Prof. Damien Galanaud, Dr Florence Laigle, Dr Anne Leger, and Prof. Vincent Navarro for their help in recruiting the patients.

Funding

This work was supported by the 'Agence Nationale de la Recherche' [grants number ANR-09-RPDOC-004-01, E.V.] the "Fondation pour la recherche médicale", and the 'Societe Française de Neurologie' (M.L.B. and D.B.). The research leading to these results received funding from the program 'Investissements d'avenir' ANR-10-IAIHU-06 and from the project PHENOTYPES, no. ANR-13-JSV4- 0001-01.

Supplementary material

Supplementary material is available at *Brain* online.

References

Ahmed FS, Miller LS. Adequate proverb interpretation is associated with performance on the independent living scales. Neuropsychol Dev Cogn B Aging Neuropsychol Cogn 2015; 22: 376–87.

Aichelburg C, Urbanski M, Thiebaut de Schotten M, Humbert F, Levy R, Volle E. Morphometry of left frontal and temporal poles predicts analogical reasoning abilities. Cereb Cortex 2016; 26: 915–32.

Andersen SM, Rapcsak SZ, Beeson PM. Cost function masking during normalization of brains with focal lesions: still a necessity? Neuroimage 2010; 53: 78–84.

Aron AR, Robbins TW, Poldrack RA. Inhibition and the right inferior frontal cortex: one decade on. [Review]. Trends Cogn Sci 2014; 18: 177–85.

Azuar C, Reyes P, Slachevsky A, Volle E, Kinkingnehun S, Kouneiher F, et al. Testing the model of caudo-rostral organization of cognitive control in the human with frontal lesions. Neuroimage 2014; 84: 1053–60.

Badre D. Cognitive control, hierarchy, and the rostro-caudal organization of the frontal lobes. [Review]. Trends Cogn Sci 2008; 12: 193–200.

Badre D, D'Esposito M. Functional magnetic resonance imaging evidence for a hierarchical organization of the prefrontal cortex. J Cogn Neurosci 2007; 19: 2082–99.
Baldo JV, Bunge SA, Wilson SM, Dronkers NF. Is relational reasoning dependent on language? A voxel-based lesion symptom mapping study. Brain Lang 2010; 113: 59–64.
Bates E, Wilson SM, Saygin AP, Dick F, Sereno MI, Knight RT, et al. Voxel-based lesion-symptom mapping. Nat Neurosci 2003; 6: 448–50.
Bethell-Fox CE, Lohman DF, Snow RE. Adaptive reasoning: componential and eye movement analysis of geometric analogy performance. Intelligence 1984; 8: 205–38.
Blanchette I, Dunbar K. How analogies are generated: the roles of structural and superficial similarity. Mem Cognit 2000; 28: 108–24.
Boroojerdi B, Phipps M, Kopylev L, Wharton CM, Cohen LG, Grafman J. Enhancing analogic reasoning with rTMS over the left prefrontal cortex. Neurology 2001; 56: 526–8.
Bugaiska A, Thibaut J-P. Analogical reasoning and aging: the processing speed and inhibition hypothesis. Aging Neuropsychol Cogn 2015; 22: 340–56.
Bunge SA, Helskog EH, Wendelken C. Left, but not right, rostrolateral prefrontal cortex meets a stringent test of the relational integration hypothesis. Neuroimage 2009; 46: 338–42.
Bunge SA, Wendelken C, Badre D, Wagner AD. Analogical reasoning and prefrontal cortex: evidence for separable retrieval and integration mechanisms. Cereb Cortex 2005; 15: 239–49.
Burgess P, Alderman N, Forbes C, Costello A, Coates L, Dawson D, et al. The case for the development and use of 'ecologically valid' measures of executive function in experimental and clinical neuropsychology. J Int Neuropsychol Soc 2006; 12: 194–209.
Burgess PW, Alderman N, Volle E, Benoit RG, Gilbert SJ. Mesulam's frontal lobe mystery re-examined. [Review]. Restor Neurol Neurosci 2009; 27: 493–506.
Cardebat D, Doyon B, Puel M, Goulet P, Joanette Y. Formal and semantic lexical evocation in normal subjects. Performance and dynamics of production as a function of sex, age and educational level. Acta Neurol Belg 1990; 90: 207–17.
Chapados C, Petrides M. Impairment only on the fluency subtest of the frontal assessment battery after prefrontal lesions. Brain 2013; 136: 2966–78.
Cho S, Holyoak KJ, Cannon TD. Analogical reasoning in working memory: resources shared among relational integration, interference resolution, and maintenance. Mem Cognit 2007; 35: 1445–55.
Cho S, Moody TD, Fernandino L, Mumford JA, Poldrack RA, Cannon TD, et al. Common and dissociable prefrontal loci associated with component mechanisms of analogical reasoning. Cereb Cortex 2010; 20: 524–33.
Christoff K, Keramatian K, Gordon AM, Smith R, Mädler B. Prefrontal organization of cognitive control according to levels of abstraction. Brain Res 2009; 1286: 94–105.
Christoff K, Prabhakaran V, Dorfman J, Zhao Z, Kroger JK, Holyoak KJ, et al. Rostrolateral prefrontal cortex involvement in relational integration during reasoning. Neuroimage 2001; 14: 1136–49.
Christoff K, Ream JM, Geddes LP, Gabrieli JD. Evaluating self-generated information: anterior prefrontal contributions to human cognition. Behav Neurosci 2003; 117: 1161–8.
Cipolotti L, Healy C, Chan E, Bolsover F, Lecce F, White M, et al. The impact of different aetiologies on the cognitive performance of frontal patients. Neuropsychologia 2015; 68: 21–30.
Cocchi L, Halford GS, Zalesky A, Harding IH, Ramm BJ, Cutmore T, et al. Complexity in relational processing predicts changes in functional brain network dynamics. Cereb Cortex 2014; 24: 2283–96.
Corbetta M, Ramsey L, Callejas A, Baldassarre A, Hacker CD, Siegel JS, et al. Common behavioral clusters and subcortical anatomy in stroke. Neuron 2015; 85: 927–41.
Crinion J, Ashburner J, Leff A, Brett M, Price C, Friston K. Spatial normalization of lesioned brains: performance evaluation and impact on fMRI analyses. Neuroimage 2007; 37: 866–75.
Crone EA, Wendelken C, van Leijenhorst L, Honomichl RD, Christoff K, Bunge SA. Neurocognitive development of relational reasoning. Dev Sci 2009; 12: 55–66.
Delis DC, Kramer JH, Kaplan E. The Delis-Kaplan executive function system. San Antonio: TX: The Psychological Corporation; 2001.
Dubois B, Slachevsky A, Litvan I, Pillon B. The FAB: a Frontal Assessment Battery at bedside. Neurology 2000; 55: 1621–6.
Dumontheil I. Development of abstract thinking during childhood and adolescence: the role of rostrolateral prefrontal cortex. [Review]. Dev Cogn Neurosci 2014; 10: 57–76.
Duncan J, Burgess P, Emslie H. Fluid intelligence after frontal lobe lesions. Neuropsychologia 1995; 33: 261–8.
Folstein MF, Folstein SE, McHugh PR. 'Mini-Mental State' - a practical method for grading the cognitive state of patients for the clinician. J Psychiatric Res 1975; 12: 189–98.
Garcin B, Volle E, Dubois B, Levy R. Similar or different? The role of the ventrolateral prefrontal cortex in similarity detection. PloS One 2012; 7: e34164.
Geake JG, Hansen PC. Neural correlates of intelligence as revealed by fMRI of fluid analogies. Neuroimage 2005; 26: 555–64.
Geake JG, Hansen PC. Functional neural correlates of fluid and crystallized analogizing. Neuroimage 2010; 49: 3489–97.
Gentner D. Structure-mapping: a theoretical framework for analogy. Cogn Sci 1983; 7: 155–70.
Gentner D, Holyoak KJ. Reasoning and learning by analogy. Am Psychol 1997; 52: 32–4.
Gentner D, Markman AB. Structure mapping in analogy and similarity. Am Psychol 1997; 52: 45–56.
Gentner D, Medina J. Similarity and the development of rules. Cognition 1998; 65: 263–97.
Gentner D, Rattermann MI, Forbus KD. The roles of similarity in transfer: separating retrievability from inferential soundness. Cogn Psychol 1993; 25: 524–75.
Geschwind N. Disconnexion syndromes in animals and man: Part I [Review]. Brain 1965; 88: 237–94.
Gick NL, Holyoak KJ. Schema induction and analogical transfer. Cogn Psychol 1983; 15: 1–38.
Gläscher J, Tranel D, Paul LK, Rudrauf D, Rorden C, Hornaday A, et al. Lesion mapping of cognitive abilities linked to intelligence. Neuron 2009; 61: 681–91.
Gratton C, Nomura EM, Pérez F, D'Esposito M. Focal brain lesions to critical locations cause widespread disruption of the modular organization of the brain. J Cogn Neurosci 2012; 24: 1275–85.
Green AE, Fugelsang JA, Kraemer DJM, Shamosh NA, Dunbar KN. Frontopolar cortex mediates abstract integration in analogy. Brain Res 2006; 1096: 125–37.
Green AE, Kraemer DJM, Fugelsang JA, Gray JR, Dunbar KN. Connecting long distance: semantic distance in analogical reasoning modulates frontopolar cortex activity. Cereb Cortex 2010; 20: 70–6.
Green AE, Kraemer DJM, Fugelsang JA, Gray JR, Dunbar KN. Neural correlates of creativity in analogical reasoning. J Exp Psychol Learn Mem Cogn 2012; 38: 264–72.
Halford GS, Wilson WH, Phillips S. Relational knowledge: the foundation of higher cognition [Review]. Trends Cogn Sci 2010; 14: 497–505.
Hampshire A, Thompson R, Duncan J, Owen AM. Lateral prefrontal cortex subregions make dissociable contributions during fluid reasoning. Cereb Cortex 2011; 21: 1–10.
Hoffman P, Jefferies E, Lambon Ralph MA. Ventrolateral prefrontal cortex plays an executive regulation role in comprehension of abstract words: convergent neuropsychological and repetitive TMS evidence. J Neurosci Off J Soc Neurosci 2010; 30: 15450–6.
Hofstadter D, Sander E. Surfaces and essences: analogy as the fuel and fire of thinking. 1st edn. New York: Basic Books; 2013.
Holyoak KJ, Thagard P. The analogical mind. Am Psychol 1997; 52: 35–44.
Holyoak KJ, Thagard P. Mental leaps: analogy in creative thought. Cambridge MA: MIT Press; 1995.

Hornberger M, Bertoux M. Right lateral prefrontal cortex—specificity for inhibition or strategy use? Brain 2015; 138: 833–5.
Jung RE, Haier RJ. The Parieto-Frontal Integration Theory (P-FIT) of intelligence: converging neuroimaging evidence [Review]. Behav Brain Sci 2007; 30: 135–54. discussion 154–187.
Kaiser NC, Lee GJ, Lu PH, Mather MJ, Shapira J, Jimenez E, et al. What dementia reveals about proverb interpretation and its neuroanatomical correlates. Neuropsychologia 2013; 51: 1726–33.
Koechlin E, Summerfield C. An information theoretical approach to prefrontal executive function [Review]. Trends Cogn Sci 2007; 11: 229–35.
Krawczyk DC. The cognition and neuroscience of relational reasoning [Review]. Brain Res 2012; 1428: 13–23.
Krawczyk DC, Hanten G, Wilde EA, Li X, Schnelle KP, Merkley TL, et al. Deficits in analogical reasoning in adolescents with traumatic brain injury. Front Hum Neurosci 2010a; 4: 62.
Krawczyk DC, McClelland MM, Donovan CM. A hierarchy for relational reasoning in the prefrontal cortex. Cortex 2011; 47: 588–97.
Krawczyk DC, McClelland MM, Donovan CM, Tillman GD, Maguire MJ. An fMRI investigation of cognitive stages in reasoning by analogy. Brain Res 2010b; 1342: 63–73.
Krawczyk DC, Morrison RG, Viskontas I, Holyoak KJ, Chow TW, Mendez MF, et al. Distraction during relational reasoning: the role of prefrontal cortex in interference control. Neuropsychologia 2008; 46: 2020–32.
Kroger JK, Sabb FW, Fales CL, Bookheimer SY, Cohen MS, Holyoak KJ. Recruitment of anterior dorsolateral prefrontal cortex in human reasoning: a parametric study of relational complexity. Cereb Cortex 2002; 12: 477–85.
Lagarde J, Valabrègue R, Corvol J-C, Garcin B, Volle E, Ber IL, et al. Why do patients with neurodegenerative frontal syndrome fail to answer: 'In what way are an orange and a banana alike?'. Brain 2015; 138: 456–71.
Mah Y-H, Husain M, Rees G, Nachev P. Human brain lesion-deficit inference remapped. Brain 2014; 137: 2522–31.
McDonald CR, Delis DC, Kramer JH, Tecoma ES, Iragui VJ. A componential analysis of proverb interpretation in patients with frontal lobe epilepsy and temporal lobe epilepsy: relationships with disease-related factors. Clin Neuropsychol 2008; 22: 480–96.
Merck C, Charnallet A, Auriacombe S, Belliard S, Hahn-Barma V, Kremin H, et al. La batterie d'évaluation des connaissances sémantiques du GRECO (BECS-GRECO): validation et données normatives. Rev Neuropsychol 2011; 3: 235–55.
Morrison RG, Krawczyk DC, Holyoak KJ, Hummel JE, Chow TW, Miller BL, et al. A neurocomputational model of analogical reasoning and its breakdown in frontotemporal lobar degeneration. J Cogn Neurosci 2004; 16: 260–71.
Murphy P, Shallice T, Robinson G, MacPherson SE, Turner M, Woollett K, et al. Impairments in proverb interpretation following focal frontal lobe lesions. Neuropsychologia 2013; 51: 2075–86.
Nachev P, Coulthard E, Jäger HR, Kennard C, Husain M. Enantiomorphic normalization of focally lesioned brains. Neuroimage 2008; 39: 1215–26.
Parkin BL, Hellyer PJ, Leech R, Hampshire A. Dynamic network mechanisms of relational integration. J Neurosci 2015; 35: 7660–73.
Preusse F, van der Meer E, Deshpande G, Krueger F, Wartenburger I. Fluid intelligence allows flexible recruitment of the parieto-frontal network in analogical reasoning. Front Hum Neurosci 2011; 5: 22.
Ramnani N, Owen AM. Anterior prefrontal cortex: insights into function from anatomy and neuroimaging. Nat Rev Neurosci 2004; 5: 184–94.
Raven JC. Standardization of progressive matrices. Br J Med Psychol 1938; 19: 137–50.
Reverberi C, Lavaroni A, Gigli GL, Skrap M, Shallice T. Specific impairments of rule induction in different frontal lobe subgroups. Neuropsychologia 2005; 43: 460–72.
Ripollés P, Marco-Pallarés J, de Diego-Balaguer R, Miró J, Falip M, Juncadella M, et al. Analysis of automated methods for spatial normalization of lesioned brains. Neuroimage 2012; 60: 1296–306.
Robin N, Holyoak KJ. Relational complexity and the functions of prefrontal cortex. In: Cazzaniga MS, editor. The cognitive neurosciences. Cambridge MA: MIT press; 1995.
Robinson GA, Cipolotti L, Walker DG, Biggs V, Bozzali M, Shallice T. Verbal suppression and strategy use: a role for the right lateral prefrontal cortex? Brain 2015; 138: 1084–96.
Rojkova K, Volle E, Urbanski M, Humbert F, Dell'Acqua F, Thiebaut de Schotten M. Atlasing the frontal lobe connections and their variability due to age and education: a spherical deconvolution tractography study. Brain Struct Funct 2015. Advance Access published on February 15, 2015, doi:10.1007/s00429-015-1001-3.
Ruff CC, Knauff M, Fangmeier T, Spreer J. Reasoning and working memory: common and distinct neuronal processes. Neuropsychologia 2003; 41: 1241–53.
Sakai K, Passingham RE. Prefrontal interactions reflect future task operations. Nat Neurosci 2003; 6: 75–81.
Schmidt GL, Cardillo ER, Kranjec A, Lehet M, Widick P, Chatterjee A. Not all analogies are created equal: associative and categorical analogy processing following brain damage. Neuropsychologia 2012; 50: 1372.
Shallice T, Burgess P. Deficits in strategy application following frontal lobe damage in man. Brain 1991; 114: 727–41.
Smith R, Keramatian K, Christoff K. Localizing the rostrolateral prefrontal cortex at the individual level. Neuroimage 2007; 36: 1387–96.
Stroop JR. Studies of interference in serial verbal reaction. J Exp Psychol 1935; 18: 643–62.
Stuss DT, Floden D, Alexander MP, Levine B, Katz D. Stroop performance in focal lesion patients: dissociation of processes and frontal lobe lesion location. Neuropsychologia 2001; 39: 771–86.
Thibaut J-P, French R, Vezneva M. Cognitive load and semantic analogies: searching semantic space. Psychon Bull Rev 2010a; 17: 569–74.
Thibaut J-P, French R, Vezneva M. The development of analogy making in children: cognitive load and executive functions. J Exp Child Psychol 2010b; 106: 1–19.
Thiebaut de Schotten M, Dell'Acqua F, Ratiu P, Leslie A, Howells H, Cabanis E, et al. From Phineas Gage and monsieur Leborgne to H.M.: revisiting disconnection syndromes. Cereb Cortex 2015; 25: 4812–27.
Thiebaut de Schotten M, Tomaiuolo F, Aiello M, Merola S, Silvetti M, Lecce F, et al. Damage to white matter pathways in subacute and chronic spatial neglect: a group study and 2 single-case studies with complete virtual 'in vivo' tractography dissection. Cereb Cortex 2014; 24: 691–706.
Tisserand DJ, Pruessner JC, Sanz Arigita EJ, van Boxtel MPJ, Evans AC, Jolles J, et al. Regional frontal cortical volumes decrease differentially in aging: an MRI study to compare volumetric approaches and voxel-based morphometry. Neuroimage 2002; 17: 657–69.
Tranel D, Manzel K, Anderson SW. Is the prefrontal cortex important for fluid intelligence? A neuropsychological study using Matrix Reasoning. Clin Neuropsychol 2008; 22: 242–61.
Tsuchida A, Fellows LK. Are core component processes of executive function dissociable within the frontal lobes? Evidence from humans with focal prefrontal damage. Cortex 2013; 49: 1790–800.
van Veen V, Carter CS. Separating semantic conflict and response conflict in the Stroop task: a functional MRI study. Neuroimage 2005; 27: 497–504.
Vartanian O. Dissociable neural systems for analogy and metaphor: implications for the neuroscience of creativity [Review]. Br J Psychol 2012; 103: 302–16.
Volle E, de Lacy Costello A, Coates LM, McGuire C, Towgood K, Gilbert S, et al. Dissociation between verbal response initiation and suppression after prefrontal lesions. Cereb Cortex 2012; 22: 2428–40.

Volle E, Gilbert SJ, Benoit RG, Burgess PW. Specialization of the rostral prefrontal cortex for distinct analogy processes. Cereb Cortex 2010; 20: 2647–59.

Volle E, Kinkingnéhun S, Pochon J-B, Mondon K, Thiebaut de Schotten M, Seassau M, et al. The functional architecture of the left posterior and lateral prefrontal cortex in humans. Cereb Cortex 2008; 18: 2460–9.

Volle E, Levy R, Burgess PW. A new era for lesion-behavior mapping of prefrontal functions. In: Stuss DT, Knight RT, editors. Principles of frontal lobe function. New York: Oxford University Press; 2013. p. 500–523.

Waechter RL, Goel V, Raymont V, Kruger F, Grafman J. Transitive inference reasoning is impaired by focal lesions in parietal cortex rather than rostrolateral prefrontal cortex. Neuropsychologia 2013; 51: 464–71.

Waltz JA, Knowlton BJ, Holyoak KJ, Boone KB, Mishkin FS, de Menerzes Santos M, et al. A system for relational reasoning in human prefrontal cortex. Psychol Sci 1999; 10: 119.

Warren DE, Power JD, Bruss J, Denburg NL, Waldron EJ, Sun H, et al. Network measures predict neuropsychological outcome after brain injury. Proc Natl Acad Sci 2014; 111: 14247–52.

Wartenburger I, Heekeren HR, Preusse F, Kramer J, van der Meer E. Cerebral correlates of analogical processing and their modulation by training. Neuroimage 2009; 48: 291–302.

Watson CE, Chatterjee A. A bilateral frontoparietal network underlies visuospatial analogical reasoning. Neuroimage 2012; 59: 2831–8.

Wechsler D. Technical Manual for the Wechsler Adult Intelligence Test. 3rd edn. San Antonio, TX: The Psychological Corporation; 1997.

Wendelken C, Bunge SA, Carter CS. Maintaining structured information: an investigation into functions of parietal and lateral prefrontal cortices. Neuropsychologia 2008; 46: 665–78.

Wendelken C, Chung D, Bunge SA. Rostrolateral prefrontal cortex: domain-general or domain-sensitive? Hum Brain Mapp 2012; 3: 1952–63.

Wharton CM, Grafman J, Flitman SS, Hansen EK, Brauner J, Marks A, et al. Toward neuroanatomical models of analogy: a positron emission tomography study of analogical mapping. Cogn Psychol 2000; 40: 173–97.

Woolgar A, Parr A, Cusack R, Thompson R, Nimmo-Smith I, Torralva T, et al. Fluid intelligence loss linked to restricted regions of damage within frontal and parietal cortex. Proc Natl Acad Sci 2010; 107: 14899–902.

Wright SB, Matlen BJ, Baym CL, Ferrer E, Bunge SA. Neural correlates of fluid reasoning in children and adults. Front Hum Neurosci 2007; 1: 8.

SUPPLEMENTARY MATERIAL

Supplementary Table 1: Descriptive data, neuropsychological scores, analogy performance, and statistical comparisons between patients and healthy subjects.

	Patients (*n* = 27)	**Healthy subjects (*n* = 54)**	**Group comparisons**
Descriptive data: Mean (SD)			
Age (years)	47.22 (15.70)	45.83 (14.43)	U = 695.0, ns
Education (years)	14.22 (3.72)	15.44 (3.03)	U = 580.5, ns
Neuropsychological data: Mean (SD)			
MMSE (/ 30)	27.67 (1.80)	29.00 (0.87)	***U = 411.0, P = 0.001***
FAB (/ 18)	15.70 (1.66)	16.70 (1.18)	***U = 459.0, P = 0.005***
Semantic Fluency	28.30 (7.73)	38.13 (8.82)	***t = 4.92, P < 0.001***
Lexical Fluency	19.81 (7.00)	26.91 (8.08)	***t = 3.89, P < 0.001***
Stroop interference	0.57 (5.19)	4.53 (7.96)	***t = 2.69, P = 0.009***
Short PPT (/ 40)	39.41 (.80)	39.06 (1.29)	U = 665.0, ns
Short naming (/ 40)	38.93 (1.07)	38.96 (1.35)	U = 677.0, ns
Main Analogy and Match scores: Mean % (SD)			
MatchApply	91.67 (8.64)	94.25 (7.95)	U = 564.0, ns
MatchFind	88.76 (11.62)	93.19 (7.08)	U = 551.0, ns
AnalogyApply	76.43 (14.03)	86.54 (9.53)	***U* = 373.0, *P* < 0 .001**
AnalogyFind	72.04 (13.36)	84.27 (9.94)	***U* = 301.0, *P* < 0 .001**
Averaged performance per task and condition			
Match mean	90.21 (8.84)	93.72 (6.08)	***U* = 507.0, *P* = 0 .025**
Analogy mean	74.23 (13.05)	85.41 (8.96)	***U* = 314.0, *P* < 0 .001**
Apply mean	82.23 (10.58)	89.50 (7.90)	***U* = 394.0, *P* = 0 .001**
Find mean	78.40 (11.36)	87.69 (7.73)	***U* = 326.5, *P* < 0 .001**
Indices			

Analogy index	-20.52 (14.93)	-9.63 (9.27)	***U* = 318.0, *P* < *0.001***
Find index	-5.03(7.30)	-2.03 (7.53)	*U* = 576.0, ns

Values are means (SD) or mean percentage of correct responses (SD) for experimental tasks. Exact *P* values significant at a $P < 0.05$ are provided. MMSE: Mini Mental State Examination; FAB: Frontal Assessment Battery; PPT: Pyramid and Palm Tree Test; ns: non significant.

Supplementary Method 1: Neuropsychological testing

With respect to semantic fluency, the participants were instructed to name as many animals as possible within a time limit of 120 seconds, without repetition of the same word. In lexical fluency, the subjects were asked to produce as many words as possible beginning by the letter P during 120 seconds, excluding proper nouns and without repetition of the same word.

The Stroop test includes three conditions that were performed in the following order: word reading, colour naming and conflict, which were presented for 45 seconds each. Interference sensitivity was measured by subtracting the predicted interference (calculated from the colour denomination and word reading conditions) and the score obtained at the conflict condition.

Semantic knowledge was assessed using short French versions of a naming test and a semantic matching test adapted from the Pyramid and Palm tree test (Merck *et al.*, 2011). In the short naming test, the subjects were asked to name drawings of 40 objects that belonged to different categories. In the short semantic matching test, which is adapted from the Pyramid and Palm tree test, the subjects were presented with 40 trials of three different written words and were told to match a target word (e.g., “swan”) with one of the two other words with which it is semantically associated (e.g., “pond” and “tree”).

Supplementary Method 2: Experimental procedure

All trials followed the same design. The instructions were displayed for 4 seconds, followed by a first set of stimuli on the left part of the screen (the source set) for 2 seconds and, then, by two other sets on the right part of the screen (the targets sets). The participants selected the correct target set by a button press on a keyboard within the 11.5 seconds following the target set display. The participants were asked to choose the target set that matched the source set based on the relationships between the stimuli that composed the sets (Analogy tasks) or based on the similarity of their visual features (Match tasks). The stimuli were letters, numbers or abstract symbols, presented in different colours, sizes or patterns. Feedback was given by displaying for 0.5 seconds a green circle for correct answers or a red circle otherwise. The trials were spaced by a 5-second interval.

The experimental procedure began by reading the written instructions to the participants and then training them on all conditions during 26 trials. All participants understood the instructions and were able to perform the tasks correctly after the training. Then, the participants completed one session under each experimental condition in the following order: MatchApply, MatchFind, AnalogyApply and AnalogyFind trials. The AnalogyApply and AnalogyFind sessions both contained 48 consecutive trials (16 trials for each of the three analogy schemas, each including eight intra-dimension and eight cross-dimension analogy trials), and the Match sessions contained 28 trials each. The participants completed the sessions in the following order: 28 MatchApply, 28 MatchFind, 48 AnalogyApply and 48 AnalogyFind trials. The trials were randomized within each session.

Supplementary Fig. 1: Patients and controls performance under each experimental condition.

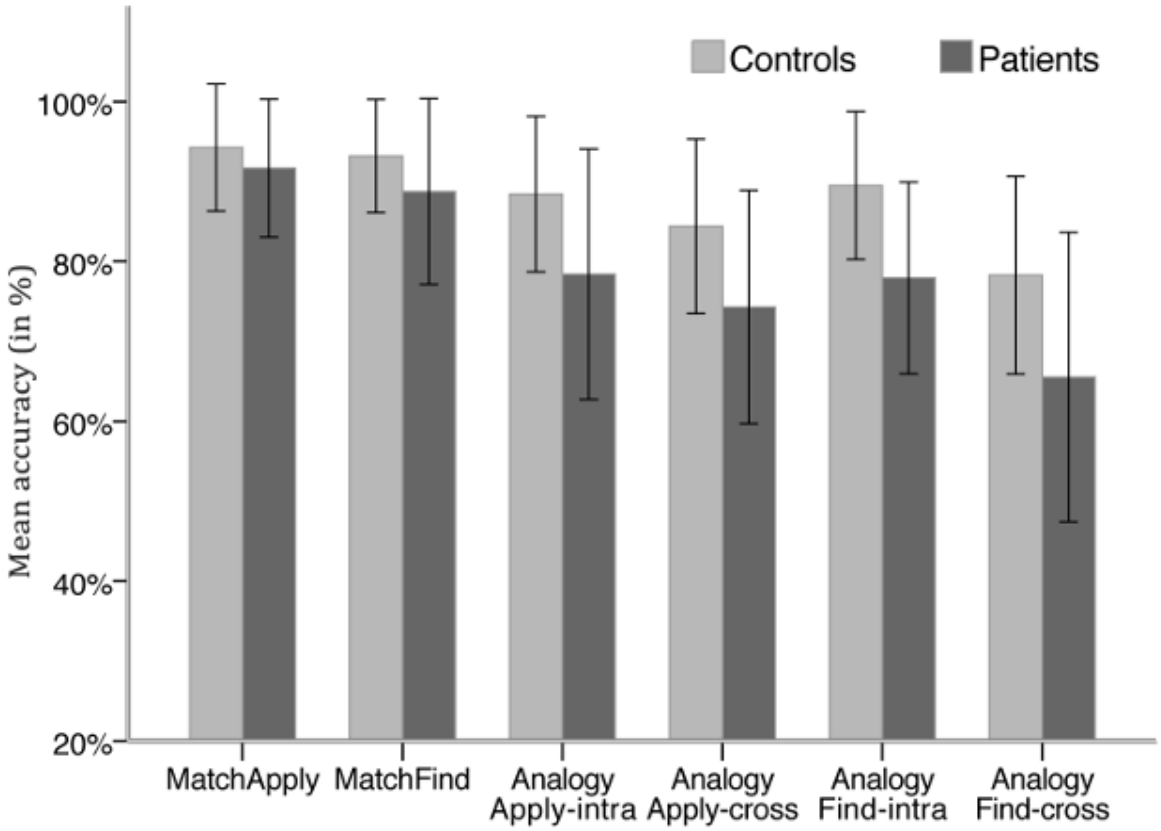

Mean accuracy (in %) and SD (error bars) in each experimental condition are displayed for patients (in dark gray) and controls (in light gray).

Supplementary Table 2: Descriptive data, neuropsychological scores, and statistical comparisons between left brain-damaged and right brain-damaged patients.

	Left lesion (*n* = 14)	**Right lesion (*n* = 9)**	**Group comparisons**
Descriptive data: Mean (SD)			
Age (years)	50.1 (17.6)	41.8 (14.6)	U = 43.5, ns
Education (years)	13.9 (4.3)	15.7 (3.0)	U = 47.0, ns
Lesion volume (cc)	29.7 (38.4)	40.0 (25.5)	U = 42.0, ns
Lesion-testing delay (months)	58.4 (49.4)	68.0 (44.5)	U = 55.0, ns
Neuropsychological data: Mean (SD)			
FAB (/18)	15.9 (1.5)	16.1 (1.5)	U = 53.5, ns
Semantic Fluency	27.6 (8.6)	32.6 (3.9)	U = 37.5, ns
Lexical Fluency	19.5 (8.3)	21.7 (3.9)	U = 48.5, ns
Stroop interference	0.04 (4.8)	1.4 (6.8)	U = 45.5, ns

Values are means (SD). Exact *P* values significant at a $P < 0.05$ are provided. FAB: frontal assessment battery; ns: non significant

Supplementary Fig. 2. The VLSM connectome map.

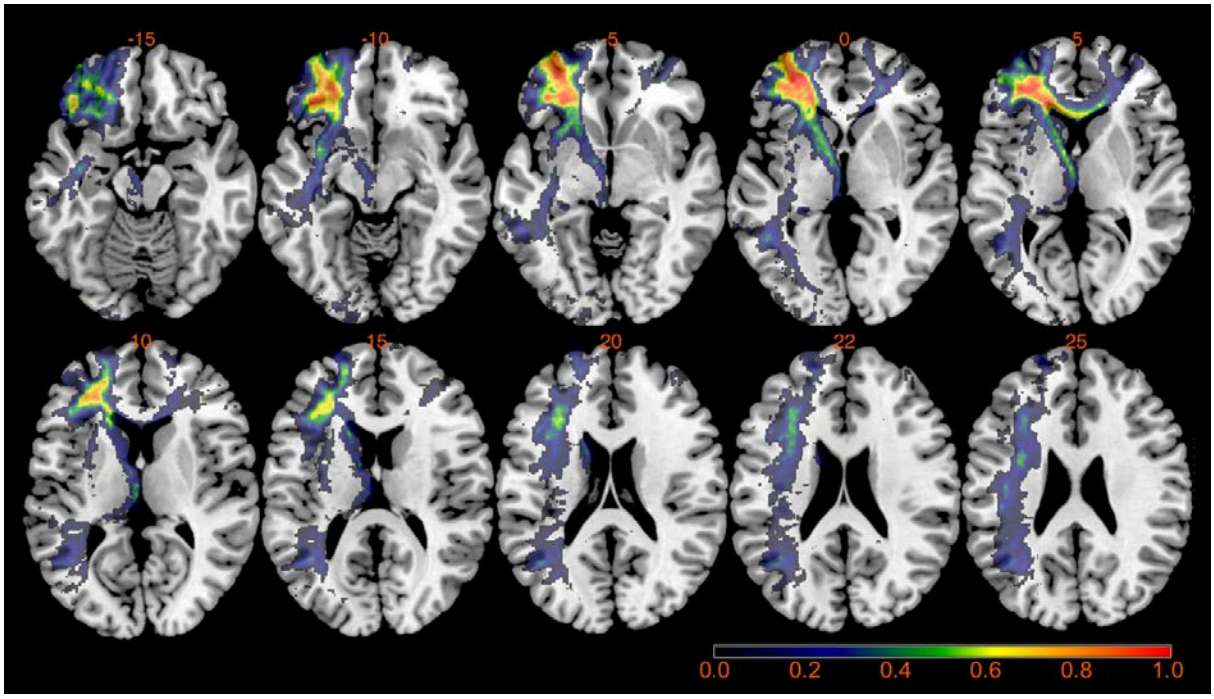

The map displays the probablility of connection to the 'VLSM Analogy region' (the tracts passing through the 'VLSM Analogy region') superimposed on a MNI template. This map was built by using the Disconnectome map software as part of the BCB toolkit (http://www.brainconnectivitybehaviour.eu/).

Z coordinates of each slice are given in red ranging from z = -15 to z = 25. The probability of connection to the 'VLSM Analogy region' is color coded.

Supplementary Table 3. Probability of each lesion to intersect the VLSM connectome map and number of tracts connected to the 'VLSM Analogy region' for each patient / lesion.

Values were obtained using the Tractotron software as part of the BCB toolkit (http://www.brainconnectivitybehaviour.eu/).

	Probability of each lesion intersecting the VSLM connectome map	Number of disconnected tracts among those connecting the 'VLSM Analogy region'
P01	0.0000	0
P02	1.0000	8
P03	0.3787	4
P04	1.0000	8
P05	0.6225	0
P06	0.0000	0
P08	1.0000	8
P09	0.6225	0
P10	0.4774	6
P11	0.3337	0
P12	0.5657	1
P13	1.0000	6
P14	0.5157	0
P15	0.6370	0
P16	0.9999	8
P17	0.8729	6
P18	0.6225	0
P19	0.5189	0

P20	1.0000	8
P21	0.5124	0
P22	1.0000	8
P23	0.1961	3
P24	0.1000	3
P25	0.1927	4
P26	0.7597	5
P27	0.1763	1
P29	1.0000	8

Supplementary Table 4. Descriptive data, neuropsychological scores, performance at the short version of the experimental tasks, and statistical comparisons between patients with a left rlPFC damage ('Damaged left rlPFC' group) and patients without a left rlPFC damage ('Intact left rlPFC' group).

	'Damaged left rlPFC' group (*n* = 7)	**'Intact left rlPFC' group (*n* = 20)**	**Group comparisons**
Descriptive data: Mean (SD)			
Age (years)	55.43 (17.86)	44.35 (14.26)	U = 41.5, ns
Education (years)	13.57 (6.00)	14.45 (2.72)	U = 61.5, ns
Lesion volume (cc)	48.66 (47.24)	26.91 (22.90)	U = 47.0, ns
Lesion-testing delay (months)	70.14 (0.63)	51.45 (47.45)	U = 47.0, ns
Neuropsychological data: Mean (SD)			
FAB (/18)	15.43 (1.40)	15.80 (1.77)	U = 53.5, ns
Semantic Fluency	31.57 (7.09)	27.15 (7.77)	U = 47.0, ns
Lexical Fluency	22.29 (6.85)	18.95 (7.01)	U = 58.5, ns
Stroop interference	-1.76 (4.22)	1.38 (5.34)	***U = 34.0, P = 0.047***
Experimental conditions: Mean % (SD)			
MatchFind - short version	86.73 (6.43)	89.46 (13.03)	U = 41.0, ns
AnalogyFind -short version	52.39 (11.50)	77.31 (12.00)	***U = 10.5, P < 0.001***
Analogy index - short version	-50.83 (16.23)	-14.58 (12.99)	***U = 6.5, P < 0.001***

Values are means (SD) or mean percentage of correct responses (SD) for experimental tasks. Exact *P* values significant at a $P < 0.05$ are provided. FAB: Frontal Assessment Battery; ns: non significant.

Supplementary Fig. 3: Receiver Operating Characteristic (ROC) curves of the short version of the experimental tasks to discriminate patients with intact versus damaged left rlPFC.

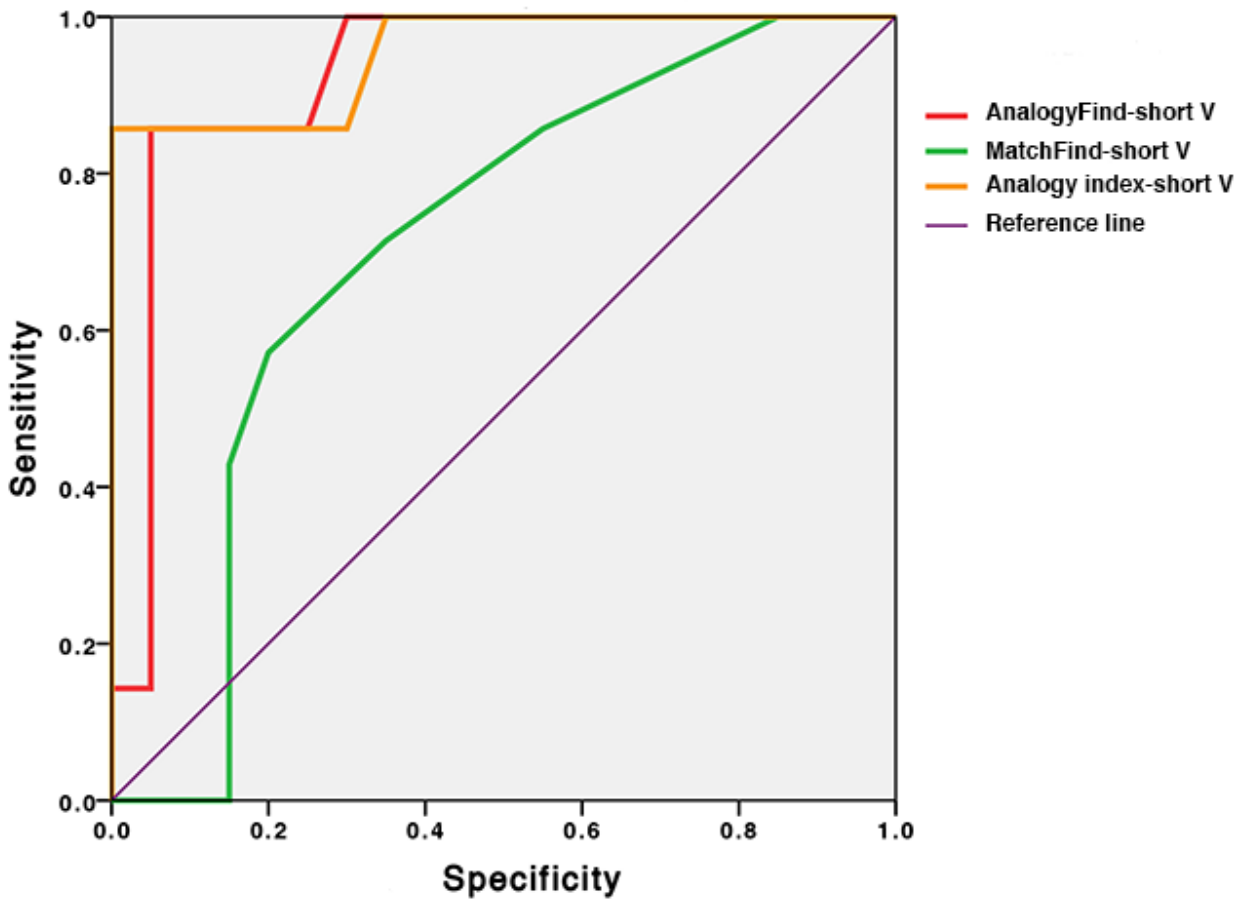

Sensitivity on the Y axis and specificity on the X axis of the short version of the analogy task are displayed for the AnalogyFind-short version condition in red, the MatchFind-short version condition in green and the Analogy index-short version in orange. The reference line is represented in violet.

Supplementary Fig. 4: Superimposition of the current result with results from other approaches that used the same analogy tasks.

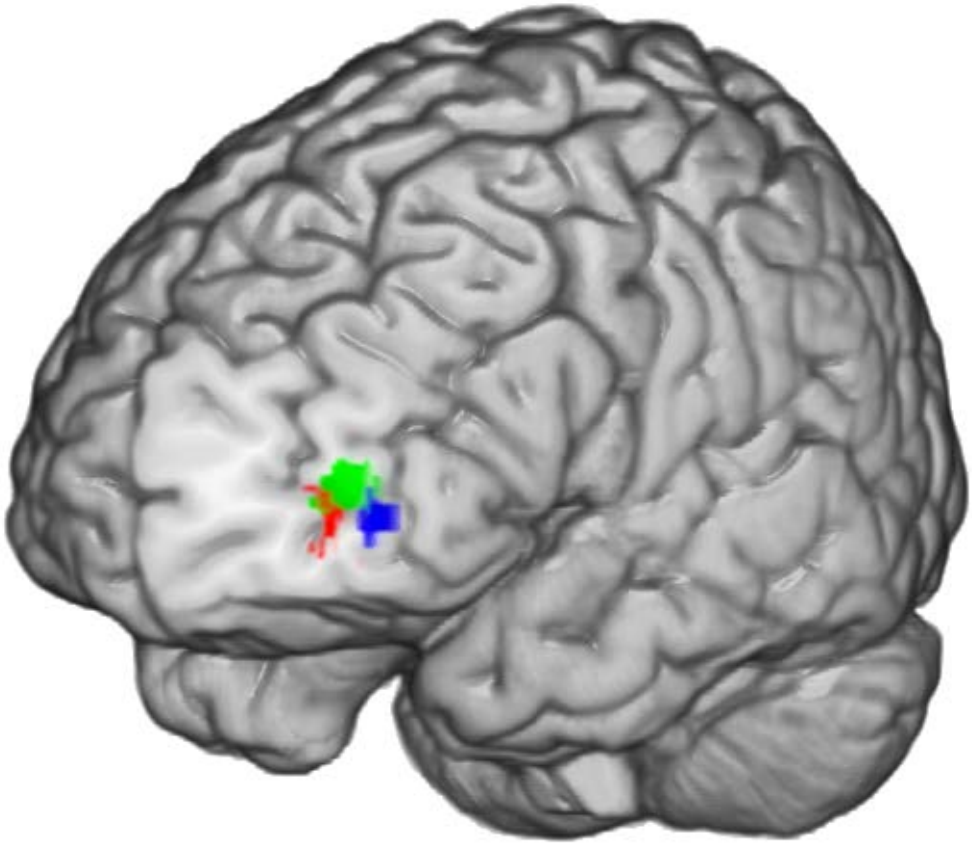

Overlap of the VLSM Analogy map (red), a VBM map of brain regions which structure correlated with analogy performance in healthy subjects (Aichelburg *et al.*, 2014; green) and a sphere centred on the peak maxima observed in a functional imaging study using the same tasks (Volle *et al.*, 2010; blue).

5 High-level cognitive functions are also supported by functional interactions

This previous research aimed to explore the brain structures involved in analogical reasoning. Beyond the critical damage area linked with decreased performance using VLSM, the study revealed an extensive network of structurally connected regions essential for the studied cognitive process. In the next study, we were interested in other cognitive functions associated with creative thinking—the abilities to generate or combine semantically distant associations. Functional imaging studies of creative cognition have identified several functional networks involved in the creative performance. Beyond anatomical connections, the integrity of the functional connectivity appeared to be crucial as well in patient studies. Hence, besides examining the critical lesions and structural disconnections linked with symptoms, we also explored if focal lesions impairing well-known functional networks were related to behavioural impairment. Like the first study, this work demonstrates the need for accurately evaluating the remote effects of brain lesions to assess the underlying mechanisms of brain functions.

Contribution: My contribution to this study was methodological. We used the disconnectome to map the disconnections linked to lower psychological scores. We were also interested in functional impairment. I participated in the analyses of the fMRI data. In addition to the exploration of the effect of damage along the default mode network (DMN) and frontoparietal control network (FPCN) on the generation and the combination of remote ideas, we also performed a seed-based functional connectivity analysis. This work was the basis for the development of the functional connectivity module of the BCBtoolkit. We chose this approach because it does not require any a priori about the systems/networks to be explored. We used the two regions found using VLSM and obtained the same functional networks; that is, the DMN functionally connected to the right medial prefrontal cortex and the FPCN to the left rostrolateral prefrontal cortex. The overlapping results led us to keep only the first functional analysis in the final version of the article. I also developed a script to examine the overlaps between the lesions and the a priori functional networks.

Résumé :

Introduction : Le concept de créativité est assimilé à deux idées contradictoires. La première considère que la créativité découle d'un comportement volontaire dirigé vers un but, qui nécessite un effort et fait appel à des fonctions élaborées, permettant d'inhiber une idée inappropriée, de manipuler mentalement des idées ou de combiner différentes idées entre elles. Ces fonctions, qu'on peut regrouper sous le terme de fonctions de contrôle, dépendent du cortex pré-frontal. La seconde idée considère que la créativité résulte au contraire d'un relâchement des inhibitions et des contraintes, lorsque l'on laisse son esprit vagabonder librement et spontanément par association d'idées sans se contrôler. Donc selon cette notion, ne pas exercer de contrôle facilite la créativité et donc les fonctions du cortex pré-frontal ne seraient pas bénéfiques à la créativité. Les études de psychologie ont montré que les deux notions ne sont pas incompatibles et que les deux types de fonctionnement, spontané et contrôlé, jouent un rôle dans la créativité (Gabora, 2010; Mok, 2014). Dans cette étude nous montrons également que les deux types de fonctionnement sont importants pour la capacité créative, et surtout qu'ils dépendent de l'intégrité de 2 réseaux cérébraux différents impliquant 2 régions différentes du cortex pré-frontal, la zone classiquement dédiée aux fonctions de contrôle, mais également une autre région.

Résultats : Grâce à la cartographie des voxels lésés, des déconnexions et des réseaux fonctionnels endommagés affectant le comportement, nous avons identifié des régions préfrontales et des connexions critiques pour des mécanismes distincts liés à la pensée créative. En explorant la créativité chez des patients qui présentaient une lésion du cortex frontal, nous avons trouvé que lorsque la lésion des patients touche un réseau frontoparietal latéral gauche, impliqué classiquement dans le contrôle cognitif, les patients sont moins efficaces dans une tâche de créativité nécessitant un contrôle cognitif. En particulier, nous avons montré que la région rostro-latérale du cortex pré-frontal est un noeud critique dans ce réseau. Mais lorsque la lésion touche un réseau médial appelé réseau du mode par défaut, en particulier dans sa région frontale médiale droite, les patients ont des difficultés dans des tâches d'association libre d'idées. Ce réseau est aussi décrit comme impliqué dans le vagabondage mental. Ces résultats indiquent que le réseau médial est critique pour générer des associations d'idées

non typiques, alors que le réseau latéral est critique pour combiner des idées de façon appropriée.

Conclusion : Nous avons montré que le cortex rostro-latéral préfrontal gauche, ainsi que ses connexions au sein du réseau de contrôle fronto-pariétal de l'hémisphère gauche et à plusieurs régions sous-corticales, jouent un rôle important dans les processus contrôlés et l'intégration/combinaison des idées pour atteindre un but. Nous avons également montré que la génération spontanée d'idées distantes semble être soutenue par le réseau du mode par défaut et le cortex rostro-médial préfrontal droit, ce qui confirme la distinction fonctionnelle rapportée dans la littérature (Beaty et al., 2016). L'importance de connexions structurelles et des réseaux fonctionnels dans l'élaboration des capacités créatives corroborent les résultats des études récentes expliquant les fonctions cognitives de haut niveau par l'interaction coordonnée de diverses structures cérébrales plutôt que l'activation localisée d'une région spécifique. Autrement dit, les aspects spontanés et contrôlés de la créativité dépendraient tous les deux du cortex pré-frontal mais impliqueraient des systèmes différents, un système médial spontané et un système latéral controlé. Ces données sont en accord avec les études récentes de connectivité fonctionnelle chez les sujets sains en IRMf, qui ont montré que le réseau latéral et le réseau médial agissent en interaction pendant la performance créative (Ellamil et al., 2012; Jung, 2014; Beaty et al., 2016; De Pisapia et al., 2016). Nos données aident à mieux comprendre le rôle de ces réseaux dans la créativité, et surtout montrent, grâce aux patients, qu'il existe des noeuds critiques au sein de ces réseaux, en particulier dans la portion la plus antérieure du cortex pré-frontal. Elles montrent également que les régions latérale et médiale du cortex pré-frontal antérieur ont des rôles distincts dans la créativité, et que la région pré-frontale du cortex intervient non seulement dans les fonctions de contrôle, mais également dans la génération d'idée plus spontanée.

doi:10.1093/brain/awx294 BRAIN 2018: 141; 217–233 | 217

BRAIN
A JOURNAL OF NEUROLOGY

Two critical brain networks for generation and combination of remote associations

David Bendetowicz,[1,2] Marika Urbanski,[1,3,4] Béatrice Garcin,[1,2] Chris Foulon,[1,4] Richard Levy,[1,2] Marie-Laure Bréchemier,[1] Charlotte Rosso,[5,6] Michel Thiebaut de Schotten[1,4] and Emmanuelle Volle[1,4]

Recent functional imaging findings in humans indicate that creativity relies on spontaneous and controlled processes, possibly supported by the default mode and the fronto-parietal control networks, respectively. Here, we examined the ability to generate and combine remote semantic associations, in relation to creative abilities, in patients with focal frontal lesions. Voxel-based lesion-deficit mapping, disconnection-deficit mapping and network-based lesion-deficit approaches revealed critical prefrontal nodes and connections for distinct mechanisms related to creative cognition. Damage to the right medial prefrontal region, or its potential disrupting effect on the default mode network, affected the ability to generate remote ideas, likely by altering the organization of semantic associations. Damage to the left rostrolateral prefrontal region and its connections, or its potential disrupting effect on the left fronto-parietal control network, spared the ability to generate remote ideas but impaired the ability to appropriately combine remote ideas. Hence, the current findings suggest that damage to specific nodes within the default mode and fronto-parietal control networks led to a critical loss of verbal creative abilities by altering distinct cognitive mechanisms.

1 Sorbonne Universités, UPMC Univ Paris 06, Inserm, CNRS, Institut du cerveau et la moelle épinière (ICM) – FrontLab, Hôpital Pitié-Salpêtrière, Boulevard de l'hôpital, F-75013, Paris, France
2 Assistance Publique-Hôpitaux de Paris, Hôpital Pitié-Salpêtrière, Neurology Department, 75013 Paris, France
3 Hôpitaux de Saint-Maurice, Medicine and Rehabilitation Department, 94410 Saint-Maurice, France
4 Institut du cerveau et la moelle épinière (ICM), Brain Connectivity and Behaviour group, 75013 Paris, France
5 Institut du cerveau et la moelle épinière (ICM), CENIR, 75013 Paris, France
6 Assistance Publique-Hôpitaux de Paris, Hôpital Pitié-Salpêtrière, Urgences cérébro-Vasculaires, 75013 Paris, France

Correspondence to: Emmanuelle Volle
FrontLab – ICM; Hôpital Pitié Salpêtrière, 47, bd de l'hôpital, 75013 Paris, France
E-mail: emmavolle@gmail.com

Keywords: creativity; lesion; disconnection; brain networks; semantic associations

Abbreviations: CAT = Combined Associates Task; DMN = default mode network; FGAT = Free Generation of Associates Tasks; FPCN = fronto-parietal control network; rl/rmPFC = rostrolateral/rostromedial prefrontal cortex; VLSM = voxel-based lesion-symptom mapping

Introduction

The concept of creativity is imbued with two contradictory notions. First, unusual and creative ideas emerge from relaxing the constraints and letting the mind wander freely and spontaneously. Second, a creative production is usually considered to be the result of goal-directed cognition that involves high-level control functions such as mental manipulation, abstract thinking, or planning. This paradox reflects the involvement of both uncontrolled spontaneous associative thinking and controlled effortful thinking in creativity (Gabora, 2010; Mok, 2014). Recent

Received April 19, 2017. Revised August 23, 2017. Accepted September 21, 2017. Advance Access publication November 22, 2017

psychological studies support this claim, by showing the contribution of controlled processes, including cognitive inhibition, switching, or working memory (Gilhooly *et al.*, 2007; Nijstad *et al.*, 2010; Nusbaum and Silvia, 2011; Benedek *et al.*, 2012*a*; De Dreu *et al.*, 2012; Lee and Therriault, 2013; Silvia *et al.*, 2013; Edl *et al.*, 2014), as well as the role of spontaneous associative thinking (Merten and Fischer, 1999; Gruszka and Necka, 2002; Faust and Lavidor, 2003; Rossmann and Fink, 2010; Benedek *et al.*, 2012*b*; Beaty *et al.*, 2014*a*), in creative abilities. The role of associative thinking abilities in creativity depends on the flexible organization of associations between elements of one's semantic knowledge (Mednick, 1962; Mednick *et al.*, 1964*a*; Kenett *et al.*, 2014; Kenett and Austerweil, 2016). Hence, creativity, defined as 'the forming of associative elements into new combinations' (Mednick, 1962; Mednick *et al.*, 1964*a*, *b*), depends on associative thinking abilities (involving the spontaneous activation of semantic associates) and on the ability to combine these elements according to given constraints (involving controlled processes; Chermahini *et al.*, 2012; Lee and Therriault, 2013; Jones and Estes, 2015). However, little is known regarding the brain mechanisms supporting the associative and controlled processes involved in the generation and the combination of creative ideas in the human brain.

Preliminary evidence from functional imaging (Dietrich and Kanso, 2010; Gonen-Yaacovi *et al.*, 2013; Boccia *et al.*, 2015) and from patient studies (Rankin *et al.*, 2007; de Souza *et al.*, 2010; Shamay-Tsoory *et al.*, 2011; Abraham *et al.*, 2012; Barbey *et al.*, 2013) demonstrated the involvement of prefrontal and posterior parietal regions in creativity, emphasizing the role of the fronto-parietal control-related network (FPCN; Vincent *et al.*, 2008; Smith *et al.*, 2009; Woolgar *et al.*, 2010; Cole *et al.*, 2013; Power and Petersen, 2013; Parlatini *et al.*, 2017) in creative thinking. Other neuroimaging approaches based on interindividual variability in morphometry (Jung *et al.*, 2010*b*, 2013, 2015; Takeuchi *et al.*, 2010; Zhu *et al.*, 2013; Fink *et al.*, 2014; Kühn *et al.*, 2014; Chen *et al.*, 2015; Jauk *et al.*, 2015) or in functional connectivity (Takeuchi *et al.*, 2012; Beaty *et al.*, 2014*a*; Chen *et al.*, 2014; Cousijn *et al.*, 2014; Wei *et al.*, 2014), have highlighted the role of the default mode network (DMN) in creative abilities. The DMN may play an important role in creative idea generation since its activity is thought to reflect associative cognition, contributing to internally-generated thoughts, mind wandering, and semantic and episodic memory (Buckner *et al.*, 2008; Binder *et al.*, 2009; Christoff *et al.*, 2009; Andrews-Hanna *et al.*, 2010; Wirth *et al.*, 2011; Fox *et al.*, 2015; Humphreys *et al.*, 2015; Xu *et al.*, 2016). Although DMN activity has been initially described as anti-correlated with FPCN activity and decreased with mental efforts and cognitive control (Raichle, 2015), several recently published articles indicate that the DMN and FPCN networks cooperate during creative performance (Ellamil *et al.*, 2012; Beaty *et al.*, 2014*b*, 2016; Chen *et al.*, 2014; Pinho *et al.*, 2014). Overall, the integration of psychological and neuroimaging findings indirectly suggests that creativity relies on associative abilities that may be supported by the DMN, combined with cognitive control processes that are supported by control-related networks. The lesion approach may be especially useful in testing this hypothesis and would clarify whether distinct damage to the two functional networks would differently affect the associative and controlled processes involved in the formation of creative ideas.

In this study, we address this new question by examining creative abilities in patients with focal frontal brain lesions with a focus on the associative and controlled processes involved in the generation and combination of remote associations. These processes were explored by using two tasks: (i) a verbal associative combination task (the Combined Associates Task, CAT), adapted from Mednick's task (1962), which allowed us to estimate the ability to form new combinations between remote associates; and (ii) a free generation of remote associates task (FGAT-distant) that consisted of a simple word-to-word generation task reflecting the ability to intentionally produce remote associations (FGAT-distant condition) with the instruction to think creatively (Prabhakaran *et al.*, 2013). In addition, another free word-to-word generation task (FGAT-first) consisted of giving the first word that came to mind with the aim of exploring spontaneous semantic associations in participants, which can reflect associative thinking abilities. Critical areas predicting performances were revealed using a voxel-based lesion mapping method (VLSM: Bates *et al.*, 2003; Kinkingnéhun *et al.*, 2007). Because various regions likely interact for cognitive functions, we also examine the impact of disconnections of white matter tracts on creative abilities using a recent approach (Thiebaut de Schotten *et al.*, 2015). Finally, we explored *a priori* the impact of damage to the DMN and to the left or right FPCN on the tasks. Together, these analyses revealed specific patterns of damage within these systems that differently affected the ability to freely generate and the ability to appropriately combine remote associations.

Materials and methods

Participants

Twenty-nine right-handed patients (French-native speakers; 17 females; mean age 47.5 years, age ranging from 23 to 75 years) who presented with a unique focal frontal lesion at the chronic stage (>3 months) were included in this study (Table 1). The patients were recruited from the departments of neurology or neuroradiology at Pitié-Salpêtrière, Saint-Antoine and Lariboisière hospitals in Paris. Patients with a history of psychiatric or neurological disease, drug or psychotropic abuse, or MRI contraindications were not included. Patients with impaired semantic memory [assessed using short French versions of a naming test and a semantic

Table 1 Demographic and clinical data for the patients included in the study

Patient	Age (years)	Gender	Education (years)	Aetiology	Lesion side	Lesion location
P01	56	F	17	Ischaemic stroke	R	Semioval centre
P03	46	F	17	Ischaemic stroke	L	Posterior MFG
P05	64	M	14	Ischaemic stroke	R	IFG and MFG
P13	67	M	15	Ischaemic stroke	L	Anterior IFG
P19	54	M	22	Ischaemic stroke	R	IFG / MFG white matter
P27	58	M	12	Ischaemic stroke	L	Precentral sulcus
P02	55	M	19	Haemorrhage	L	Rostral PFC / VMPFC
P07	51	M	11	Haemorrhage	B	Rostral PFC
P09	47	M	11	Haemorrhage	R	Cingulate / VMPFC
P10	62	F	13	Haemorrhage	B	Cingulate / VMPFC
P12	46	M	12	Haemorrhage	B	Cingulate / VMPFC
P14	49	M	9	Haemorrhage	B	Cingulate / VMPFC
P16	40	F	22	Haemorrhage	L	Rostral PFC
P17	40	M	14	Haemorrhage	B	Rostral PFC / VMPFC
P20	71	M	17	Haemorrhage	L	Rostral PFC / VMPFC
P25	59	F	16	Haemorrhage	L	VMPFC
P26	26	F	13	Haemorrhage	L	Posterior IFG
P29	75	F	12	Haemorrhage	L	Rostral PFC
P04	50	F	11	Low-grade glioma (excision)	L	Rostral PFC + / VMPFC
P08	70	F	5	Meningioma (excision)	L	Rostral PFC
P30	52	F	13	Low-grade glioma (excision)	R	MFG
P06	32	F	16	Epilepsy surgery	R	Posterior SFG
P11	41	M	16	Epilepsy surgery	R	IFG / MFG / posterior SFG
P15	36	F	14	Epilepsy surgery	R	Rostral PFC / VMPFC
P18	23	F	16	Epilepsy surgery	R	Rostral PFC
P21	23	F	15	Epilepsy surgery	R	Rostral PFC
P22	27	F	9	Epilepsy surgery	L	Lateral rostral PFC
P23	26	F	13	Epilepsy surgery	L	Precentral gyrus
P24	32	F	14	Epilepsy surgery	L	Posterior medial PFC

Ischaemic strokes affected the middle cerebral artery territory. Haemorrhages were caused by a ruptured aneurism, a spontaneous hematoma, or by a vascular malformation for one patient. Epileptic patients underwent a surgical resection of their epileptic focus, whose origin was cryptogenic, except for two patients who had a dysplasia removed (Patients P21 and P23). Education level corresponds to the number of years since the beginning of school (usually at age 6). The interval is the delay (in months) between the onset of the lesion and testing. B = bilateral; F = female; IFG = inferior frontal gyrus; L = left; M = male; MFG = middle frontal gyrus; R = right; SFG = superior frontal gyrus; vmPFC = ventromedial PFC.

matching test, as described in Merck *et al.* (2011)] or who were not able to understand task instructions were excluded from the study. Descriptive and clinical data are reported in Supplementary Table 1.

The patient performances were compared to those of a group of 54 healthy right-handed, French-native speaker controls (Supplementary Table 2), and who had no history of psychiatric or neurological disease, drug or psychotropic abuse, or MRI contraindication and no cognitive impairment [Mini-Mental State Examination (MMSE) $\geqslant$ 27/30; Folstein *et al.*, 1975]. Controls were matched to patients for age and years of formal education.

The local ethics committee approved the experiment; all participants provided written informed consent and were paid for their participation.

Neuropsychological testing and control tasks

Neuropsychological tests were administered to all participants, assessing their cognitive status (by MMSE), cognitive and behavioural executive functions (by the Frontal Assessment Battery; Dubois *et al.*, 2000). In addition, participants performed the Stroop test (Stroop, 1935), a phonemic and a category fluency task, and short French versions of a naming test and a semantic matching test as described in Merck *et al.* (2011), to control for some executive and semantic processes that play roles in the experimental tasks. The Stroop test assesses the ability to inhibit a prepotent response. The performance of fluency tasks depends on a complex set of cognitive processes, including self-initiation of action, semantic retrieval, switching between categories of responses, inhibition, updating and monitoring the content of working memory (Perret, 1974; Troyer *et al.*, 1997; Unsworth *et al.*, 2011). In the naming task, the participant was asked to provide the name of each of the 40 black and white pictures displayed one by one on a computer screen. The participants gave their response orally, and the examiner wrote down and scored their responses. The semantic matching task was adapted from the Pyramids and Palm Trees Test (Howard and Patterson, 1992). In each trial, three words were presented on the computer screen, with the target word presented above the other two words. For each triad, participants were asked to select, through finger pointing, the bottom item that was semantically related to that at the top (the target). Among the bottom items, one was linked to the target with a functional or a category relationship; the other item was a semantic

distractor. A total of 40 trials was performed and scored. The naming and semantic matching tasks aimed to ensure the absence of semantic memory deficits in our patients [i.e. scores $\geqslant 37$ correct responses on the naming task and 38 on the semantic matching task (Merck *et al.*, 2011)].

The participants also underwent the short version of the Torrance test, a divergent thinking test, to assess creative abilities based on a well-validated test (Goff and Torrance, 2002).

Experimental tasks

Combined Associates Task

See Supplementary material (Method 1) and Bendetowicz *et al.* (2017) for detailed information on this task.

We built a new verbal task adapted from Mednick's remote associates task (Mednick, 1962), in which subjects were required to find a word related to all three cue words that were presented to them when there was no obvious link between these cue words. The construct validity and reliability of the remote associate task has been shown in previous studies (Mednick, 1962; Mednick *et al.*, 1964*a*; Chermahini *et al.*, 2012). Performance on such tasks depends both on the organization of spontaneous associations between words or concepts (associative thinking), and on the constrained generation and combination of remote associates, likely using controlled processes (as detailed in Table 2; Mednick *et al.*, 1964*a*; Ward and Kolomyts, 2010; Chermahini *et al.*, 2012; Benedek and Neubauer, 2013; Lee and Therriault, 2013; Kenett *et al.*, 2014; Jones and Estes, 2015).

Based on the hypothesis that the more remote the elements to combine, the more creative the process (Mednick, 1962), we adapted the remote associates task and varied the semantic distance between the written cue words and the solution word(s). We used free association norms to quantify mean associative distance (association strength; Debrenne, 2011; http://dictaverf.nsu.ru/) between the cue words and the solution word(s) for each trial. We built 72 CAT trials and classified the trials according to the median of the association strength. Thirty-six trials with mean association strength greater than the median (>7) were classified as 'close CAT' trials [for example, 'rue' (street), 'campagne' (countryside), 'centre' (centre); the solution is 'ville' (town)]. Thirty-six trials were classified as 'distant CAT' trials [e.g. 'pont' (bridge), 'social' (social), 'attacher' (to tie); the solution is 'lien' (link)]. A previous study showed that healthy participants performed close trials significantly more accurately and with shorter reaction times than distant trials (Bendetowicz *et al.*, 2017).

The three cue words were displayed on the screen until the participants produced a response, within a time limit of 30 s. After giving their response, participants provided ratings on insight (by pressing V/N keys on the keyboard for yes/no 'Eureka' experience) as it is commonly assessed in the remote associate task, and as detailed in the Supplementary material, and in Bendetowicz *et al.* (2017).

The percentage of trials solved was measured (CAT-solving) for all trials and separately for close and distant trials. To obtain a score that would be more specifically related to the creative potential than to a global solving performance, an index (CAT-index) was calculated as the difference between performance on close and distant trials, divided by the mean performance in both conditions. This index operationalizes Mednick's hypothesis ('the more remote the elements to be combined, the more creative the process or solution'), as distant trials involve a solution that is more distant from the elements to be combined than close trials. Hence, CAT-distant and CAT-close conditions are both remote associate tasks, but correspond to high and low creative conditions, respectively. The CAT-index reflects the ability to solve distant trials (the more creative condition) when controlling for performance in the less creative condition (close trials). In particular, the CAT-index measure allows one to control for processes such as word reading and understanding, vocabulary and lexical retrieval and verbal response selection and production, sensorimotor processing, and the overall ability to solve problems. Importantly, CAT-index also controls for the effects of lexical frequency (of cue and solution words) and word salience (or steepness inducing fixation) of the cue words, which are essential factors influencing remote word associate tasks (Mednick *et al.*, 1964*a*; Gupta *et al.*, 2012; Klein and Badia, 2015) (Supplementary material). Correlation analyses in healthy controls have previously indicated that the CAT-index was related to other creativity measures (Bendetowicz *et al.*, 2017).

Free Generation of Associates Tasks

See Supplementary material (Method 2) for detailed information on this task.

FGAT were free word generation tasks. On each FGAT trial, a cue word was displayed on a computer screen, and the participants were asked to produce another word in response to the cue word according to two conditions, a 'first' and a 'distant' condition.

Table 2 Task requirements in terms of cognitive processes or mechanisms

	FGAT-first	FGAT-distant	CAT
Spontaneous semantic associations Low cognitive control	+	+	+
Generation of remote associates Involving controlled retrieval of semantic elements, inhibition of usual and inappropriate associates, selection among the retrieved associates, working memory	–	+	+
Combination of remote associates Involving relational integration, multitasking and subgoal integration, branching, evaluation and selection of candidate solutions to meet the constraints of the task, updating and switching in working memory	–	–	+

In the 'distant' condition (FGAT-distant), the participants were asked to say aloud a word that was unusually associated with the cue word, with an original but existing link between the cue word and their response. FGAT-distant aimed to assess the ability to intentionally generate unusual word associations. The uncommonness of responses in a word-to-word generation task with the instruction to be creative has been found to be a reasonably strong correlate of creative performance. Other studies have used similar tasks in which participants were presented with a noun and were asked to say a verb related to the noun, with the instruction to think creatively. Lower semantic similarity or higher semantic distance of the noun–verb pairs correlated positively with a creativity factor derived from a battery of measures, including achievement-based measures (Green *et al.*, 2012*a*, 2015; Prabhakaran *et al.*, 2013). Overall, both the CAT and FGAT-distant tasks were creativity-related tasks and involve the ability to generate remote associations, while the CAT additionally requires combination processes (Table 2).

In contrast, the 'first' condition or FGAT-first was not a creativity task but was aimed to assess to what extent semantic associations were common, typical (or 'steep' according to Mednick's hypothesis) in individuals. In the FGAT-first condition, the subjects were asked to say aloud the first word that came to mind. This condition involved associative thinking with minimal control demands.

The same list of 58 words was used in the first and the distant conditions (Supplementary material). We measured the frequency or commonness of the responses of each participant, relative to normative data from 96 healthy subjects ('FGAT-first/distant frequency') as the main FGAT measure. We also measured the uniqueness (percentage of responses that were not given by subjects from our normative data: 'FGAT-first/distant unique responses') and the typical nature [percentage of responses that corresponded to the first associate of the cue word according to French association norms (Debrenne, 2011): 'FGAT-first/distant typical responses'] of the patients' responses.

Testing and procedure

The tasks were programmed using MeyeParadigm [e(ye)Brain Inc., 2009] running on a PC. Participants performed the FGAT-first before the FGAT-distant condition for duration of about 10 min. The CAT task was performed thereafter. After the instructions of the CAT task, participants were trained on 10 trials and then performed the 72 test trials for a total duration of ~40 min.

Statistical analyses

Statistical analyses were performed using SPSS software (v22.0; IBM Corp.). Between-group differences were analysed using parametric *t*-tests when the assumption of normality was met or non-parametric tests otherwise, using exact *P*-values for comparison within our patient group. Scores were Z transformed to compare the performance across CAT and FGAT tasks. The alpha-level used to determine significance was set to 0.05.

Neuroimaging analyses

Imaging lesion preprocessing

Patients underwent a high-resolution T_1-weighted MRI acquisition that was spatially normalized to the Montreal Neurological Institute (MNI) template using the 'unified segmentation' approach combined with a lesion masking to limit the impact of a brain lesion on the spatial normalization (Crinion *et al.*, 2007; Andersen *et al.*, 2010; Ripollés *et al.*, 2012). Lesions were manually segmented on the normalized MRIs by trained neurologists. The resulting lesion volumes in the MNI space were used for further analyses. The lesions of all the patients overlapped on a brain template are displayed in Supplementary Fig. 1. The lesion method has been used previously (Urbanski *et al.*, 2016) and is detailed in the Supplementary material (Method 3).

Lesion-deficit mapping approach

To investigate lesion-deficit relationships, we ran a VLSM analysis (Bates *et al.*, 2003) using the NPM software (http://www.nitrc.org/projects/mricron). This approach statistically compares for each voxel the performance of the patients damaged in that voxel to those of other patients. We used the non-parametric Brunner-Munzel test. VLSM results were reported with a significance threshold of $P < 0.05$ with a family-wise errors (FWE) correction for multiple comparisons using permutations. Given the small number of patients, we prioritized a larger coverage with a permissive minimal overlap threshold of three lesions, i.e. only the voxels having a lesion overlap from at least three patients were considered. Seventy-two per cent of the prefrontal cortex was concerned by at least one lesion, but the percentage of prefrontal voxels that satisfied the three overlaps threshold was 36% (Supplementary material, Method 4). We also report the results of the VLSM analysis when using a higher overlap threshold of four lesions in the Supplementary material. Separate VLSM maps were run for the two tasks related to creative thinking: FGAT-distant and CAT-index. Subsequent group comparison analyses were performed to examine the specificity of the deficits according to the critical lesion locations revealed by the VLSM analyses. In this analysis, patient groups were selected from the VLSM analysis based on their deficit on either the CAT-index or the FGAT-distant score, and were compared to other patients and to each other regarding their demographic characteristics and performance in the other cognitive tasks. Although this selective analysis can be biased by its lack of independence from the VLSM study, it allowed directly comparing the impact of critical lesion locations when looking for an interaction between tasks and lesion location.

Impact of disconnections: a disconnection-deficit mapping approach

To explore the impact of tract disconnection on creative performance, we used a disconnection-deficit approach by calculating the probability of disconnection of white matter tracts caused by each lesion, using Disconnectome maps software (Thiebaut de Schotten *et al.*, 2015) as part of the BCBtoolkit (http://www.bcblab.com). For each patient, a disconnectome map was obtained by diffusion-based tractography of white matter fibres passing by the lesion. Tractography was performed in a group of 10 healthy controls. First, lesions were

registered to the diffusion images of the group of healthy controls (Rojkova *et al.*, 2016) using affine and diffeomorphic deformations (Klein *et al.*, 2009; Avants *et al.*, 2011). The registered lesions were used as seed points to track streamlines passing through the damaged regions in each healthy dataset. For each patient, we created a binary visitation map of the streamlines intersecting the lesion. These maps were normalized to MNI space using the inverse of the deformations mentioned above. We created percentage overlap maps by summing at each point in MNI space the normalized visitation map of each subject; hence, the value in each voxel of the visitation maps varied according to intersubject variability. For each lesion we obtained a disconnectome map that approximates the disconnections provoked by the lesion of each patient with a probability of disconnection >50% (disconnectome page on http://toolkit.bcblab.com/). Then we enter these maps in a regression analysis in FSL (http://fsl.fmrib.ox.ac.uk/fsl/fslwiki/) to examine the disconnections that were associated with a deficit. Age, years of education, and lesion volume were covaried out.

Impact of damage to the default mode and the fronto-parietal control networks

Based on the functional imaging literature, we hypothesized that patients with a lesion affecting the DMN and/or the FPCN would have a creativity loss. To test this hypothesis, we examined how damage to these networks impacted the patients' performance. We used the functional networks described by Smith *et al.* (2009) to define the DMN and FPCN (Supplementary Fig. 2). We determined for each patient if his/her lesion damaged these functional networks using FSL routines (http://fsl.fmrib.ox.ac.uk/fsl/fslwiki/) in the MNI152 space. The functional networks from Smith *et al.* (2009) were arbitrarily thresholded at a conservative $z = 4$ (a threshold that these authors also used in their original paper). Each of the networks was considered as damaged if at least 1% of the network was affected by the lesion to avoid considering a network as damaged when only a few voxels of the lesion were overlapping it. The main creativity measures, CAT-index and FGAT-distant frequency scores, in the patients with damaged versus intact networks were compared statistically (Table 4 and Supplementary Fig. 3). As lesions often overlapped with more than one network, the impact of damage to the distinct resting state networks could not be directly compared to each other.

Results

Behavioural analyses

Compared to controls, patients had significantly lower scores on the CAT, especially when the words to combine were more distant (assessed based on a CAT-index score). In patients, there was no significant correlation between CAT performance and age [r = −0.109, not significant (ns)], lesion volume ($r_s = -0.351$, ns) and lesion delay (r = 0.059, ns). In patients, there was no significant correlation between CAT-index and phonemic fluency (r = −0.345, ns), category fluency (r = −0.054, ns), Stroop interference (r = −0.338, ns), naming task ($r_s = -0.271$, ns) and semantic matching task ($r_s = 0.145$, ns). CAT-index did not correlate with response times in the FGAT conditions (FGAT-first-reaction times: $r_s = 0.001$, ns; FGAT-distant-reaction times: $r_s = -0.059$, ns).

The commonness of the words produced in the FGAT-first and FGAT-distant conditions was not significantly different between the patient and control groups (Supplementary Table 2). There was also no significant correlation between the commonness of the patient responses in the FGAT-distant and -first frequency scores and age (first: $r_s = -0.196$, ns; distant: r = 0.118, ns), lesion volume (first: $r_s = 0.232$, ns; distant: $r_s = 0.296$, ns) and lesion delay (first: $r_s = 0.113$, ns; distant: r = 0.155, ns). There was no significant correlation in patients between the FGAT-first and -distant frequency scores and phonemic fluency (first: $r_s = -0.091$, ns; distant: r = −0.282, ns), category fluency (first: $r_s = 0.028$, ns; distant: r = −0.237, ns), Stroop interference (first: $r_s = -0.062$, ns; distant: r = −0.351, ns), naming task (first: $r_s = -0.096$, ns; distant: $r_s = -0.077$, ns) and semantic matching task (first: $r_s = 0.286$, ns; distant: $r_s = 0.167$, ns).

These results indicate that our experimental measures were not correlated with scores on control tasks measuring the inhibition of prepotent responses, fluency processes and semantic memory.

In healthy controls, the uniqueness of responses provided in the FGAT-distant condition correlated with the originality and fluency scores on the Torrance test (r = 0.339, $P = 0.015$; r = 0.317, $P = 0.023$), and the CAT-index score correlated with the originality scores on the Torrance test (r = −0.282, $P = 0.045$). These results suggest that FGAT-distant and CAT-index are related to creativity as assessed by divergent thinking tasks.

Lesion-deficit mapping analyses

VLSM statistics revealed specific frontal regions responsible for lower creative abilities. One such region was located in the left rostrolateral prefrontal cortex [rlPFC; volume 0.23 cm^3; Brodmann area (BA) 10; MNI coordinates $x = -30$, $y = 50$, $z = 2$ mm; $P < 0.05$, FWE-corrected] that was associated with a significant deficit on the CAT, especially for distant trials (CAT-index; Fig. 1A and Supplementary Fig. 4). Damage to this region impaired the ability to combine remote semantic associations, but its effect on the ability to generate remote associates (FGAT-distant) was not significant (Table 3). Additionally, the right rostromedial region [rostromedial prefrontal cortex (rmPFC); volume 0.38 cm^3, BA 10/11; MNI coordinates $x = 12$, $y = 43$, $z = -6$ mm; $P < 0.05$, FWE-corrected] was critical for generating distant associates, as patients with a lesion in this region produced more common and less unique responses in the FGAT-distant condition than other patients (Fig. 1B). Importantly, patients with a lesion in the right rmPFC produced more common and less unique responses in the FGAT-first condition than did

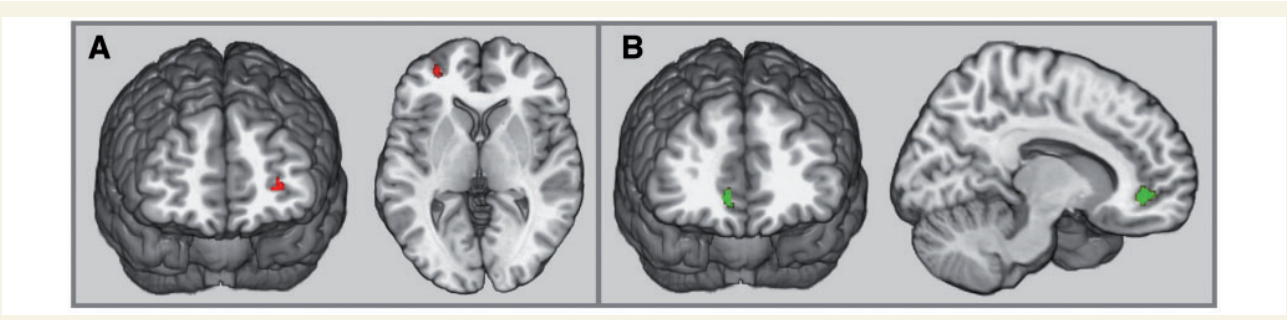

Figure 1 Lesion-deficit mapping associated with CAT-index and FGAT-distant performance. Coloured clusters show the lesion location associated with a significant impairment on the CAT-index (red) (**A**) and on the FGAT-distant condition (green) (**B**) ($P < 0.05$, FWE-corrected).

Table 3 Descriptive data and experimental task performance according to lesion location, along with statistical comparisons of the three groups of patients

	Left rlPFC lesion ($n = 6$)[a]	Right rmPFC lesion ($n = 6$)[a]	Other patients ($n = 16$)	Left rlPFC versus other patients groups	Right rmPFC versus other patient groups
Descriptive data: mean (SD)					
Age (years)	52.8 (18.1)	42.8 (12.2)	47.1 (15.6)	$t(20) = 0.743$, $P = 0.466$	$t(20) = -0.589$, $P = 0.563$
Education (years)	13.0 (6.4)	12.8 (2.5)	15.1 (2.5)	$t(20) = -1.150$, $P = 0.264$	$t(20) = -1.903$, $P = 0.072$
Lesion volume (cc)	50.6 (51.4)	31.6 (13.4)	25.5 (24.5)	$t(20) = 1.572$, $P = 0.132$	$t(20) = 0.573$, $P = 0.573$
Lesion delay (months)	66.7 (43.3)	47.3 (43.2)	53.5 (48.9)	$t(20) = 0.578$, $P = 0.569$	$t(20) = -0.271$, $P = 0.789$
Neuropsychological data: mean (SD)					
FAB (/18)	15.7 (1.4)	15.2 (2.3)	15.9 (1.5)	$U = 40.5$, $P = 0.590$	$U = 42$, $P = 0.693$
Category fluency (animals)	31.3 (7.7)	27.7 (8.0)	27.7 (7.7)	$U = 37.5$, $P = 0.449$	$U = 47.5$, $P = 0.971$
Phonemic fluency (letter P)	22.0 (7.5)	18.2 (6.6)	19.8 (7.0)	$U = 45.5$, $P = 0.858$	$U = 41$, $P = 0.641$
Short naming (/40)	39.2 (1.2)	38.7 (1.0)	39.0 (1.1)	$U = 43.5$, $P = 0.747$	$U = 38$, $P = 0.494$
Short PPT (/40)	39.3 (0.5)	39.8 (0.4)	39.3 (0.9)	$U = 43.0$, $P = 0.747$	$U = 33.5$, $P = 0.294$
Stroop conflict	32.5 (7.4)	37.0 (9.9)	37.4 (9.4)	$U = 29.0$, $P = 0.178$	$U = 45.0$, $P = 0.858$
Creative combination task					
CAT-index	41.5 (18.3)	35.6 (10.9)	20.5 (12.8)	**Significant based on the VLSM analysis**	**$t(20) = 2.547$, $P = 0.019$**
CAT-solving (close trials)	47.7 (10.6)	50.0 (11.5)	51.0 (10.7)	$t(20) = -0.655$, $P = 0.520$	$t(20) = -0.199$, $P = 0.844$
CAT-solving (distant trials)	20.4 (9.7)	23.6 (5.8)	34.4 (11.1)	**$t(20) = -2.714$, $P = 0.013$**	**$t(20) = -2.240$, $P = 0.037$**
CAT-omissions	11.3 (11.6)	20.6 (21.3)	17.3 (15.6)	$U = 39.5$, $P = 0.541$	$U = 42.0$, $P = 0.693$
Creative generation task					
FGAT-distant (frequency)	3.15 (1.34)	4.75 (1.07)	3.13 (1.04)	$t(20) = 0.033$, $P = 0.974$	**Significant based on the VLSM analysis**
FGAT-distant (typical responses)	5.0 (4.5)	9.5 (6.5)	5.3 (4.9)	$t(20) = -0.109$, $P = 0.914$	$t(20) = 1.659$, $P = 0.113$
FGAT-distant (unique responses)	30.0 (12.1)	17.5 (7.2)	29.3 (8.2)	$t(20) = 0.154$, $P = 0.879$	**$t(20) = -3.108$, $P = 0.006$**

The impact of the two lesion locations identified in the VLSM analyses (left rlPFC associated with CAT and right rmPFC associated with FGAT) was further explored in *post hoc* analyses to better characterize the cognitive profile of the patients. Based on the VLSM results of CAT-index and FGAT-distant frequency scores, patients were distributed into three groups according to their lesion location: patients with a lesion affecting the left rlPFC VLSM region ('left rlPFC group'), patients with a lesion in the right rmPFC region ('right rmPFC group'), and patients with a lesion that preserved these two regions ('other patients group'). The three groups did not differ significantly in terms of age, years of education, lesion volume or lesion delay. Note that some of the statistics reported for the generation and the combination tasks may be subject to a selection bias and were not used to draw conclusions.

[a]One patient with a lesion affecting both the rlPFC and the rmPFC regions has been removed from these analyses.

Results are shown as the means (SD) or mean percentages of correct responses (SD) for experimental tasks. 'CAT-solving' refers to the percentage of correct responses in the CAT task, and is reported separately for close and distant trials. 'CAT-omissions' refers to the percentage of omissions among failed trials (the remaining failed trials were trials in which participants provided incorrect solution words). Exact *P*-values significant at $P < 0.05$ are provided.

patients with a spared right rmPFC (Fig. 2 and Supplementary Table 3). Patients with a right rmPFC lesion did not differ from other patients in performance on the conflict condition of the Stroop test (Table 3) or in mean reaction times in the FGAT-first and FGAT-distant trials (Supplementary Table 3), which indicated that they did not experience inhibition difficulties or impulsive behaviours. Hence, the impairment of the rmPFC patients in the creativity-related tasks could not be entirely explained by a lack of response inhibition or by increased impulsivity.

In addition, patients with a right rmPFC lesion had slightly (but not significantly) longer reaction times in FGAT-first trials but shorter reaction times in FGAT-distant trials, which does not argue for energization difficulties (the process of initiation and sustaining of any response; Stuss and Alexander, 2007). These findings suggest that a right rmPFC lesion impacts spontaneous semantic associations (FGAT-first) as well as the voluntary generation of remote associations (FGAT-distant). Additionally, patients with a right rmPFC lesion were also impaired in the CAT task (Table 3).

To better understand the consequences of the two lesion locations, we ran a mixed ANOVA comparing CAT-index and FGAT-distant commonness Z-scores between the 'left rlPFC' and 'right rmPFC' groups [patients with left rostrolateral prefrontal cortex (rlPFC) versus right rmPFC lesions], using lesion volume, age, and years of education as covariates (Fig. 2). Although this analysis allowed us to directly compare the impact of different lesion locations on different tasks, it may be subject to a selection bias, since the patient groups were formed based on the VLSM regions. Hence, the results will be interpreted with caution and in integration with the other findings of the study. The ANOVA showed no significant task effect [$F(1,7) = 1.299$, ns] and no significant group effect [$F(1,7) = 0.158$, ns] but did show a significant interaction between tasks and groups [$F(1,7) = 5.766$, $P = 0.047$]. Left rlPFC and right rmPFC lesions both impacted the CAT but only a right rmPFC lesion was associated with difficulties in the FGAT task (Table 3 and Fig. 2).

Finally, there was no significant difference between patient groups in Stroop scores, verbal fluency scores, naming and semantic matching scores (Table 3). The lesion overlap of each patient group is provided in Supplementary Fig. 5.

Overall, these results show that different lesion locations were associated with different profiles of performance in generation and combination tasks, suggesting that left rlPFC and right rmPFC lesions affect different brain mechanisms involved in creativity. As shown in Fig. 2, patients with a right rmPFC lesion were impaired in both creativity-related tasks (generation in the FGAT-distant, combination in the CAT) and produced more common associates in the spontaneous word association task (FGAT-first), whereas patients with a left rlPFC lesion were impaired in the CAT only.

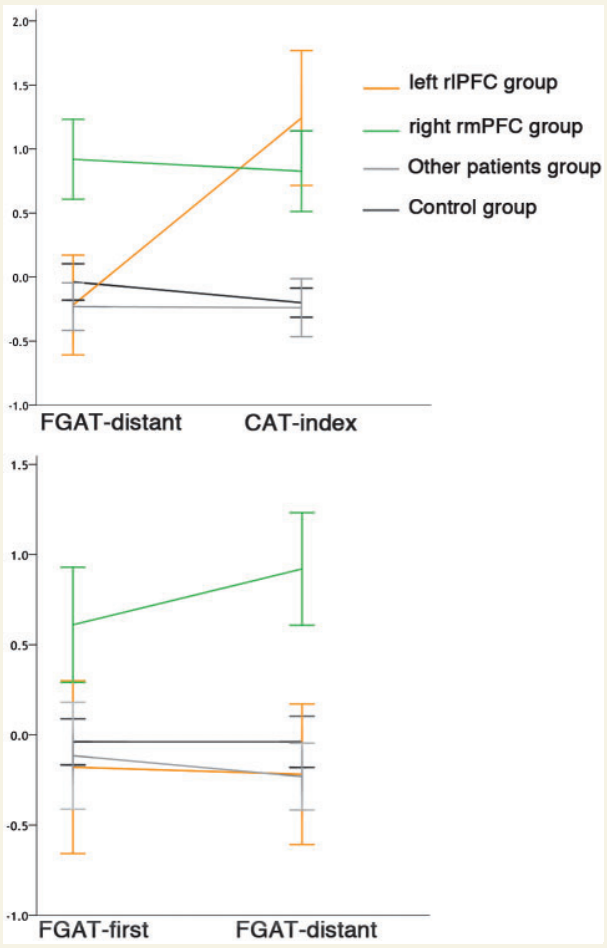

Figure 2 ***Post hoc* analysis of CAT and FGAT performance in the distinct patient groups.** Patients in the 'left rlPFC group' had a lesion affecting the left rlPFC as identified in the VLSM analysis; patients in the 'right rmPFC group' had a lesion affecting the right rmPFC as identified in the VLSM analysis. Patients with a lesion that spared these two regions were pooled in the 'other patient group'. The 'control group' included paired healthy subjects. The 'right rmPFC group' showed significantly poorer results than the other groups for both FGAT-distant and CAT-index performance whereas patients in the 'left rlPFC group' were only impaired in the CAT-index (*top*). Patients in the 'right rmPFC group' generated more common responses than any other group in the FGAT-distant and FGAT-first conditions (*bottom*). Error bars represent standard errors. Note that the higher the FGAT scores were, the more common the responses of the participants, and the higher the CAT-index scores were, the poorer the creative performance. *Y*-axes: performance expressed as Z-scores.

Disconnection-deficit mapping analyses

The disconnection-deficit mapping method showed that the disconnection of tracts connecting the left rlPFC was associated with difficulties in combining remote ideas (CAT), especially when connections from the left anterior thalamic radiations and the left fronto-marginal tract were disconnected (Fig. 3A; $P < 0.05$, FWE-corrected). This result remained significant when the FGAT-distant frequency score was entered as a covariate in the regression, indicating that the deficit in CAT-index associated with the reported disconnections was not related to a deficit in the FGAT-distant task.

In contrast, the difficulties in generating distant ideas (FGAT-distant frequency) were associated with a disconnection of the right cingulate fasciculus (Fig. 3B; $P < 0.01$, not surviving FWE correction).

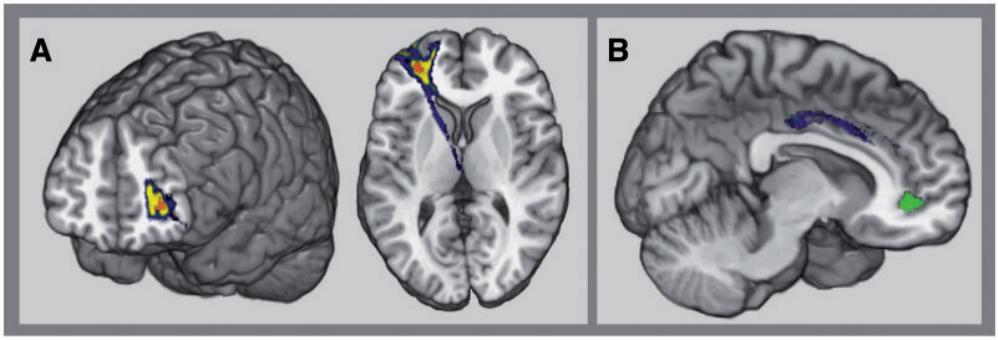

Figure 3 Disconnection-deficit mapping. The disconnection-deficit map of the CAT-index score ($P < 0.05$, FWE-corrected) (**A**) and of the FGAT-distant commonness of responses ($P < 0.01$, uncorrected) (**B**) are superimposed on a 3D brain rendering and displayed in a blue-to-green gradient. The VLSM regions associated with CAT-index and FGAT-distant commonness are superimposed in red and green, respectively.

Table 4 Demographic data, experimental task performance, and statistical comparisons of the three groups of patients as a function of the integrity of the default mode and the fronto-parietal control networks

	Damaged DMN ($n = 9$)	Intact DMN ($n = 20$)	Damaged left FPCN ($n = 10$)	Intact left FPCN ($n = 19$)	Damaged right FPCN ($n = 12$)	Intact right FPCN ($n = 17$)
Descriptive data						
Age (years)	48.8 (13.4)	47.0 (16.2)	50.7 (16.9)	45.8 (14.4)	44.4 (13.7)	49.7 (16.2)
Education (years)	12.7 (2.6)	14.7 (3.9)	13.4 (5.0)	14.4 (2.8)	14.7 (3.3)	13.7 (3.9)
Lesion volume (cm^3)	53.7 (54.9)	28.2 (23.4)	50.5 (53.6)	28.5 (23.0)	**50.2 (35.7)***	26.1 (35.7)
Lesion delay (months)	59.4 (45.8)	53.0 (45.1)	74.5 (44.8)	44.7 (42.1)	60.3 (43.0)	51.2 (46.7)
Creative combination task						
CAT-index	36.6 (13.1)	25.8 (17.4)	**39.2 (16.3)***	23.9 (14.7)	27.1 (16.7)	30.6 (17.0)
Creative generation task						
FGAT-distant (frequency)	**4.3 (1.0)***	3.2 (1.3)	3.6 (1.3)	3.5 (1.3)	4.0 (1.6)	3.2 (1.0)

There was no significant difference between damaged and intact networks for age, education, and lesion volume or delay, except for the right FPCN. Patients with a damaged DMN (compared to patients with intact DMN) produced statistically more common responses in the FGAT-distant task [$t(27) = 2.318$, $P = 0.028$], their performance on the CAT was poorer but not statistically significantly [CAT-index: $t(27) = 1.650$, $P = 0.110$]. Conversely, patients with a damaged left FPCN produced responses in the FGAT task similar to those of patients with intact left FPCN [$t(27) = 0.051$, $P = 0.960$], but their performance on the CAT was significantly poorer [CAT-index: $t(27) = 2.573$, $P = 0.016$]. Performance of patients with a damaged right FPCN did not differ significantly from performance of patients with an intact right FPCN [FGAT task: $t(27) = 1.610$, $P = 0.119$; CAT-index: $t(27) = -0.552$, $P = 0.586$]. Means (SD) are provided. Significant differences between damaged and intact groups are indicated in bold (*$P < 0.05$).

Both results (disconnections associated with CAT-index and disconnections associated with FGAT-distant frequency) remained significant at the same respective thresholds when age, years of education, and lesion volume were not covaried out, and when semantic matching scores and semantic fluency scores were covaried out.

The disconnection-deficit mapping of the FGAT-first score was not significant.

Overall, these results indicate that distinct brain disconnections differently support the ability to freely generate distant associates and the ability to combine these associates.

Resting state network-based analyses

The status of the DMN and FPCN damage for each patient is reported in Supplementary Table 1. We compared the FGAT and CAT performance of the patients with damaged versus intact networks (Table 4 and Supplementary Fig. 3). The results confirmed that patients with a damaged DMN had difficulties in generating remote associates (FGAT-distant task; $P = 0.028$), whereas patients with a damaged left FPCN had difficulties in combining remote associates (CAT-index; $P = 0.002$). Damage to the right FPCN did not impair either FGAT-distant or CAT performance. Overall, these results indicate that damage to the DMN and the left FPCN may have a different impact on CAT and FGAT task performance.

Discussion

Based on three complementary methods performed on the same set of data (lesions and scores), the novel findings of this study demonstrate that distinct frontal regions, likely parts of two separate networks, are critical for two aspects

of creative thinking: lesions to the right rmPFC, its connections, or the DMN impaired the ability to generate remote associates, whereas lesions to the left rlPFC, its connections, or the left FPCN impaired the ability to combine remote associates. The cognitive deficits associated with damage to these distinct regions have implications for understanding the associative and controlled processing involved in creative abilities, as discussed below.

Critical role of the right rostromedial prefrontal cortex in generating remote associations: associative thinking mechanisms?

Patients with a lesion in the right rmPFC region had difficulty in generating remote associations in the FGAT-distant condition, and additionally generated more typical responses in the FGAT-first condition, a task that explores spontaneous word associations. Word-association tasks similar to the FGAT-first condition are used to measure semantic distance in association norms, a measure that correlates with the priming effect (Mednick *et al.*, 1964*b*; Gruszka and Necka, 2002; Faust and Lavidor, 2003). The priming effect estimates how two words or concepts are automatically associated in semantic memory. Hence, more typical word responses in the FGAT-first task may reflect that patients with a right rmPFC lesion have stronger semantic associations, suggesting that they have a different organization or access to semantic associations. Right rmPFC patients performed similarly to the other patient groups in naming, semantic matching and category fluency tasks, and had similar response times under the FGAT conditions, indicating that they had no major impairments or slowness in semantic memory. We can nevertheless not exclude the possibility that patients had a subtle semantic memory impairment that was undetected by the semantic neuropsychological tests that were used. Hence, although the relationships between word association tasks and classical semantic memory tasks—and their related brain networks—remain to be clarified (Bar *et al.*, 2007; Humphreys *et al.*, 2015), our results suggest that the right rmPFC plays a role in associative thinking abilities. Overall, the FGAT-first task is not a creativity task *per se* but reflects associative mechanisms that have been shown to play a role in creative abilities (Merten and Fischer, 1999; Gruszka and Necka, 2002; Faust and Lavidor, 2003; Rossmann and Fink, 2010; Benedek *et al.*, 2012*b*; Beaty *et al.*, 2014*a*), and more particularly, computational methods have shown that the organization of semantic memory is related to creativity (Kenett *et al.*, 2014; Benedek *et al.*, 2017).

The differences in the spontaneous access to semantic associations in right rmPFC patients can explain their difficulties in generating distant associates in the FGAT-distant condition. As Mednick stated, 'if an individual's associative response to a stimulus element of a creative problem is of excessive strength, this will tend to reduce the likelihood of occurrence of more remote associative responses . . . and will reduce the probability and speed of creative solution' (Mednick, 1962). FGAT-distant correlated with the originality and fluency scores on the Torrance test, suggesting this task involves a divergent thinking component. Right rmPFC patients did not differ from other patients in the conflict condition of the Stroop score or in phonemic and category fluency tasks, suggesting that their difficulties in generating remote associates may not be explained by difficulties in inhibition, lexical retrieval, controlled search in memory and working memory. However, as these neuropsychological tasks were not directly matched to the FGAT-distant task, we cannot exclude the possibility that they placed fewer demands on executive processes than FGAT-distant tasks, which could explain the dissociation of performance in these patients. Hence, whether the difficulties of right rmPFC patients in voluntary generating remote ideas (observed in their FGAT-distant responses) could be solely explained by less flexible spontaneous semantic associations (typicality of their FGAT-first responses) or also by additional semantic control processes required in the FGAT-distant task remains an open question.

The role of the rmPFC in the generation of distant or creative ideas has been shown in a previous lesion study (Shamay-Tsoory *et al.*, 2011) and in functional imaging studies (Seger *et al.*, 2000; Green *et al.*, 2015). Using a word association task, Green *et al.* (2015) found that the generation of unusual associations co-activated the rmPFC and other regions such as the parahippocampal region and the cingulate cortex that are part of the DMN. The current results also showed that damage to the DMN (resting state network analysis) and a disconnection of the cingulate fasciculus (disconnection analysis) altered the free generation of distant ideas (FGAT-distant), suggesting that the rmPFC, as part of the DMN, is critical for the generation of remote ideas. This interpretation is consistent with several morphometry studies in healthy subjects that have shown a link between different structures of the DMN regions and/or the cingulate fasciculus and creativity tasks (Takeuchi *et al.*, 2010; Jung *et al.*, 2013; Chen *et al.*, 2014, 2015; Fink *et al.*, 2014; Kühn *et al.*, 2014; Jauk *et al.*, 2015). Overall, the current results and recent neuroimaging data point to the DMN, especially the core DMN including the rmPFC (Andrews-Hanna *et al.*, 2014; Christoff *et al.*, 2016), as being critical for remote thinking and unusual idea generation.

Furthermore, the poor performance of rmPFC patients on the combination task, CAT, may also be explained by an excessive strength in semantic associations and/or a difficulty in generating distant ideas in the FGAT conditions (Mednick, 1962; Mednick *et al.*, 1964*a*). A few previous studies have demonstrated that there is a link between the ability to freely generate distant associates (as in the FGAT-distant condition) and creative performance, including performance on Mednick's task (similar to the CAT;

Rossmann and Fink, 2010; Benedek *et al.*, 2012*b*; Benedek and Neubauer, 2013; Smith *et al.*, 2013; Hass, 2016). Neuro-computational methods using semantic graphs have also demonstrated that more creative people have more flexible semantic associations (Kenett *et al.*, 2014, 2016; Kenett and Austerweil, 2016; Benedek *et al.*, 2017). Conversely, if a patient is characterized by typicality and excessive strength in semantic associations, when solving the CAT, he/she may be fixated on the strong associates of each cue word, which would prevent the activation of more remote associates and of the solution word (Fig. 4A). Our results support this hypothesis, showing that rmPFC patients had excessively typical spontaneous semantic associations that could explain that they had difficulties to solve the CAT. This interpretation might also be related to the observation that right rmPFC patients reported more Eureka experiences than the other patients in both correct and incorrect CAT trials (Supplementary Table 4). Indeed,

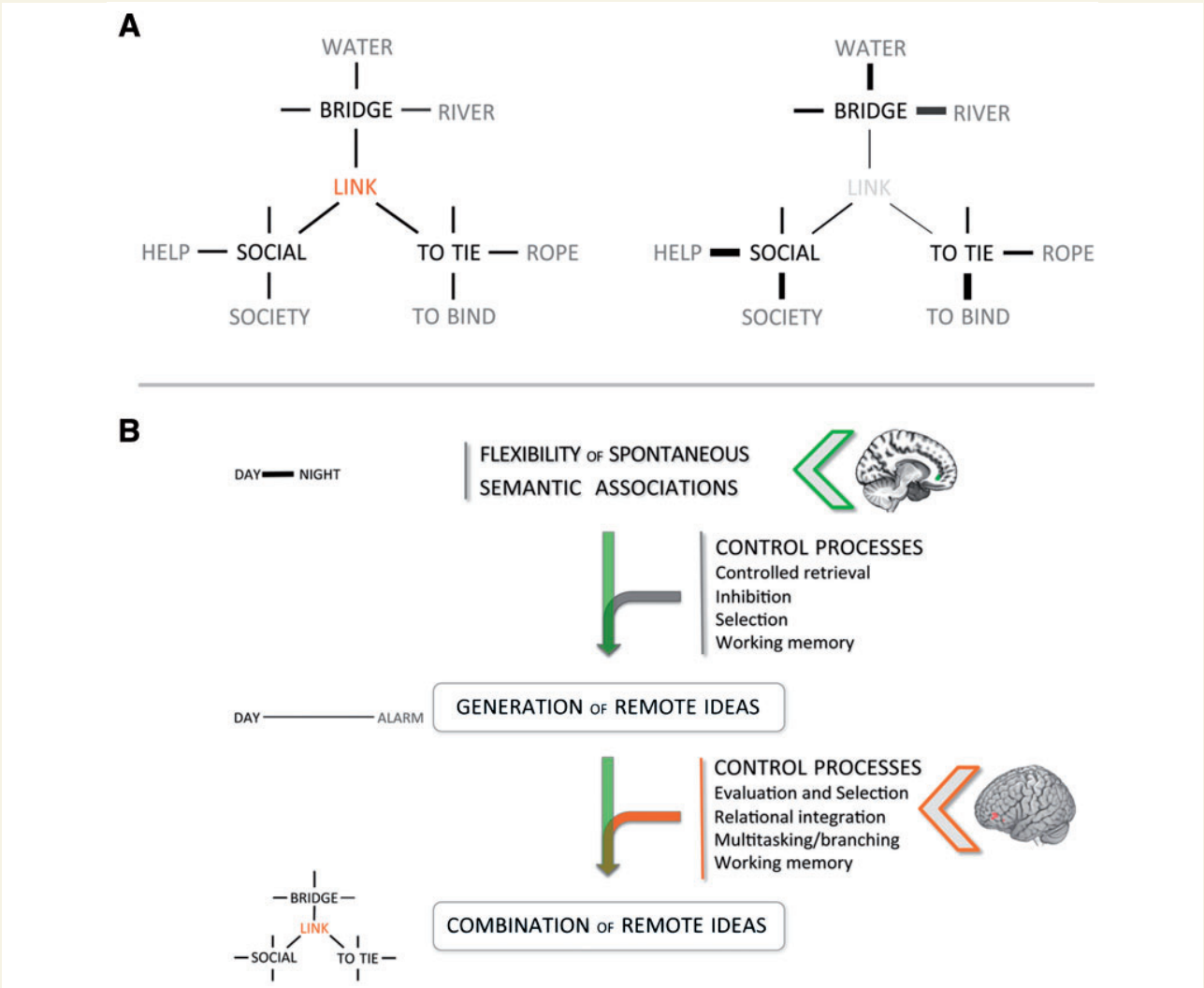

Figure 4 Schematic interpretation of the results. (**A**) This schematic representation of the CAT illustrates that compared to people with flexible semantic associations (*left*), patients with typicality in semantic associations (including patients with right rmPFC damage) may be fixated on the strong associates of each cue word when solving the CAT (*right*, for instance 'river' or 'water' for 'bridge', 'help' for 'social' and 'rope' for 'to tie'). These strong associations prevent the activation of more remote associates, including the solution word 'link'. For instance, if we present a right rmPFC patient with the word 'bridge' he may tend to be restricted to stereotyped responses, such as 'water' or 'river', and would be characterized as having an associative hierarchy with a steep slope (Mednick, 1962), preventing him/her from getting past the first one or two conventional responses to the stimulus and acceding to the solution. (**B**) Cognitive mechanisms likely affected by a right rmPFC/DMN lesion (green open arrow) and by a left rlPFC/FPCN lesion (orange open arrow) and their consequences in further processing for creative activities (green and orange filled arrows). Alteration of associative thinking abilities after right rmPFC damage affects further steps of creative thinking, i.e. on generation and combination mechanisms. Controlled processes, supported in part by the left rlPFC and its connections, manage the generated ideas for further integration and the selection of an appropriate response to satisfy the constraints of the task.

an increased rate of Eureka reports may suggest that these patients rely more than the other patients on strong and spontaneous semantic associations to generate their response. However, this result is difficult to interpret because the link between strong semantic associations and Eureka experiences is not straightforward.

Overall, the deficits in right rmPFC patients support Mednick's hypothesis, which had previously only been explored in healthy subjects, and indicate a role for right rmPFC in associative thinking. This interpretation may not be entirely supported by the resting state network analysis, as patients with DMN damage experienced difficulties in generating remote associates (FGAT-distant), although their FGAT-first (spontaneous associations) and CAT-index (combination of remote associates) scores failed to reach significance. However, this interpretation is in line with a growing body of literature showing the role of the DMN in spontaneous cognition (Andrews-Hanna *et al.*, 2010, 2014), in mind wandering and daydreaming (Fox *et al.*, 2015; Christoff *et al.*, 2016), and in contextual associations (Bar, 2009*a*, *b*), suggesting its involvement in spontaneous associative thinking. Rather than specific processes or content of thoughts, the DMN may underlie a thinking mode characterized by a spontaneous and associative progression of thoughts that favours creative thinking. A schematic representation of the interpretation of the results according to previous literature is provided in Fig. 4B.

Additional results of this study showed that other cognitive and cerebral mechanisms are necessary for creative combination abilities, as revealed by the cognitive profile of patients with left rlPFC damage.

Critical role of the left rostrolateral prefrontal cortex in combining remote ideas

Damage to the left rlPFC impaired CAT performance, whereas the generation of remote associates was preserved. Damage to some of the connections of the left rlPFC, and damage to the left FPCN also impaired CAT performance. This indicates that a left rlPFC lesion altered CAT performance by a mechanism different from that of a right rmPFC lesion (Fig. 4B).

In addition to associative thinking, solving CAT-like tasks indeed involves controlled cognitive mechanisms (Table 2; Mednick, 1962; Lee and Theriault, 2013) such as the strategic search and controlled retrieval in memory (Smith *et al.*, 2013), the inhibition of interference caused by frequent and more salient associates (Gupta *et al.*, 2012), the integration or combination of the retrieved associates (Taft and Rossiter, 1966), and the selection and evaluation of a solution that satisfies the constraints of the task (Mednick, 1962). The preserved FGAT-first performance of left rlPFC patients suggests that they did not have a different organization of semantic associations compared with healthy controls. Their preserved FGAT-distant performance suggests that the controlled processes allowing for the generation of remote associations were also preserved, including controlled retrieval in memory or the inhibition of prepotent associates (Table 3). This interpretation is consistent with the preserved performance of left rlPFC patients in the Stroop interference task and verbal fluency tasks. Hence, a remaining hypothesis is that a left rlPFC lesion (or a disconnection of this region) impacted the CAT performance at the integration or combination step. This integration/combination step likely corresponds to the convergent component identified in recent studies that explored the remote associates task using computational method and simulations, as opposed to the divergent component (Klein and Badia, 2015; see also Smith *et al.*, 2013).

The role of the left rlPFC in the processes involved in the combination of remote elements remains poorly understood. Only a few functional MRI and EEG studies have been performed using CAT-like tasks, and most of them have focused on the insight component of the task over other information-processing aspects (Jung-Beeman *et al.*, 2004; Sandkühler and Bhattacharya, 2008; Subramaniam *et al.*, 2009; Dietrich and Kanso, 2010). However, two studies support the role of the left rlPFC in creative combination. A meta-analysis of functional imaging studies of creativity showed that the tasks requiring the combination of separate and remote elements, i.e. 'creative combination tasks' were associated with more activation in the left rlPFC than other types of creativity tasks (Gonen-Yaacovi *et al.*, 2013). A morphometry study in healthy subjects showed a correlation between creative combination abilities and grey matter volume in the left rlPFC (Bendetowicz *et al.*, 2017). Thus, despite the limitations of the current study (including its small sample size, the non-independence between VLSM and group analyses, and the use of control tasks that were not strictly matched to the experimental tasks), the convergence with previous findings on creativity using different approaches reinforces the strength and interpretations of the current results.

The hypothesis regarding the role of the left rlPFC, and possibly of the FPCN, in the integration or combination of remote elements in our creativity-related task is also consistent with neuroimaging studies from other fields of research. Previous functional imaging studies have established the role of the rlPFC—in connection with the FPCN—in the integration of relational information (Kroger *et al.*, 2002; Krawczyk, 2012; Parkin *et al.*, 2015; Aichelburg *et al.*, 2016; Hobeika *et al.*, 2016), especially in the integration of semantically remote (Green *et al.*, 2012*b*) or multiple (Christoff *et al.*, 2001; Bunge *et al.*, 2005; Cho *et al.*, 2010) relationships. Relational integration has been shown to depend on the integrity of the left but not right rlPFC in patients (Urbanski *et al.*, 2016). In this regard, it is noteworthy that CAT-like tasks have shown strong correlations with relational reasoning tasks (Chermahini and Hommel, 2010; Lee and Therriault, 2013; Jones and Estes, 2015). Hence, left rlPFC patients may have

difficulties in integrating several pieces of information to solve the CAT. This hypothesis is in agreement with the established roles of the rostral PFC in multitasking (enacting the sequence of subgoals required to achieve a behaviour without any cue in the environment to indicate when to switch subgoals) (Burgess *et al.*, 2007, 2009) and in branching (maintaining a subtask in a reversible pending state during the execution of another one) (Hyafil and Koechlin, 2016). These complex types of processing likely occur when solving the CAT (Table 2 and Fig. 4). However, the computation performed to combine remote associates is not yet fully understood (Ward and Kolomyts, 2010; Thagard and Stewart, 2011; Gupta *et al.*, 2012; Smith *et al.*, 2013; Klein and Badia, 2015), and further studies are needed to better understand this computation and its cerebral substrate.

Finally, the disconnection-mapping results revealed that the role of the left rlPFC in creative combination may be supported by its connections through the anterior thalamic radiations and the fronto-marginal tract in the CAT. This suggests that the involvement of the left FPCN in the CAT is supported by cortico-subcortical connections rather than by a direct long-range fronto-parietal system. The anterior thalamic radiations carry association fibres projecting from the thalamus to frontal cortical structures and reciprocal projections to the anterior part of the prefrontal cortex originating from the mediodorsal nucleus, and they are involved in executive functions, working memory and drive (Catani and Thiebaut de Schotten, 2012). The microstructure of the left anterior thalamic radiations has been reported to relate to creative abilities in healthy subjects (Jung *et al.*, 2010*a*, 2013). The fronto-marginal tract connects the lateral and the medial portion of the frontal pole (Rojkova *et al.*, 2016); however, the role of this fasciculus in cognition remains undocumented. Overall, in agreement with previous functional MRI and morphometry data, the current results show that the left rlPFC or some of its connections are critical for combining remote associates, and suggest their role in the integration of multiple and remote elements.

Integration of the results with recent functional connectivity studies and existing theories

A recent series of functional connectivity studies has indicated that creative thinking involves dynamic interactions of large-scale brain systems that include the DMN and FPCN, which are usually anti-correlated at rest, but appear to cooperate during creative tasks and artistic performance (Ellamil *et al.*, 2012; Jung, 2014; Beaty *et al.*, 2016; De Pisapia *et al.*, 2016). Previous studies have also shown that the FPCN and the DMN work in interaction to allow deliberate control or constraints on thoughts (Christoff *et al.*, 2009, 2016). Based on this literature, Beaty *et al.* (2016) proposed that creative performance involves both generative functions possibly supported by the default network and the control functions supported by control-related networks. Our findings are consistent with these data and additionally demonstrate the necessary regions within each anatomical network in patients. We showed that the left rlPFC, likely in connection with other FPCN and subcortical regions, plays a role in controlled processes and is possibly involved in the integration/combination of the generated ideas to meet task-specific goals, whereas the right rmPFC, a region of the DMN, is critical for the generation of remote ideas. Moreover, we showed that damage to the right medial prefrontal region impacted the associative component of idea generation as reflected by spontaneous semantic associations. Hence, the current results add evidence for the concept of associative and controlled interacting modes of creative thinking that is supported by existing psychological and recent neuroimaging data (for reviews see Dietrich, 2004; Gabora, 2010; Jung, 2014; Beaty *et al.*, 2016; Volle, 2017). These interactive thinking modes are likely not unique to creativity but are probably general in cognition, as soon as we control our stream of thought (Christoff *et al.*, 2009, 2016; Spreng *et al.*, 2010; Chen *et al.*, 2013). They may be linked with classical dual-process theories that generally oppose an intuitive-heuristic system (automatic system 1) to a deliberate analytic system (controlled system 2) (Lieberman *et al.*, 2004; De Neys, 2006; Allen and Thomas, 2011; Kahneman, 2011; Evans and Stanovich, 2013; Varga and Hamburger, 2014; Sowden *et al.*, 2015; Cassotti *et al.*, 2016).

The right lateralization of the region associated with spontaneous semantic associations is consistent with the hypothesis of a right hemispheric dominance for coarse coding of semantic associations (Jung-Beeman, 2005; Kounios and Beeman, 2014). This theory emphasizes the importance of right hemispheric structures for the activation, the selection and the integration of coarser semantic elements, whereas left hemisphere structures may be related to fine-grained processing of semantic knowledge by activating smaller semantic fields. In light of this hypothesis, our results suggest that right prefrontal structures are necessary for the activation of larger semantic fields and to generate distant semantic relations. The experimental distinction between associative and controlled processes and their brain correlates may help reconcile some paradoxical results between insight functional MRI studies that emphasized the role of right brain regions in creativity (Jung-Beeman *et al.*, 2004; Kounios and Beeman, 2014) and meta-analyses of functional imaging studies that highlighted the left dominance of brain regions associated with various creativity tasks (Dietrich and Kanso, 2010; Gonen-Yaacovi *et al.*, 2013; Boccia *et al.*, 2015; Wu *et al.*, 2015).

Limitations

The lesion approach in general, and our results in particular, do not take into account the neuroplasticity that occurs

after a brain lesion. Patients with lesions from different aetiologies that have distinct time courses and different mechanisms of plasticity have been included in this study. However, we did not find significant differences in performance between aetiologies, as it has previously been shown for executive functions (Cipolotti *et al.*, 2015). Inclusion of various lesion aetiologies allowed us to obtain a broader brain distribution of lesions, especially in the rostral PFC, which is rarely the site of ischaemic strokes. The small number of patients included ($n = 29$) may limit the possibility to identify all the critical PFC regions related to our tasks. We cannot exclude the possibility that the VLSM analyses missed other critical prefrontal regions or underestimated the size of the critical functional area because of a lack of statistical power in some of the regions and because of only partial coverage of the frontal lobes. We favoured quality over quantity: the selection criteria were restricted to focal and unique lesions in the prefrontal regions (excluding traumatic brain injury that also provokes diffuse axonal lesion). The current study focused on the frontal region based on its importance in the existing literature on creative cognition; however, the necessity of non-frontal brain regions for creative abilities, especially regions belonging to the DMN, the semantic network, and the control-related networks, should be further tested.

In addition, correlations between CAT-index and FGAT-distant scores with divergent thinking measures and creative achievement in control subjects indicate that CAT and FGAT tasks are creativity-related tasks. However, the precise cognitive processes involved in FGAT-distant and CAT tasks, and their relationships with other creativity tasks, will need to be clarified. The respective critical role of the left rlPFC and right rmPFC and their related networks in these creative processes should also be confirmed in a further independent patient study. Furthermore, creativity is a complex construct that is not fully explored by CAT and FGAT tasks that focus on the semantic domain using word associations. Thus, it is possible that other domains of creativity, for instance non-verbal or more ecological creativity tasks, would involve other or additional brain networks.

Conclusions

Recent findings have shown that creative abilities depend on the interaction between the DMN and the FPCN that may support associative and controlled processing of information. Our results converge and add more causal evidence to these findings by showing using verbal creativity-related tasks that there are critical nodes in these networks supporting associative and controlled processing. The integrity of the right rmPFC was shown critical for associative thinking and to generate remote associates, while the integrity of the left rlPFC and some of its connections was critical for constraining this process at the combination step. The precise role of the DMN in the organization or activation of semantic associations is an important question for future research, which could benefit from neuro-computational methods using semantic graphs. Finally, how the current results based on word association tasks can be generalized to various creativity tasks or domains is an essential issue that could be tested in healthy subjects and in patients.

Acknowledgements

The authors thank the participants of this study, and thank Prof. Claude Adam, Dr Carole Azuar, Dr Dorian Chauvet, Dr Frédéric Clarençon Dr Vincent Degos, Prof. Sophie Dupont, Prof. Damien Galanaud, Dr Florence Laigle, Dr Marc-Antoine Labeyrie, Dr Anne Leger, Prof. Vincent Navarro, and Prof. Pascale Pradat-Diehl for their help in recruiting the patients.

Funding

This work was supported by the 'Agence Nationale de la Recherche' [grant numbers ANR-09-RPDOC-004-01, EV and ANR-13-JSV4-0001-01, MTS], the 'Fondation pour la recherche medicale' [grant numbers: FDM20150632801 and DEQ20150331725], and the 'Societe Française de Neurologie' (MLB and DB). The research received funding from the program 'Investissements d'avenir' ANR-10-IAIHU-06.

Supplementary material

Supplementary material is available at *Brain* online.

References

Abraham A, Beudt S, Ott DVM, Yves von Cramon D. Creative cognition and the brain: dissociations between frontal, parietal–temporal and basal ganglia groups. Brain Res 2012; 1482: 55–70.

Aichelburg C, Urbanski M, Thiebaut de Schotten M, Humbert F, Levy R, Volle E. Morphometry of left frontal and temporal poles predicts analogical reasoning abilities. Cereb Cortex 2016; 26: 915–32.

Allen AP, Thomas KE. A dual process account of creative thinking [review]. Creat Res J 2011; 23: 109–18.

Andersen SM, Rapcsak SZ, Beeson PM. Cost function masking during normalization of brains with focal lesions: still a necessity? Neuroimage 2010; 53: 78–84.

Andrews-Hanna JR, Reidler JS, Huang C, Buckner RL. Evidence for the default network's role in spontaneous cognition. J Neurophysiol 2010; 104: 322–35.

Andrews-Hanna JR, Smallwood J, Spreng RN. The default network and self-generated thought: component processes, dynamic control, and clinical relevance [review]. Ann NY Acad Sci 2014; 1316: 29–52.

Avants BB, Tustison NJ, Song G, Cook PA, Klein A, Gee JC. A reproducible evaluation of ANTs similarity metric performance in brain image registration. Neuroimage 2011; 54: 2033–44.

Bar M. The proactive brain: memory for predictions [review]. Philos Trans R Soc B Biol Sci 2009a; 364: 1235–43.

Bar M. A cognitive neuroscience hypothesis of mood and depression [review]. Trends Cogn Sci 2009b; 13: 456–63.

Bar M, Aminoff E, Mason M, Fenske M. The units of thought. Hippocampus 2007; 17: 420–8.
Barbey AK Colom R, Grafman J. Architecture of cognitive flexibility revealed by lesion mapping. Neuroimage 2013; 82: 547–54.
Bates E, Wilson SM, Saygin AP, Dick F, Sereno MI, Knight RT, et al. Voxel-based lesion-symptom mapping. Nat Neurosci 2003; 6: 448–50.
Beaty RE, Benedek M, Wilkins RW, Jauk E, Fink A, Silvia PJ, et al. Creativity and the default network: a functional connectivity analysis of the creative brain at rest. Neuropsychologia 2014a; 64: 92–8.
Beaty RE, Silvia PJ, Nusbaum EC, Jauk E, Benedek M. The roles of associative and executive processes in creative cognition. Mem Cognit 2014b; 42: 1186–97.
Beaty RE, Benedek M, Silvia PJ, Schacter DL. Creative cognition and brain network dynamics [review]. Trends Cogn Sci 2016; 20: 87–95.
Bendetowicz D, Urbanski M, Aichelburg C, Levy R, Volle E. Brain morphometry predicts individual creative potential and the ability to combine remote ideas. Cortex 2017; 86: 216–29.
Benedek M, Franz F, Heene M, Neubauer AC. Differential effects of cognitive inhibition and intelligence on creativity. Personal Individ Differ 2012a; 53–334: 480–5.
Benedek M, Könen T, Neubauer AC. Associative abilities underlying creativity. Psychol Aesthet Creat Arts 2012b; 6: 273–81.
Benedek M, Neubauer AC. Revisiting Mednick's model on creativity-related differences in associative hierarchies. Evidence for a common path to uncommon thought. J Creat Behav 2013; 47: 273–89.
Benedek M, Kenett YN, Umdasch K, Anaki D, Faust M, Aljoscha CN. How semantic memory structure and intelligence contribute to creative thought: a network science approach. Think Reason 2017; 23: 158–83.
Binder JR, Desai RH, Graves WW, Conant LL. Where is the semantic system? A critical review and meta-analysis of 120 functional neuroimaging studies. Cereb Cortex 2009; 19: 2767–96.
Boccia M, Piccardi L, Palermo L, Nori R, Palmiero M. Where do bright ideas occur in our brain? Meta-analytic evidence from neuroimaging studies of domain-specific creativity. Front Psychol 2015; 6: 1195.
Buckner RL, Andrews-Hanna JR, Schacter DL. The brain's default network [review]. Ann N Y Acad Sci 2008; 1124: 1–38.
Bunge SA, Wendelken C, Badre D, Wagner AD. Analogical reasoning and prefrontal cortex: evidence for separable retrieval and integration mechanisms. Cereb Cortex 2005; 15: 239–49.
Burgess PW, Dumontheil I, Gilbert SJ. The gateway hypothesis of rostral prefrontal cortex (area 10) function [review]. Trends Cogn Sci 2007; 11: 290–8.
Burgess PW, Alderman N, Volle E, Benoit RG, Gilbert SJ. Mesulam's frontal lobe mystery re-examined [review]. Restor Neurol Neurosci 2009; 27: 493–506.
Cassotti M, Agogué M, Camarda A, Houdé O, Borst G. Inhibitory control as a core process of creative problem solving and idea generation from childhood to adulthood. New Dir Child Adolesc Dev 2016; 2016: 61–72.
Catani M, Thiebaut de Schotten M. Atlas of human brain connections. Oxford, New York: Oxford University Press; 2012.
Chen AC, Oathes DJ, Chang C, Bradley T, Zhou Z-W, Williams LM, et al. Causal interactions between fronto-parietal central executive and default-mode networks in humans. Proc.Natl Acad Sci USA 2013; 110: 19944–9.
Chen Q, Yang W, Li W, Wei D, Li H, Lei Q, et al. Association of creative achievement with cognitive flexibility by a combined voxel-based morphometry and resting-state functional connectivity study. Neuroimage 2014; 102 Pt 2: 474–83.
Chen Q-L, Xu T, Yang W-J, Li Y-D, Sun J-Z, Wang K-C, et al. Individual differences in verbal creative thinking are reflected in the precuneus. Neuropsychologia 2015; 75: 441–9.
Chermahini SA, Hommel B. The (b)link between creativity and dopamine: spontaneous eye blink rates predict and dissociate divergent and convergent thinking. Cognition 2010; 115: 458–65.
Chermahini SA, Hickendorff M, Hommel B. Development and validity of a Dutch version of the Remote Associates Task: an item-response theory approach. Think Ski Creat 2012; 7: 177–86.
Cho S, Moody TD, Fernandino L, Mumford JA, Poldrack RA, Cannon TD, et al. Common and dissociable prefrontal loci associated with component mechanisms of analogical reasoning. Cereb Cortex 2010; 20: 524–33.
Christoff K, Gordon AM, Smallwood J, Smith R, Schooler JW. Experience sampling during fMRI reveals default network and executive system contributions to mind wandering. Proc Natl Acad Sci USA 2009; 106: 8719–24.
Christoff K, Prabhakaran V, Dorfman J, Zhao Z, Kroger JK, Holyoak KJ, et al. Rostrolateral prefrontal cortex involvement in relational integration during reasoning. Neuroimage 2001; 14: 1136–49.
Christoff K, Irving ZC, Fox KCR, Spreng RN, Andrews-Hanna JR. Mind-wandering as spontaneous thought: a dynamic framework [review]. Nat Rev Neurosci 2016; 17: 718–31.
Cipolotti L, Healy C, Chan E, MacPherson SE, White M, Woollett K, et al. The effect of age on cognitive performance of frontal patients. Neuropsychologia 2015; 75: 233–41.
Cole MW, Reynolds JR, Power JD, Repovs G, Anticevic A, Braver TS. Multi-task connectivity reveals flexible hubs for adaptive task control. Nat Neurosci 2013; 16: 1348–55.
Cousijn J, Zanolie K, Munsters RJM, Kleibeuker SW, Crone EA. The relation between resting state connectivity and creativity in adolescents before and after training. PLoS One 2014; 9: e105780.
Crinion J, Ashburner J, Leff A, Brett M, Price C, Friston K. Spatial normalization of lesioned brains: performance evaluation and impact on fMRI analyses. Neuroimage 2007; 37: 866–75.
De Dreu CKW, Nijstad BA, Baas M, Wolsink I, Roskes M. Working memory benefits creative insight, musical improvisation, and original ideation through maintained task-focused attention. Pers Soc Psychol Bull 2012; 38: 656–69.
De Neys W. Automatic-heuristic and executive-analytic processing during reasoning: chronometric and dual-task considerations. Q J ExpPsychol 2006; 59: 1070–100.
Debrenne M. Le dictionnaire des associations verbales du français et ses applications. In: Bertrand O, Schaffner I, editors. Variétés, variations and formes du français. Palaiseau: Éditions de l'École polytechnique; 2011. p. 355–66.
De Pisapia N, Bacci F, Parrott D, Melcher D. Brain networks for visual creativity: a functional connectivity study of planning a visual artwork. Sci Rep 2016; 6: 39185.
de Souza LC, Volle E, Bertoux M, Czernecki V, Funkiewiez A, Allali G, et al. Poor creativity in frontotemporal dementia: a window into the neural bases of the creative mind. Neuropsychologia 2010; 48: 3733–42.
Dietrich A. The cognitive neuroscience of creativity. Psychon Bull Rev 2004; 11: 1011–26.
Dietrich A, Kanso R. A review of EEG, ERP, and neuroimaging studies of creativity and insight [review]. Psychol Bull 2010; 136: 822–48.
Dubois B, Slachevsky A, Litvan I, Pillon B. The FAB: a frontal assessment battery at bedside. Neurology 2000; 55: 1621–6.
Edl S, Benedek M, Papousek I, Weiss EM, Fink A. Creativity and the Stroop interference effect. Personal Individ Differ 2014; 69: 38–42.
Ellamil M, Dobson C, Beeman M, Christoff K. Evaluative and generative modes of thought during the creative process. Neuroimage 2012; 59: 1783–94.
Evans JSBT, Stanovich KE. Dual-process theories of higher cognition: advancing the debate [review]. Perspect Psychol Sci J Assoc Psychol Sci 2013; 8: 223–41.
Faust M, Lavidor M. Semantically convergent and semantically divergent priming in the cerebral hemispheres: lexical decision and semantic judgment. Cogn Brain Res 2003; 17: 585–97.

Fink A, Koschutnig K, Hutterer L, Steiner E, Benedek M, Weber B, et al. Gray matter density in relation to different facets of verbal creativity. Brain Struct Funct 2014; 219: 1263–9.
Folstein MF, Folstein SE, McHugh PR. 'Mini-mental state'. A practical method for grading the cognitive state of patients for the clinician. J Psychiatr Res 1975; 12: 189–98.
Fox KCR, Spreng RN, Ellamil M, Andrews-Hanna JR, Christoff K. The wandering brain: meta-analysis of functional neuroimaging studies of mind-wandering and related spontaneous thought processes. Neuroimage 2015; 111: 611–21.
Gabora L. Revenge of the 'Neurds': characterizing creative thought in terms of the structure and dynamics of memory [review]. Creat Res J 2010; 22: 1–13.
Gilhooly KJ, Fioratou E, Anthony SH, Wynn V. Divergent thinking: strategies and executive involvement in generating novel uses for familiar objects. Br J Psychol 2007; 98: 611–25.
Goff K, Torrance EP. The abbreviated torrance test for adults. Bensenville, IL: Scholastic Testing Service, Inc.; 2002.
Gonen-Yaacovi G, de Souza LC, Levy R, Urbanski M, Josse G, Volle E. Rostral and caudal prefrontal contribution to creativity: a meta-analysis of functional imaging data. Front Hum Neurosci 2013; 7: 465.
Green AE, Cohen MS, Kim JU, Gray JR. An explicit cue improves creative analogical reasoning. Intelligence 2012a; 40: 598–603.
Green AE, Kraemer DJM, Fugelsang JA, Gray JR, Dunbar KN. Neural correlates of creativity in analogical reasoning. J Exp Psychol Learn Mem Cogn 2012b; 38: 264–72.
Green AE, Cohen MS, Raab HA, Yedibalian CG, Gray JR. Frontopolar activity and connectivity support dynamic conscious augmentation of creative state: neuroimaging augmented state creativity. Hum Brain Mapp 2015; 36: 923–34.
Gruszka A, Necka E. Priming and acceptance of close and remote associations by creative and less creative people. Creat Res J 2002; 14: 193–205.
Gupta N, Jang Y, Mednick SC, Huber DE. The road not taken: creative solutions require avoidance of high-frequency responses. Psychol Sci 2012; 23: 288–94.
Hass RW. Tracking the dynamics of divergent thinking via semantic distance: analytic methods and theoretical implications. Mem Cognit 2016; 45: 233–44.
Hobeika L, Diard-Detoeuf C, Garcin B, Levy R, Volle E. General and specialized brain correlates for analogical reasoning: a meta-analysis of functional imaging studies. Hum Brain Mapp 2016; 37: 1953–69.
Howard D, Patterson K. The Pyramids and Palm Trees Test: a test for semantic access from words and pictures. Bury St Edmunds: Thames Valley Test Company; 1992.
Humphreys GF, Hoffman P, Visser M, Binney RJ, Lambon Ralph MA. Establishing task- and modality-dependent dissociations between the semantic and default mode networks. Proc Natl Acad Sci USA 2015; 112: 7857–62.
Hyafil A, Koechlin E. A neurocomputational model of human frontopolar cortex function [Internet]. bioRxiv 2016. Available from: http://biorxiv.org/content/early/2016/01/21/037150
Jauk E, Neubauer AC, Dunst B, Fink A, Benedek M. Gray matter correlates of creative potential: a latent variable voxel-based morphometry study. Neuroimage 2015; 111: 312–20.
Jones LL, Estes Z. Convergent and divergent thinking in verbal analogy. Think Reason 2015; 21: 473–500.
Jung RE. Evolution, creativity, intelligence, and madness: 'Here Be Dragons'. Front Psychol 2014; 5: 784.
Jung RE, Grazioplene R, Caprihan A, Chavez RS, Haier RJ. White matter integrity, creativity, and psychopathology: disentangling constructs with Diffusion Tensor Imaging. PLoS One 2010a; 5: e9818.
Jung RE, Mead BS, Carrasco J, Flores RA. The structure of creative cognition in the human brain. Front Hum Neurosci 2013; 7: 330.
Jung RE, Segall JM, Jeremy Bockholt H, Flores RA, Smith SM, Chavez RS, et al. Neuroanatomy of creativity. Hum Brain Mapp 2010b; 31: 398–409.
Jung RE, Wertz CJ, Meadows CA, Ryman SG, Vakhtin AA, Flores RA. Quantity yields quality when it comes to creativity: a brain and behavioral test of the equal-odds rule. Front Psychol 2015; 6: 864.
Jung-Beeman M. Bilateral brain processes for comprehending natural language [review].Trends Cogn Sci 2005; 9: 512–18.
Jung-Beeman M, Bowden EM, Haberman J, Frymiare JL, Arambel-Liu S, Greenblatt R, et al. Neural activity when people solve verbal problems with insight. PLoS Biol 2004; 2: E97.
Kahneman D. Thinking, fast and slow. 1st ed. New York, NY: Farrar, Straus and Giroux; 2011.
Kenett YN, Anaki D, Faust M. Investigating the structure of semantic networks in low and high creative persons. Front Hum Neurosci 2014; 8: 407.
Kenett YN, Austerweil JL. Examining search processes in low and high creative individuals with random walk. In: Papafragou A, Grodner D, Mirman D, Trueswell JC, editors. Proceedings of the 38th Annual Conference of the Cognitive Science Society. Austin, TX: Cognitive Science Society; 2016. p. 313–18.
Kenett YN, Beaty RE, Silvia PJ, Anaki D, Faust M. Structure and flexibility: investigating the relation between the structure of the mental lexicon, fluid intelligence, and creative achievement. Psychol Aesthet Creat Arts 2016; 10: 377–88.
Kinkingnéhun S, Volle E, Pélégrini-Issac M, Golmard J-L, Lehéricy S, du Boisguéheneuc F, et al. A novel approach to clinical-radiological correlations: Anatomo-Clinical Overlapping Maps (AnaCOM): method and validation. Neuroimage 2007; 37: 1237–49.
Klein A, Andersson J, Ardekani BA, Ashburner J, Avants B, Chiang M-C, et al. Evaluation of 14 nonlinear deformation algorithms applied to human brain MRI registration. Neuroimage 2009; 46: 786–802.
Klein A, Badia T. The usual and the unusual: solving Remote Associates Test tasks using simple statistical natural language processing based on language use. J Creat Behav 2015; 49: 13–37.
Kounios J, Beeman M. The cognitive neuroscience of insight [review]. Annu Rev Psychol 2014; 65: 71–93.
Krawczyk DC. The cognition and neuroscience of relational reasoning [review]. Brain Res 2012; 1428: 13–23.
Kroger JK, Sabb FW, Fales CL, Bookheimer SY, Cohen MS, Holyoak KJ. Recruitment of anterior dorsolateral prefrontal cortex in human reasoning: a parametric study of relational complexity. Cereb Cortex 2002; 12: 477–85.
Kühn S, Ritter SM, Müller BCN, van Baaren RB, Brass M, Dijksterhuis A. The importance of the default mode network in creativity—a structural MRI study. J Creat Behav 2014; 48: 152–63.
Lee CS, Therriault DJ. The cognitive underpinnings of creative thought: a latent variable analysis exploring the roles of intelligence and working memory in three creative thinking processes. Intelligence 2013; 41: 306–20.
Lieberman MD, Jarcho JM, Satpute AB. Evidence-based and intuition-based self-knowledge: an FMRI study. J Pers Soc Psychol 2004; 87: 421–35.
Mednick SA. The associative basis of the creative process. Psychol Rev 1962; 69: 220–32.
Mednick MT, Mednick SA, Jung CC. Continual association as a function of level of creativity and type of verbal stimulus. J Abnorm Psychol 1964a; 69: 511–15.
Mednick MT, Mednick SA, Mednick EV. Incubation of creative performance and specific associative priming. J Abnorm Psychol 1964b; 69: 84–8.
Merck C, Charnallet A, Auriacombe S, Belliard S, Hahn-Barma V, Kremin H, et al. La batterie d'évaluation des connaissances sémantiques du GRECO (BECS-GRECO): validation et données normatives. Rev Neuropsychol 2011; 3: 235–55.
Merten T, Fischer I. Creativity, personality and word association responses: associative behaviour in forty supposedly creative persons. Personal Individ Differ 1999; 27: 933–42.
Mok LW. The interplay between spontaneous and controlled processing in creative cognition [review]. Front Hum Neurosci 2014; 8: 663.

Nijstad BA, Dreu CKWD, Rietzschel EF, Baas M. The dual pathway to creativity model: creative ideation as a function of flexibility and persistence [review]. Eur Rev Soc Psychol 2010; 21: 34–77.
Nusbaum EC, Silvia PJ. Are intelligence and creativity really so different? Fluid intelligence, executive processes, and strategy use in divergent thinking. Intelligence 2011; 39: 36–45.
Parkin BL, Hellyer PJ, Leech R, Hampshire A. Dynamic network mechanisms of relational integration. J Neurosci 2015; 35: 7660–73.
Parlatini V, Radua J, Dell'Acqua F, Leslie A, Simmons A, Murphy DG, et al. Functional segregation and integration within fronto-parietal networks. Neuroimage 2017; 146: 367–75.
Perret, E. The left frontal lobe of man and the suppression of habitual responses in verbal categorical behavior. Neuropsychologia 1974; 12: 323–30.
Pinho AL, de Manzano Ö, Fransson P, Eriksson H, Ullén F. Connecting to create: expertise in musical improvisation is associated with increased functional connectivity between premotor and prefrontal areas. J Neurosci 2014; 34: 6156–63.
Power JD, Petersen SE. Control-related systems in the human brain [review]. Curr Opin Neurobiol 2013; 23: 223–8.
Prabhakaran R, Green AE, Gray JR. Thin slices of creativity: using single-word utterances to assess creative cognition. Behav Res Methods 2013: 1–19.
Raichle ME. The restless brain: how intrinsic activity organizes brain function [review]. Phil Trans R Soc B 2015; 370: 20140172.
Rankin KP, Liu AA, Howard S, Slama H, Hou CE, Shuster K, et al. A case-controlled study of altered visual art production in Alzheimer's and FTLD. Cogn Behav Neurol 2007; 20: 48–61.
Ripollés P, Marco-Pallarés J, de Diego-Balaguer R, Miró J, Falip M, Juncadella M, et al. Analysis of automated methods for spatial normalization of lesioned brains. Neuroimage 2012; 60: 1296–306.
Rojkova K, Volle E, Urbanski M, Humbert F, Dell'Acqua F, Thiebaut de Schotten M. Atlasing the frontal lobe connections and their variability due to age and education: a spherical deconvolution tractography study. Brain Struct Funct 2016; 221: 1751–66.
Rossmann E, Fink A. Do creative people use shorter associative pathways? Personal Individ Differ 2010; 49: 891–5.
Sandkühler S, Bhattacharya J. Deconstructing insight: EEG correlates of insightful problem solving. PLoS One 2008; 3: e1459.
Seger CA, Desmond JE, Glover GH, Gabrieli JD. Functional magnetic resonance imaging evidence for right-hemisphere involvement in processing unusual semantic relationships. Neuropsychology 2000; 14: 361–9.
Shamay-Tsoory SG, Adler N, Aharon-Peretz J, Perry D, Mayseless N. The origins of originality: the neural bases of creative thinking and originality. Neuropsychologia 2011; 49: 178–85.
Silvia PJ, Beaty RE, Nusbaum EC. Verbal fluency and creativity: general and specific contributions of broad retrieval ability (Gr) factors to divergent thinking. Intelligence 2013; 41: 328–40.
Smith KA, Huber DE, Vul E. Multiply-constrained semantic search in the Remote Associates Test. Cognition 2013; 128: 64–75.
Smith SM, Fox PT, Miller KL, Glahn DC, Fox PM, Mackay CE, et al. Correspondence of the brain's functional architecture during activation and rest. Proc Natl Acad Sci USA 2009; 106: 13040–5.
Sowden PT, Pringle A, Gabora L. The shifting sands of creative thinking: connections to dual-process theory. Think Reason 2015; 21: 40–60.
Spreng RN, Stevens WD, Chamberlain JP, Gilmore AW, Schacter DL. Default network activity, coupled with the frontoparietal control network, supports goal-directed cognition. Neuroimage 2010; 53: 303–17.
Stroop J. Studies of interferences in serial verbal reactions. J Exp Psychol 1935; 18: 643–62.
Stuss DT, Alexander MP. Is there a dysexecutive syndrome? Philos Trans R Soc Lond B Biol Sci 2007; 362: 901–15.
Subramaniam K, Kounios J, Parrish TB, Jung-Beeman M. A brain mechanism for facilitation of insight by positive affect. J Cogn Neurosci 2009; 21: 415–32.
Taft R, Rossiter JR. The remote associates test: divergent or convergent thinking? Psychol Rep 1966; 19: 1313–14.
Takeuchi H, Taki Y, Sassa Y, Hashizume H, Sekiguchi A, Fukushima A, et al. Regional gray matter volume of dopaminergic system associate with creativity: evidence from voxel-based morphometry. Neuroimage 2010; 51: 578–85.
Takeuchi H, Taki Y, Hashizume H, Sassa Y, Nagase T, Nouchi R, et al. The association between resting functional connectivity and creativity. Cereb Cortex 2012; 22: 2921–9.
Thagard P, Stewart TC. The AHA! experience: creativity through emergent binding in neural networks. Cogn Sci 2011; 35: 1–33.
Thiebaut de Schotten M, Dell'Acqua F, Ratiu P, Leslie A, Howells H, Cabanis E, et al. From Phineas Gage and Monsieur Leborgne to H.M.: revisiting disconnection syndromes. Cereb Cortex 2015; 25: 4812–27.
Troyer AK, Moscovich M, Winocur G. Clustering and switching as two components of verbal fluency: evidence from younger and older healthy adults. Neuropsychology 1997; 11: 138–46.
Unsworth N, Spillers GJ, Brewer GA. Variation in verbal fluency: a latent variable analysis of clustering, switching, and overall performance. Q J Exp Psychol 2011; 64: 447–66.
Urbanski M, Bréchemier M-L, Garcin B, Bendetowicz D, Thiebaut de Schotten M, Foulon C, et al. Reasoning by analogy requires the left frontal pole: lesion-deficit mapping and clinical implications. Brain 2016; 139: 1783–99.
Varga AL, Hamburger K. Beyond type 1 vs. type 2 processing: the tridimensional way [review]. Front Psychol 2014; 5: 993.
Vincent JL, Kahn I, Snyder AZ, Raichle ME, Buckner RL. Evidence for a frontoparietal control system revealed by intrinsic functional connectivity. J Neurophysiol 2008; 100: 3328–42.
Volle E. Associative and controlled cognition in divergent thinking: theoretical, experimental, neuroimaging evidence, and new directions. In: Jung RE, Vartanian O, editors. The Cambridge handbook of the neuroscience of creativity. New York, NY: Cambridge University Press; 2017.
Ward TB, Kolomyts Y. Cognition and creativity. In: Kaufman JC, Sternberg RJ, editors, The Cambridge handbook of creativity. New York, NY: Cambridge University Press; 2010. p. 93–112.
Wei D, Yang J, Li W, Wang K, Zhang Q, Qiu J. Increased resting functional connectivity of the medial prefrontal cortex in creativity by means of cognitive stimulation. Cortex 2014; 51: 92–102.
Wirth M, Jann K, Dierks T, Federspiel A, Wiest R, Horn H. Semantic memory involvement in the default mode network: a functional neuroimaging study using independent component analysis. Neuroimage 2011; 54: 3057–66.
Woolgar A, Parr A, Cusack R, Thompson R, Nimmo-Smith I, Torralva T, et al. Fluid intelligence loss linked to restricted regions of damage within frontal and parietal cortex. Proc Natl Acad Sci USA 2010; 107: 14899–902.
Wu X, Yang W, Tong D, Sun J, Chen Q, Wei D, et al. A meta-analysis of neuroimaging studies on divergent thinking using activation likelihood estimation. Hum Brain Mapp 2015; 36: 2703–18.
Xu Y, Lin Q, Han Z, He Y, Bi Y. Intrinsic functional network architecture of human semantic processing: modules and hubs. Neuroimage 2016; 132: 542–55.
Zhu F, Zhang Q, Qiu J. Relating inter-individual differences in verbal creative thinking to cerebral structures: an optimal voxel-based morphometry study. PLoS One 2013; 8: e79272.

Supplementary Table 1. Lesion characteristics and grouping of the patients.

Patient	Interval (months)	Lesion volume (cc)	VLSM group	DMN damaged	Left FPCN damaged	Right FPCN damaged
P01	7	0.27	Other	0	0	0
P02	76	38.87	Left rlPFC group	0	1	0
P03	126	21.22	Other	0	1	1
P04	137	150.85	Left rlPFC group	1	1	0
P05	119	76.63	Other	0	0	1
P06	129	22.43	Other	0	0	1
P07	54	146.42	None*	1	1	1
P08	85	55.60	Left rlPFC group	0	1	0
P09	115	13.79	Right rmPFC group	1	0	0
P10	14	44.12	Right rmPFC group	1	0	1
P11	29	67.13	Other	0	0	1
P12	51	9.29	Other	1	0	0
P13	133	4.71	Other	0	1	0
P14	19	23.17	Right rmPFC group	1	0	1
P15	82	49.67	Right rmPFC group	0	0	1
P16	56	27.59	Left rlPFC group	0	1	0
P17	7	26.71	Right rmPFC group	1	0	0
P18	47	32.13	Right rmPFC group	1	0	1
P19	48	60.11	Other	0	0	1
P20	91	37.06	Other	1	0	0
P21	36	37.79	Other	0	0	1
P22	30	16.45	Left rlPFC group	0	1	0
P23	19	2.95	Other	0	0	0
P24	4	14.81	Other	0	0	0
P25	9	0.87	Other	0	0	0
P26	32	29.19	Other	0	1	0
P27	3	1.22	Other	0	0	0
P29	16	14.21	Left rlPFC group	0	1	0
P30	20	22.11	Other	0	0	1

This table indicates whether the patient's lesion affected the Voxel-Lesion Symptom Mapping (VLSM) regions (rlPFC and rmPFC regions), and the Fronto-Parietal Control Network (FPCN) or the Default Mode Network (DMN) (0: no/ 1: yes).

Left rlPFC: the lesion affected the VLSM region associated with a deficit on the CAT (in the left rlPFC region); right rmPFC: the lesion affected the VLSM region associated with a deficit on the FGAT (in the rmPFC region); other: the lesion spared both VLSM regions. The interval is the delay between the occurrence of the lesion and the inclusion in this study.

* Patient P07 was excluded from post hoc group analyses because his lesion damaged both the left rlPFC and the right rmPFC VLSM regions.

Supplementary Table 2: Descriptive data, neuropsychological scores, experimental task performance in patients and healthy subjects.

	Patients (n=29)	**Healthy subjects (n=54)**	**Group comparisons**
Descriptive data: Mean (SD)			
Age (years)	47.5 (15.2)	45.8 (14.4)	U = 741.0, ns
Education (years)	14.1 (3.6)	15.4 (3.0)	U = 594.0, ns
Neuropsychological data: Mean (SD)			
MMSE (/30)	27.6 (1.7)	29.0 (0.9)	***U* = 413.0, *P* < 0.001**
FAB (/18)	15.6 (1.8)	16.7 (1.2)	***U* = 473.5, *P* = 0.002**
Category Fluency	28.2 (7.6)	38.1 (8.8)	***t* = 5.01, *P* < .001**
Phonemic Fluency	19.6 (7.0)	26.9 (8.1)	***t* = 4.12, *P* < .001**
Stroop conflict	35.97 (9.0)	46.3 (11.6)	***t* = -4.167, *P* < 0.001**
Short PPT (/40)	39.5 (0.8)	39.1 (1.3)	U = 695.0, ns
Short naming (/40)	39.9 (1.0)	39.0 (1.3)	U = 729.0, ns
CAT: Mean % (SD)			
CAT-solving	39.08 (9.66)	48.33 (8.93)	***t* = 4.370, *P* < 0.001**
CAT-index	29.16 (16.69)	21.04 (11.82)	***t* = -2.575, *P* = 0.012**
FGAT: Mean % (SD)			
FGAT-first (frequency)	22.57 (9.33)	21.66 (7.79)	U = 700.0, P = 0.428
FGAT-distant (frequency)	3.56 (1.31)	3.40 (1.46)	t = -0.474, P = 0.636

The CAT-solving score represents the percentage of correct responses (for close and distant trials). The CAT-index score represents the performance on close minus distant trials, divided by the mean performance on both trials. Performance on the FGAT is represented by the frequency of the subject's response based on data collected on 96 healthy subjects (50 females; mean age = 44.4 years, SD = 14.9 and mean education = 15.3 years, SD = 3.2).

Results are reported as the means (SD) or mean percentage of correct responses (SD) for the experimental tasks. Exact P values significant at $P < 0.05$ are provided. MMSE: Mini Mental State Examination; FAB: Frontal Assessment Battery; PPT: Pyramid and Palm Tree Test.

Supplementary Table 3. Impact of a right rmPFC lesion on FGAT performances.

	Damaged right rmPFC region	**Intact right rmPFC region**	**Damaged vs intact groups**
FGAT-first (frequency)	27.92 (6.37)	20.87 (9.60)	***U* = 36.0, *P* = 0.037***
FGAT-first (typical responses)	25.29 (8.16)	18.55 (9.84)	*U* = 41.0, *P* = 0.067
FGAT-first (unique responses)	9.71 (4.72)	17.50 (11.71)	***U* = 38.0, *P* = 0.046***
FGAT-first RT (ms)	3481 (1229)	3357 (1065)	U = 69.0, ns
FGAT-distant (frequency)	4.88 (1.04)	3.14 (1.1)	***t*(27) = 3.696, *P* = 0.001***
FGAT-distant (typical responses)	9.57 (6.0)	5.18 (4.68)	*t*(27) = 2.026, *P* = 0.053
FGAT-distant (unique responses)	17.57 (6.55)	29.50 (9.10)	***t*(27) = -3.196, *P* = 0.004***
FGAT-distant RT (ms)	6619 (1868)	6760 (2071)	U = 71.0, ns
Stroop conflict score	35.71 (9.62)	36.05 (8.96)	*t*(27) = -0.084, *P* = 0.934

RT: Reaction Time

This table provides the means (SD) or mean percentage of correct responses (SD) for the experimental tasks and the Stroop conflict score in patients with damaged and intact right rmPFC. Exact *P* values significant at $P < 0.05$ are provided.

Whether the lesion spared or damaged the rmPFC region, patients did not differ in performance on the conflict condition of the Stroop test and patients with an rmPFC damage had a higher mean RT in FGAT trials, suggesting that a lack of response inhibition or impulsivity could not entirely explain our results. In addition, the group with the right rmPFC damaged had slightly longer RTs at FGAT-first but shorter RTs at the FGAT-distant which does not argue for an energization difficulty.

The semantic distance was calculated using the association frequency using, the frequency association norms from the dictionary of Debrenne (2011).

Supplementary Table 4

Insight subjective reports in the three groups of patients

	Left rlPFC lesion	**Right rmPFC lesion**	**Other patients**	**Left rlPFC vs other patients groups**	**Right rmPFC vs other patient groups**
CAT-Eureka (percent of correct responses)	85.6 (16.1)	98.9 (1.6)	84.2 (22.9)	U = 43, P = 0.711	**U = 16, P= 0.017**
CAT-Eureka (%incorrect trials)	53.8 (22.7)	90.0 (8.3)	90.0 (8.3)	*U* = 34, *P* = 0.302	*U* = 34, *P* = 0.302

Results are shown as the mean percentage of Eureka reports (SD) among correct and incorrect CAT trials. Exact *P* values significant at $P < 0.05$ are provided.

Supplementary Fig. 1: Coverage of all lesions in the frontal lobe.

Warmer color shows a higher number of lesion overlaps.

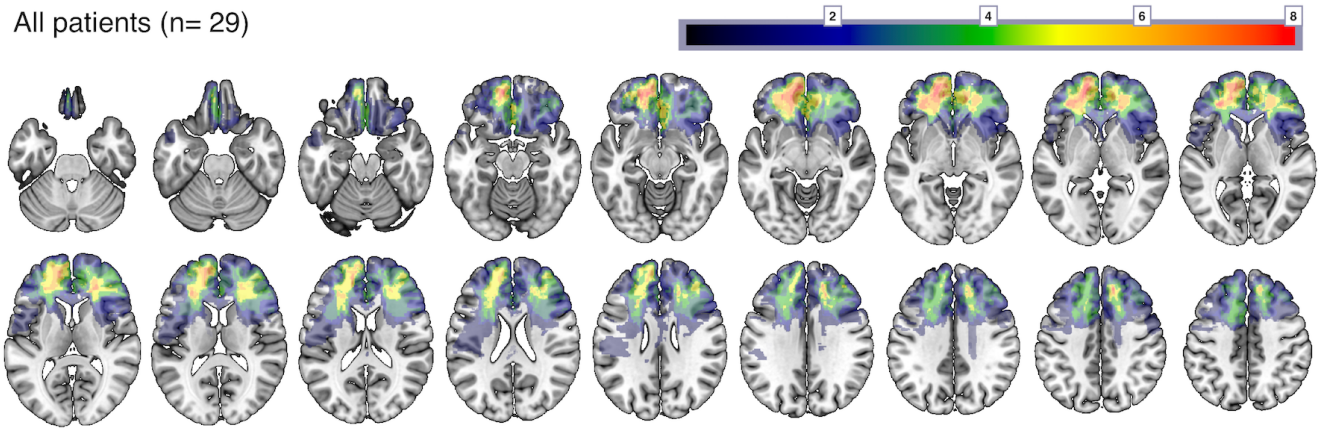

Supplementary Fig.2: Functional networks described by Smith et al. (2009).

This figure depicts the functional networks described by Smith et al. (2009) as the Fronto-Parietal Control Network (FPCN) represented here in orange for the left hemisphere (network 10) and in blue for the right hemisphere (network 9) and the Default Mode Network (DMN; network 4) in green.

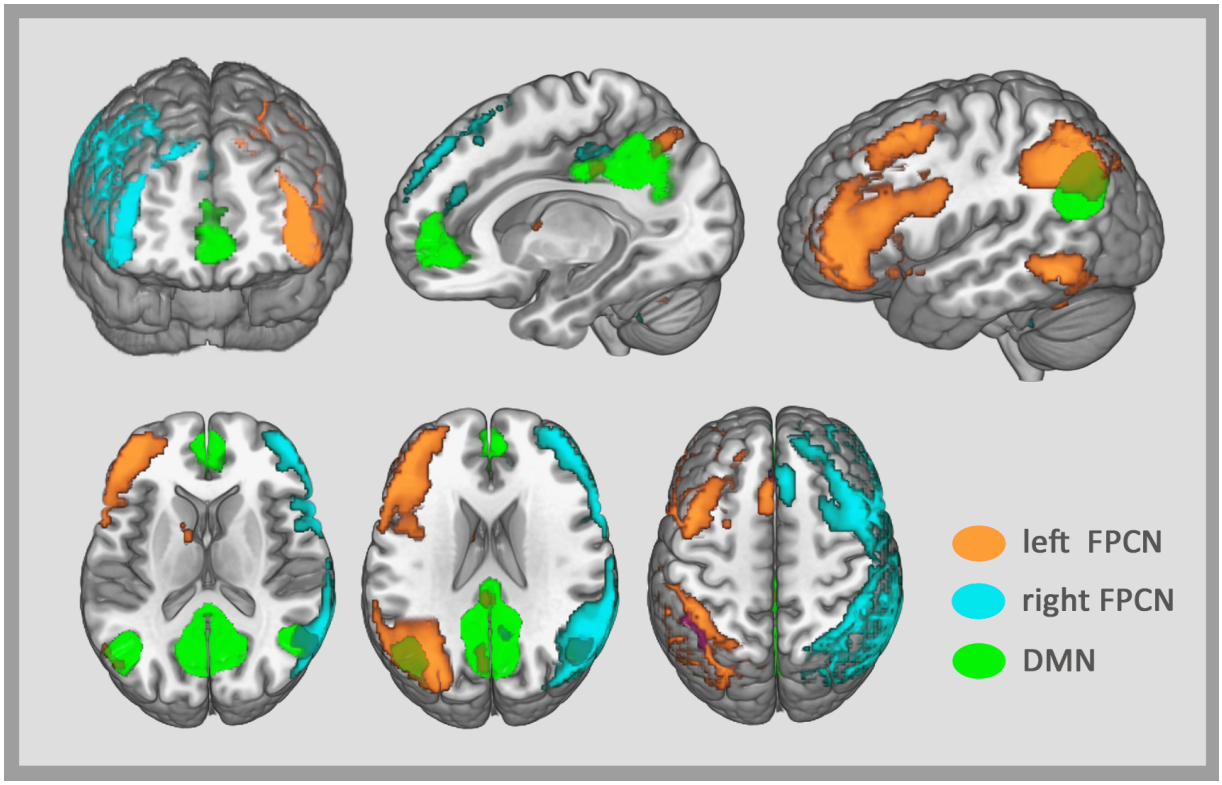

Supplementary Fig. 3: Main scores according to damage to functional networks.

This figure depicts the frequency scores on the Y axis at the FGAT-first (first row) and FGAT-distant (second row) conditions, and mean scores on the Y axis on the CAT-index (third row) according to damage to the DMN (spared: gray / damaged: green) or the left FPCN (spared: gray / damaged: orange). *: significant at $P < 0.05$.

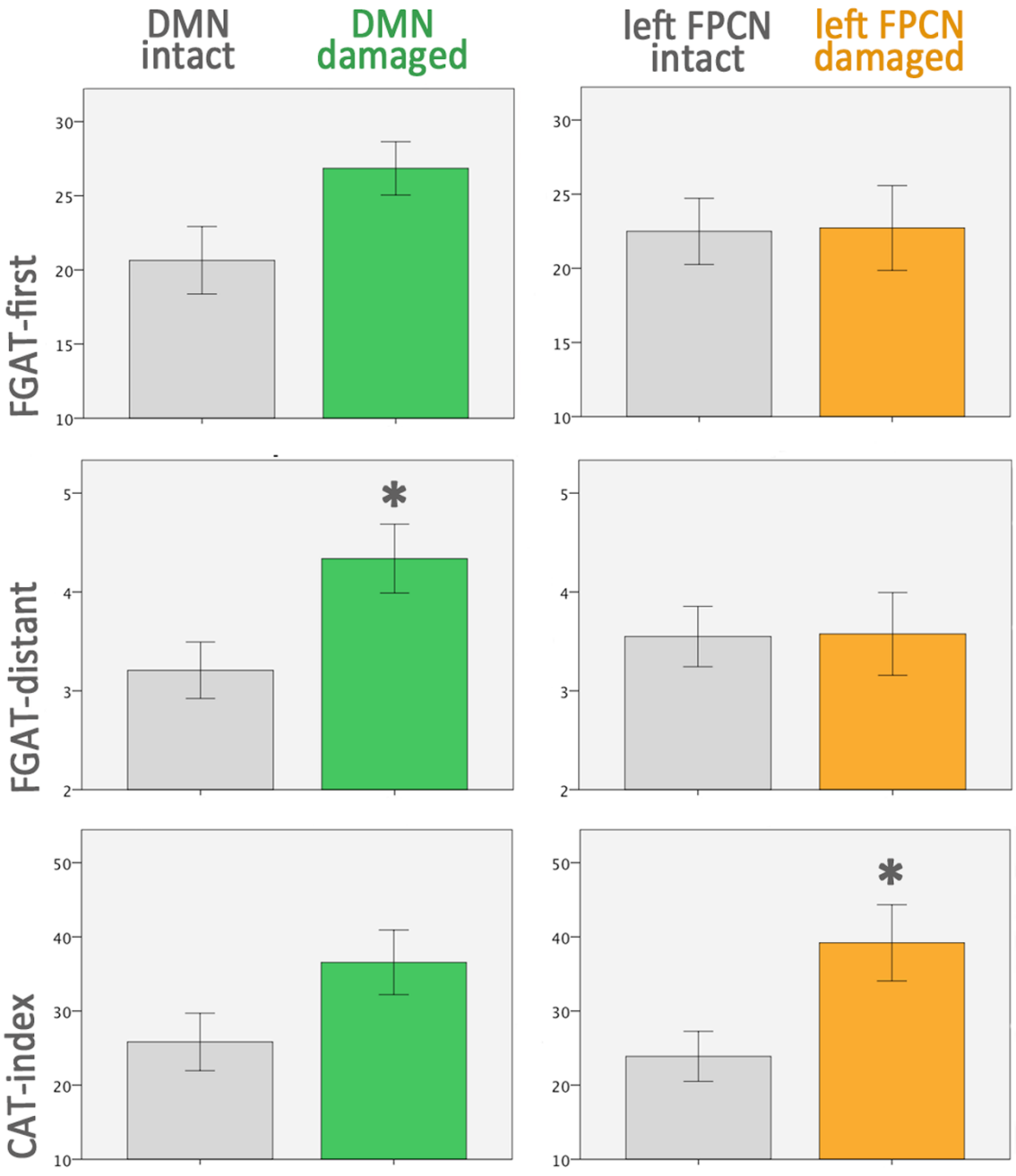

Supplementary Fig. 4

Lesion-deficit mapping associated with CAT-index and FGAT-distant performance: comparative results between a 3 and a 4 lesion overlaps threshold.

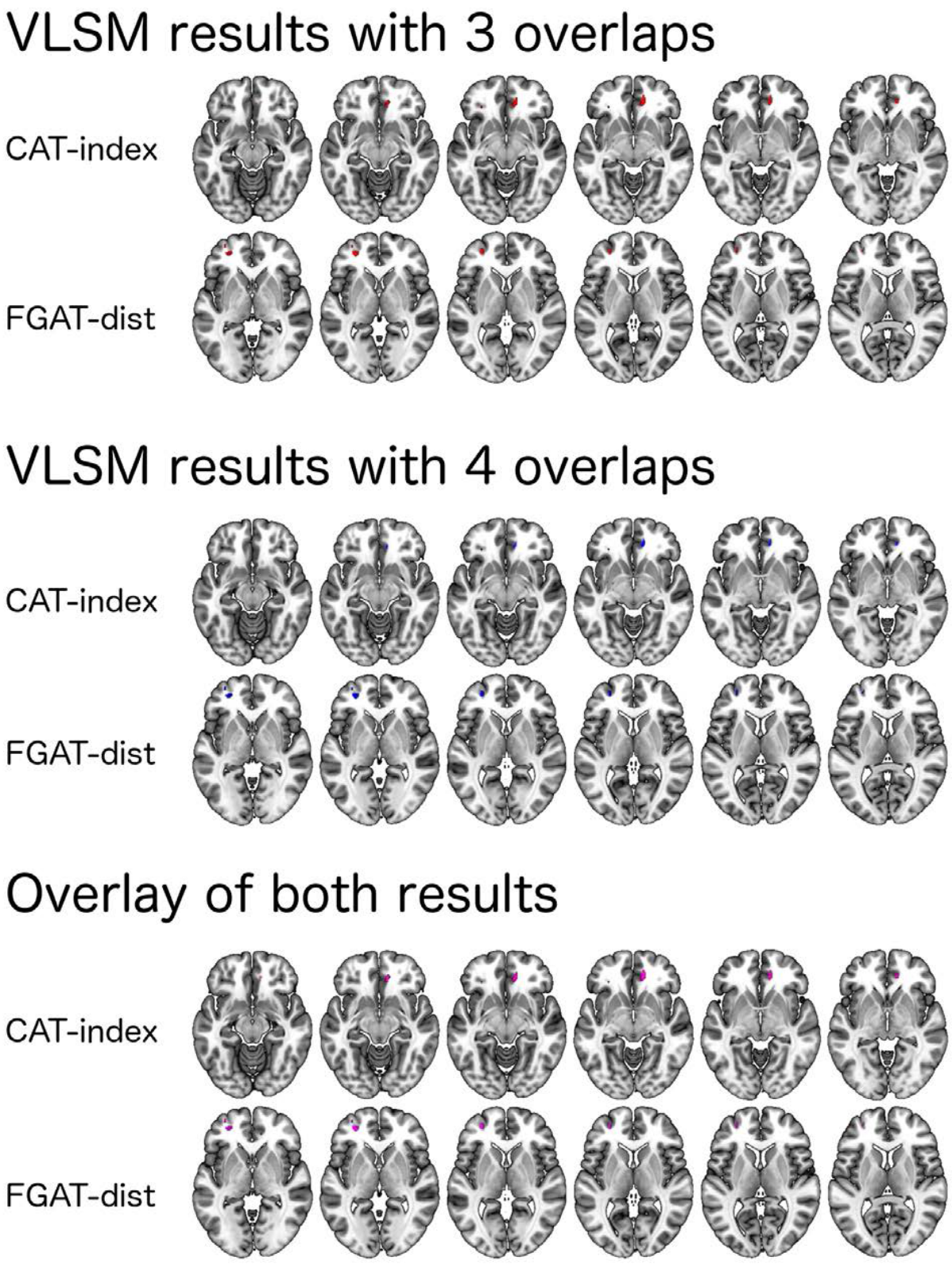

Significant regions are superimposed on axial slices of a brain template in the MNI space. VLSM results using an overlap threshold of 3 lesions are displayed in red, results using an overlap threshold of 4 lesions are shown in blue, and the overlay of both results is displayed in purple. All results were thresholded at $P < 0.05$ with a family-wise errors (FWE) correction for multiple comparisons using permutations. The percentage of prefrontal voxels that satisfied the four overlaps threshold was 22%.

In the left rlPFC region associated with poor CAT-index scores, at an overlap threshold of 4 lesions, Z = 3.540, exceeding the threshold for significance after correction for multiple comparisons using a permutation FWE corrected threshold that was Z > 3.26361632). At an overlap threshold of 3 lesions, Z = 3.615 in the same significant area, exceeding the threshold for significance after correction for multiple comparisons using a permutation FWE corrected threshold that was Z > 3.35279489).

In the right rmPFC region associated with poor FGAT-distant scores, at an overlap threshold of 4 lesions, Z = 3.891, exceeding the threshold for significance after correction for multiple comparisons using a permutation FWE corrected threshold that was Z > 3.32005405). At an overlap threshold of 3 lesions, Z = 3.891 in the same significant area, exceeding the threshold for significance after correction for multiple comparisons using a permutation FWE corrected threshold that was Z > 3.38957906).

Supplementary figure 5: Overlap of the lesions for each patient group.

Warmer color shows a higher number of lesion overlaps.

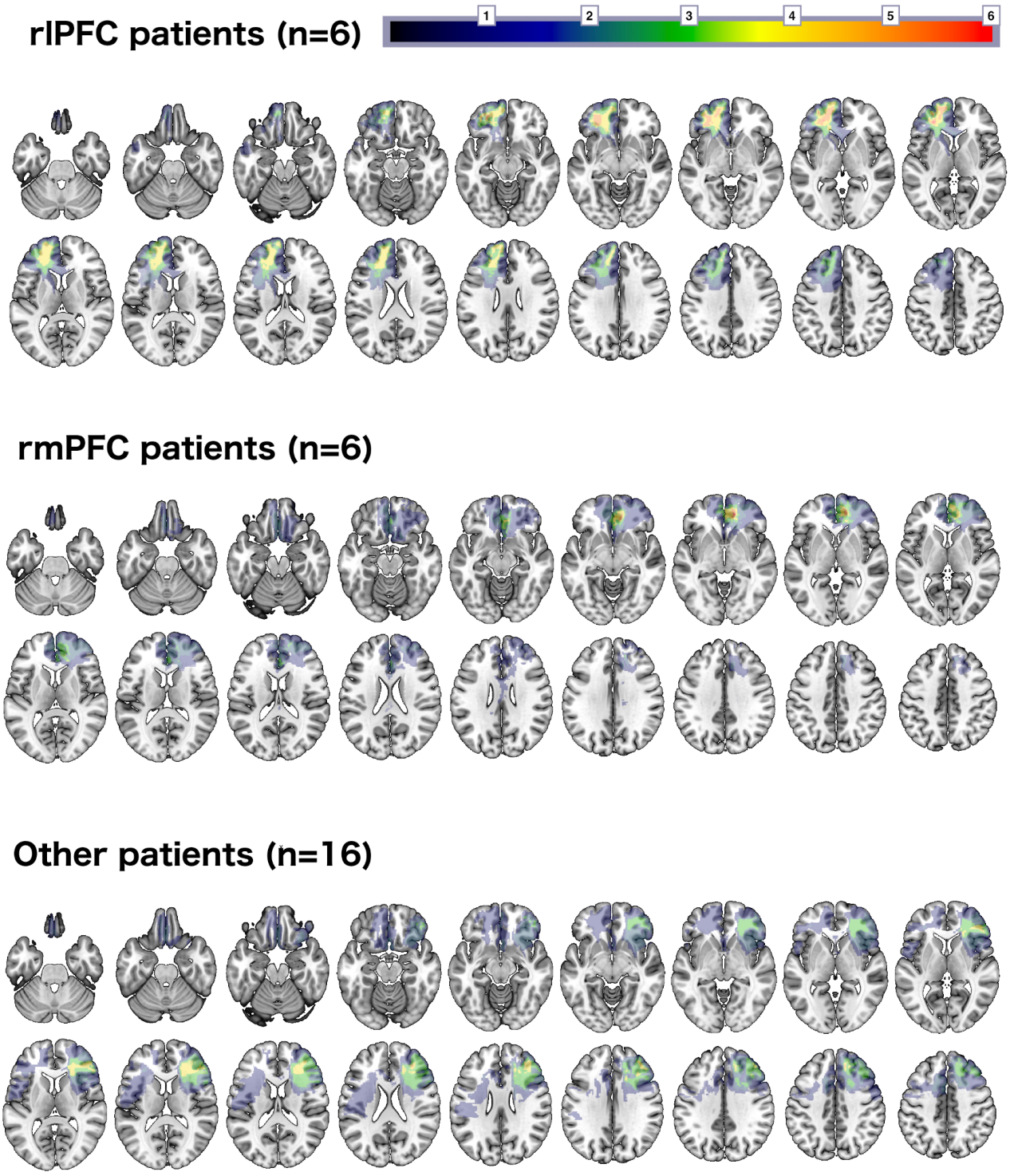

Supplementary Method 1.

Material and experimental procedure for the Combined Association Task (CAT)

We built a new verbal task adapted from Mednick's RAT (Mednick, 1962), in which subjects were required to find a word related to three cue words that were presented to them when there was no usual association between these cue words. In the current adaptation of the task, we varied the semantic distance between the cue words and the solution word(s) using association norms. This task has been used in a previous study in healthy subjects (Bendetowicz *et al.*, 2017).

Construction of the material based on measures of semantic distance/strength

Triplets of cue words of variable semantic distance with their solution were created based on free association norms in French, which were available through a published database (Debrenne, 2011) available online (http://dictaverf.nsu.ru/). We used the associative frequency between two words as a measure of semantic distance (or "association strength"). This measure quantifies the proportion of subjects who produced the word B when they were given the word A (for instance, if 334 of 519 participants who were presented the word "woman" responded "man", then the association strength was 334 / 519 * 100 = 64). We selected from the database measures of association strengths obtained from at least 450 adult native French speakers. Associative strength measured from free generation tasks may better capture free word associations (De Deyne *et al.*, 2016) than word co-occurrences in text corpora (such as latent semantic analysis, which has been used before, see Smith *et al.*, 2013; Green *et al.*, 2015) and appeared to be closer to our task condition because participants were required to generate a word based on its associations.

Based on these measures of associative strength, we built 72 trials in the CAT, i.e., 72 triads of unrelated cue words that shared one (or a few) semantic associate(s). We computed the average association strength between the three cue words and the solution word. In cases in which the triad had several possible solution words, the mean association strengths between the cue words and the solution words were summed because each solution word was considered a correct response. The mean association strength of the 72 trials was 9.13 (SD = 7.49), and the median was 7. We classified the trials according to the median of the association strength; 36 trials were classified as "close CAT" trials (associative strength > 7;

for instance “rue” (street) – “campagne” (countryside) - “centre” (center), leading to the solution “ville” (town)), 36 trials were classified as “distant CAT” trials (associative strength < 7; for instance “pont” (bridge) – “social” (social) – “attacher” (to tie), leading to the solution “lien” (link)). The characteristics of the close and distant CAT trials are provided in (Bendetowicz *et al.*, 2017, Table 2). Close and distant CAT trials differed significantly with respect to the mean association strength between the cue words and the solution words, but they did not differ significantly in their mean lexical frequency computed with Lexique 3.80 (http://www.lexique.org; New *et al.*, 2004) as detailed in Bendetowicz et al., 2017.

Words vary in terms of the extent to which they are strongly associated with other words, i.e., associative steepness (Mednick *et al.*, 1964), which may play a role in word generation. We thus controlled the steepness of the cue words in the experiment. A steep word is one for which there is a highly constrained association to one associate, with a much stronger association to this associate than to all the other associates. A flat word is one for which there is a minimally constrained association to other words. The steepness was calculated as the frequency ratio between the second and the first associates of a given word. We defined a word as a steep word when its steepness (the ratio between the associative strengths of its first and second associates) was > 4 and a word as a flat word when steepness was ≤ 3 (Mednick, 1962). The average steepness of cue words in each trial did not differ between close and distant trials (respectively, mean = 2.55, SD = 1.14 and mean = 2.67; SD = 1.76; $U = 627.5$, $P = 0.82$).

Reports of insight

As in Bendetowicz et al (2017), we assessed the individual tendency to solve the task with insight by collecting subjective reports of these “Eureka moments” on a trial-by-trial basis, as has been done previously (e.g., Kounios & Beeman, 2014). Insight or Eureka is the sudden awareness of the solution to a problem (i.e., the “Aha!” or “Eureka!” phenomenon) and is accompanied by little or no conscious access to the processing leading up to that solution (Bowden, Jung-Beeman, Fleck, & Kounios, 2005; Kounios & Beeman, 2014; Topolinski & Reber, 2010; Weisberg, 2013). This sudden awareness of the solution is often elicited by problem solving tasks such as the Mednick’s task (Kounios and Beeman, 2014).

Experimental procedure

After the instructions were displayed on a computer screen and explained by the examiner, participants completed 10 practice trials before performing the experimental tasks. In each

trial, a set of three unrelated cue words that were arranged in a triangle was displayed on the screen. Participants were asked to give a unique word that was related to all three cue words. The cue words were displayed on the screen until the participants produced a response, within a time limit of 30 s, and with a visual signal 2 s before the end of the display to warn the participants that time was up. Response times were recorded on the computer by button press, and response words were given orally. The examiner wrote down the subjects' answers.

Five hundred milliseconds after the participant gave his/her answer to each CAT problem, a new screen appeared with the word "Eureka?". Participants were asked to report whether their response came to their mind spontaneously and suddenly or was the direct result of a conscious effortful search. To report their subjective "Eureka" experience, the subjects pressed the keyboard letter "V" if their previous response word had come to mind spontaneously and suddenly without conscious effort. They pressed the keyboard letter "N" otherwise. The participants had 5 seconds to respond. We registered and measured the percentage of "Eureka" reports separately for correctly solved trials (CAT-Eureka).

Trials were separated by two-second inter-trial intervals. The order of trials was randomized between participants, mixing close and distant trials.

Supplementary Method 2

Material and experimental procedure for the free generation association task (FGAT)

Participants were asked to generate a word in response of a given cue word according to two distinct conditions. In the "first" condition, the subjects were asked to produce the first word that came to mind. In the "distant" condition, the participants were asked to produce a word that was associated with the cue word in an unusual way. The subjects were instructed to answer with a single word, avoiding phrases, compound words and proper nouns. The same list of 58 words was used in the first and distant conditions.

Construction of the material based on measures of semantic distance/strength

To build the verbal material for the FGAT and to analyze the participants' responses, we used the same published free-association norms as for the CAT (Debrenne, 2011; http://dictaverf.nsu.ru/). We selected words in the database for which associative norms were established based on more than 450 adults who were native French speakers. Ambiguous words such as words corresponding either to an adjective or to a conjugated form of a verb were avoided.

As in the CAT, we explored the steepness of the cue words used. Steepness ranged from 5.58 to 38.00 (mean 12.15) for steep words and from 1.05 to 2.43 (mean 1.58) for flat words. The list of 58 words used in this task included equal proportions of steep and flat words (29 steep words including 11 adjectives, 16 nouns and 2 verbs; and 29 flat words, including 11 adjectives, 16 nouns and 2 verbs). Cue words were reasonably frequent according to mean written frequencies (text- and web-based words computed with Lexique 3.8; www.lexique.org, (New *et al.*, 2004) with a mean lexical frequency of 197 occurrences per millions. Mean lexical frequency did not differ significantly between steep and flat word lists (flat words: 140.98 occurrences per million; steep words: 144.46; $U = 396.0$, $P = 0.70$). Because we were interested in the effect of instruction in the patients, responses to steep and flat cue words were pooled for FGAT-first and FGAT-distant analyses in the current study. Internal reliability was good for both FGAT conditions (Cronbach alpha = 0.911 for FGAT-first and 0.893 for FGAT-distant).

Measures and normative data

Response frequency was calculated in order to estimate the commonness of the words produced by the participants. Response frequency (FGAT-first/distant frequency) was

computed for each response as the proportion of healthy subjects who gave this same response based on normative data acquired in a group of 96 healthy subjects (50 females). Mean age = 44.4 years (SD = 14.9), and mean education = 15.3 years (SD = 3.2).

In this sample, there was a significant difference in FGAT frequency between the first and the distant condition for both flat words (FGAT-first flat frequency = 9.91 (2.76); FGAT-distant flat frequency = 3.02 (1.11); Wilcoxon Z = -8.507, $P < 0.001$) and steep words (FGAT-first steep frequency = 35.45 (12.81); FGAT-distant steep frequency = 4.03 (1.75); Wilcoxon Z = -8.507, $P < 0.001$). As the steepness of the cue words had similar effects on response commonness, steep and flat words have been pooled for the analyses.

In addition to FGAT-first/distant frequency, we measured the number of unique responses (FGAT-first/distant unique responses), i.e. the responses provided by a given participant that was not produced by any subject of the normative dataset. We used our sample of normative data rather than the dictaverf database to calculate the commonness of the responses and the number of unique responses because our normative data include both the FGAT-first and FGAT-distant conditions, whereas dictaverf norms were established by asking participants to provide the first word that came to mind (as in our FGAT-first condition) only.

Finally, we also measured the number of typical responses (FGAT-first/distant typical responses). Typical responses corresponded to the most frequent associate for each given cue word based on the association norms (Debrenne, 2011; http://dictaverf.nsu.ru/) obtained in more than 450 participants.

All the responses were screened for general appropriateness. Responses for which there was no intelligible link with the cue, or for which the participant could not explain this link, and responses that were repetition of the cue word were excluded from all analyses. In total, 0.6% of trials in healthy subjects and 0.1% of trials in patients were excluded. In addition, healthy subjects produced no answer in 1.5% of the trials, and patients produced no answer in 5.5% of the trials.

Experimental procedure

After the instructions were displayed on a computer screen and clarified by the examiner, participants performed the experimental tasks as follows. Each trial began with a cue word displayed on a computer screen, and the participant was asked to produce a response word according to the instruction (first or distant). For each word, participants were given a maximal time of 10 s (FGAT-first) or 20 s (FGAT-distant) to indicate their response by speaking aloud. Responses were written down by the examiner, and RTs were recorded by button press on the keyboard. Once the participant had given his/her response, a blank screen

was displayed, and after 2 s, the next trial began. Subjects always performed the first condition before the distant condition. The order of words for both conditions was randomized between subjects.

Supplementary Method 3

Image acquisition, lesion segmentation and spatial normalization.

Patients underwent a high-resolution T1-weighted structural MRI acquisition on a Siemens 3 Tesla (VERIO TIM system) with a 32-channel head coil. A three-dimensional MPRAGE acquisition of 176 axial slices covered the whole brain with a voxel isometric resolution of 1 mm^3 (TE = 2.98 ms, TR = 2300 ms, and flip angle = 9°). Behavioral testing took place on the same day or a few days apart from MRI acquisition for all the participants.

Patient MRIs were preprocessed with SPM8 software (Wellcome Department of Imaging Neuroscience, London, UK), running on Matlab (Mathworks Inc., Natick, USA; www.mathworks.com/matlabcentral). The MRIs were spatially normalized to the Montreal Neurological Institute (MNI) template using the 'unified segmentation' approach combined with lesion masking to limit the impact of a brain lesion on spatial transformations (Crinion *et al.*, 2007; Andersen *et al.*, 2010). This approach appeared to be a good compromise between normalization accuracy and lesion shrinkage (Ripollés *et al.*, 2012). The parameters in SPM were set to the defaults, except that we used a medium regularization (Andersen *et al.*, 2010; Ripollés *et al.*, 2012). Spatially normalized images were resliced to a final voxel size of 1.5 × 1.5 × 1.5 mm3. Normalized MRIs were visually checked and compared with the template to evaluate the normalization accuracy. Signal abnormalities due to the lesions were manually segmented on the normalized MRIs using MRIcron (https://www.nitrc.org/projects/mricron) by trained and experienced neurologists (DB, BG, MLB, EV), who were blind to the performances of the patients at the time of the lesion segmentation. The resulting normalized and segmented lesion volumes were then used in the following analyses.

Supplementary Method 4

We created a prefrontal mask using WFU Pickatlas tool in SPM (http://fmri.wfubmc.edu/software/pickatlas), including all frontal labels of the AAL atlas, and excluding prefrontal gyri and SMA (Frontal_Sup_L, Frontal_Sup_R, Frontal_Sup_Orb_L, Frontal_Sup_Orb_R, Frontal_Mid_L, Frontal_Mid_R, Frontal_Mid_Orb_L, Frontal_Mid_Orb_R, Frontal_Inf_Oper_L, Frontal_Inf_Oper_R, Frontal_Inf_Tri_L, Frontal_Inf_Tri_R, Frontal_Inf_Orb_L, Frontal_Inf_Orb_R, Frontal_Sup_Medial_L, Frontal_Sup_Medial_R, Frontal_Med_Orb_L, Frontal_Med_Orb_R, Cingulum_Ant_L, Cingulum_Ant_R, Rectus_L, Rectus_R). We additionally included in the mask the adjacent

white matter. The percentage overlap of the lesion map (that included only regions coverage by 3 lesions or more) and the prefrontal mask was calculated using MRIcron.

Supplementary references

Andersen SM, Rapcsak SZ, Beeson PM. Cost function masking during normalization of brains with focal lesions: still a necessity? NeuroImage 2010; 53: 78–84.

Bendetowicz D, Urbanski M, Aichelburg C, Levy R, Volle E. Brain morphometry predicts individual creative potential and the ability to combine remote ideas. Cortex 2017; 86: 216–229.

Bowden EM, Jung-Beeman M, Fleck J, Kounios J. New approaches to demystifying insight. Trends Cogn Sci 2005; 9: 322-328.

Crinion J, Ashburner J, Leff A, Brett M, Price C, Friston K. Spatial normalization of lesioned brains: performance evaluation and impact on fMRI analyses. NeuroImage 2007; 37: 866–875.

De Deyne S, Kenett YN, Anaki D, Faust M, Navarro D. Large-scale network representations of semantics in the mental lexicon [Internet]. In: Big data in cognitive science: From methods to insights. In M. N. Jones (Ed.); 2016.

Debrenne M. Le dictionnaire des associations verbales du français et ses applications. In: Bertrand O, Schaffner I, editors. Variétés, variations & formes du français. Palaiseau: Éditions de l'École polytechnique; 2011. p. 355–366.

Green AE, Cohen MS, Raab HA, Yedibalian CG, Gray JR. Frontopolar activity and connectivity support dynamic conscious augmentation of creative state. Hum Brain Mapp 2015; 36: 923–934.

Kounios J, Beeman M. The cognitive neuroscience of insight. [Review]. Annu Rev Psychol 2014; 65: 71–93.

Mednick MT, Mednick SA, Jung CC. Continual association as a function of level of creativity and type of verbal stimulus. J Abnorm Psychol 1964; 69: 511–515.

Mednick SA. The associative basis of the creative process. Psychol Rev 1962; 69: 220–232.

New B, Pallier C, Brysbaert M, Ferrand L. Lexique 2: a new French lexical database. Behav Res Methods Instrum Comput J Psychon Soc Inc 2004; 36: 516–524.

Ripollés P, Marco-Pallarés J, de Diego-Balaguer R, Miró J, Falip M, Juncadella M, et al. Analysis of automated methods for spatial normalization of lesioned brains. NeuroImage 2012; 60: 1296–1306.

Smith KA, Huber DE, Vul E. Multiply-constrained semantic search in the Remote Associates Test. Cognition 2013; 128: 64–75.

Topolinski S, Reber R. Immediate truth—temporal contiguity between a cognitive problem and its solution determines experienced veracity of the solution. Cognition 2010; 114:117-122.

Weisberg, R. W. On the "Demystification" of Insight: A Critique of Neuroimaging Studies of Insight. Creativity Research Journal 2013; 25: 1–14.

6 The rise of a new associationist school for lesion-symptom mapping

The advanced non-invasive neuroimaging techniques allowed the creation of lesion-symptom analyses, which aim to relate brain injuries to behavioural changes statistically. The first methods, however, suffered from selection biases, as the groups were selected a priori according to either their common functional deficit or their similar damage location (Damasio and Damasio, 1989; Burgess and Shallice, 1996a,b). More recent methods, such as VLSM (Bates et al., 2003) and AnaCOM (Kinkingnehun et al., 2004), allow the use of unselected patient groups by combining the damage location information and the behavioural assessment. These voxel-wise methods statistically compare the neuropsychological performance of patients having a lesion in the voxels with the other patients in VLSM case and with control population scores in AnaCOM. As previously mentioned, these approaches still suffer from several shortcomings. We demonstrated in the three presented studies that the impact of brain lesions goes far beyond the damaged area alone. Hence, the interpretation of lesion-symptom approaches has to consider the disruption of structural and functional networks. The three previous papers demonstrate the importance of taking into account the disconnections and provide methods and tools to do so. These tools have been designed to be user-friendly and useful for clinicians, even when multimodal imaging is not available for their patients (see Figure 2). However, even if we don't select the patients according to their lesion location, there can still be a location bias because of the studied pathology; Mah and colleagues (2014) showed that ischaemic strokes' locations are driven by the organisation of the vascular tree, causing a shift in the results found using classical lesion-symptom analyses. This bias can be reduced by mixing the pathologies in the datasets (Volle et al., 2013). In the next publication, we commented on a study by Xu et al. (2018) in which the authors used a high-dimensional multivariate approach to address the location shift of ischaemic strokes. This work highlighted the poor translation of lesion-symptom approaches to clinical practice and their poor accuracy in therapeutic inference. In our commentary, we discussed what directions should take the future research to assess the effect of brain lesions better and to reconcile the research and clinical practice.

Contribution: For this scientific commentary, I participated in discussing the article and its integration in the future research perspectives. I also took part in the writing and the choice of the references.

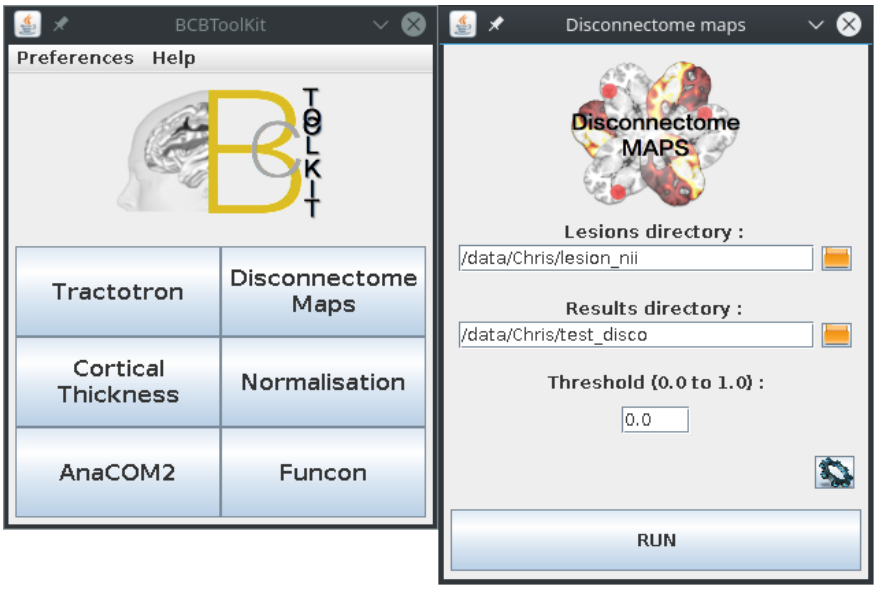

Figure 2: View of the user interface of the BCBtoolkit. The left panel is the main menu, and the right panel is the Disconnectome Maps module. While the interface allows a readily use with default parameters of the analysis, the open source package contains all the scripts which can be modified to optimise the settings.

Résumé :

Les accidents vasculaires cérébraux (AVC) affectent chaque année plus de 2 millions de personnes, rien qu'en Europe. Cependant, malgré des améliorations notables de la prise en charge de ces patients, il est encore très difficile de prédire quels seront l'évolution et le rétablissement des patients après un dommage cérébral. Bien que l'on trouve de nombreux résultats significatifs dans la littérature, notre compréhension des effets des troubles cérébraux et de leur évolution reste lacunaire. Ceci est dû à l'échec de transposition de ces résultats à la pratique clinique causé par un faible pouvoir prédictif des méthodes classiquement utilisées. Ce commentaire scientifique porte sur l'article 'High-dimensional therapeutic inference in the focally damaged human brain', par Xu et al. (2018), qui propose une méthode d'évaluation des effets d'un traitement sur le rétablissement de patients cérébro-lésés. Ce commentaire nous a également permis

de discuter des développements, présents comme futurs, de l'étude des effets des lésions cérébrales.

L'article de Xu et collègues propose une approche multivariée d'apprentissage artificiel prenant en compte un très grand nombre de dimensions pour évaluer les effets des traitements utilisés dans les cas d'AVC. Les auteurs ont ainsi comparé la capacité de prédiction de cette approche avec celle des méthodes classiques qui ne prennent en compte que des paramètres très généraux. Pour ce faire, les auteurs ont simulé des effets de traitements dans le plus grand jeu de données d'AVC actuellement disponible. Ils ont comparé deux types de traitements sur la déviation du regard après un AVC, l'un n'affectant pas la taille de la lésion (e.g. neuroréhabilitation) et l'autre réduisant la taille de la lésion (e.g. thrombolyse). Ils ont ainsi analysé l'efficacité de leur approche et celle des méthodes classiques en simulant un traitement dans une partie, sélectionnée aléatoirement, du jeu de données tandis que le reste faisait office de population contrôle. Cet article démontre une amélioration significative de la détection d'effets thérapeutiques pour un traitement n'affectant pas la taille de la lésion et une supériorité amplifiée de leur méthode si le traitement modifie la taille de la lésion.

Cet article met en exergue les biais des méthodes classiques d'évaluation des symptômes liés aux lésions et propose une solution statistique pour de futures recherches cliniques. Grâce aux initiatives de partage de données, les chercheurs seront à même de répliquer ces résultats et d'appliquer ces méthodes à de futures recherches. Ce partage permettra un accés à une plus grande quantité de données, contribuant à réduire les biais de sélection qui entravent la transposition des recherches au domaine clinique. La méthode présentée permet de prendre plus efficacement en compte les interactions entre les régions anatomiques et en démontre l'importance. Une démarche qui fait écho au développement récent de plusieurs méthodes qui visent à prendre en compte de manière plus complète les interactions et la complexité des connexions du cerveau. La combinaison de ces différentes approches permet d'étudier de façon plus précise les changements provoqués par des pathologies neurologiques. Des méthodes permettent par exemple de prendre en compte les connexions de la matière blanche interrompues par les lésions à l'aide de l'imagerie de diffusion et des algorithmes de tractographie (Thiebaut de Schotten et al., 2015). Il est également possible d'étudier les interactions fonctionnelles entre les différentes régions du cerveau à l'aide de l'IRM fonctionnelle (Boes et al., 2015; Foulon et al., 2018). Ces approches sont

d'autant plus importantes à l'aune des récentes études suggérant que les fonctions cognitives de haut niveau émergent de l'interaction entre de nombreuses structures cérébrales à travers un mécanisme d'intégration et non de l'activité d'une seule zone localisée (Siegel et al., 2016). Pour conclure, bien qu'il reste de nombreux défis à relever pour mieux comprendre les mécanismes de la cognition et l'évolution des troubles neurologiques, la combinaison de ces différentes méthodes pourraient permettre d'importantes avancées. Ce n'est qu'en développant de nouvelles idées et en partageant données et technologies que la communauté scientifique parviendra à relever ces défis au bénéfice des patients et de la société dans son ensemble.

BRAIN
A JOURNAL OF NEUROLOGY

SCIENTIFIC COMMENTARIES

The rise of a new associationist school for lesion-symptom mapping

This scientific commentary refers to 'High-dimensional therapeutic inference in the focally damaged human brain', by Xu *et al.* (doi:10.1093/brain/awx288).

In Europe, more than 2 million individuals each year will have their brain integrity and function challenged by stroke. Despite the progress achieved through the use of thrombolysis with alteplase in acute stroke patients (Wahlgren *et al.*, 2007), many have persistent deficits, affecting their personality, degrading their quality of life and preventing their return to work. Patients need to know, in a timely manner, to what extent their symptoms will resolve. This knowledge reduces the burden and stress associated with stroke, and allows patients to make appropriate arrangements with their family, their health insurance provider and their employer. The mechanics of recovery also provide a framework in which to study the organization of the human brain. Despite the large body of statistically significant lesion-symptom studies in the literature, there has been relatively little translation of these studies into clinical practice, mainly because of their weak predictive power. In effect, the methods currently employed in clinical neuroanatomical studies of stroke are unfit for clinical practice. Research is currently failing practitioners and patients alike. Radical changes in clinical-neuroanatomical correlations are required in order to make significant progress in the field of stroke research. In this issue of *Brain*, Xu and co-workers provide novel insights into the therapeutic inferences that can be derived from a focally damaged human brain (Xu *et al.*, 2017).

The authors used a large dataset of stroke patients ($n = 1172$), with no subselection of the population other than exclusion of very large lesions involving an entire hemisphere to avoid potential bias. As there is no ground truth regarding the impact of any therapeutic intervention, Xu *et al.* instead simulated interventions and their potential effects on a specific outcome, namely gaze deviation after stroke. The authors used two types of simulated interventions: a 'lesion non-altering intervention', which changes the brain's response to the lesion but not the lesion *per se* (e.g. neurorehabilitation), and a 'lesion-altering intervention', which reduces the size of the lesion (e.g. thrombolysis). In both cases, after iteratively randomizing the patients to 'intervention' and 'control' cohorts, Xu *et al.* tested whether statistical models could detect different effect sizes of treatment. A high-dimensional multivariate approach exhibited a significantly higher predictive power than that of the classical low-dimensional approach for the non-altering intervention. This effect was amplified for the lesion-altering intervention. The work of Xu *et al.* thus demonstrates the biases inherent in the classic lesion-symptom approach, and offers a statistical solution to help investigators draw clinically meaningful inferences in future.

Thanks to data-sharing initiatives, any investigator can replicate the methods of Xu *et al.* or apply them to a different question. Such initiatives have provided the scientific community with a wealth of data for analysis. For instance, the Enigma Consortium stroke recovery initiative (http://enigma.ini.usc.edu/ongoing/enigma-stroke-recovery/) recently made available 304 T_1-weighted MRIs with manually segmented lesions and metadata (Liew *et al.*, 2017). Many authors now recognize the importance of analysing large numbers of unselected stroke patients in order to increase sensitivity, rather than drawing conclusions derived from carefully selected groups and exceptional clinical cases (Corbetta *et al.*, 2015).

There are several approaches available for modelling the interactions between anatomical regions (Fig. 1), including statistical modelling (Xu *et al.*, 2017), and use of *a priori* anatomical knowledge derived from diffusion-weighted imaging tractography (disconnectome approaches, http://toolkit.bcblab.com). Statistical modelling (i.e. a high-dimensional multivariate approach) captures interactions between damaged areas across patients and can help avoid bias (Xu *et al.*, 2017). Other authors have used pre-established atlases of white matter connections to estimate the association between damaged regions (Thiebaut de Schotten *et al.*, 2015). This approach has identified

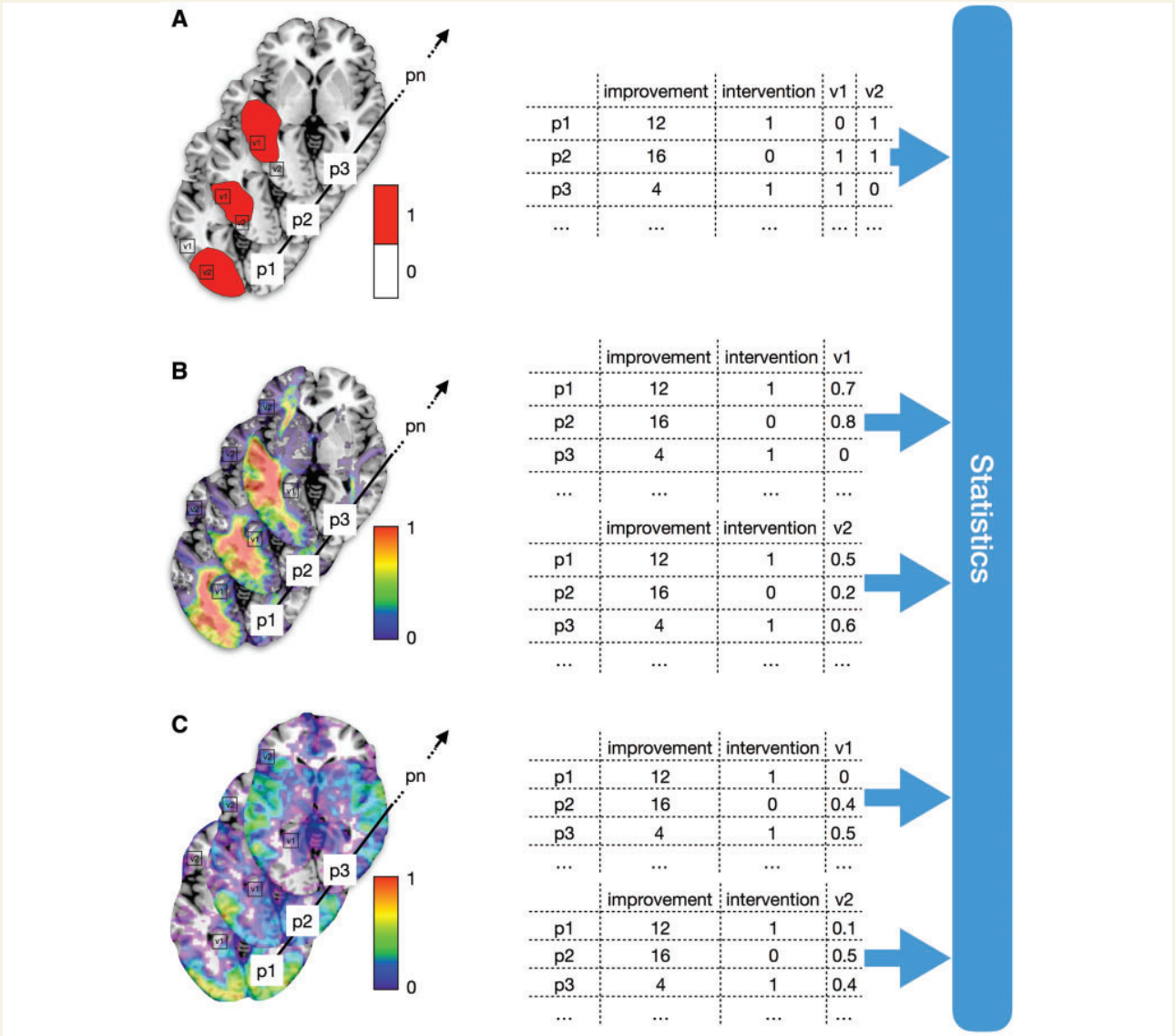

Figure 1 Three models capture the association between brain regions in clinical-neuroanatomical correlations. Analyses were reduced to three patients (Patients p1, p2 and p3) and two voxels (v1, v2) for simplification purposes and performed with BCBtoolkit (http://toolkit.bcblab.com). (**A**) Mass multivariate approach whereby all voxels of the brain are considered variables of interest. The interaction between lesioned voxels is integrated into the statistical model used to predict patient outcomes. (**B**) Disconnectome maps, whereby the probability of disconnection in each voxel is considered a variable of interest. Unlike the mass-multivariate approach, voxels are tested independently in the statistical model used to predict patient outcomes. (**C**) Functional connectivity maps, whereby the correlation between the average time course of the BOLD signal in the lesion and each of the other voxels in the brain is considered a variable of interest. The voxels are tested independently in the statistical model used to predict patient outcomes.

biomarkers with high sensitivity and specificity for chronic visuospatial neglect (Thiebaut de Schotten *et al.*, 2014). Finally, functional MRI at rest (resting state functional MRI) can be used to measure the spontaneous association between brain areas (i.e. functional connectivity) (Boes *et al.*, 2015; Foulon *et al.*, 2017). Recent results demonstrate that higher order cognitive symptoms, such as impairments in memory and attention, are better explained by changes in functional connectivity than by lesion location, whereas lesion location better explains primary disorders (e.g. motor and visual disorders) (Siegel *et al.*, 2016). This finding suggests that the highest level of cognitive function emerges from the interaction between primary and lower level areas through a mechanism of integration, which is not localized to a single brain area. The dynamics of functional connectivity closely reflect the state of recovery within the brain, which in turn

makes resting state functional MRI an excellent method for studying the mechanisms associated with brain recovery. However, functional connectivity is not ideal for predicting future symptoms, as it fluctuates during the recovery process.

There are significant challenges ahead in improving approaches based on lesion-symptom statistics, diffusion-weighted imaging tractography, and resting state functional connectivity. A framework that takes advantage of all three methods could provide a more comprehensive understanding of the biology of recovery after stroke. For instance, tractography can reveal the long-range effects of a brain lesion, whereas functional connectivity measures the dynamic changes associated with brain recovery through plasticity. As proposed by Xu *et al.*, high-dimensional multivariate statistics can control the relationship between various dimensions under study and the distribution of the lesion in space to avoid any bias and optimize the ability of the model to detect interactions. This framework could be used to revisit classic syndromes and provide biomarkers with large effect sizes, which would be applicable in the clinic. Another challenge will be to quantify the percentage of shared variance between the model and individual measurements. Most of these methods assume that all brains are equivalent or identical (Thiebaut de Schotten and Shallice, 2017). Preliminary evidence suggests that different brain connectivity phenotypes are associated with different profiles of recovery. For instance, Forkel *et al.* showed that the size of the arcuate fasciculus in the right hemisphere predicts some of the improvements in speech impairment after a stroke in the left hemisphere (Forkel *et al.*, 2014). Again, reporting the effect size of this interindividual variability is crucial in order to estimate its importance in everyday clinical practice.

In conclusion, associationist principles (Geschwind, 1965; Catani and ffytche, 2005) indicate that brain lesions should not be considered random focal impairments, but rather anatomically predetermined imbalances in a vast system of interconnected areas. Previous attempts to build on this framework were limited by the available methodology and by a lack of access to large cohorts of patients. Newer ideas involving optimized statistics, anatomical models and functional measures have already demonstrated their validity and superiority over classical lesion overlapping approaches in predicting symptoms and the likely outcomes of clinical interventions. We now must reach out and engage with other scientific teams, and promote the sharing of technologies and datasets, to build up a common framework that will be beneficial to patients and to society as a whole.

Michel Thiebaut de Schotten[1,2] *and Chris Foulon*[1,2]

1 *Brain Connectivity and Behaviour Laboratory, Brain and Spine Institute, Paris, France*
2 *Frontlab, Institut du Cerveau et de la Moelle épinière (ICM), UPMC UMRS 1127, Inserm U 1127, CNRS UMR 7225, Paris, France*

Correspondence to: Michel Thiebaut de Schotten
E-mail: michel.thiebaut@gmail.com

doi:10.1093/brain/awx332

Funding

We thank Lauren Sakuma for discussion and the "Agence Nationale de la Recherche" [grant numbers ANR-13-JSV4-0001-01 and ANR-10-IAIHU-06] for their generous support.

References

Boes AD, Prasad S, Liu H, Liu Q, Pascual-Leone A, Caviness VS Jr, et al. Network localization of neurological symptoms from focal brain lesions. Brain 2015; 138 (Pt 10): 3061–75.

Catani M, ffytche DH. The rises and falls of disconnection syndromes. Brain 2005; 128 (Pt 10): 2224–39.

Corbetta M, Ramsey L, Callejas A, Baldassarre A, Hacker CD, Siegel JS, et al. Common behavioral clusters and subcortical anatomy in stroke. Neuron 2015; 85: 927–41.

Forkel SJ, Thiebaut de Schotten M, Dell'Acqua F, Kalra L, Murphy DG, Williams SC, et al. Anatomical predictors of aphasia recovery: a tractography study of bilateral perisylvian language networks. Brain 2014; 137 (Pt 7): 2027–39.

Foulon C, Cerliani L, Kinkingnehun S, Levy R, Rosso C, Urbanski M, et al. Advanced lesion symptom mapping analyses and implementation as BCBtoolkit. bioRxiv 2017; 133314. doi: 10.1101/133314.

Geschwind N. Disconnexion syndromes in animals and man. I. Brain 1965; 88: 237–94.

Liew SL, Anglin JM, Banks NW, Sondag M, Ito KL, Kim H, et al. A large, open source dataset of stroke anatomical brain images and manual lesion segmentations. bioRxiv 2017; 179614.

Siegel JS, Ramsey LE, Snyder AZ, Metcalf NV, Chacko RV, Weinberger K, et al. Disruptions of network connectivity predict impairment in multiple behavioral domains after stroke. Proc Natl Acad Sci USA 2016; 113: E4367–76.

Thiebaut de Schotten M, Dell'Acqua F, Ratiu P, Leslie A, Howells H, Cabanis E, et al. From Phineas Gage and Monsieur Leborgne to H.M.: revisiting disconnection syndromes. Cereb Cortex 2015; 25: 4812–27.

Thiebaut de Schotten M, Shallice T. Identical, similar or different? Is a single brain model sufficient? Cortex 2017; 86: 172–5.

Thiebaut de Schotten M, Tomaiuolo F, Aiello M, Merola S, Silvetti M, Lecce F, et al. Damage to white matter pathways in subacute and chronic spatial neglect: a group study and 2 single-case studies with complete virtual "*in vivo*" tractography dissection. Cereb Cortex 2014; 24: 691–706.

Wahlgren N, Ahmed N, Davalos A, Ford GA, Grond M, Hacke W, et al. Thrombolysis with alteplase for acute ischaemic stroke in the Safe Implementation of Thrombolysis in Stroke-Monitoring Study (SITS-MOST): an observational study. Lancet 2007; 369: 275–82.

Xu T, Jaüger H, Husain M, Rees G, Nachev P. High-dimensional therapeutic inference in the focally damaged human brain. Brain 2017; 141: 48–54.

Discussion

7 The dark side of brain lesions

In this thesis, we present three principal results. We first developed, implemented, and applied a set of complementary multimodal methods to assess the indirect effects of focal brain lesions. This study was a proof of concept that unveiled brain structures outside the lesioned area that contributed significantly to the neuropsychological performance and changed their structural and functional organisation. We then applied these methods to explore the neural bases of higher cognitive functions, namely category fluency, reasoning by analogy, and creativity. Finally, we demonstrated the role of large-scale networks in higher cognitive functions. Overall, these results indicate that the extent of the disruption spreads far beyond the lesioned area and that decades of lesion-based mapping can now be re-assessed in light of the associationist paradigm.

First, the tool we developed (BCBtoolkit) allows for the study of different dimensions of the indirect effects of focal brain lesions. Our point was to demonstrate that the location of a lesion is insufficient in informing us about the real effects of brain damage. We started by mapping the white matter connections—using the disconnectome maps method—impaired by the injury to investigate the disconnections potentially related to behavioural impairment. This approach revealed both cortical and subcortical disconnection areas linked with a deficit in category fluency. The accuracy of our findings was confirmed by the nearly systematic correspondence of significant cortical and subcortical disconnection with the functional activations observed in fMRI studies during categorisation and/or fluency tasks. Importantly, this correspondence strengthens the idea that high-level cognitive functions such as category fluency are recruiting numerous structurally and functionally connected regions to be performed. Following this logic, we calculated—using functional connectivity—the set of regions connected to each critical disconnection. We noticed that some redundancy existed in the functional network extracted. Therefore, we performed a principal component analysis to summarise the results in three main networks. This data reduction approach indicated that the critical disconnected areas belonged to

similar functional networks. Next, we assessed whether the lesions indeed impair these broad networks (i.e., broader than the structural disconnections). We found that patients with disconnections in two on three of these main networks have significantly more diminished functional connectivity than those without. Hence, brain damage is, besides affecting structurally disconnected regions, disrupting larger-scale functional networks. As functional impairment should result from microstructural changes caused by diaschisis, we explored how these networks are structurally affected and if these disruptions are impairing the studied cognitive function. Among the three networks, the integrity of the ventral frontoparietal network, known for its pivotal role in language functions, appeared to be linked with the category fluency performance—a thinner cortex leading to poorer performance. This network connects the core language territories and is strongly left lateralised, contrary to the other two other networks identified. The strong lateralisation of this network limiting brain recovery alternatives (Bartolomeo and Thiebaut de Schotten, 2016) together with its functional involvement in language may explain its essential contribution to the task. Beyond the investigation of category fluency, we extended the use of our tool to the investigation of the neural bases of other higher cognitive functions.

In Urbanski et al. (2016), we showed that analogical reasoning abilities in the visual domain requires various structural connections. When we compared the disconnections of well-known white matter tracts with the performance in the tasks, we identified four critical fibre pathways. The analysis revealed that the more tract disconnected from the left rostrolateral prefrontal cortex (rlPFC), the lower the ability of reasoning by analogy, which was not the case with the tracts not connected to the rlPFC. Hence, the rlPFC appears to be the convergence point of several large-scale brain structures and white matter connections, the backbone of its interaction with the rest of the brain. As for the category fluency, this is convergent with functional imaging and may explain why this is the most consistent region shown activated across fMRI studies (Hobeika et al., 2016).

Analogical reasoning partially relates to the ability to generate and combine distant associations, two essential functions for creativity. In Bendetowicz et al. (2018), we explored whether the generation and combination of distant associations in the semantic domain relate to brain disconnections. This time, we not only mapped the structural disconnections but also explored how damages to functional networks impact the ability to perform the tasks. With the same

perspective as the precedent study, we first tried to relate brain damages to an alteration of the patients' performances. Particularly, the disconnection of the right cingulate fasciculus, as well as the DMN, impairs the ability to generate distant associations. Both the DMN's structures and the cingulate fasciculus are known to be involved in creative tasks (Takeuchi et al., 2010; Jung et al., 2013; Chen et al., 2014, 2015; Fink et al., 2014; Kühn et al., 2014; Jauk et al., 2015). Alternatively, the ability to combine remote ideas seems to require different structures in the left hemisphere, such as the anterior thalamic radiations, the fronto-marginal tract, and to rely on the integrity of the frontoparietal control network (Gonen-Yaacovi et al., 2013; Bendetowicz et al., 2017; Green et al., 2012). Consequently, the generation and combination of distant associations require separate functional and structural networks—in agreement with recent functional connectivity findings on creativity-related networks in healthy subjects (Beaty et al., 2016).

We successfully identified and mapped various brain structures dedicated to the generation of the higher cognitive functions of the human brain. Though not comprehensive, our studies showed these structures interacting together, which allows these complex cognitive processes to happen. While we are aware of these interactions, we still lack knowledge about how these interactions occur and how they generate the various complex behaviours we are capable of. Together, the three articles we published (Foulon et al., 2018; Urbanski et al., 2016; Bendetowicz et al., 2018) demonstrated that the digital application of the associationist paradigm allows for a better understanding of the impact of focal brain lesions. Exploring long-range effects on both structural and functional networks provides more insights into the underlying mechanisms of high-level cognitive functions than the lesioned area alone. As we suggested in our commentary (Thiebaut de Schotten and Foulon, 2018), the lesion location is not sufficient to study higher cognitive functions. It is only by taking into account how cortical and subcortical regions are connected and how large-scale functional networks are interacting together so that we will be able to gather clues on the real effect of focal brain damage.

8 Can we model the interactions between brain structures?

Beyond the work presented in the PhD, future research might want to focus on the modality of interaction that occurs between the different structures of the brain. To this purpose, we can imagine a simple model to illustrate the interactions between what we will call "modules", which can be either brain regions or networks, functionally or structurally defined. We can consider that they can bear two states depending on their participation in a given cognitive function. The state 1 will indicate that the module participates in the function and 0 otherwise. The state 0 can either be when the module is not required to perform the function or because the module is impaired and cannot communicate with the other modules.

Theoretically, if we want to model the interactions between 3 modules, A, B and C, each one being able to be active or not to perform a function, they can either work independently, sequentially or integratively (see Figure 3). Independently, the zero state of our model, A, B, and C, can be active or not separately without influence on the others (see Figure 3A). Each of the three modules will bear two states, 1 or 0, and the sum of the potential states is 6—the sum of the potential information is the sum of the system's constituents. Now, let's consider that A is connected to B and B to C and that B needs the output information from A to send its own to C and C needs it to send it in turn (see Figure 3B). We will call that a sequence. In the case of this sequence, the system has only two possibilities, either the system achieves the function by processing and sending the information through the string of modules or not—the sum of the potential information is less than the sum of the system's constituents. Finally, the modules can be connected reciprocally, not acting sequentially but rather integratively together, to produce a function (see Figure 3C). The number of different potential states combinations is 8, and the sum of the potential information is more than the sum of the system's constituents.

This simple demonstration parallels with information theory (Shannon, 1948). In information theory, we store the information on bits, which can be in two different states associated with 0 and 1, like the simple modules of our model. Similar to our representation of integration, the bits are considered as a whole

to calculate the amount of data we can store in a given number of bits. The amount of information we can store in n bits is 2^n, 2 being the number of possible states of a bit. Similarly, in our model, the number of possible states of modules interacting together integratively would be 2^n with n the number of modules. Moreover, the number of possibilities of an integrative system would grow exponentially with the number of modules. We can then extend the model to more complex structures, which could bear more than two states. The number of combinations offered by integration would grow even faster.

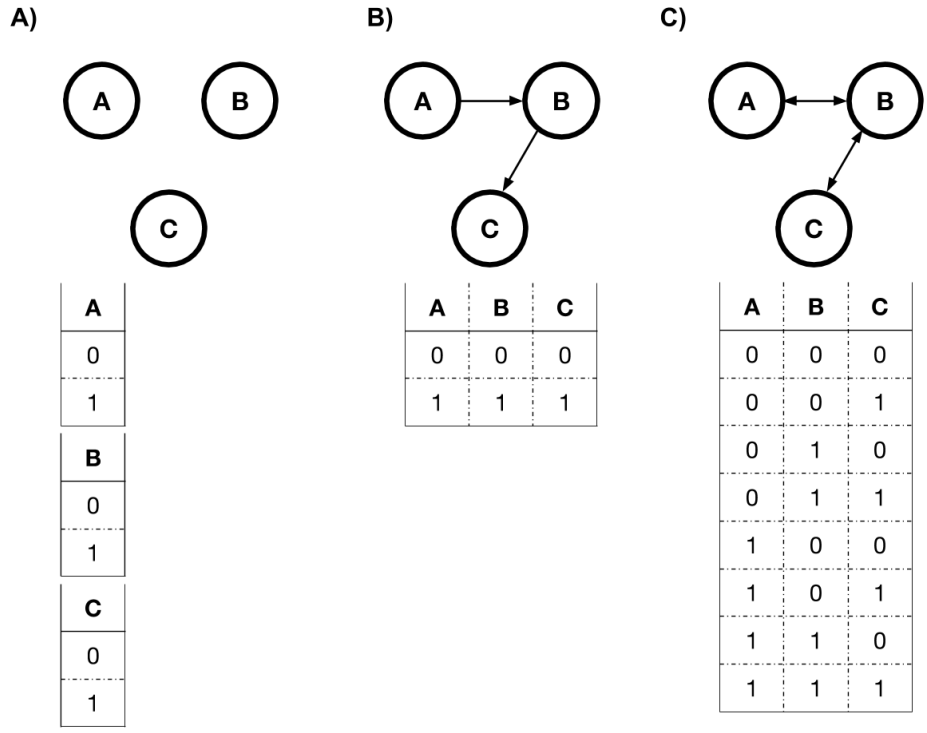

Figure 3: A) represents the possible states of independant modules. B) represents the possible states of modules linked through undirectional connections. C) represents the possible states of modules linked with bidirectional connections

9 Does integration occur in the brain?

Theoretically, a sequence of brain modules can perform a complex task requiring several steps. When someone throws me a balloon, my brain will identify the balloon. The module gathering the visual input will then send it to another coordinate calculation system. Then, once it has estimated the trajectory of the balloon, it will forward the right information to activate my motor system allowing me to catch it. If any part of the sequence is missing, I will miss the balloon. And, it will be the case for any task requiring the sequential activation of modules in the brain. The proportional increase of reaction time that reflects different steps in sequences between perception and action (Ledlow et al., 1978) partially supports this model. Now, let's consider the integration of numerous modules acting together in producing a behaviour. The different brain structures must work like an orchestra; they have to follow the right music score and rhythm together, although they can play different instruments; this is the whole which produces the symphony. In that configuration, we can observe that losing one musician from the orchestra will not destroy the symphony; the sound will be slightly simpler. Consequently, the symphony is resilient to missing musicians and integrative configurations in the brain should be more resilient to focal damages. This model has been preferentially adopted for higher cognitive functions such as consciousness which require the integration of many signals in short time periods (Edelman, 2003). Hence, both models, sequential and integrative, find support in the literature, and both organisations may well work together in the brain.

However, there is an open question about the model of the integration: Is there a located conductor, or is the music score distributed and coordinated through the white matter connections? A brain module with a conductor would rely on one critical node that would communicate the rhythm to every other node of the network. In such a case, the conductor would be a weak spot for the whole function—which might be a way to disentangle it from the other hypothesis. Therefore, we could find a difference between sequential and integrative functions. Sequential functions should be entirely disabled with the disruption of whichever node or its connection along the sequence while the conductor should be the only weak point that leads to the total disabling of the function. Nevertheless, it would make integration more resilient to random damage. A conductor

should be connected to every other node of the structure that performs a given function. Such structures may exist in the brain, for instance, the two thalami at the hemispheric scale. The cases of damage in these regions have a dreadful impact on the brain—for example, the destruction of the two thalami leads to death. Several measures have already been tried to identify highly interactive regions. The functional entropy and different measures from graph theory such as node degree, centrality, or "hubiness" may help us disentangle the conductors of functions whenever they exist. The other hypothesis is that the conductor's role in integrative functions is spread through the white matter connections. The different regions of the brain would organise themselves, neighbour to neighbour. Hence, to spread the rhythm to play the symphony, the first region of the module would need to send the music score to its neighbours, which would, in turn, send it to their neighbours, and so on. This would produce a lag along the module's processing—a lag that could reflect the number of synapses that the message has to pass. Such a delay has already been shown in studies of synchrony using EEG measures (Varela et al., 2001). Travelling upstream may reveal the first region that initiates the symphony and informs us on the organisation of the orchestra. The self-organisation of the brain modules would be highly resilient to all kinds of damage. The total disruption of such modules would require the destruction of every part of it. However, what we define as the high-level cognitive functions may be possible only from a threshold of integration. We could imagine that the function would falter with an insufficient number of structures interacting together to generate the symphony. The actual organisation of the brain modules for integrative functions may also be a gradient or a combination of these two models. The resilience, the efficiency, and the variety of combinations enabled by the integrative interactions between brain modules may lead us to think it should be the preferred organisation of brain networks. However, if we consider an example such the one used above, it is difficult to find a way to perform the action of catching a balloon using integration as it will always require our brain to wait for the computation of the precedent link of the sequence. It is more likely that among the tremendous amount of different functions our brains are performing, we need both types of interactions combined at different levels. Hopefully, future development will enable us to refine our model and maybe disentangle the different interactions.

10 Limitations and future developments

The three studies presented in this thesis, however, present potential location biases. Firstly, all our patients had frontal lesions, preventing us from studying the more posterior parts of the brain. Even though the structural and functional disconnections influence regions outside of the frontal regions, we cannot exclude the participation of other networks in the studied functions. It would be interesting to reproduce these studies on datasets with broader distribution and varieties of lesions. Another location bias lies in the distribution of the areas where the pathologies occur. Indeed, the location of the brain damages, even without any selection, is not random. For instance, with strokes, the lesions' locations are linked to the vascular tree's anatomy (Mah et al., 2014). Highly multivariate analyses might achieve more accurate results, as they allow one to remove the part of the variance explained by the non-random distribution of damages. They, however, require a much larger amount of data than what we had for these studies. It is, therefore, primordial to support the open science initiatives that are developing around the world. It is probably the most efficient way to develop accurate and reproducible science. Moreover, all the patient data used in our studies are at the chronic stage of the pathologies; we cannot exclude an effect of the recovery on the functional and structural changes found. In the two publications of Urbanski et al. (2016) and Bendetowicz et al. (2018), we used the VLSM methods to find a critical spot to explain the decreased performance in the different psychological tests. As we mentioned, this method suffers from several biases. The location shift pointed out in Mah and colleagues' work (2014) might concern these findings. However, this location shift concerns the ischemic strokes; the variety of disorders of our datasets may prevent, or at least mitigate, this bias in our studies. The advantage of the disconnectome methods is subject to limitations as we provide an estimation of the severed connections from a dataset of healthy subjects. This estimation might partially miss structural interindividual differences that influence the patient's recovery. For instance, the size of spared fibre pathways can have a significant impact on recovery (Forkel et al., 2014) This latter limitation would require further development to bring our approach closer to individual data to be addressed.

So far, the analyses we performed are always in a standard reference space in order to compare the neuroimaging data between different subject populations.

As discussed in Thiebaut de Schotten and Foulon (2018), many methods used in group studies fail the translation to clinical usage. However, further improvement and adjustment to map the patients' lesion's indirect effects in the native space could benefit clinical practice (see Figure 4). Indeed, it would allow a more personalised diagnosis and follow-up of recovery and would improve the accuracy of a single-patient approach. The first step would be to bring the disconnectome maps in the native space to map the lost connections. While it is still an estimation of the connections severed by the lesion, it gives more information about the potential brain structures that may be indirectly affected by the damage than structural information alone. Besides, our multimodal framework could also be adapted for a more personalised diagnosis or a monitoring-oriented purpose. In addition to mapping the structural disconnections, we can also estimate the functional differences—we can use the seed-based functional connectivity, for instance—between a patient and a healthy population. Similar to our approach with the BCBtoolkit publication, the functional connectivity combined with the disconnectome maps may help us to investigate a wider extent of the indirect impact of a lesion at the individual level.

Besides the translation of our group analyses to clinical practice, we may want to increase the variety of brain disorders that we can study through this multimodal associationist framework. In the present work, we analysed only focal brain lesions. Further research could focus on extending the framework to neurodegenerative diseases. This will require adapting the methods to partial disconnections and diffusing damages. The disconnectome maps may be an advance in that field, as the diffusion measures of patient data suffer from other, but not less critical, flaws (Jones et al., 2013) than focal lesions. The cortical thickness measurement, for instance, appears to be sensible enough to detect diffuse damage (Gefen et al., 2012; Eskildsen et al., 2015; Mesulam et al., 2015); in combination with the disconnectome maps, it could provide more accurate information on the structurally affected regions. Functional imaging is also widely used to study neurodegenerative diseases (Buckner et al., 2009; Farb et al., 2013; Migliaccio et al., 2016), and it would undoubtedly benefit from a combination with the disconnectome maps once adapted to neurodegenerative disorders. The two potential evolutions for this framework may also be developed together; extending our methods to neurodegenerative diseases would also benefit from being adapted for clinical practice.

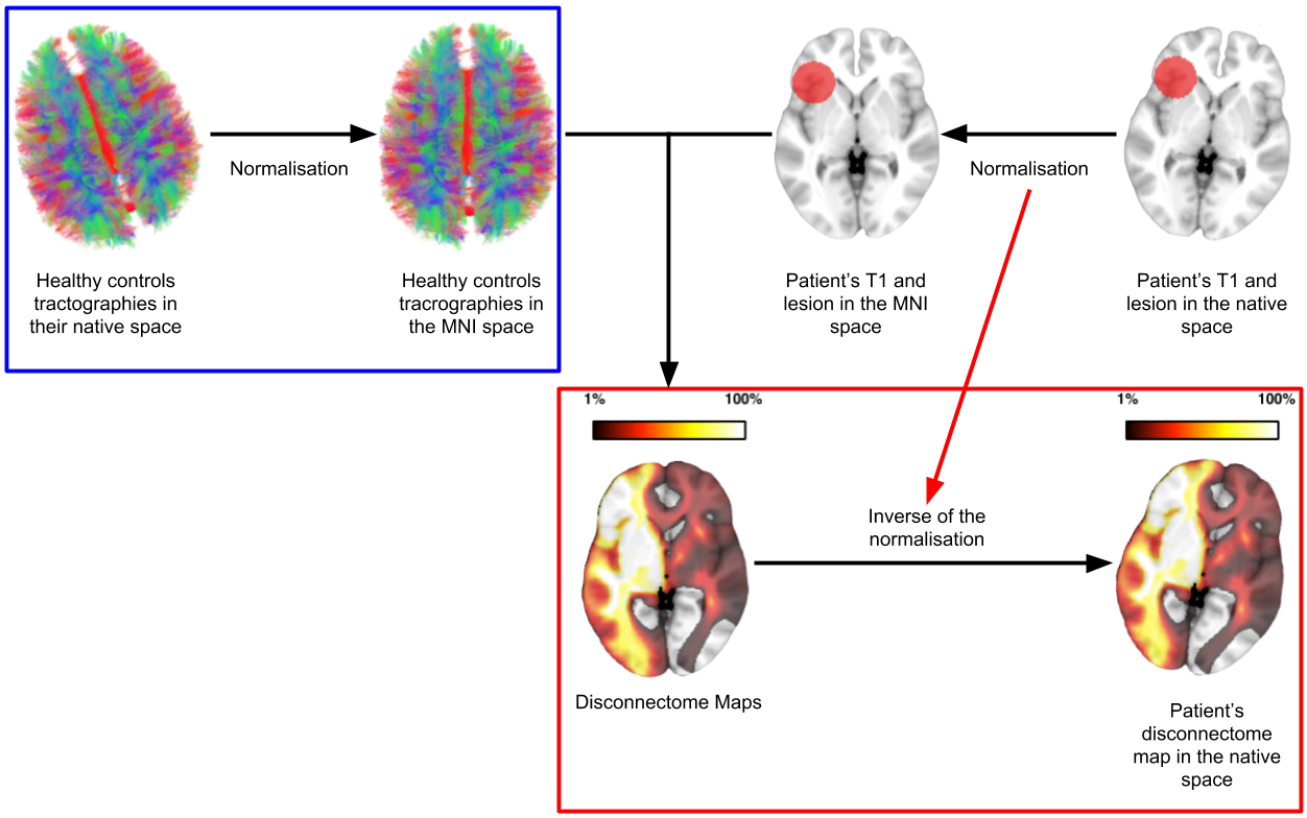

Figure 4: Possible pipeline to bring the disconnectome daps in the native space. Registering the controls' tractographies in the MNI, as in the blue step of the pipeline, will spare us one transformation of the images compared to the classical disconnectome maps. The red step shows how we could calculate the disconnectome maps in the patient's native space, by reversing the transformations we used to bring the patient's images in the MNI on the disconnectome maps.

Bibliography

Ahmed, F. S. and Miller, L. S. (2015). Adequate proverb interpretation is associated with performance on the Independent Living Scales. *Aging, Neuropsychology, and Cognition*, 22(3):376–387. 4

Ashburner, J. and Friston, K. J. (2000). Voxel-Based Morphometry—The Methods. *NeuroImage*, 11(6):805–821. 1

Bartheld, C. S. v., Bahney, J., and Herculano-Houzel, S. (2016). The search for true numbers of neurons and glial cells in the human brain: A review of 150 years of cell counting. *Journal of Comparative Neurology*, 524(18):3865–3895. 2

Bartolomeo, P. (2011). The quest for the 'critical lesion site' in cognitive deficits: Problems and perspectives. *Cortex*, 47(8):1010–1012. 2

Bartolomeo, P. and Thiebaut de Schotten, M. (2016). Let thy left brain know what thy right brain doeth: Inter-hemispheric compensation of functional deficits after brain damage. *Neuropsychologia*, 93:407–412. 2, 7

Bates, E., Wilson, S. M., Saygin, A. P., Dick, F., Sereno, M. I., Knight, R. T., and Dronkers, N. F. (2003). Voxel-based lesion–symptom mapping. *Nature Neuroscience*, 6(5):448–450. 2, 6

Beaty, R. E., Benedek, M., Silvia, P. J., and Schacter, D. L. (2016). Creative Cognition and Brain Network Dynamics. *Trends in Cognitive Sciences*, 20(2):87–95. 5, 7

Bendetowicz, D., Urbanski, M., Aichelburg, C., Levy, R., and Volle, E. (2017). Brain morphometry predicts individual creative potential and the ability to combine remote ideas. *Cortex*, 86:216–229. 7

Bendetowicz, D., Urbanski, M., Garcin, B., Foulon, C., Levy, R., Bréchemier, M.-L., Rosso, C., Thiebaut de Schotten, M., and Volle, E. (2018). Two critical brain networks for generation and combination of remote associations. *Brain*, 141(1):217–233. 7, 10

Biswal, B., Zerrin Yetkin, F., Haughton, V. M., and Hyde, J. S. (1995). Functional connectivity in the motor cortex of resting human brain using echo-planar MRI. *Magnetic resonance in medicine*, 34(4):537–541. 1

Boes, A. D., Prasad, S., Liu, H., Liu, Q., Pascual-Leone, A., Caviness, V. S., and Fox, M. D. (2015). Network localization of neurological symptoms from focal brain lesions. *Brain*, 138(10):3061–3075. 6

Bonnelle, V., Ham, T. E., Leech, R., Kinnunen, K. M., Mehta, M. A., Greenwood, R. J., and Sharp, D. J. (2012). Salience network integrity predicts default mode network function after traumatic brain injury. *Proceedings of the National Academy of Sciences*, 109(12):4690–4695. 3

Breasted, J. H. (1930). *The Edwin Smith Surgical Papyrus: published in facsimile and hieroglyphic transliteration with translation and commentary in two volumes*, volume 3. Chic. UP. 1

Bredesen, D. E. (1995). Neural apoptosis. *Annals of Neurology*, 38(6):839–851. 3

Broca, P. (1861). Perte de la parole, ramollissement chronique et destruction partielle du lobe antérieur gauche du cerveau. *Bull Soc Anthropol*, 2(1):235–238. 1

Buckner, R. L., Sepulcre, J., Talukdar, T., Krienen, F. M., Liu, H., Hedden, T., Andrews-Hanna, J. R., Sperling, R. A., and Johnson, K. A. (2009). Cortical Hubs Revealed by Intrinsic Functional Connectivity: Mapping, Assessment of Stability, and Relation to Alzheimer's Disease. *Journal of Neuroscience*, 29(6):1860–1873. 10

Burgess, P. W. and Shallice, T. (1996a). Bizarre responses, rule detection and frontal lobe lesions. *Cortex*, 32(2):241–259. 6

Burgess, P. W. and Shallice, T. (1996b). Response suppression, initiation and strategy use following frontal lobe lesions. *Neuropsychologia*, 34(4):263–272. 6

Capurso, S. A., Calhoun, M. E., Sukhov, R. R., Mouton, P. R., Price, D. L., and Koliatsos, V. E. (1997). Deafferentation Causes Apoptosis in Cortical Sensory Neurons in the Adult Rat. *The Journal of Neuroscience*, 17(19):7372–7384. 3

Carrera, E. and Tononi, G. (2014). Diaschisis: past, present, future. *Brain*, 137(9):2408–2422. 3

Catani, M. and Ffytche, D. H. (2005). The rises and falls of disconnection syndromes. *Brain*, 128(10):2224–2239. 3

Catani, M. and Mesulam, M. (2008). What is a disconnection syndrome? *Cortex*, 44(8):911–913. 2

Catani, M. and Thiebaut de Schotten, M. (2012). *Atlas of Human Brain Connections*. OUP Oxford. 1

Chen, Q., Yang, W., Li, W., Wei, D., Li, H., Lei, Q., Zhang, Q., and Qiu, J. (2014). Association of creative achievement with cognitive flexibility by a combined voxel-based morphometry and resting-state functional connectivity study. *NeuroImage*, 102:474–483. 7

Chen, Q.-L., Xu, T., Yang, W.-J., Li, Y.-D., Sun, J.-Z., Wang, K.-C., Beaty, R. E., Zhang, Q.-L., Zuo, X.-N., and Qiu, J. (2015). Individual differences in verbal creative thinking are reflected in the precuneus. *Neuropsychologia*, 75:441–449. 7

Chouiter, L., Holmberg, J., Manuel, A. L., Colombo, F., Clarke, S., Annoni, J.-M., and Spierer, L. (2016). Partly segregated cortico-subcortical pathways support phonologic and semantic verbal fluency: A lesion study. *Neuroscience*, 329:275–283. 3

Ciaraffa, F., Castelli, G., Parati, E. A., Bartolomeo, P., and Bizzi, A. (2013). Visual neglect as a disconnection syndrome? A confirmatory case report. *Neurocase*, 19(4):351–359. 2

Clarke, E. and O'Malley, C. D. (1996). *The Human Brain and Spinal Cord: A Historical Study Illustrated by Writings from Antiquity to the Twentieth Century*. Norman Publishing. 1

Corbetta, M., Kincade, M. J., Lewis, C., Snyder, A. Z., and Sapir, A. (2005). Neural basis and recovery of spatial attention deficits in spatial neglect. *Nature Neuroscience*, 8(11):1603–1610. 3

Cowan, W. M. (1970). Anterograde and Retrograde Transneuronal Degeneration in the Central and Peripheral Nervous System. In *Contemporary Research Methods in Neuroanatomy*, pages 217–251. Springer, Berlin, Heidelberg. 3

Crivellato, E. and Ribatti, D. (2007). Soul, mind, brain: Greek philosophy and the birth of neuroscience. *Brain Research Bulletin*, 71(4):327–336. 1

Damasio, H. and Damasio, A. R. (1989). *Lesion analysis in neuropsychology*. Oxford University Press, USA. 2, 6

De Pisapia, N., Bacci, F., Parrott, D., and Melcher, D. (2016). Brain networks for visual creativity: a functional connectivity study of planning a visual artwork. *Scientific Reports*, 6:39185. 5

Deiters, O. (1865). *Untersuchungen über Gehirn und Rückenmark des Menschen und der Säugethiere*. F. Veiweg. 1

Dronkers, N. F., Plaisant, O., Iba-Zizen, M. T., and Cabanis, E. A. (2007). Paul Broca's historic cases: high resolution MR imaging of the brains of Leborgne and Lelong. *Brain*, 130(5):1432–1441. 2, 3

Edelman, G. M. (2003). Naturalizing consciousness: A theoretical framework. *Proceedings of the National Academy of Sciences*, 100(9):5520–5524. 9

Ellamil, M., Dobson, C., Beeman, M., and Christoff, K. (2012). Evaluative and generative modes of thought during the creative process. *NeuroImage*, 59(2):1783–1794. 5

Eskildsen, S. F., Coupé, P., Fonov, V. S., Pruessner, J. C., and Collins, D. L. (2015). Structural imaging biomarkers of Alzheimer's disease: predicting disease progression. *Neurobiology of Aging*, 36:S23–S31. 10

Farb, N. A. S., Grady, C. L., Strother, S., Tang-Wai, D. F., Masellis, M., Black, S., Freedman, M., Pollock, B. G., Campbell, K. L., Hasher, L., and Chow, T. W. (2013). Abnormal network connectivity in frontotemporal dementia: Evidence for prefrontal isolation. *Cortex*, 49(7):1856–1873. 10

Feeney, D. M. and Baron, J.-c. (1986). Diaschisis. *Stroke*, 17(5):817–830. 3

Fields, R. D. (2008). White Matter Matters. *Scientific American*, 298(3):54–61. 2

Finger, S., Koehler, P. J., and Jagella, C. (2004). The Monakow Concept of Diaschisis: Origins and Perspectives. *Archives of Neurology*, 61(2):283–288. 1, 3

Fink, A., Koschutnig, K., Hutterer, L., Steiner, E., Benedek, M., Weber, B., Reishofer, G., Papousek, I., and Weiss, E. M. (2014). Gray matter density in relation to different facets of verbal creativity. *Brain Structure and Function*, 219(4):1263–1269. 7

Forkel, S. J., Schotten, M. T. d., Dell'Acqua, F., Kalra, L., Murphy, D. G. M., Williams, S. C. R., and Catani, M. (2014). Anatomical predictors of aphasia recovery: a tractography study of bilateral perisylvian language networks. *Brain*, 137(7):2027–2039. 3, 10

Fornito, A., Zalesky, A., and Breakspear, M. (2015). The connectomics of brain disorders. *Nature Reviews Neuroscience*, 16(3):159. 3

Foulon, C., Cerliani, L., Kinkingnéhun, S., Levy, R., Rosso, C., Urbanski, M., Volle, E., and Thiebaut de Schotten, M. (2018). Advanced lesion symptom mapping analyses and implementation as BCBtoolkit. *GigaScience*, 7(3):1–17. 6, 7

Fox, M. D., Corbetta, M., Snyder, A. Z., Vincent, J. L., and Raichle, M. E. (2006). Spontaneous neuronal activity distinguishes human dorsal and ventral attention systems. *Proceedings of the National Academy of Sciences*, 103(26):10046–10051. 3

Friedman, B. R., Jones, J. P., Chavez-Munoz, G., Salmon, A. P., and Merritt, C. R. B. (1989). *Principles of MRI*. McGraw Hill Book Co. 1

Gabora, L. (2010). Revenge of the "Neurds": Characterizing Creative Thought in Terms of the Structure and Dynamics of Memory. *Creativity Research Journal*, 22(1):1–13. 5

Gall, F. J. .-. A. d. t. and Spurzheim, J. G. .-. A. d. t. (1810). *Anatomie et physiologie du système nerveux en général et du cerveau en particulier. Tome 2*

/ , avec des observations sur la possibilité de reconnaître plusieurs dispositions intellectuelles et morales de l'homme et des animaux par la configuration de leurs têtes, par J. F. Gall et G. Spurzheim,... 1

Gefen, T., Gasho, K., Rademaker, A., Lalehzari, M., Weintraub, S., Rogalski, E., Wieneke, C., Bigio, E., Geula, C., and Mesulam, M.-M. (2012). Clinically concordant variations of Alzheimer pathology in aphasic versus amnestic dementia. *Brain*, 135(5):1554–1565. 10

Geschwind, N. (1965a). Disconnexion syndromes in animals and man - Part I. *Brain*, 88(2):237–294. 3

Geschwind, N. (1965b). Disconnexion syndromes in animals and man - Part II. *Brain*, 88(3):585–644. 3

Ghosh, S. K. (2015). Human cadaveric dissection: a historical account from ancient Greece to the modern era. *Anatomy & Cell Biology*, 48(3):153–169. 1

Gonen-Yaacovi, G., Souza, D., Cruz, L., Levy, R., Urbanski, M., Josse, G., and Volle, E. (2013). Rostral and caudal prefrontal contribution to creativity: a meta-analysis of functional imaging data. *Frontiers in Human Neuroscience*, 7. 7

Gratton, C., Neta, M., Sun, H., Ploran, E. J., Schlaggar, B. L., Wheeler, M. E., Petersen, S. E., and Nelson, S. M. (2017). Distinct Stages of Moment-to-Moment Processing in the Cinguloopercular and Frontoparietal Networks. *Cerebral Cortex*, 27(3):2403–2417. 3

Green, A. E., Kraemer, D. J., Fugelsang, J. A., Gray, J. R., and Dunbar, K. N. (2012). Neural correlates of creativity in analogical reasoning. *Journal of Experimental Psychology: Learning, Memory, and Cognition*, 38(2):264. 7

Hobeika, L., Diard-Detoeuf, C., Garcin, B., Levy, R., and Volle, E. (2016). General and specialized brain correlates for analogical reasoning: A meta-analysis of functional imaging studies. *Human Brain Mapping*, 37(5):1953–1969. 7

Jauk, E., Neubauer, A. C., Dunst, B., Fink, A., and Benedek, M. (2015). Gray matter correlates of creative potential: A latent variable voxel-based morphometry study. *NeuroImage*, 111:312–320. 7

Jones, D. K., Knösche, T. R., and Turner, R. (2013). White matter integrity, fiber count, and other fallacies: The do's and don'ts of diffusion MRI. *NeuroImage*, 73:239–254. 10

Jones, O. P., Alfaro-Almagro, F., and Jbabdi, S. (2018). An empirical, 21st century evaluation of phrenology. *bioRxiv*, page 243089. 1

Jung, R. E. (2014). Evolution, creativity, intelligence, and madness: "Here Be Dragons". *Frontiers in Psychology*, 5. 5

Jung, R. E., Mead, B. S., Carrasco, J., and Flores, R. A. (2013). The structure of creative cognition in the human brain. *Frontiers in Human Neuroscience*, 7. 7

Keith, A. (1927). The Brain of Anatole France. *British Medical Journal*, 2(3491):1048. 1

Kinkingnehun, S. R. J., du Boisgueheneuc, F., Golmard, J.-L., Zhang, S. X., Levy, R., and Dubois, B. (2004). Anatomo-clinical overlapping maps (AnaCOM): a new method to create anatomo-functional maps from neuropsychological tests and structural MRI scan of subjects with brain lesions. volume 5369, pages 583–592. 6

Krawczyk, D. C. (2012). The cognition and neuroscience of relational reasoning. *Brain Research*, 1428:13–23. 4

Kühn, S., Ritter, S. M., Müller, B. C. N., Baaren, R. B. v., Brass, M., and Dijksterhuis, A. (2014). The Importance of the Default Mode Network in Creativity—A Structural MRI Study. *The Journal of Creative Behavior*, 48(2):152–163. 7

Lashley, K. S. (1950). In search of the engram. In *Physiological mechanisms in animal behavior. (Society's Symposium IV.)*, pages 454–482. Academic Press, Oxford, England. 1

Ledlow, A., Swanson, J. M., and Kinsbourne, M. (1978). Differences in reaction times and average evoked potentials as a function of direct and indirect neural pathways. *Annals of Neurology: Official Journal of the American Neurological Association and the Child Neurology Society*, 3(6):525–530. 9

Liepmann, H. (1900). Das Krankheitsbild der Apraxie (motorische Asymbolie) auf Grund aines Falles von einseitiger Apraxie. *Monatschrie Psychiatrie Neuroligie*, 10:214–227. 1

Liew, S.-L., Anglin, J. M., Banks, N. W., Sondag, M., Ito, K. L., Kim, H., Chan, J., Ito, J., Jung, C., Khoshab, N., Lefebvre, S., Nakamura, W., Saldana, D., Schmiesing, A., Tran, C., Vo, D., Ard, T., Heydari, P., Kim, B., Aziz-Zadeh, L., Cramer, S. C., Liu, J., Soekadar, S., Nordvik, J.-E., Westlye, L. T., Wang, J., Winstein, C., Yu, C., Ai, L., Koo, B., Craddock, R. C., Milham, M., Lakich, M., Pienta, A., and Stroud, A. (2018). A large, open source dataset of stroke anatomical brain images and manual lesion segmentations. *Scientific Data*, 5:180011. 3

Lissauer, H. (1890). Ein Fall von Seelenblindheit nebst einem Beitrage zur Theorie derselben. *Archiv für Psychiatrie und Nervenkrankheiten*, 21(2):222–270. 1

Lo, E. H., Dalkara, T., and Moskowitz, M. A. (2003). Neurological diseases: Mechanisms, challenges and opportunities in stroke. *Nature Reviews Neuroscience*, 4(5):399–414. 2

MacPherson, S. E., Della Sala, S., Cox, S. R., Girardi, A., and Iveson, M. H. (2015). *Handbook of Frontal Lobe Assessment*. Oxford University Press. Google-Books-ID: S_sJCAAAQBAJ. 3

Mah, Y.-H., Husain, M., Rees, G., and Nachev, P. (2014). Human brain lesion-deficit inference remapped. *Brain*, 137(9):2522–2531. 2, 6, 10

Mesulam, M.-M., Thompson, C. K., Weintraub, S., and Rogalski, E. J. (2015). The Wernicke conundrum and the anatomy of language comprehension in primary progressive aphasia. *Brain*, 138(8):2423–2437. 10

Meynert, T. (1885). Psychiatry: Clinical Treatise on the Diseases of the Fore-Brain, trans. *B. Sachs. New York & London: GP Putnam*. 1

Migliaccio, R., Gallea, C., Kas, A., Perlbarg, V., Samri, D., Trotta, L., Michon, A., Lacomblez, L., Dubois, B., Lehericy, S., and Bartolomeo, P. (2016). Functional Connectivity of Ventral and Dorsal Visual Streams in Posterior Cortical Atrophy. *Journal of Alzheimer's Disease*, 51(4):1119–1130. 10

Mok, L. W. (2014). The interplay between spontaneous and controlled processing in creative cognition. *Frontiers in Human Neuroscience*, 8. 5

Morrison, R. G., Krawczyk, D. C., Holyoak, K. J., Hummel, J. E., Chow, T. W., Miller, B. L., and Knowlton, B. J. (2004). A neurocomputational model of analogical reasoning and its breakdown in frontotemporal lobar degeneration. *Journal of Cognitive Neuroscience*, 16(2):260–271. 4

Nachev, P. (2015). The first step in modern lesion-deficit analysis. *Brain*, 138(6):e354–e354. 2

Parker Jones, O., Alfaro-Almagro, F., and Jbabdi, S. (2018). An empirical, 21st century evaluation of phrenology. *Cortex*, 106:26–35.

Parlatini, V., Radua, J., Dell'Acqua, F., Leslie, A., Simmons, A., Murphy, D. G., Catani, M., and Thiebaut de Schotten, M. (2017). Functional segregation and integration within fronto-parietal networks. *NeuroImage*, 146:367–375. 3

Power, J. D. and Petersen, S. E. (2013). Control-related systems in the human brain. *Current Opinion in Neurobiology*, 23(2):223–228. 3

Saenger, V. M., Ponce-Alvarez, A., Adhikari, M., Hagmann, P., Deco, G., and Corbetta, M. (2017). Linking Entropy at Rest with the Underlying Structural Connectivity in the Healthy and Lesioned Brain. *Cerebral Cortex*, pages 1–11. 3

Shannon, C. E. (1948). A mathematical theory of communication. *The Bell System Technical Journal*, 27(3):379–423. 8

Siegel, J. S., Ramsey, L. E., Snyder, A. Z., Metcalf, N. V., Chacko, R. V., Weinberger, K., Baldassarre, A., Hacker, C. D., Shulman, G. L., and Corbetta, M. (2016). Disruptions of network connectivity predict impairment in multiple behavioral domains after stroke. *Proceedings of the National Academy of Sciences*, 113(30):E4367–E4376. 6

Smith, S. M., Fox, P. T., Miller, K. L., Glahn, D. C., Fox, P. M., Mackay, C. E., Filippini, N., Watkins, K. E., Toro, R., Laird, A. R., and Beckmann, C. F. (2009). Correspondence of the brain's functional architecture during activation

and rest. *Proceedings of the National Academy of Sciences*, 106(31):13040–13045. 1, 3

Takeuchi, H., Taki, Y., Sassa, Y., Hashizume, H., Sekiguchi, A., Fukushima, A., and Kawashima, R. (2010). Regional gray matter volume of dopaminergic system associate with creativity: Evidence from voxel-based morphometry. *NeuroImage*, 51(2):578–585. 7

Thiebaut de Schotten, M., Dell'Acqua, F., Ratiu, P., Leslie, A., Howells, H., Cabanis, E., Iba-Zizen, M. T., Plaisant, O., Simmons, A., Dronkers, N. F., Corkin, S., and Catani, M. (2015). From Phineas Gage and Monsieur Leborgne to H.M.: Revisiting Disconnection Syndromes. *Cerebral Cortex*, 25(12):4812–27. 2, 6

Thiebaut de Schotten, M. and Foulon, C. (2018). The rise of a new associationist school for lesion-symptom mapping. *Brain*, 141(1):2–4. 7, 10

Tononi, G., Edelman, G. M., and Sporns, O. (1998). Complexity and coherency: integrating information in the brain. *Trends in Cognitive Sciences*, 2(12):474–484. 3

Urbanski, M., Bréchemier, M.-L., Garcin, B., Bendetowicz, D., Thiebaut de Schotten, M., Foulon, C., Rosso, C., Clarençon, F., Dupont, S., Pradat-Diehl, P., Labeyrie, M.-A., Levy, R., and Volle, E. (2016). Reasoning by analogy requires the left frontal pole: lesion-deficit mapping and clinical implications. *Brain*, 139(6):1783–1799. 4, 7, 10

Varela, F., Lachaux, J.-P., Rodriguez, E., and Martinerie, J. (2001). The brainweb: Phase synchronization and large-scale integration. *Nature Reviews Neuroscience*, 2(4):229–239. 9

Vartanian, O. (2012). Dissociable neural systems for analogy and metaphor: implications for the neuroscience of creativity. *British Journal of Psychology (London, England: 1953)*, 103(3):302–316. 4

Volle, E., Levy, R., and Burgess, P. W. (2013). A New Era for Lesion-Behavior Mapping of Prefrontal Functions. In Stuss, D. T. and Knight, R. T., editors, *Principles of Frontal Lobe Function*, pages 500–523. Oxford University Press. 6

von Monakow, C. (1914). *Die Lokalisation im Grosshirn und der Abbau der Funktion durch kortikale Herde*. JF Bergmann. 1

Waller, A. (1850). Experiments on the Section of the Glossopharyngeal and Hypoglossal Nerves of the Frog, and Observations of the Alterations Produced Thereby in the Structure of Their Primitive Fibres. *Philosophical Transactions of the Royal Society of London*, 140:423–429. 2

Wernicke, C. (1906). Grundrisse der psychiatrie. Leipzig. *Verlag von Georg Thieme*. 1

Xu, T., Rolf Jäger, H., Husain, M., Rees, G., and Nachev, P. (2018). High-dimensional therapeutic inference in the focally damaged human brain. *Brain*, 141(1):48–54. 2, 6, 6

Yarkoni, T. (2011). Neurosynth. 3

Yarkoni, T., Poldrack, R. A., Nichols, T. E., Essen, D. C. V., and Wager, T. D. (2011). Large-scale automated synthesis of human functional neuroimaging data. *Nature Methods*, 8(8):665–670. 3

Chris FOULON **Thèse de doctorat** **2018**

Sujet : Implémentation d'analyses néo-associationistes avancées du cerveau

Résumé : Les nouvelles techniques d'imagerie cérébrales, notamment les différentes modalités de l'imagerie par résonance magnétique (IRM), permettent pour la première fois dans l'histoire des neurosciences, d'étudier le cerveau humain in vivo. Ces technologies rendent désormais possible l'étude des symptômes provoquées par des lésions cérébrales chez les patients vivants. Mais ceci requiert le développement de nouvelles analyses, adaptées à ces données encore inaccessibles quelques décennies plus tôt. La plupart des méthodes actuelles pour relier des déficits neuropsychologiques aux dommages cérébraux se concentrent sur la région lésée elle même, négligeant les connexions structurelles et fonctionnelles affectées. Dans cette thèse, nous présentons tout d'abord un ensemble de méthodes, implémentées dans notre logiciel, le BCBtoolkit, permettant l'étude des déconnexions à la fois structurelles et fonctionnelles, ainsi que leur impact sur le comportement. Nous avons utilisé ces analyses pour cartographier les effets de lésions focales frontales sur la performance dans la tâche de fluence catégorielle. Nous présentons ensuite deux études dans lesquelles nous avons utilisé ces approches pour étudier les mécanismes cérébraux de plusieurs fonctions associées à la créativité. Et nous terminons cette thèse par une discussion sur les interactions entre les différentes structures du cerveau, qui permettent de générer les comportements humains. Nos études dévoilent la participation de nombreux réseaux, aussi bien structurels que fonctionnels, dans les différentes fonctions cognitives de haut niveau. Nous tentons, ultimement, de modéliser théoriquement leurs interactions.

Mots clés : Neuroimagerie, lésion, connectivité, disconnexion, tractographie, IRMf

Subject: Implementing Advanced Neo-Associationist Analyses of the Brain

Summary: The new brain imaging techniques, notably the different magnetic resonance imaging (MRI) modalities, allow the study of the human brain in vivo for the first time in neuroscience's history. These technologies now make possible to study the symptoms caused by brain lesions in living patients. However, it requires the development of new analyses adapted for this new kind of data which was not available a few decades ago. Most of the classical lesion–symptom analyses are focused on the lesioned area, often neglecting the affected structural and functional connections. In this thesis, we begin by presenting a set of methods, implemented in our software the BCBtoolkit, enabling the study of both structural and functional disconnections and their effect on the behaviour. We applied these analyses to map the impact of focal brain lesions on the performance in category fluency. We then present two studies using this approach to investigate the underlying mechanisms of several cognitive functions associated with creativity. We finally discuss the possible interaction between the different brain structures, which generate human behaviours. Our studies unveil numerous networks, both structural or functional, participating in the different high-level cognitive functions. Ultimately, we propose a theoretical model for these interactions.

Keywords: Neuroimaging, lesion, connectivity, disconnection, tracrography, fMRI